Dissertation zur Erlangung des Doktorgrades der
Fakultät für Chemie und Pharmazie der
Ludwig-Maximilians-Universität München

Genetic engineering of adenoviral vectors for improved therapeutic applications

Martin Andreas Mück-Häusl

aus

Bad Reichenhall

2011

Erklärung

Diese Dissertation wurde im Sinne von § 13 Abs. 3 bzw. 4 der Promotionsordnung vom 29. Januar 1998 (in der Fassung der sechsten Änderungssatzung vom 16. August 2010) von Frau Prof. Dr. Anja Ehrhardt betreut und von Herrn Prof. Dr. Roland Beckmann von der Fakultät für Chemie und Pharmazie vertreten.

Ehrenwörtliche Versicherung

Die vorliegende Dissertation wurde selbstständig, ohne unerlaubte Hilfe erarbeitet.

München, den

_____

(Martin Mück-Häusl)

Promotionskommission

Prof. Dr. Roland Beckmann
Prof. Dr. Anja Ehrhardt
Prof. Dr. Klaus Förstemann
PD Dr. Manfred Ogris
Prof. Dr. Christian Wahl-Schott
Prof. Dr. Karl-Peter Hopfner

Eckdaten

Dissertation eingereicht am:	04.11.2011
1. Gutachter:	Prof. Dr. Roland Beckmann
2. Gutachterin:	Prof. Dr. Anja Ehrhardt
Mündliche Prüfung am:	08.12.2011

Table of content

Summary

Genetic aberrations are one of the major causes for a broad range of diseases. Gene therapeutic approaches based on the transfer of functional genes into affected cells resemble an attractive alternative for treatment of genetic disorders. For transport of genetic material vectors are used, which are mainly based on recombinant viruses. Newest generation of vectors based on non-enveloped adenoviruses called high-capacity adenoviral vectors (HCAs) are devoid of all viral coding sequences and generation depends on an adenoviral helper-virus (HV) providing the viral proteins *in trans*. Therefore, vector-associated toxicity and immunogenicity is low, whereas the capacity for cargo sequences is high (>36kb). In this thesis, I focused on improving features and generation of HCAs by genetic engineering.

First, a standardized protocol for cloning of HCA genomes with a single cargo sequence of up to 14 kb and large-scale preparation of HCA utilizing a bioreactor system was established in the content of this thesis. Details of the protocol highlight critical steps during vector preparation and titration and an extensive trouble-shooting guide is provided enabling establishment of this method in any laboratory.

Next, to circumvent clearance of naturally episomal HCA genomes, a hybrid vector system was established combining efficient delivery by HCAs with the integration machinery of the Sleeping Beauty transposase (SB). In this study, I optimized the system by replacing SB with the hyperactive variant HSB5, which exhibited a 10-fold higher activity. Efficacy of the system was demonstrated in mice delivering a hepatocyte-specific expression cassette for the canine coagulation factor IX (cFIX). Application of this system for treatment of a hemophilia B dog resulted in phenotypic correction of the blood clotting disorder for approximately 3 years mediated by stable and therapeutic cFIX expression levels (60 ng/ml). Additional analysis revealed no vector-associated acute toxicity, no anti-cFIX antibodies and only low levels of neutralizing anti-adenovirus antibodies indicating no potent induction of the immune system. Molecular analysis of hepatocyte-derived DNA revealed that the main portion of transposons was integrated into the host genome. However, increase of dosage resulted in a total loss of therapeutic effects probably due to significantly increased induction of the immune response. In conclusion, even for the improved hybrid vector system the therapeutic window is narrow and therefore, I aimed at improving the HCA vector system into several directions.

To circumvent restrictions of cloning methods currently used for incorporation of therapeutic DNA into HCA genomes and modulation of HV genomes, I established a novel cloning

platform based on bacterial artificial chromosomes (BACs), which allows arbitrary sequence modulations by homologous recombination. In sharp contrast to common cloning strategies, no intermediate clones have to be generated. Furthermore, I demonstrated simple generation of BACs utilizing isolated viral genomes or the newly invented backbone-exchange method for conversion of plasmids into BACs. Traceless modification in a 2-step procedure was exemplified by construction of BACs with HV genomes containing capsid-modifications fib5/35 and hex5/48. Furthermore, I invented a recombination pipeline based on iterative recombination steps utilizing alternating bacterial selection cassettes. This enables generation of complex HCAs genomes such as B-HCA-2indsys containing two independent systems for cell type-specific and inducible expression. In addition, ion-exchange columns were shown to allow easy and rapid purification of several small-scale HCA preparations in parallel.

To broaden the spectrum of HCA applications, I modified the hypervariable regions (HVRs) located within the surface region of the major capsid protein hexon, which mediate liver-tropism of unmodified adenoviral vectors via interaction with coagulation factor X after intravenous administration. Chimeric hexon genes were generated by precise exchange of HVRs or exchange of the complete surface domains with respective sequences of other human adenovirus serotypes. Expressed chimeric hexon proteins were shown to enable initial capsid assembly steps and therefore, respective hexon-modified HV genomes were constructed by BAC cloning technology. Challenging reconstitution was successful for HVs with HVRs precisely exchanged with sequences of serotypes 12 (HV-HVR12) and 48 (HV-HVR48) and with completely exchanged surface domains of serotypes 4 (HV-SD4) and 12 (HV-SD12). Analysis of FX-mediated transduction in cell culture revealed high transduction efficiency for HV-HVR12 indicating a newly created binding site. Bioluminometric measurements after intravenous injection of HV-HVR12 in mice demonstrated enhanced expression levels located within the liver with 500-fold higher maximum signal strength compared to unmodified HVs. In contrast, for HV-SD12 neither enhanced transduction rates in cell culture were observed nor transduction of liver tissue was detected in mice. Therefore, the whole hexon surface domain seems to be responsible for the interaction with FX, which is in contrast to the current hypothesis claiming that exclusively HVR sequences bind to FX.

In summary, improvements introduced in this thesis for generation of genetically modified adenoviruses will pave a new path towards widespread in gene therapeutic approaches, anti-cancer treatments and vaccination purposes as well as basic research.

Zusammenfassung

Genetische Aberrationen sind eine der Hauptursachen für eine Vielzahl von Krankheiten. Gentherapeutische Ansätze, die auf dem Transfer von funktionellen Genen in die betroffenen Zellen basieren, repräsentieren eine attraktive Alternative für die Behandlung von genetisch bedingten Erkrankungen. Für den Transport von genetischem Material werden hauptsächlich Vektoren verwendet, die auf rekombinanten Viren basieren. Die neueste Generation von Vektoren genannt „high-capacity adenovirale Vektoren“ (HCAs), die auf nicht-umhüllten Adenoviren basieren, enthalten keine viralen, kodierenden Sequenzen. Ihre Herstellung beruht auf einem adenoviralen Helfer-Virus (HV), das die viralen Proteine *in trans* zur Verfügung stellt. Daher ist die Vektor-assoziierte Toxizität und Immunogenität gering, während die Kapazität für Fracht-Sequenzen hoch ist (> 36kb). In dieser Arbeit habe ich mich auf die Verbesserung der Eigenschaften und der Erzeugung von HCAs mit Hilfe gentechnischer Manipulationen konzentriert.

Zunächst wurde im Rahmen dieser Arbeit ein standardisiertes Protokoll etabliert, das die Klonierung von HCA-Genomen mit einzelnen Sequenzen von bis zu 14 kb ermöglicht sowie die Herstellung von HCAs im großen Maßstab unter Verwendung eines Bioreaktor-Systems erlaubt. Details des Protokolls heben kritische Schritte innerhalb des Herstellungsverfahrens und der Titration der Vektoren hervor. Zudem stellt es einen umfangreicher Leitfaden zur Fehleranalyse zur Verfügung, der die Etablierung dieser Methode in jedem Labor ermöglicht.

Um den Abbau von naturgemäß episomal vorliegenden HCA-Genomen zu umgehen, wurde daraufhin ein Hybrid-Vektor-System etabliert, das den effizienten Transport mittels HCAs mit der Integrationsmaschinerie der Sleeping Beauty Transposase (SB) kombiniert. In dieser Studie optimierte ich das System durch den Austausch der SB mit der hyperaktiven Variante HSB5, die eine 10-fach höhere Aktivität aufweist. Die Wirksamkeit des Systems konnte in Mäusen durch den stabilen Transport einer Expressionskassette gezeigt werden, die eine leber-spezifische Expression des Blutgerinnungsfaktor IX von Hunden (cFIX) bewirkte. Die Anwendung des Systems zur Behandlung eines Hundes mit Hämophilie B führte zur Korrektur des Phänotyps der Blutgerinnungsstörung für ca. 3 Jahren, die durch die stabile Expression von cFIX auf einem therapeutischen Level (60 ng / ml) bewirkt wurde. Zusätzliche Analysen zeigten keine akute, vektor-assoziierte Toxizität, keine Bildung von anti-cFIX Antikörpern und nur geringe Mengen von neutralisierenden anti-Adenovirus Antikörpern und damit kein Anzeichen für eine starke Induktion des Immunsystems. Die molekulare Analyse der DNA, die aus Hepatozyten isoliert wurde, ließ erkennen, dass der

Hauptteil der Transposons in das Wirtsgenom integriert wurde. Allerdings führte die Erhöhung der Dosis zu einem vollständigen Verlust des therapeutischen Effekts, der vermutlich auf die deutlich angestiegene Induktion der Immunantwort zurückzuführen ist. Zusammenfassend ist selbst für das verbesserte Hybrid-Vektor-System das therapeutische Fenster schmal und deshalb strebte ich auf mehreren Ebenen die Verbesserung des auf HCA basierenden Vektorsystems an.

Um die Limitierungen der derzeitigen Klonierungsmethoden zu umgehen, die für den Einbau von therapeutischer DNA in HCA-Genome und für die Veränderung von HV-Genomen verwendet werden, etablierte ich eine neue Klonierungsplattform. Diese basiert auf künstlichen bakteriellen Chromosomen (BACs), die beliebige Veränderungen von Sequenzen mit Hilfe homologer Rekombination ermöglicht. Im Gegensatz zu anderen Klonierungsstrategien müssen dabei keine Zwischen-Klone generiert werden. Darüber hinaus habe ich gezeigt, dass die Generierung von BACs sowohl unter Verwendung isolierter viraler Genome als auch mit Hilfe der neu entwickelten Methode des „Backbone-Austausches“, der die Konvertierung von Plasmiden in BACs ermöglicht, einfach ist. Des Weiteren erlaubt ein 2-stufiges Verfahren rückstandsfreie Modifikationen wie am Beispiel der Konstruktionen von BACs veranschaulicht wurde, die HV Genome mit den Kapsid-Modifikationen fib5/35 und der Hexon-Modifikation hex5/48 beinhalten. Des Weiteren entwickelte ich eine Rekombination-Pipeline, die auf iterativen Rekombinationsschritten unter Benutzung von sich abwechselnden bakteriellen Selektionskassetten basiert. Dies ermöglicht die Erzeugung komplexer HCA-Genome wie beispielsweise B-HCA-2indsys, das zwei unabhängige Systeme für Zelltyp-spezifische und induzierbare Expression enthält. Außerdem wurde gezeigt, dass Ionenaustausch-Säulen eine einfache und schnelle Aufreinigung von mehreren kleinen Mengen von HCAs parallel ermöglichen.

Zur Erweiterung des Spektrums der HCA-Anwendungen, modifizierte ich die hypervariablen Regionen (HVRs) im oberflächennahen Bereich des Haupt-Kapsidproteins Hexon, das über die Interaktion mit dem Gerinnungsfaktor X den Leber-Tropismus von unmodifizierten adenovirale Vektoren nach intravenöser Gabe bestimmt. Chimäre Hexon-Gene wurden durch präzisen Austausch der HVRs oder durch Austausch der kompletten Oberflächenbereiche mit den entsprechenden Sequenzen von anderen humanen Adenovirus-Serotypen erzeugt. Nachdem gezeigt wurde, dass die chimären Hexon-Proteine die anfänglichen Assemblierungsschritte ermöglichen, wurden Hexon-modifizierte HV-Genome mit Hilfe der BAC-Klonierungstechnologie konstruiert. Die an sich anspruchsvolle Rekonstitution war

erfolgreich für die HVs, bei denen die HVRs exakt mit den Sequenzen der Serotypen 12 (HV-HVR12) und 48 (HV-HVR48) ausgetauscht wurden und bei denen die kompletten Oberflächenbereiche mit denen der Serotypen 4 (HV-SD4) und 12 (HV-SD12) ersetzt wurden. Die Analyse der FX-vermittelten Transduktion in der Zellkultur ergab eine hohe Transduktionseffizienz für HV-HVR12, was auf eine neu geschaffene Bindungsstelle hinweist. Bioluminometrische Messungen nach intravenöser Injektion von HV-HVR12 in Mäuse zeigten eine erhöhte Expression in der Leber mit 500-fach höherer maximaler Signalstärke im Vergleich zu unmodifizierten HVs. Im Gegensatz dazu war für HV-SD12 weder eine erhöhte Transduktionsrate in Zellkultur noch Transduktion von Lebergewebe in vivo beobachtet worden. Daher scheint der gesamte Oberflächenbereich des Hexons für die Interaktion mit FX verantwortlich zu sein, im Gegensatz zu der aktuellen Hypothese, die besagt, dass ausschließlich HVR-Sequenzen an FX binden.

Zusammenfassend werden die Verbesserungen, die in dieser Arbeit für die Erzeugung von gentechnisch veränderten Adenoviren vorgestellt wurden, den Weg für die Verbreitung in gentherapeutischen Ansätzen, Anti-Krebs-Behandlungen, Impfstrategien und Gebieten der Grundlagenforschung ebnen.

1. Introduction

In general diseases could be classified in contagious diseases and non-communicable diseases. Contagious diseases are caused by pathogens, for instance the acquired immune deficiency syndrome (AIDS) is caused by the human immunodeficiency virus (HIV), tuberculosis by mycobacterium tuberculosis or malaria by plasmodium malariae. In contrast, main risk factors, which cause non-communicable diseases, are inherited genetic aberrations as well as the environment and the life-style, which could affect a person directly or by generation of spontaneous genomic mutations by physical (UV light), chemical (reactive oxygenic substances) or biological damage (virus infection). Most of the non-communicable diseases like cancer, cardiovascular diseases of neurological disorders are caused by multiple genetic defects affecting expression of cellular proteins. Therefore, a single mutation in one of these genes represents a predisposition of the affected person for the respective disease but does not necessarily result in clinical symptoms, whereas accumulation of mutations finally initializes the onset of the disease and the related phenotype (Bos 1989; Bertram 2000; Setel, Saker et al. 2004; Hamosh, Scott et al. 2005; Antonarakis and Beckmann 2006).

For a small fraction of non-communicable diseases called monogenetic diseases a mutation of a single gene is sufficient to cause clinical symptomes. These diseases are classified in dominant, recessive and X-linked disorders. For dominant genetic disorders like the Huntington disease one affected allel is sufficient to cause the phenotype, whereas for patients with a recessive disease for instance cystic fibrosis or phenylketonuria both allels of the respective gene have to be affected. Genetic diseases caused by mutated genes located on the X chromosome like hemophilia A and B or Duchenne muscular dystrophy are called x-linked, which mainly affect male patients. Mutations causing a monogenetic disease affect either regulatory elements or coding sequences of the respective gene. In detail, sequences are altered by point mutations, deletions of endogenous sequences, insertion of additional sequences into the coding sequence or chromosomal aberrations such as rearrangements. As a consequence, the gene product is non-functional or instable or the expression is altered in strength, location or regulation. Generally, impact of the mutation on the functionality of the protein is directly related with the severity of the clinical symptoms (Scriver and Waters 1999; Weatherall 2001; Hamosh, Scott et al. 2005; Antonarakis and Beckmann 2006).

Currently used therapies for monogenetic diseases mainly focus on treatment of clinical symptoms such as skin transplantations for patients with epidermolysis bullosa, a disorder in

collagen VII causing strongly decreased connectivity of skin tissue (Lin and Carter 1993). Other monogenetic diseases can be treated by protein replacement therapy. Herein, synthetic functional protein is injected intravenously to replace the non-functional endogenous protein, which leads to compensation of the pathogenic effect, for example to treat the clotting disorder hemophilia B patients are repeatedly treated with recombinant coagulation factor IX. Nevertheless, this kind of therapy is cost intensive and inconvenient as well as repeated intravenous injections restrict the application of this kind of therapy to diseases caused by a defect of a secreted protein (Konkle, Josephson et al. 1993). In addition, for many severe monogenetic diseases like SCID, dermolysis bullosa or Duchenne muscular dystrophy current therapies are insufficient (Darras, Korf et al. 1993). Therefore, to face the challenges of treating genetic diseases scientists aim at elimination of disease, origins on DNA level utilizing gene therapeutic approaches.

1.1. Gene therapy

Gene therapy is defined as the delivery of therapeutic DNA to a certain tissue or cell type to treat the genetic defect. For example hemophilia B is caused by a mutation located within the gene encoding coagulation factor IX and therefore blood coagulation is severely impaired, which causes spontaneous bleedings in affected patients. In a gene therapeutic approach the gene encoding functional factor IX is delivered to hepatocytes and is subsequently expressed and secreted resulting in phenotypic correction. In contrast to therapeutic treatments based on gene addition for correction of a genetic disease, gene replacement therapies aim for the repair of the endogenous mutated gene or the replacement with the correct gene in the genomic context. These approaches are applied for dominant mutations or gene products, which are toxic for the cell. Furthermore, gene knock-down approaches could be applied for toxic gene products as long as the encoded protein is not essential for the cell or the organism (O'Connor and Crystal 2006).

1.1.1. Classifications of gene therapeutic approaches

In principle, for a gene therapeutic application the therapeutic DNA is packaged in or coupled to a gene vector, which enables the transfer of the DNA into the respective target cell. Based on the strategy used gene therapeutic applications are classified in direct (*in vivo*) and cell-

mediated (*ex vivo*) approaches (Fig. 1.1) (O'Connor and Crystal 2006). *In vivo* applications are based on direct application of the therapeutic agent to the patient (Zabner, Couture et al. 1993), whereas for *ex vivo* approaches cells derived from the patient are transduced and subsequently expanded and reimplanted (Blaese, Culver et al. 1995). Besides classical gene therapeutic approaches aiming for compensation of gene defects, therapy forms based on similar principles are evaluated for vaccination purposes. Herein, the antigen encoding gene is transfered to cells enabling the establishment of a robust antigen-specific immune response (Rollier, Reyes-Sandoval et al. 2011). Furthermore, gene therapeutic setups were used for anti-viral treatments either delivering genes encoding for proteins, which inhibit virus replication, or siRNAs targeting viral mRNAs (Arbuthnot 2010). Last but not least treatments of cancer with conditionally replicating viruses can be included in the category of gene therapeutic strategies. These modified therapeutic viruses mainly replicate in cancer cells causing cell death and therefore reduction or even elimination of cancer tissue can occur (Hernandez-Alcoceba 2011).

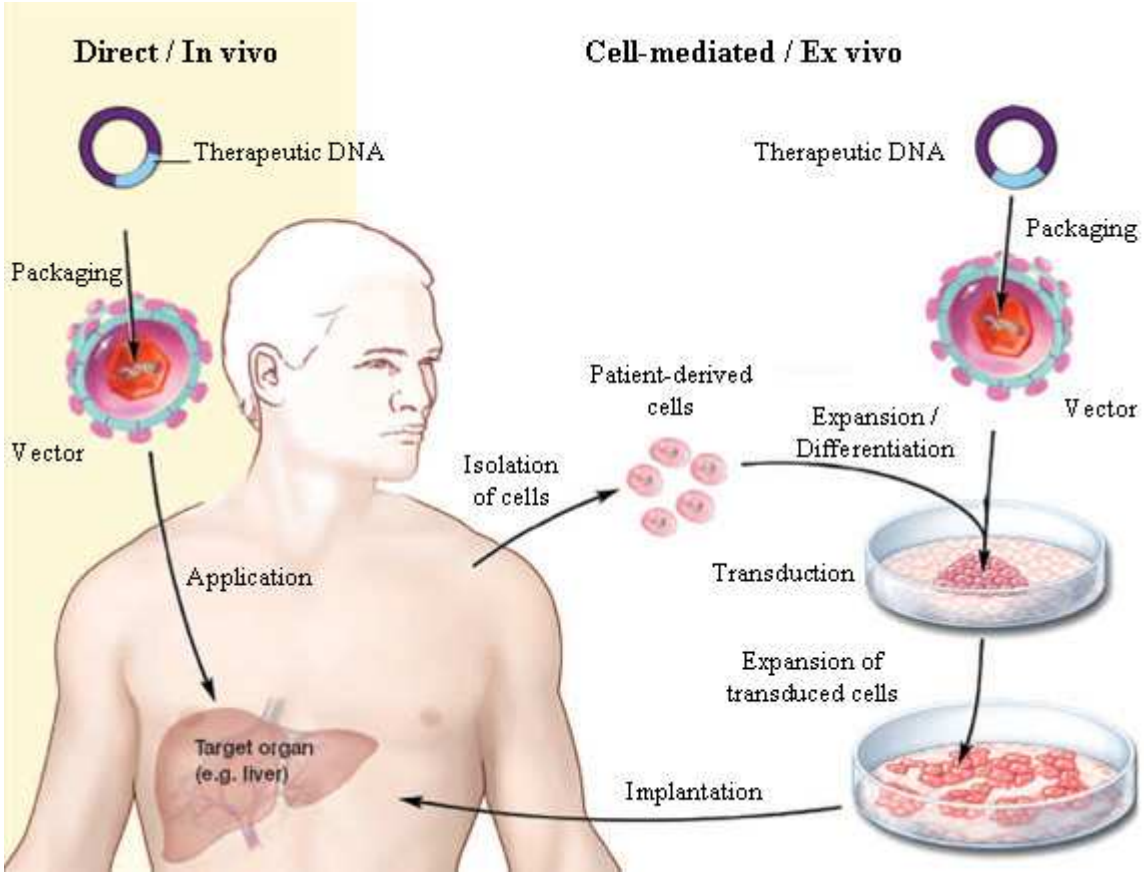

Figure 1.1: Schematic illustration of direct (in vivo) and cell-mediated (ex vivo) gene therapeutic strategies. Modified from The National Institutes for Health resource for stem cell research (http://stemcells.nih.gov/info/2006report/2006Chapter4.htm).

1.1.2. Clinical and pre-clinical studies

For establishment of a gene therapeutic application efficiency and persistence of the therapeutic effect as well as adverse effects like toxicity or immunogenicity have to be evaluated in small and large animals before tested in phase I clinical studies. In these studies, the lowest dose resulting in a therapeutic effect and the highest dose with tolerable side effects are determined. Defined therapeutic windows are transferred to humans including all data sets gained from related studies (Van Spall, Toren et al. 2007). First gene therapeutic attempts were performed in the early 1990s treating patients with monogenetic diseases causing severe symptoms with no alternative therapies such as severe combined immunodeficiency (SCID) (Blaese, Culver et al. 1995; Cavazzana-Calvo, Hacein-Bey et al. 2000). Due to the death of patient Gessie Gelsinger in 1999 treated with a high dose of a gene therapeutic agent (Raper, Chirmule et al. 2003), restrictions for gene therapeutic applications were tightened and the progress in this field slowed down. Nevertheless, recent successes led to an increase of clinical trials and over the past years two gene therapeutic treatments for nasopharyngeal carcinomas were legalized in China (Wilson 2005). Up to now clinical trials include monogenetic disease as well as the treatment of infectious diseases, polygenetic diseases like diverse cancer types, cardiovascular diseases and neurological disorders (Fig. 1.2) (Edelstein, Abedi et al. 2004).

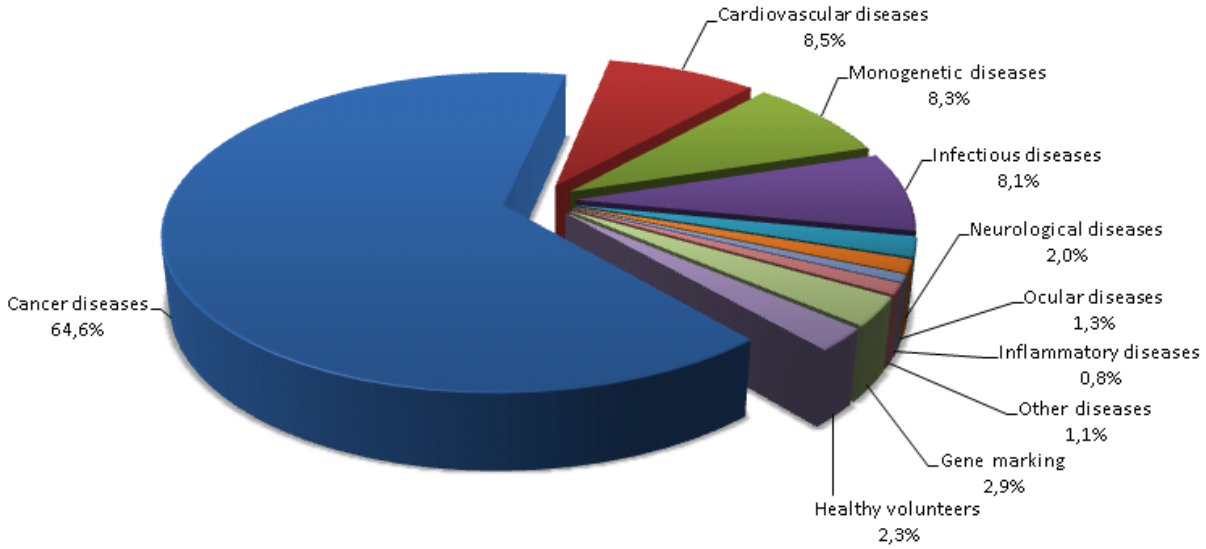

Figure 1.2: Indications addressed by gene therapy clinical trials. Modified from the journal of gene medicine 2011 (http://www.wiley.com/legacy/wileychi/genmed/clinical/)

1.2. Variables defining therapeutic window of a gene therapeutic approach

Main determinants affecting the efficiency of a gene therapeutic treatment are the composition of the therapeutic DNA and the route of administration as well as the type and composition of the vector used for delivery (O'Connor and Crystal 2006).

1.2.1. Application route

For *in vivo* application, vectors are either distributed systemically via intravenous injection or administration is locally restricted. The latter option includes several application routes such as intramuscular injection, intranasal application, inhalation or direct injection into the target organ or specific tissue (Knowles, Hohneker et al. 1995; Perricone, Morris et al. 2001; Harvey, Maroni et al. 2002). Furthermore, administration could be combined with standard chirurgical procedures, for instance ballon-catheters to enable local restriction of vectors transported via the blood stream (Brunetti-Pierri, Stapleton et al. 2007). In general, it was demonstrated, that local administrations are often more efficient and cause less immune response, but application procedures are usually sophisticated and often invasive.

Ex vivo gene therapeutic applications include a broad subset of strategies, which significantly differ in the experimental setup (Naldini 2011). For example often certain types of stem cells like hematopoietic stems are used for cell-mediated gene therapy (Malatack, Consolini et al. 2003). Isolation of these stem cells from patient material is often challenging and cells have to be characterized before further processing. Therefore, standardized stem cells not derived from the patient were used as an alternative in some studies (Fairchild, Cartland et al. 2004). In other approaches complete tissue pieces composed of several cell types were transduced with the therapeutic DNA. Efficiency of *ex vivo* approaches is often limited by the number of processing steps such as isolation or expansion of transduced cells and therefore alterations, which may result in cancer formation or induction of the immune response after implantation.

1.2.2. Therapeutic DNA

The design of the therapeutic DNA has also a major influence on the efficiency of the gene therapeutic approach. For expression of a therapeutic gene the coding cDNA sequence could be used, but often utilization of the enogenous sequence encoding all regulatory elements or usage of an optimized gene is more suitable (Nott, Meislin et al. 2003; Bollenbach, Vetsigian

et al. 2007). Furthermore, regulatory elements like enhancers, promoters or miRNA-target sites represent tools, which enable tissue-specific expression (Pastore, Morral et al. 1999; Wolff, Wolff et al. 2009), induction of expression in presence or absence of certain drugs (Osterwalder, Yoon et al. 2001; Mohr, Arapovic et al. 2010) or inhibition of expression in cells, which are not targeted (Brown and Naldini 2009). Moreover, internal ribosomal entry sites or synthetic protease cleavage sites facilitate coupled expression of two or more transgenes whereas insulator sequence provide the option to separate two expression cassette allowing independent transcription. In contrast to gene insertion and replacement approaches, gene knock-down strategies are mainly based on targeting mRNA transcripts of the mutated gene with specific siRNAs to decrease expression of the affected gene. Delivery of multiple siRNA expression cassettes specific for the same mRNA may enhance efficiency and specificity of the knock-down effect (Castanotto and Rossi 2009; Sliva and Schnierle 2010).

To enable long-term expression of transgenes essential for the treatment of genetic disorders, additional sequences could be used enabling persistence and amplification of the transgene expression cassette in replicating cells. For instance, persistence of episomal vector DNA could be mediated by vector-associated sequences or DNA maintenance could be supported by additional non-coding sequences such as the EBNA-binding sequences (Yates, Warren et al. 1985). These mediate attachment to the chromosomal DNA via the Eppstein-Barr virus derived EBNA1 protein or non-viral S/MAR sequences, which interact with histones to anchor the DNA and which also act as origins of replication enabling DNA replication during the S phase in cycling cells (Ehrhardt, Haase et al. 2008). As an attractive alternative, therapeutic DNA can be incorporated into the host genome. Most prominent enzymes mediating somatic integration are provided by viral integration machineries e.g. retroviral integrases or Rep proteins from the adeno-associated virus. Furthermore, non-viral integration machineries based on transposases like the Sleeping Beauty transposase and the PiggyBac transposase or bacterial integrases such as the phiC31 integrase are used for incorporation of foreign DNA into the host chromosomes (Ehrhardt, Xu et al. 2005; Sorrell and Kolb 2005; Ehrhardt, Yant et al. 2007; Muther, Noske et al. 2009). The integration patterns of these systems differ significantly with varying preferences for transcriptional active regions or distinct genomic loci. Although integration into the host chromosomes is efficient for these enzymes resulting in long-term effects, unwanted genotoxic side effects such as insertional mutagenesis could occur. This could lead to activation of endogenous proto-oncogenes initializing transformation of transduced cells in cancer cells (Baum 2007). In contrast, zinc

finger nucleases and transcription activator like effectors (TALEs) can mediate specific modulation of a single location within the host genome allowing precise gene replacement or gene corrections with no or low genotoxic side effects (Wood, Lo et al. 2011). As a further alternative, homologous recombination dependent on cellular proteins was used for targeted integration of therapeutic DNA (Katada and Komiyama 2011). Although off-target integration and associated oncogenic potential is significantly reduced, efficiency of these gene replacement strategies *in vivo* have been shown to be low in comparison to non-targeted integration machineries. Although maintenance of therapeutic DNA could be provided by described strategies, expression of a therapeutic protein generally decreases due to transcriptional silencing mediated by DNA-methylation (Brooks, Harkins et al. 2004). Therefore bacterial sequences like the origin of replication or selection markers as well as CpG islands of the cargo sequence can be depleted, resulting in a significantly improved expression profile and reduction of induced intracellular defense mechanisms (Haase, Argyros et al. 2010).

1.2.3. Vectors for gene therapeutic applications

Preclinical as well as clinical applications demonstrated, that the vector type used for the treatment is the major determinant for the outcome of a gene therapeutic approach. It determines the efficacy for somatic transfer of the therapeutic DNA and most of the adverse effects such as toxicity and immune response are associated with the vector. Furthermore, other aspects like the persistence of the therapeutic effect or genotoxicity are dependent on the vector type. Due to their natural ability to invade a cell and transport their genomic cargo into the nucleus of a cell, several virus types were utilized as a shuttle for DNA transfer. In parallel, non-viral strategies were developed to deliver therapeutic DNA mimicking viral entry methods (Gonin and Gaillard 2004; Gardlik, Palffy et al. 2005).

1.3. Vector types

In principle, vector design aims at achieving optimal features concerning all aspects of the respective gene therapeutic application. Ideally, the vector should mediate highly efficient transduction of cells and intracellular transport into the cell nucleus as well as specificity for target cells to avoid adverse effects especially for direct *in vivo* applications. Furthermore,

after delivery of the therapeutic DNA, the therapeutic effect should either persist life-long or for a sufficient time period dependent on the demands of the respective disease. In addition, the vector should induce neglegible toxicity and immune responses either directed against vector components or the therapeutic gene product. In case of viral vectors the latter issue includes unwanted expression of viral proteins and virus replication. For transfer into clinical studies the final vector preparations should yield high purity and high titers. Moreover, vector production should be easy and fast including adoption to the respective application by cloning, amplification, purification and titration. Moreover, the vectors should feature high stability enabling at least medium-term storage (Crystal 1995).

Currently, viral vectors commonly used are based on retroviruses, lentiviruses, adeno-associated viruses or adenoviruses, whereas common non-viral vectors are mainly based on polymers complexing therapeutic DNA, artificial liposomes encapsulating the DNA or naked DNA administered with specific delivery methods (Gonin and Gaillard 2004; Gardlik, Palffy et al. 2005). So far, however, none of these vectors could unify all features required for the optimal vector and therefore different vectors are used for a specific application due to individual requirements (Table 1.1).

1.3.1. Non-viral vector types

For proof-of-principle experiments in cell culture as well as in small animal models often naked DNA-circles are used, because they are easy to produce in high amounts and regularly no toxicity or immunogenicity is related with pure DNA. However, yielded effects are transient due to degradation of the DNA-circles by endogenous nucleases. Furthermore, the transduction efficiency is low due to repulsive electrostatic interactions between DNA molecules and the cellular surface and the lack of an import mechanism for the transfer of the DNA molecules into the cellular nucleus. In contrast, transduction efficiency of non-viral DNA-polymer complexes and artificial liposomes for transport of plasmids are significantly higher due to charge-based interactions between positive-charged polymers or lipids with the negative-charged cellular surface. However, no nuclear import is enabled inhibiting transduction of resting cells and long-term effects are limited by nuclease-mediated degradation as seen for naked plasmid DNA. Therefore, applications of these vector types are limited to a few approaches including transduction of certain cell types ex vivo and direct application into target organs in vivo. Nevertheless, perspectives of these vector types are

Vector type	Description	Advantages	Disadvantages	Application field
Naked plasmid-DNA	Circular plasmids; Often mini-circles or variants of episomal stable plasmids (pEpi);	Easy production; High capacity (<20 kb); Low toxicity; Low immunogenicity; In vivo delivery by hydrodynamic injection;	Low transduction rates; No active nuclear import; Transient effects due to degradation by nucleases;	Preliminary experiments in cell culture and small animals; Part of prime-boost vaccination approaches;
Lipoplexes	DNA (Plasmids) encapsulated by cationic lipids;	Easy production; High capacity (< 20 kb); Low immunogenicity; Modification of lipids or addition of components; Moderate transduction rates for certain cell types;	Substantial toxicity; No active nuclear import; Transient effects due to degradation by nucleases;	Direct local administration in vivo for transient effects;
Polyplexes	DNA (Plasmids) complexed with cationic polymers like poly-L-lysine or polyethylenimine (PEI);	Easy production; High capacity (<20 kb) Low immunogenicity; Modification of polymers or addition of components; Moderate transduction rates for certain cell types;	Substantial toxicity; No active nuclear import; Transient effects due to degradation by nucleases;	Direct local administration in vivo for transient effects;
Retroviruses	Enveloped ssRNA-virus; Mainly based on MLV;	Moderate capacity (9-10 kb); High transduction efficiency for a broad range of host cells; Integrating and therefore stable expression (integration);	Low titers (10^5-10^6); Oncogenic potential due to insertional mutagenesis (biased towards transcriptional active regions); Low capsid stability; No transduction of resting cells;	Transduction of cells in ex vivo approaches for example modification of T cells or hematological diseases;
Lentiviruses	Enveloped ssRNA-virus; Mainly based on HIV-1;	Moderate capacity (9-10 kb); High transduction efficiency for a broad range of host cells; Transduction of resting cells; Low toxicity; Low immunogenicity; Stable expression (integration);	Moderate titers (10^6-10^9 tu/ml); Oncogenic potential due to insertional mutagenesis (almost random); Low capsid stability;	Transduction of cells in ex vivo approaches for example modification of T cells or hematological diseases;
Adeno-associated viruses (AAV)	Non-enveloped ssDNA-virus Based on various serotypes (1,2,5,6,8,9);	High titers (10^{10}-10^{11} tu/ml); Genome persistance in Resting cells (long-term effect); Non-pathogenic in humans; Modified targeting by capsid-modifications;	Substantial immunogenicity in humans; Low capacity (< 5 kb); Low transduction efficiency in cell culture;	Direct systemic or local application to treat genetic disorders or neurological, cardiovascular and ocular diseases;
First-generation adenoviruses (FG-AdVs)	Non-enveloped dsDNA-virus deleted for early genes; Mainly based on serotype 5;	Moderate capacity (7.5-8 kb); High titers (10^{11}-10^{12} tu/ml); High transduction efficiency for a broad range of host cells; Transduction of resting cells; Liver-targeting in vivo; Modified targeting by capsid-modifications;	High acute toxicity; High immunogenicity; Transient effects in cycling cells; Clearance of vector genomes; Low transduction of CAR^- cells; liver-targeting in vivo;	Vaccination (intramuscular injection); Transient transduction of cells in cell culture;
High-capacity adenoviruses (HC-AdVs or HCAs)	Non-enveloped dsDNA-virus deleted for all coding sequences; Mainly based on serotype 5;	High capacity (36 kb); No acute toxicity; High titers (10^{11}-10^{12} tu/ml); High transduction efficiency for a broad range of host cells; Transduction of resting cells; Liver-targeting in vivo; Genome persistance in resting cells	Substantial immunogenicity; Transient effects in cycling cells; Low transduction of CAR^- cells; Liver-targeting in vivo;	Systemic application in vivo; Treatment of diverse cancer types; Vaccination (intramuscular injection); Transient transduction of cells in cell culture;

Table 1.1: Features and application fields of vector types most commonly used in gene therapeutic approaches. Modified from (Gonin and Gaillard 2004; Mintzer and Simanek 2009). tu: transducing units; kb: kilobases; ssRNA: single-strand RNA; MLV: murine leukaemia virus; HIV-1: human immunodeficiency virus 1; ssDNA: single-strand DNA; dsDNA: double-strand DNA; CAR^-: negative for Cosackievirus and adenovirus receptor.

promising, because features could be improved by additional or modified components for example to increase the transduction efficiency, to enable nuclear import or to allow targeting of specific cell surface markers. However, new components could affect other vector properties such as the vector-associated toxicity (Douglas 2008; Mintzer and Simanek 2009).

1.3.2. Viral vector types

For most gene therapeutic applications viral vector types are used (Thomas, Ehrhardt et al. 2003). For ex vivo approaches often retroviral vectors mainly based on the murine leukemia virus (MLV) were used in the past, with cargo sequences replacing viral coding sequences. They are able to transduce a broad range of cell types, especially various stem cells, and transduction efficiency is even improved for retroviral vectors, which are pseudo-typed with the glycoprotein of the Vesicular Stomatitis Virus (VSV-G) (Yang, Vanin et al. 1995). MLV vector genomes usually integrate into the host genome mediating stable and persistent expression levels of the transported transgene or siRNA. However, somatic integration can be associated with cancer formation due to the integration profile, which is biased towards transcription active regions leading to induction of proto-oncogenes (Yi, Hahm et al. 2005). Therefore, currently lentiviral vectors based on the human immunodeficiency virus 1 (HIV-1) are mainly used for ex vivo approaches. Features of this vector type are similar to vectors based on MLV, but 5' and 3' of lentiviral vector genomes have significantly lower transcriptional activity and therefore vectors have lower oncogenic potential (Pluta and Kacprzak 2009; Dropulic 2011). For direct in vivo applications mainly vectors based on adeno-associated viruses are used. Vector preparations with high titers can be generated and direct in vivo administration of this vector type results in high transduction rates not accompanied by vector-associated toxicity. Furthermore, AAV genomes persist episomally in non-diving cells resulting in relatively stable long-term effects and AAV capsid-modifications enable more specific targeting of defined organs or cell types in vivo. However, clinical studies revealed an immunological response after systemic administration of AAVs in humans resulting in a strong decrease of the therapeutic effect. Another limiting factor is the low capacity for cargo sequences (<5kb) within the AAV vector genomes and additionally, evaluation of vectors in cell culture is hampered by low transduction efficiencies in ex vivo (Warrington and Herzog 2006; Daya and Berns 2008). As an alternative for in vivo applications, first-generation adenoviral vectors deleted for up to three early viral genes were

used providing higher capacity for transgenic sequences (7.5-8 kb) and mediating highly efficient transduction of a broad range of cell types. However, due to acute toxicity after systemic administration and potent vector-related immunogenicity adenoviral vectors were mainly used for vaccination purposes or for treatment of diverse cancer types by conditional replicating oncolytic adenoviruses (Nasz and Adam 2001; Douglas 2002). In sharp contrast, evaluation of the newest generation of adenoviral vectors called high-capacity adenoviral vectors revealed almost undetectable vector-associated toxicity and strongly reduced immunogenicity due to deletion of all viral coding sequences. Furthermore, these vectors allow transport of sequences up to 36 kb and vector genomes are stable in resting cells. These features provide new options for vaccination studies as well as direct in vivo applications (Palmer and Ng 2005; Segura, Alba et al. 2008). Considering the high potential of high-capacity adenoviral vectors further optimization is a desirable goal.

1.4. Features of adenoviruses

Human adenoviruses (hAds) belong to the genus of mastadenoviridae of the family of adenoviridae. Based on neutralization assays 56 serotypes have been identified up to now (Robinson, Singh et al. 2011), which are divided in six subgroups (A-F) based on the GC content of the viral genome and the ability of the adenovirus to agglutinate erythrocytes (Norrby, van der Veen et al. 1970). In general, human adenoviruses cause mild infections of the upper respiratory tract (Hilleman and Werner 1954), the gastrointestinal tract (Flewett, Bryden et al. 1973) or the eyes (Jawetz 1959), but for immune-compromised patients especially after organ transplantations, infections could cause severe complications (Kojaoghlanian, Flomenberg et al. 2003; Echavarria 2008).

1.4.1. Structure of the adenoviral particle

Adenoviruses are non-enveloped particles with a diameter of about 70-100 nanometers (Stewart, Burnett et al. 1991). The main structure features are shared by all serotypes, although they could differ slightly in details (Chiu, Mathias et al. 1999). For structural analysis serotypes 2 and 5 of adenovirus subgroup C were used (Fig. 1.3a), which were historically characterized in great detail and which were used for generation of most recombinant adenoviral vectors (Schmid and Hearing 1998).

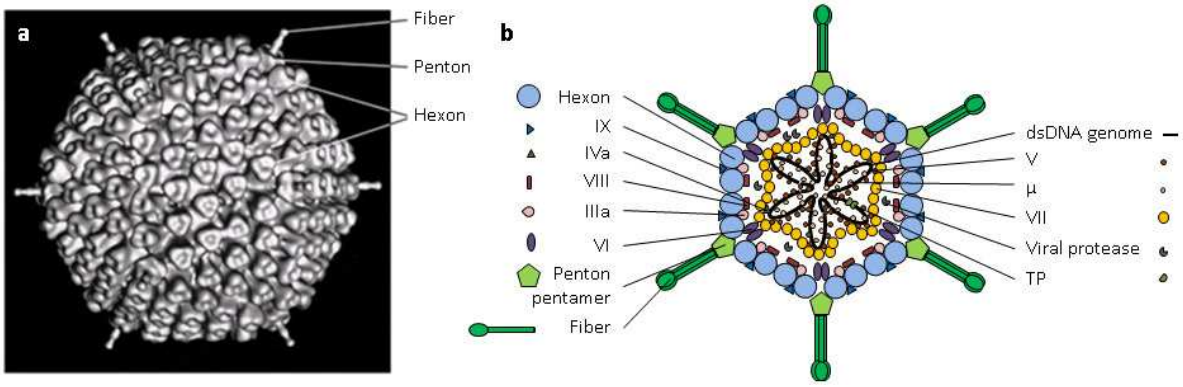

Figure 1.3: Structure of the adenovirus particle. (a) Structure of the human adenovirus serotype 5 particle reconstructed based on data derived of electron microscopy measurements and x-ray christallography measurements (Saban, Silvestry et al. 2006). (b) Schematic composition of an adenovirus particle. The virus capsid consists of major capsid proteins hexon, penton and fiber as well as minor proteins IIIa, VIII and IX. The protein VI connects the capsid with the core consisting of the dsDNA genome associated with the proteins μ, V, VII, IVa and the terminal proteins (TPs). In addition, a mature particle contains several viral protease molecules.

In general, the viral particle consists of an icosaedric capsid and the inner matrix including the viral genome (Fig. 1.3b) (Stewart, Burnett et al. 1991). The capsid shell is composed of three major capsid proteins called hexon, penton and fiber and three minor proteins pIX, pIIIa and pVIII (Stewart, Fuller et al. 1993; Chiu, Mathias et al. 1999; Liu, Jin et al. 2010; Reddy, Natchiar et al. 2010). In detail, 240 hexon timers build the scaffold of the icosaedric capsid structure, which are fixed by 12 penton pentameres located at the vertices (Burnett, Grutter et al. 1985; Stewart, Fuller et al. 1993). Hexon trimeres are organized in 20 groups of nine (GONs), which are stabilized by several hexon-hexon interactions and form the facets of the icosaeder, and five peripentonal hexon trimers per vertex tightening the interaction between penton pentameres and GONs by additional hexon-hexon and hexon-penton interactions (Fabry, Rosa-Calatrava et al. 2005). Fiber proteins are organized in 12 trimeres, each of them interacting with a penton pentamer, respectively (Svensson, Persson et al. 1981). A protein network consistent of 240 copies of pIX proteins stabilizes the facets on the outer surface of the capsid (Fabry, Rosa-Calatrava et al. 2009) whereas the network built by 60 IIIa proteins and 120 VIII proteins steel the capsid at the inner surface (San Martin, Glasgow et al. 2008; Liu, Jin et al. 2010). The pVI protein is bound to the cavity of hexon trimers at the inner surface, mediating the connection of the capsid with the adenovirus core. The core of an adenoviral particle contains the linear, double-strand DNA genome and each end of the genome is covalently linked to a terminal protein (TP) (Rekosh 1981; Smart and Stillman 1982). Highly basic core proteins pVII and Mu are directly associated with the adenoviral genome mediating condensation of DNA similar to histones into a nucleosome-like structure (Mirza and Weber 1982; Chatterjee, Vayda et al. 1985). pV proteins are suggested to form a

core shell interacting with core protein pVII (Newcomb, Boring et al. 1984) and the capsid proteins pVI, penton and pIIIa (Matthews and Russell 1998; Liu, Jin et al. 2010). Therefore, pV proteins anchor the genomic DNA in the capsid. In addition, in every intact virus capsid about 10 copies of the viral cysteine protease are present, which are essential for maturation of the virus capsid and the cell entry during infection (Webster, Russell et al. 1989).

1.4.2. The adenoviral genome organization

The adenoviral genome is a linear DNA double-strand and about 36 kb in size with variations depending on the adenovirus serotype (Chroboczek, Bieber et al. 1992). In general the adenovirus genome is organized in four early transcribed genome regions (E1-E4) and five late transcribed genome regions (L1-L5) as depicted in Fig. 1.4. Early genes encode for several proteins, which enable efficient expression of viral proteins and viral genome replication as well as interaction with the host immune system (Nevins 1987). Proteins encoded by late transcribed regions are mainly structural proteins and proteins essential for efficient capsid assembly and release from the cell (Russell 2009). The genome is secluded by homologous sequences of about 100-150 bp called inverted terminal repeats (ITRs) (Hay, Stow et al. 1984). ITR sequences form so called panhandle structures, which are recognized by the terminal proteins (TPs) facilitating initialization of genome replication and protection against degradation by cellular exonucleases. Within the first 300 bp downstream of the 5'ITR the packaging signal ψ is located consisting of 7 repeats (Grable and Hearing 1990) with the consensus sequence motif 5'-TTTGN$_8$CG-3'(Hearing, Samulski et al. 1987; Schmid and Hearing 1998). This sequence is essential for incorporation of the viral genome into an empty capsid during virus assembly in the cell nucleus (Hearing, Samulski et al. 1987). Additionally, 1-2 viral miRNAs are encoded within the genome (Mathews and Shenk 1991). These are transcribed by the cellular RNA polymerase III and were shown to be essential for efficient virus replication.

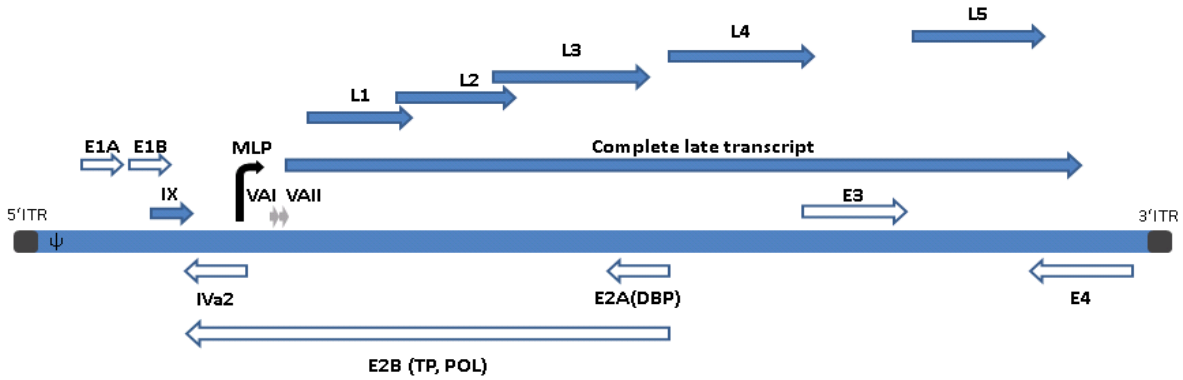

Figure 1.4: Genomic organization of the human adenovirus serotype 5. The adenoviral genome depicted in blue is secluded by inverted terminal repeats (ITRs) and contains the packaging signal ψ at the 5' end.. Regions E1-E4 encoding early genes and spliced transcripts E2A encoding the DNA-binding protein (DBP), E2B containing genes for terminal proteins (TP) and the adenoviral polymerase (Pol) and the transcript for IVa are shown as white arrows. The late regions L1-L5 encoding the late proteins and the complete late transcript generated under control of the major late promoter (MLP) are shown as blue arrows. Adenoviral non-coding RNAs VAI and VAII are depicted as gray arrows.

1.4.3. The adenoviral replication cycle

The replication cycle of human adenovirus serotype 5 (hAd5) can be divided in the phases of cell entry (Fig. 1.5), virus replication and formation of viral particles with subsequent release from the cell.

Primary interaction during cell entry, called attachment, is mediated by the knob domain of the adenoviral fiber proteins. These domains are recognized by the Coxsackie- and Adenovirus Receptor (CAR) (Bergelson, Cunningham et al. 1997), which is mainly located in tight junctions of epithelial cells. This initial interaction is postulated to be a universal mechanism for all adenoviruses but targeted cellular receptors differ upon serotype-specific sequence and structure of the adenovirus fiber knobs, although most serotypes target the CAR receptor (Bergelson, Cunningham et al. 1997). For example a recent study demonstrated that human adenovirus serotypes 3, 7, 11 and 14 belonging to subgroup B attach to the cellular receptor desmoglein-2 (DSG-2) expressed at intercellular junctions of polarized cells but also present on nonpolarized erythrocytes or granulocytes (Wang, Li et al. 2010). In contrast, earlier studies report interaction between cell surface marker CD46 and fiber proteins of other human adenoviruses of subgroup B (serotypes 16, 21, 35 and 50) (Tuve, Wang et al. 2006; Nilsson, Storm et al. 2011). Furthermore, human adenovirus serotype 37, which causes epidemic kerato-conjunctivitis, was shown to interact with GD1 gangliosides demonstrating that other cell surface structures than extracellular protein domains could be utilized by an adenovirus for cell entry (Nilsson, Storm et al. 2011).

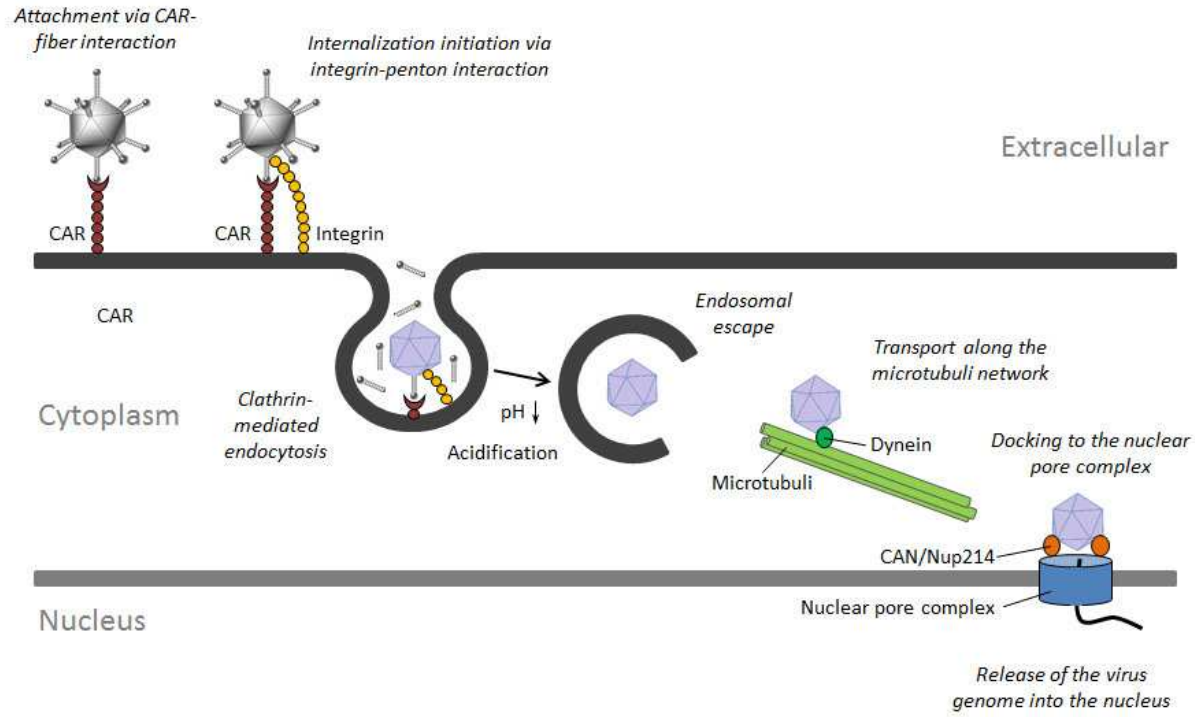

Figure 1.5: CAR-mediated cell entry of human adenovirus serotype 5. During cell entry fibers of the adenoviral particle attach to the cosackie- and adenovirus receptor (CAR) and clathrin-mediated endocytosis is initiated via interaction of adenoviral penton proteins with cellular integrins. Acidification in the endosome triggers partial shedding of the capsid mediating endosomal escape. Subsequently, the capsid binds to dynein proteins and is transported along microtubuli to a nuclear pore complex. There, nuclear pore filament proteins Can/Nup214 enable docking to the nuclear pore complex. Finally, the virus genome is released into the nucleus during disassemble of the virus capsid.

After attachment of the virus capsid to the cell surface cellular integrins $\alpha_v\beta_3$ and $\alpha_v\beta_5$ interact with penton proteins via a RGD-motif displayed in a loop located at the particle surface initializing internalization of the viral particle by clathrin-mediated endocytosis (Patterson and Russell 1983; Bai, Harfe et al. 1993; Wickham, Mathias et al. 1993; Mathias, Wickham et al. 1994). Acidification of the endosomal compartment (pH > 6.0) activates the viral protease, which triggers the removal of the vertices of the virus particle. In addition adenoviral pVI proteins are processed by protease cleavage enabling escape of viral particles from the endosome (Greber, Webster et al. 1996; Wiethoff, Wodrich et al. 2005). Due to partially disruption, released viral particles are able to interact with the cellular microtubule network, facilitating the transport from the periphery to the nuclear membrane (Suomalainen, Nakano et al. 1999; Wodrich, Henaff et al. 2010). There, particles dock to the nuclear pore complex via interaction of hexon proteins with nuclear pore filament CAN/Nup214 (Trotman, Mosberger et al. 2001; Strunze, Engelke et al. 2011). Subsequently viral particles disassemble releasing the adenoviral genomes associated with proteins pV, pVII and mu into the cell nucleus 1-2 h after initial attachment (Matthews and Russell 1998).

After entering the nucleus, the viral genome attaches to the nuclear matrix via the terminal proteins (Fredman and Engler 1993) and it is stabilized by cellular histones. Subsequently, the adenovirus replication takes place by expression of viral proteins in a temporally coordinated manner. Initially, proteins encoded by the E1 region are transcribed and expressed (Akusjarvi 1993). These proteins modulate the cellular transcription pattern, promote entering into the S phase and prevent induction of apoptosis. Furthermore, E1A induces transcription of all other early regions E2-E4 (Akusjarvi 1993; Flint and Shenk 1997). Respective proteins interfere with pathways for induction of apoptosis and further modulate the transcription profile for optimized virus amplification, prevent from induction of the innate immune response, and enable escape from the cellular immune response. Furthermore, expressed factors facilitate efficient RNA transport as well as correct splicing of the mRNAs (Wold, Doronin et al. 1999). Proteins responsible for the synthesis of viral genomes are mainly encoded by E2 and it was shown that upon replication of the viral genome the major late promoter is activated mediating the transcription of late protein (Ramachandra and Padmanabhan 1995). In detail, a single mRNA of about 30 kb is transcribed containing all late regions L1-L5, which is processed by alternative polyadenylation and splicing into 18 separated mRNAs (Shaw and Ziff 1980). These mRNAs encode for capsid proteins as well as for proteins essential for correct folding, nuclear transport, protein processing and capsid assembly.

Capsid assembly is assumed to take place in several stages. First, hexon trimeres form groups of nine (GONs), which subsequently assemble with hexon trimeres and penton pentameres as well as minor capsid proteins forming an intermediate virus capsid. During maturation the double-strand DNA genome connected to viral core proteins is imported together with viral cysteine-protease, which is essential for final processing steps in capsid formation (Schmid and Hearing 1995; Weber 1995). Newly generated viruses are released by cell death called cytopathic effect, which is caused by accumulation of adenovirus death protein as well as other adenoviral proteins (Tollefson, Scaria et al. 1992).

1.4.4. Fate of adenoviral particles after intravenous injection

Adenoviral vectors based on human adenovirus serotype 5 used for gene therapy are often applied intravenously when tested *in vivo*. After entering the blood stream the adenoviral capsids initially bind to coagulation factor X (FX) (Kalyuzhniy, Di Paolo et al. 2008; Waddington, McVey et al. 2008) or to other vitamin K-dependent serine proteases

(coagulation factor IX and VII) as well as protein C (Fig. 1.6a) (Parker, Waddington et al. 2006). In detail, this interaction occurs between amino acids located within the hypervariable regions of hexon monomers located in a cavity built by hexon trimerization and the γ-carboxylated glutamic acid (Gla) domain of factor X (Fig. 1.6b, c) (Waddington, McVey et al. 2008; Alba, Bradshaw et al. 2009). Heparin binding exosites of virus-associated factor X molecules bind to N- or O-sulfated heparan sulfate proteoglycans (HSPGs) presented on cell surfaces, therefore bridging the viral particle to these cells (Bradshaw, Parker et al. 2010). Due to the fact, that a major portion of the blood passes the liver tissue and liver cells as well as liver-associated macrophages called Kupffer cells present a high number of heparin sulfate proteoglycans on their surface, intravenously applied adenoviral vectors mainly transduce the liver tissue. Nevertheless, recent studies demonstrated, that primary attachment receptor CAR as well as the alternative receptor complement receptor CR1 is present on human erythrocytes (Fig. 1.6a). Therefore, it was suggested, that efficiency of adenovirus-mediated gene transfer via intravenous injection is reduced. Furthermore, adenovirus particles interacting with erythrocytes might be recognized or taken up by immune cells activating or triggering the anti-adenoviral immune response. Unfortunately, murine erythrocytes were shown to be negative for both receptors. Thus, translation of vectors evaluated in mouse experiments to large animals models or humans is challenging (Carlisle, Di et al. 2009).

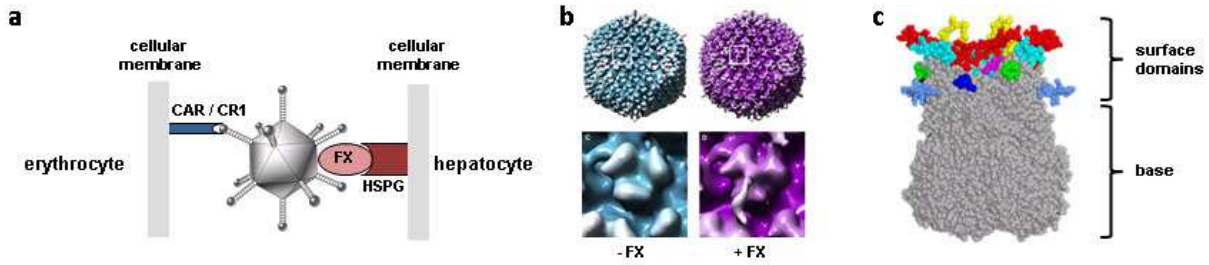

Figure 1.6: Interaction of human adenovirus 5 particles (hAd5) after intravenous injection. (a) hAd5 particles interact with erythrocytes via binding of viral fiber proteins to cosackievirus and adenovirus receptor (CAR) or complement receptor 1 (CR1). Furthermore, coagulation factor X (FX) and other proteins vitamin K dependent serine proteases as well as protein C bind to surface domains of hexon protein. This mediates interaction with heparan sulfate proteoglycans (HSPGs) presented on the surface of hepatocytes and other cells such as Kupffer cells. **(b)** Structural details of FX-binding to surface domains of hexon timers were analyzed by cryoelectron microscopy (modified from Waddington et. al, 2008). **(c)** Hexon trimers can be devided into the base, which is orientated to the virus core and highly conserved, and the surface domains harboring 7 hypervariable region (depicted in colours), which are essential for FX-binding.

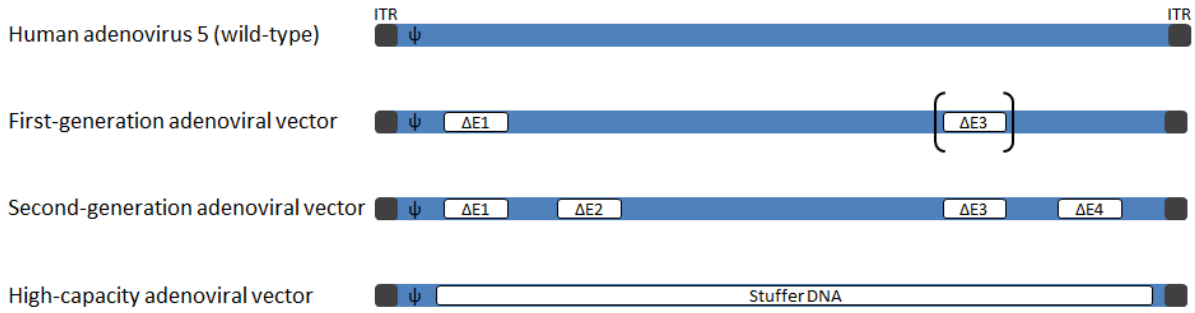

Figure 1.7: Organization of recombinant adenoviral vector genomes. At the top the genome of the human adenovirus 5 is depicted in blue secluded by inverted terminal repeats (ITRs) and with the packaging signal ψ at the 5' end. First-generation adenoviral vectors are depleted for the early region 1 (E1) and fakultatively early region 3 (E3) is also deleted. For second-generation adenoviral vectors additionally early region E2 or E4 is deleted. High-capacity adenoviral vectors are composed of stuffer DNA (28-36 kb) flanked by 5'- and 3'-ends of the wild-type adenoviral genome.

1.5. Adenoviral vectors

Historically, most adenoviral vectors are based on adenovirus serotype 5, although vector systems based on several other serotypes were established in the past. In principle, deletion of certain regions in the adenoviral genome guaranties complete inhibition of viral replication in native cells and provides the space for incorporation of the therapeutic DNA. Amplification of adenoviral vectors containing modified genomes is feasible by providing missing adenoviral components *in trans* (Benihoud, Yeh et al. 1999; Zhang 1999).

1.5.1. First-generation adenoviral vectors (FG-AdVs)

FG-AdVs are based on the deletion of the early region 1 (E1), which encodes factors essential for initiation of adenovirus replication (Fig. 1.7) (Akusjarvi 1993). Therefore cells could be infected efficiently resulting in efficient transport of the vector genome but initiation of virus replication is inhibited. Depletion of the E1 region enables incorporation of a cargo sequence of up to 4.5 kb (McGrory, Bautista et al. 1988). For amplification of these vectors, cell lines were generated providing E1 proteins or homologs *in trans*. The most commonly used cell line is the human embryonic kidney HEK293 cell line containing a fragment of the wild-type human adenovirus 5 genome including the E1 region (Benihoud, Yeh et al. 1999; Zhang 1999). However, during amplification spontanous homologous recombination could occur between a FG-AdV genome and the cell-encoded genome fragment resulting in replication competent adenoviruses (RCAs) (Hehir, Armentano et al. 1996). To avoid this effect the cell line PERC.6 was generated, which is based on human embryonic retinoblasts. These cells

contain an expression cassette for the adenovirus E1 region under control of the ubiquitous phosphoglycokinase (PGK) promoter sharing no homologies with the adenoviral vector genomes (Fallaux, Bout et al. 1998). FG-AdVs were further development by partial or complete deletion of the E3 region allowing incorporation of larger cargo sequences (up to 8 kb) and offering the option for incorporation of two separated sequences in the E1 and the E3 region, which are transcribed independent from each other (Bett, Haddara et al. 1994). Proteins encoded by the E3 region mainly inhibit immunological pathways (Wold, Tollefson et al. 1995). Therefore the effect of the E3 deletion on virus replication is low during amplification in cell culture (Wold, Doronin et al. 1999). Although viral transcription activation of other early proteins and late proteins encoded by the vector genome is not activated due to the lack of E1 encoded proteins, viral proteins are expressed at low levels due to partial complementation by cellular factors (Yang, Nunes et al. 1994). Some of the expressed viral proteins were shown to be toxic and furthermore, expressed viral proteins are processed and presented as antigen. Therefore transduction with adenoviral vectors cause cell death in a dose-dependent manner and *in vivo* applications of FG-AdVs cause a strong and robust cytotoxic T-cell response (Yang, Nunes et al. 1994).

1.5.2. Second-generation adenoviral vectors

FG-AdVs were further developed by deletion of E2 or E4 region (Fig. 1.7) (Engelhardt, Litzky et al. 1994; Lusky, Christ et al. 1998; Schaack 2005). Proteins encoded by these regions are essential for replication in cell culture. Therefore, they are provided *in trans* by respective producer cell lines based on HEK293 cells. These adenoviral vectors are classified as second generation adenoviral vectors, which provide additional space for larger cargo sequences (10.5 kb) and up to four independent expression cassettes. Moreover, deletions of additional early gene regions prevent generation of replication-competent adenoviruses during amplification. Nevertheless, trans-complementation during amplification of these vectors could be less efficient due to the fact that some E2- and E4-encoded proteins are toxic. Despite utilization of inducible expression systems the vector replication rate might be decreased during amplification reducing significantly vector yields as well as vector titers (Krougliak and Graham 1995; Lusky, Christ et al. 1998). Additionally, reduction in transgene expression indicated leaky expression of viral proteins. Therefore, vector-related toxicity and immunogenicity are still major obstacles for usage of these vectors (Fang, Wang et al. 1996).

1.5.3. High-capacity adenoviral vectors (HCAs)

As a logical consequence third generation adenoviral vectors called high-capacity adenoviral vectors (HCAs) were created containing an artificial vector genome deleted of all viral sequences except for the ITRs and the packaging signal (Fig. 1.7) (Parks, Chen et al. 1996). In contrast to first- and second-generation adenoviral vectors, viral proteins are not provided *in trans* by producer cells but instead a adenoviral helper-virus (HV) is used for vector amplification. For this reason high-capacity adenoviral vectors were also called helper-dependent, gutless or gutted adenoviral vectors in the literature (Fisher, Choi et al. 1996; Hardy, Kitamura et al. 1997; Hartigan-O'Connor, Amalfitano et al. 1999). The helper-virus is a first-generation adenoviral vector with a packaging signal flanked by loxP-sites. For production modified HEK293 cells are used, which constitutively express high levels of Cre recombinase. During amplification the producer cell is transduced with a HV and the HCA genome (Fig. 1.8). Transcription of the HV genome provides viral proteins and enables assembly of viral capsids, but packaging of the HV genome is prevented due to excision of the packaging signal by Cre-mediated recombination of the loxP-sites. Therefore, only HCA vector genomes are packaged. Alternative production systems are based on other recombinases like the Flp recombinase from Saccharomyces cerevisiae (Ng, Beauchamp et al. 2001) or the bacteriophage-derived phiC31 integrase (Alba, Hearing et al. 2007).

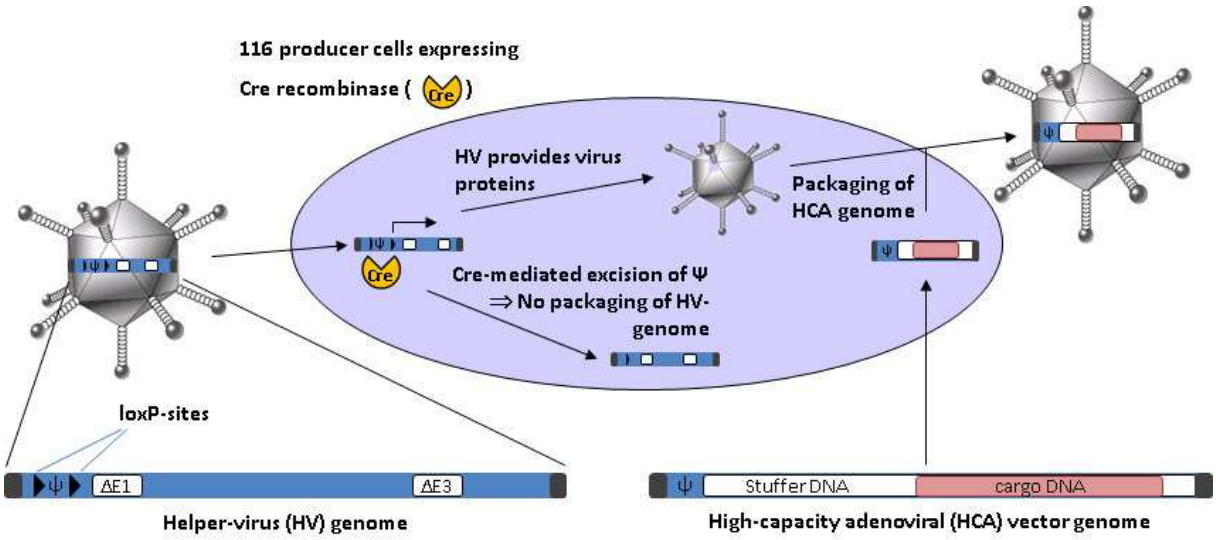

Figure 1.8: Schematic overview for production of high-capacity adenoviral vectors. For production of high-capacity adenoviral vectors 116 producer cells expressing the Cre recombinase (Cre) are co-transduced with a helper-virus and the high-capacity adenoviral (HCA) vector genome. Transcription of the helper-virus genomes allows production of virus proteins, but packaging the helper-virus genome is inhibited due to Cre-mediated excision of the packaging signal ψ, which is flanked by loxP-sites. Therefore, only HCA genomes are packaged resulting in the formation of high-capacity adenoviral vectors.

HCAs enable transport of cargo sequences of up to 36 kb and for this reason large transgenes or multiple expression cassette as well as endogenous regulatory sequences or complex expression system such as inducible systems can be used (Kochanek, Clemens et al. 1996; Kawano, Ishizaki et al. 2008; Puntel, Muhammad et al. 2010). Importantly, deletion of all viral coding sequences results in decrease of vector-associated acute toxicity, which was only detected for high doses of HCAs (Morral, Parks et al. 1998). Moreover, the adaptive immune response is significantly reduced such as formation of anti-adenoviral neutralizing antibodies interfering with efficient transduction (Chen, Mack et al. 1997; Muruve, Cotter et al. 2004). In addition, separation of capsid-encoding sequences and packaged sequences containing the therapeutic DNA increases the flexibility of the system, although generation of HCAs is also more complex. Nevertheless, HCA production remains a sophisticated method and Cre-mediated excision of the helper-virus packaging signal is not complete resulting in contaminations of high-capacity adenoviral vector preparations with 0.1-1% HV (Palmer and Ng 2003). Furthermore, generation of replication competent adenovirus due to homologous recombination of HV genomes with E1 region encoded by the producer cells can not be excluded (Hehir, Armentano et al. 1996).

1.5.4. Vector preparation

In general, preparations of all generations of adenoviral vectors are similar except for the construction of the vector genome used for vector production. For initial generation of the first and second generation adenoviral vectors, human embryonic kidney 293 cells are transfected with the respective linearized vector genome. After cytopathic effect was observed due to formation of adenoviral vector particles, cells are harvested. Viral particles are released by consecutive freezing and thawing steps and virus lysate is used for the next amplification round. This procedure is repeated with increasing numbers of cells and final amplification is performed utilizing approximately 4 x 10^8 HEK293 cells (Luo, Deng et al. 2007). HCAs are produced using a similar methodology, but instead utilizing the Cre-expressing HEK293-based cell line 116 and co-infection with HVs. Newest protocols for large-scale amplification of HCAs use 116 cells growing in suspension utilizing bioreactors (Palmer and Ng 2003).

For adenoviral vector purification cell lysates are harvested, vector particles released from the cells and separated from cellular debris as well as from unpackaged adenoviral particles by ultracentrifugation utilizing a CsCl step gradient and successively a CsCl continuous gradient

(Kanegae, Makimura et al. 1994). Isolated particles are stored in physiological buffer by dialysis and finally the physical titer of the vector preparation is determined by optical density measurement for the vector DNA. For detection of the infectious titer DNA is isolated from HEK293 cells 2h post infection and vector genome copies are determined by real-time PCR (Ma, Bluyssen et al. 2001).

For incorporation of a cargo sequence into the vector genome or for modification of a capsid protein three cloning methods are currently used (Fig. 1.9). These are based on homologous recombination in HEK293 cells (McGrory, Bautista et al. 1988) or E.coli strain BJ5183 (Chartier, Degryse et al. 1996) or based on rare restriction enzymes and in vitro ligation of fragments (Mizuguchi and Kay 1998). Homologous recombination in HEK293 cell is mainly used for incorporation of a transgene into the E1-region of a first generation adenoviral vector genome. Therefore, cells are transfected with a genome fragment lacking the 5'end and a plasmid containing the 5'ITR, the packaging signal, the transgene expression cassette and more than 1000 bp sequence homologous to the 5' end of the genome fragment (Berkner and Sharp 1983). Homologous recombination is mediated by cellular proteins resulting in formation of the final vector genome. This method was also used for modification of the fiber gene located at the 3'end of the FG-AdV genome containing a reporter gene in the E1 region. For several cloning methods commercial kit are available.

In contrast, cloning with rare restriction enzymes is based on generation of the final vector genome prior to transfection into HEK293 cells. In detail, a plasmid is generated containing the transgene or the modified genome region flanked by recognition site for a rare restriction enzyme. Furthermore, the vector genome encoded by a plasmid is modified by flanking the region, which should be replaced, with identical restriction enzyme recognition sites. For generation of the final vector genome fragments of these two plasmids generated by respective restriction digests are ligated and subsequently transformed in E.coli for amplification. Due to the binding sites of the restriction enzymes, this method is not traceless, which is essential for precise modifications of capsid proteins. For these modulations homologous recombination in E.coli strain BJ5183 is the method of choice. Similar to the ligation based method intermediate clones have to be constructed, containing the modification flanked by at least 200 bp of homologous sequences at each side. Furthermore, a plasmid encoding the adenoviral vector genome with a binding site for a rare restriction enzyme in the region of interest has to be generated. For construction the linearized genome and the modified sequence are recombined in recombinase-expressing BJ5183 E.coli bacteria.

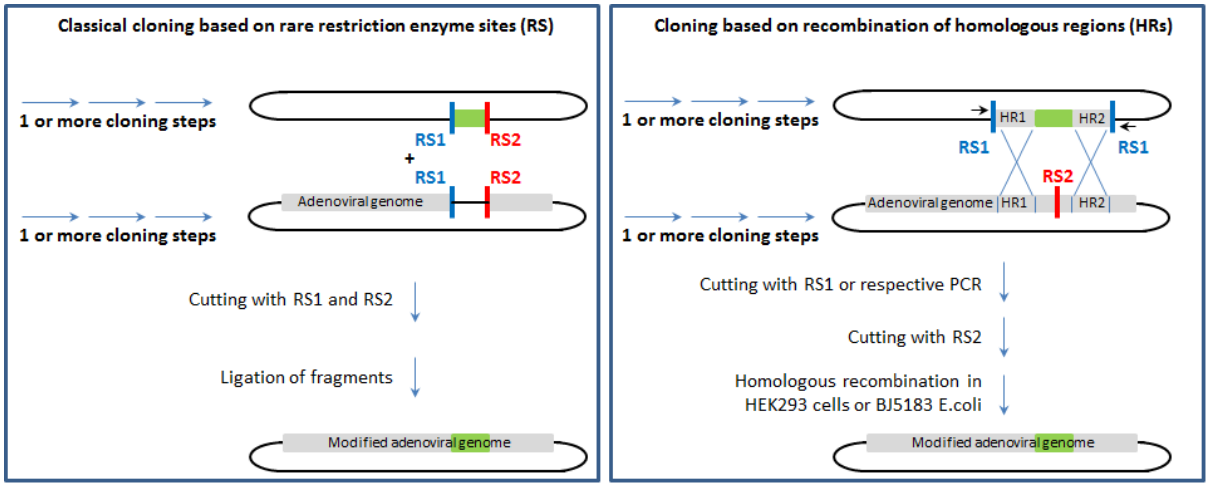

Figure 1.9: Current cloning strategies for manipulation of adenoviral genomes. For generation of modified adenoviral genomes using the classical cloning strategy based on rare restriction enzymes (left) a plasmid containing the modified sequence flanked by restriction enzyme binding sites (RS1 and RS2) is generated by several cloning steps. In addition, a plasmid is created containing the adenoviral genome with identical restrictions enzyme binding sites in the target region, which should be modified. Both plasmids are cutted with the respective restriction endonucleases and fragments are ligated resulting in a plasmid containing the modified adenoviral genome. For cloning based on homologous recombination (right) a plasmid containing the modification flanked by homologous regions and a plasmid with a restriction enzyme binding site (RS2) within the target region have to be created. For generation of the plasmid containing the modified adenovirus genome, the modified genome region is amplified by PCR (black arrows) or excised by a restriction endonuclease (RS1). In parallel, the plasmid with the adenovirus is cutted with RS2. Subsequently sequences are combined by homologous recombination of HR1- and HR2-regions in human embryonic kidney 293 cells (HEK293) or bacteria of the Escherichia coli (E.coli) strain BJ5183.

In summary the last two methods enable targeting of any genome region, but intermediate clones have to be constructed newly for every region. In addition, generation of intermediate vector genomes with binding sites for rare restriction enzymes is highly challenging (Youil, Toner et al. 2002). It is of note, that most modulations were tested with FG-AdVs. However, for adoption to second or third generation adenoviral vectors, cloning steps had to be repeated and construction might be hampered by differences in the vector genome with respect to binding sites of restriction enzymes (Khare, May et al. 2011). Therefore, established capsid-modifications are rare for these vectors, whereas for incorporation of cargo sequences into second generation adenoviral vectors or high-capacity adenoviral vector genomes cloning strategies are established, which are often based on rare restriction enzymes (Ehrhardt and Kay 2002; Shi, Graham et al. 2006). These could be adopted easily for new approaches, although alteration of the respective genome is restricted to a single site and often limited in size.

1.5.5. Optimization of adenoviral vectors by capsid modifications and hybrid vector systems

To optimize adenoviral vector properties virus capsid can be modified for retargeting of the vector or to escape from the immune response (Smith, Mehaffey et al. 1993; Yei, Mittereder et al. 1994). For example adenoviral vectors could be modified chemically by components bound to capsid components (Kreppel and Kochanek 2008; Wortmann, Vohringer et al. 2008). This enables shielding from recognition by components of the immune system as well as partial or complete detargeting from the liver tissue. However, often transduction efficiency of these vectors is severely affected. Another option to modulate vector features is to use other human or non-human adenoviruses for gene transfer. In general, these serotypes have a lower seroprevalences and enable more efficient transduction of certain cell types for defined applications. However, respective vectors are rarely used and little is known about the fate of these serotypes after application in cell culture and in vivo and moreover, construction of respective vector genomes is challenging (Seshidhar Reddy, Ganesh et al. 2003; Keriel, Rene et al. 2006). For these reasons studies are mainly concentrating on capsid manipulations precisely altering specific capsid proteins or protein domains of a vector based on hAd5, which has been extensively investigated in the past. In detail, for detargeting of an adenoviral vector from the liver, interaction of hexon proteins with coagulation factor X can be prevented by alteration of the hypervariable regions of the hexons. Therefore, either point mutations can be introduced or hypervariable regions can be precisely exchanged with respective sequences of other adenovirus serotypes (Roberts, Nanda et al. 2006; Waddington, McVey et al. 2008; Alba, Bradshaw et al. 2009). Moreover, modulations of the fiber by exchanging of the knob domain with other adenovirus serotypes or by introduction of peptide ligands can significantly increase transduction efficiency for various cell types (Henning, Andersson et al. 2005; Wang, Shayakhmetov et al. 2005; Terashima, Oka et al. 2009). In addition, fiber modifications can lead to retargeting *in vivo* from the liver to other organs or tissues, but efficiencies of these approaches are usually low. Similar effects were shown for several capsid-modified vectors based on pIX fusion proteins or with altered RGD loops of the penton protein (Wickham, Carrion et al. 1995; Poulin, Lanthier et al. 2010). For the escape from neutralizing anti-adenovirus antibodies, modulations of the hypervariable regions of the hexon proteins have shown high efficacy (Sumida, Truitt et al. 2005; Pichla-Gollon, Drinker et al. 2007), whereas fiber modifications have rather small effects and pIX or penton modifications have no significant influence on the humoral immune response.

Another set of options for improvements is provided by the high capacity of the HCA genome. This allows transport of additional foreign DNA, which could improve vector features or add new vector properties. For example expression of a toxic transgene product could be realized by combination with an inducible expression system, for instance the Tet-systems for doxycycline-based induction (Puntel, Muhammad et al. 2010). Furthermore, combinations with systems for somatic integration such as the Sleeping Beauty transposase enable incorporation of a transgene expression cassette into the cellular genome resulting in long-term expression in dividing cells (Yant, Ehrhardt et al. 2002). Additionally, genes with supporting effects for virus replication could be incorporated into the vector genome. For instance it was shown, that the miRNA suppressor protein p19 significantly improves vector production due to increase of viral protein expression (Rauschhuber, C. T., Muck-Hausl, M.H. et al., manuscript in preparation).

Most of these vector modifications either affecting capsid structure or gene expression were evaluated individually and in context of first generation adenovirus vector. This is mostly due to challenges regarding cloning procedures of respective genomes. In principle, capsid modifications affecting different capsid proteins and systems modulating transgene expression profiles could be combined in a single vector unifying new vector features. Nevertheless, the latter approaches are strongly hampered by limitations of currently available cloning methods. Therefore the number of available vectors containing multiple modifications is very low.

1.6. Aim of this study

High-capacity adenoviral vectors provide high capacity for cargo sequences, high stability and high titer yields, low cell toxicity after administration as well as no relation to cancer or other severe malignancies in humans. Therefore, they are attractive tools for gene and cell therapy as well as for vaccination purposes and basic research. Nevertheless, usage of HCAs is restricted due to labor-intensive production procedures, limited persistence of episomal genomes in replicating cells, low transduction efficiency of certain cell types, strong liver-tropism after intravenous application and induction of a robust adaptive immune response after first in vivo administration. Although previous preclinical and clinical studies based on cellular transduction with first-generation adenoviral vectors and HCAs showed some success, major limitations for this type of vector need to be overcome. In this study a system should be established allowing transfer of information obtained from first-generation

adenoviral vectors to high-capacity adenoviral vectors as well as optimization of HCA features should be achieved. This should significantly improve HCA vector performance in current applications and it should pave a new path towards new application fields for this type of vector.
To realize this aim, I worked on following projects:

1. A standardized protocol for large-scale production of high-capacity adenoviral vectors should be established containing a trouble-shooting guide. This represents a prerequisite to establish this method in other laboratories. Furthermore, an established protocol is necessary for adoption of modifications to components required for generation of HCAs as exemplified by capsid-modified helper-viruses in this thesis.

2. The established hybrid vector system combining high-capacity adenoviral vectors for efficient delivery and the Sleeping Beauty transposase for sustained transgene expression should be improved by utilization of hyperactive sleeping beauty variant HSB5. The improved system has to be tested in mice for functionality and it should be evaluated for therapeutic efficiency in the context of a large animal model for a monogenetic disease.

3. Fast and smooth modulations of adenoviral vector genomes should be enabled utilizing an alternative cloning technology based on bacterial artificial chromosomes and manipulation by homologous recombination. This technique should be evaluated for capsid-modifications of helper-viruses. Furthermore, an advanced cloning technique for generation of complex high-capacity adenoviral vector genomes should be established.

4. Modification of surface domains of major capsid protein hexon should be generated by serotype switch and evaluated with respect to early capsid assembly steps. Promising candidates should be incorporated into the helper-virus genome and the respective virus reconstituted. Generated hexon-modified helper-viruses should be evaluated in cell culture and also biodistribution after intravenous administration in mice should be determined.

PROTOCOL

A rapid protocol for construction and production of high-capacity adenoviral vectors

Lorenz Jager[1,4], Martin A Hausl[1,4], Christina Rauschhuber[1,4], Nicola M Wolf[1], Mark A Kay[2,3] & Anja Ehrhardt[1]

[1]Department of Virology, Max von Pettenkofer-Institute, Ludwig-Maximilians University Munich, 80336 Munich, Germany. [2]Department of Pediatrics, [3]Department of Genetics, School of Medicine, Stanford University, 269 Campus Drive, CCSR Building, Room 2105, Stanford, CA 94305-5164, USA. [4]These authors contributed equally to this work. Correspondence should be addressed to A.E. (ehrhardt@mvp.uni-muenchen.de).

Published online 2 April 2009; doi:10.1038/nprot.2009.4

High-capacity adenoviral vectors (HC-AdVs) lacking all viral coding sequences were shown to result in long-term transgene expression and phenotypic correction in small and large animal models. It has been established that HC-AdVs show significantly reduced toxicity profiles compared with early-generation adenoviral vectors. Furthermore, with capsid-modified HC-AdV becoming available, we are just starting to understand the full potential of this vector system. However, for many researchers, the wide-scale use of HC-AdV is hampered by labor-intensive and complex production procedures. Herein, we provide a feasible and detailed protocol for efficient generation of HC-AdV. We introduce an efficient cloning strategy for the generation of recombinant HC-AdV vector genomes. Infection and amplification of the HC-AdV are performed in a spinner culture system. For purification, we routinely apply cesium chloride gradients. Finally, we describe various methods for establishing vector titers. Generation of high-titer HC-AdV can be achieved in 3 weeks.

INTRODUCTION

Adenoviral vectors

Adenoviral vectors are widely used for gene transfer into a broad variety of cell types. To date, the majority of adenovirus-based gene transfer studies in basic research and gene therapy are predicated on first- or second-generation recombinant adenoviral vectors lacking the early adenoviral gene E1 and/or E3, respectively. These vector types are easy to produce, and commercial kits are available for recombinant adenoviruses derived from the human adenovirus serotype 5 (see ref. 1). However, in transduced cells *de novo* adenoviral protein synthesis of early and late adenoviral genes still contained in the vector genome remains problematic. A major drawback of early-generation vectors are the cytotoxic effects induced in the target cell due to the production of toxic viral proteins. In addition, these proteins can result in an antigen-dependent immune response as a result of their association with the major histocompatibility complex class I on the cell surface[2].

For many research applications, adenovirus is simply used as a transfer vehicle for the introduction of foreign DNA into a target cell. To study cellular effects of introduced foreign DNA sequences, it is important to keep undesired side effects at a minimum. Owing to toxic effects of expressed adenoviral proteins, production of HC-AdV devoid of all viral coding sequences is of great interest to the research community.

High-capacity adenoviral vectors for gene delivery

Alternative terms for the HC-AdVs include 'gutless', 'gutted', 'fully-deleted' or 'helper-dependent' adenoviral vectors[3–6]. For this type of vector, the only adenoviral sequences required for genome packaging are noncoding sequences: the inverted terminal repeats (ITRs) at both ends and the packaging signal at the 5′-end. The deletion of viral sequences allows gene transfer of up to 36 kb of foreign DNA. Besides the transgene expression cassette, this viral genome may contain stuffer DNA for stabilization. This stuffer DNA may enhance transcriptional levels of transgenes or it may optimize packaging efficiencies.

Adenovirus is able to transduce a wide variety of different cell types and organs depending on the serotype used [7–10]. At this time, there are 51 known human adenoviral serotypes characterized by a respiratory, intestinal, renal, ocular or intestinal tropism dependent on the subgroup[7]. On the basis of this feature, HC-AdVs were used for therapeutic applications for monogenetic diseases, such as Duchenne muscular dystrophy[11–13], hemophilia A[14–16], glycogen storage disease type Ia (see ref. 17), hypoalphalipoproteinemia[18], hyperbilirubinemia[19], ornithine transcarbamylase deficiency[20], familial hypercholesterolemia[21], hemophilia B[22–24] as well as acquired diseases such as oxygen-induced retinopathy[25] and multiple sclerosis[26]. For these therapeutic applications, insertion of therapeutic transgenes into the HC-AdV genome and administration of these viral vectors was shown to result in long-term transgene expression and phenotypic correction in mice[11,13,16–18,20,21,24,26], rats[19,25], dogs[14,15,22,23] and nonhuman primates[27] without chronic toxicity.

Although long-term transgene expression after adenoviral gene transfer was observed in quiescent cells, vector genome copy numbers and transgene expression decrease in rapidly dividing cells[28]. This phenomenon is a result of the predominantly episomal state of recombinant adenoviral vector genomes. To maintain the transgene expression cassette contained in the adenovirus, genetic elements for persistent transgene expression were introduced into the adenoviral vector.

For somatic integration of the transgene from the adenoviral vector genome into the host genome adenovirus/retrovirus[29], adenovirus/foamy virus[30], adenovirus/Sleeping Beauty transposase[31], adenovirus/phiC31 integrase[32] and adenovirus/adeno-associated virus hybrid vectors[33,34] were created (reviewed in ref. 28). Furthermore, adenovirus was used in concert with components of the episomally maintained Epstein–Barr virus episome[35,36] or for homologous recombination and subsequent somatic integration[37,38].

In addition to *in vivo* applications, HC-AdVs were used to transduce a broad variety of cell types in culture, including neurons[39] and embryonic stem cells[37]. Additionally, capsid-modified HC-AdVs

PROTOCOL

with the adenovirus serotype 35 fiber were used to transduce cells resistant to many transfection reagents, such as human hematopoietic stem cells[40] and other hematopoietic cell lines[41].

Limitations and potential of high-capacity adenoviral vectors

Although HC-AdV lacks all viral-coding sequences, there are still limitations that need to be overcome. These include toxicity and/or immunogenicity due to the viral capsid particles themselves, and/or an immune response directed against the transgene product itself. Furthermore, the synthetic viral genome may be recognized by components of the innate immune response, such as Toll-like receptors. There is evidence that adenoviral vectors trigger the innate immune response through Toll-like receptor-dependent pathways[42,43]. Moreover, there may be a risk of low-level random integration of recombinant adenoviral vector genomes that may lead to insertional mutagenesis.

To reduce acute toxicity due to the incoming capsid particles themselves, different application methods were tested. It was shown that delivery to the cerebrospinal fluid targeting the brain[26], pseudo-hydrodynamic delivery targeting the liver[27], intramuscular injection to target muscle cells[13] and aerosol delivery using an intratracheal catheter targeting lung epithelial cells[44] make adenoviral vectors less toxic. Moreover, these approaches enabled or enhanced transduction efficiency and specificity to the respective targeted organs, and furthermore, it was shown that coating of the adenoviral capsid with polyethylene glycol makes this type of vector less immunogenic[45].

In addition, novel methodologies for cloning and manipulating adenoviral genomes derived from virtually any serotype are now available. On the basis of bacterial artificial chromosomes containing the adenoviral vector genome and methods for precise genetic manipulation, any gene can be deleted or inserted[46]. Importantly, capsid-modified vectors based on alternative adenoviral serotypes, for which the prevalence in the human population is rather low, may lower the immune response. Moreover, serotype switching will provide a broader tropism, and repetitive *in vivo* administration may be feasible.

In total, due to the broad natural tropism of adenovirus, the high potential of chimeric capsids, the possibility to generate hybrid vectors and the different application methods make this vector system very attractive for basic research, biotechnology and gene therapy.

Systems for production of high-capacity adenoviral vectors

The first system for the production of HC-AdV was described in 1996 by Parks *et al.*[6]. All protocols available at present are still based on this principle. During the production of HC-AdVs, an adenoviral helper virus lacking the early adenoviral genes E1 and E3 provides all adenoviral gene products needed for amplification, generation of viral particles and packaging in *trans*. To minimize unwanted packaging of helper virus genomes, the helper virus contains a packaging signal, which was flanked by loxP sites. During production in an adenoviral producer cell line stably expressing Cre recombinase, loxP sites are recognized and the packaging signal is excised. This leads to unpackagable helper virus genomes and HC-AdV genomes being efficiently packaged. Similar to systems based on Cre/loxP recombination, alternative amplification methodologies were based on Flp recombinase-mediated excision of the packing signal. Flp recombinase systems are available for adherent cells[47,48] and suspension cultures[49]. Furthermore, other HC-AdV systems using helper viruses based on E1/E2a-deleted[50] and E1/E2a/E3-deleted[51] adenoviral vectors were established.

Many researchers are restricted to using first- or second-generation adenoviral vectors because of the complex and sophisticated production procedure of HC-AdVs. Earlier protocols for HC-AdV production required several preamplification steps. Large-scale amplification was usually performed in many tissue-culture plates (up to sixty 150-mm dishes per HC-AdV preparation) using adherent human embryonic kidney cells[23,24,52,53].

Production and amplification of high-capacity adenoviral vectors in a producer cell line grown in suspension

To date, there are only very few laboratories, including ours, using producer cells grown in suspension for production of HC-AdV[29,54,55]. The procedure for HC-AdV production is summarized in a schematic diagram in **Figure 1**.

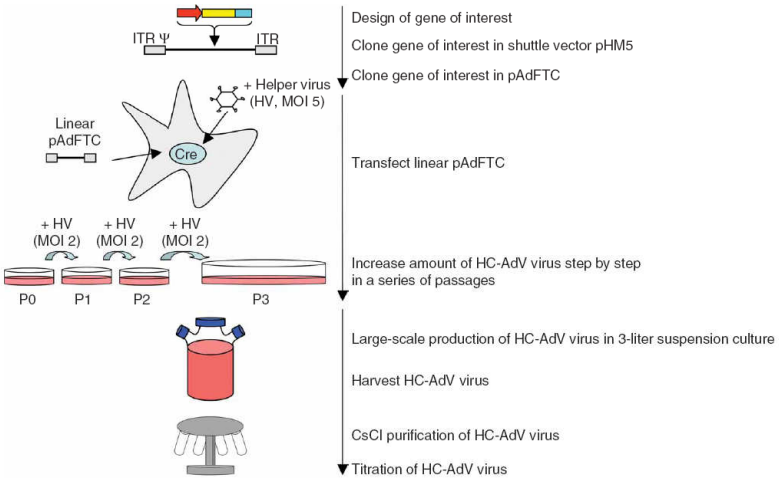

Figure 1 | Schematic diagram for high-capacity adenoviral vector (HC-AdV) production. The flowchart shows on the top the transgene expression cassette, which is inserted into the shuttle vector pHM5 (ref. 59). The red arrow represents the promoter, the yellow bar represents the gene of interest and the blue bar represents the polyadenylation signal. After cloning the complete transgene expression cassette into the HC-AdV production plasmid pAdFTC (see ref. 24) (both orientations work), the linearized construct is transfected into the cells of the HC-AdV producer cell line (116 cells (see ref. 55)), which is subsequently infected with the helper virus AdNG163R-2 (ref. 55). After three serial preamplification steps, large-scale production is performed in a 3-liter suspension culture. For purification, virus is isolated by cesium chloride gradients using ultracentrifugation. HC-AdV, high-capacity adenoviral vector; ITR, adenovirus serotype 5 inverted terminal repeat; Ψ, packaging signal; HV, helper virus; MOI, multiplicity of infection.

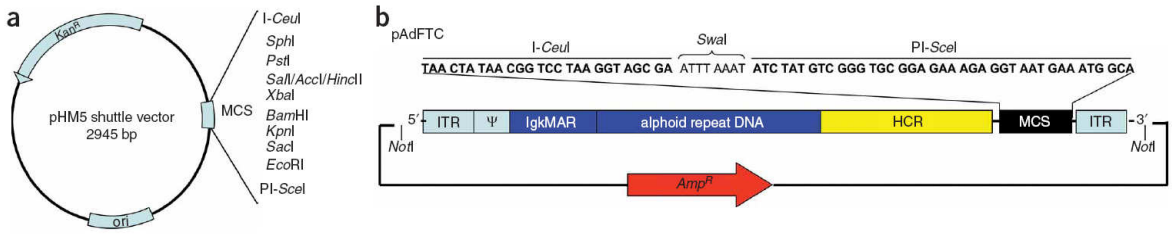

Figure 2 | Schematic maps of pHM5 and pAdFTC. (**a**) pHM5 shuttle vector[59]. All unique cloning sites are indicated. This plasmid is derived from the cloning vector pUC18 (ref. 62) and contains a kanamycin-resistance gene. Construction of pHM5 was described earlier[59]. (**b**) pAdFTC (see ref. 24) is ~31 kb in size. This plasmid contains the human adenovirus serotype 5 inverted terminal repeats (5′- and 3′-ITR), a packaging signal (Ψ), the matrix attachment region of the murine immunoglobulin κ locus (IgkMAR), alphoid repeat DNA sequences from human chromosome 17 and a liver-specific enhancer (hepatic control region, HCR). The MCS includes unique recognition sites for I-*Ceu*I, *Swa*I and PI-*Sce*I. The recognition sequences of these enzymes are indicated. The *Not*I sites are used for release of the linear HC-AdV construct (22 kb in size without insert) from the plasmid backbone (9 kb in size). pAdFTC is based on pDYAL and bears an ampicillin-resistance gene. Further information on pDYAL is provided in a previous publication[68].

In this protocol, the procedure starts with the cloning of HC-AdV production plasmid. Virus is amplified by three subsequent passaging steps and finally amplified using 3-liter suspension culture of 116 cells. HC-AdV particles are released from cells, purified by cesium chloride gradients and subsequently dialyzed. Finally, the number of viral particles is determined by measuring the absorbance at 260 nm. The number of transducing units per ml is determined by infection of adherent cells and subsequent determination of HC-AdV genomes by either quantitative real-time PCR (qPCR) or Southern blot analyses.

Cloning of high-capacity adenoviral vector production plasmids

Various HC-AdV systems for cloning of HC-AdV production plasmids are available. For efficient packaging, the total size of the DNA sequence between the 5′- and 3′-ITR, and the ITRs themselves need to exceed 27.7 kb. HC-AdVs contain optimized stuffer DNA sequences[53] or DNA of the transgene expression cassette exclusively (if the transgene expression cassette is larger than 27 kb). Alternative cloning strategies are also based on rare restriction enzymes[56,57] or homologous recombination using backbone vectors with different mammalian centromeric DNA fragments[58]. For all systems, the HC-AdV production plasmid is linearized by restriction enzyme digest and transfected into the producer cell line. Herein, we describe a simplified and efficient cloning procedure based on rare restriction enzymes for inserting the transgene expression cassette into the HC-AdV genome. The cloning strategy uses the shuttle plasmid pHM5[24,59] and the HC-AdV production plasmid pAdFTC (see ref. 24).

The shuttle plasmid pHM5 was described earlier[59] and contains a multiple cloning site (MCS) flanked by the rare restriction enzyme sites I-*Ceu*I and PI-*Sce*I and a kanamycin resistance gene. A kanamycin resistance may be advantageous for counter selection when cloning into the ampicillin-resistant HC-AdV production plasmid pAdFTC. Alternatively, any other shuttle vector in which the complete transgene expression cassette is flanked by the restriction enzyme sites I-*Ceu*I and PI-*Sce*I can be used. The cloning procedure starts with inserting the complete transgene expression cassette including promoter and polyadenylation signal into the MCS of the shuttle vector pHM5. This step is followed by releasing the transgene from the shuttle vector pHM5 by restriction enzyme digest with I-*Ceu*I and PI-*Sce*I. This DNA fragment is then ligated by the same restriction enzymes into the plasmid pAdFTC. The plasmid pAdFTC contains stuffer DNA derived from a centromere region on human chromosome 17 and a matrix attachment region from the murine immunglobuline κ locus, and the rare restriction enzyme sites I-*Ceu*I and PI-*Sce*I. One may insert up to 12 kb, but not less than 5 kb of foreign DNA into the MCS of pAdFTC. Larger insertions will exceed the optimal range for efficient packaging (maximum packaging capacity: 37.6 kb). Also, smaller insertions resulting in viral genomes less than 27.7 kb may lead to inefficient virus assembly[60,61]. To package larger foreign DNA sequences, one needs to remove stuffer DNA. For smaller inserts, stuffer DNA needs to be added. Each orientation of the insert in pAdFTC is possible. Plasmid maps and the cloning strategy of the present system are depicted in **Figures 2** and **3**.

MATERIALS

REAGENTS

- Albumin fraction V (Roth, cat. no. 8076.2)
- Calf intestinal alkaline phosphatase (CIP) (New England Biolabs, cat. no. M0290)
- Alpha-P32-dCTP (Hartmann Analytic, cat. no. SRP105) **! CAUTION** Radioactive material. When dealing with radioactive materials, appropriate safety precautions and national regulations must be followed.
- Bomix (Bode Chemie Hamburg, cat. no. 973573) **! CAUTION** Corrosive.
- Cesium chloride, CsCl (Invitrogen, cat. no. 8627.2)
- E-Toxa clean (Sigma-Aldrich, cat. no. E9029)
- I-*Ceu*I (New England Biolabs, cat. no. R0694)
- *Hind*III (New England Biolabs, cat. no. R0103)
- *Not*I (New England Biolabs, cat. no. R0189)
- PI-*Sce*I (New England Biolabs, cat. no. R0696)
- *Swa*I (New England Biolabs, cat. no. R0604)
- T4 DNA ligase (New England Biolabs, cat. no. M0202)
- RNase A, 100 mg ml^{-1}; 17,500 U (Qiagen, cat. no. 19101)
- UltraPure phenol:chloroform:isoamyl alcohol (24:24:1 vol/vol) (Invitrogen, cat. no. 15593-031) **! CAUTION** Organic solvent; work under a fume hood, use eye protection and a lab coat when using substances with chloroform. Chloroform can perforate latex gloves, therefore consider double-gloving or nitril gloves for safety.
- Ethanol (EtOH; >99.8%) (Roth, cat. no. 5054.2)
- Trypan blue (Roth, cat. no. CN76.1)
- DH10B electroporation competent cells (Invitrogen, cat. no. 18290-015)
- Superfect transfection reagent (Qiagen, cat. no. 301305)

PROTOCOL

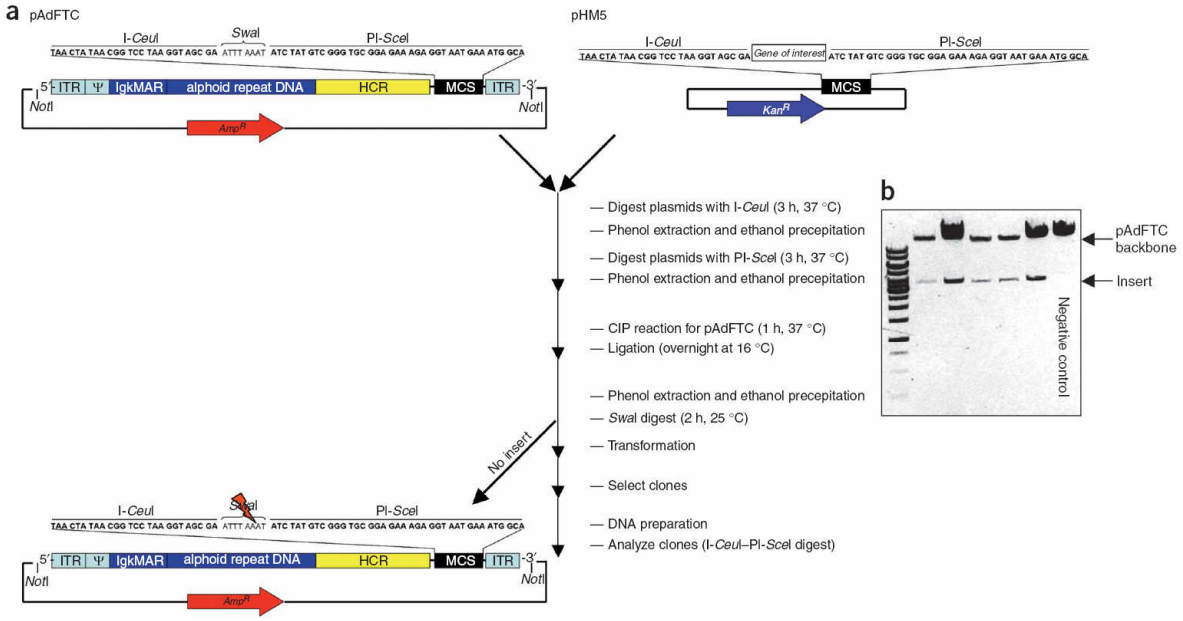

Figure 3 | Flowchart of cloning the transgene expression cassette into pAdFTC. (**a**) Step-by-step cloning procedure. For a detailed description of the single working steps, refer to Steps 1–13. In brief, digest plasmids pAdFTC and pHM5, containing the complete transgene expression cassette, with the restriction enzyme I-*Ceu*I and purify DNA by phenol–chloroform extraction and ethanol precipitation. After that, digest purified, I-*Ceu*I cutted vectors overnight with the restriction enzyme PI-*Sce*I. The digested pHM5 is loaded on a preparative agarose gel to purify the gene of interest (see also Step 6), whereas the pAdFTC is purified as described in Step 7. Set up ligation with CIP-treated pAdFTC and the transgene expression cassette overnight (see Step 8). The ligation mixture is then purified by phenol–chloroform extraction and ethanol precipitation. The *Swa*I digest of the ligation product (Step 10) is performed to prevent the growth of pAdFTC plasmids without insert. (**b**) Example analysis of clones on a 1% agarose gel. Following this cloning procedure, up to 90% of the clones are positive.

- Hygromycin B, 20 mg ml^{-1}, liquid (PAA, cat. no. P02-015) **! CAUTION** Hazardous to humans and the environment. Wear a labcoat and gloves when handling this harmful agent.
- L-Glutamine, 200 mM, liquid (PAA, cat. no. M11-004)
- Fetal bovine serum (FBS) **▲ CRITICAL** Testing of different FBS batches should be performed for optimal cell growth (e.g., Sigma, cat. no. F9665, batch no. 085K3395)
- Minimal essential medium (MEM) (PAA, cat. no. E15-825)
- EX-CELL 293 serum-free medium for HEK 293 cells (Sigma, cat. no. 14571C-500ML)
- Dulbecco's minimal essential medium (PAA, cat. no. E15-843)
- OPTI-MEM I reduced serum medium (Invitrogen, cat. no. 31985)
- Trypsin-EDTA, 0.05% (wt/vol) (PAA, cat. no. L11-004)
- Trypan blue (Roth, cat. no. CN76.1)
- Dulbecco's phosphate buffer saline (DPBS) (PAA, cat. no. H15-002)
- Producer cell line 116, which is based on the human embryonic kidney cell line 293 stably expressing Cre recombinase[55]. This cell line is obtainable from Philip Ng (Department of Molecular and Human Genetics, Baylor College of Medicine, Houston, Texas, USA)
- Human embryonic kidney cells, 293 cells (American Tissue Culture Collection, ATCC Cell Biology Collection)
- Helper virus AdNG163R-2 (see ref. 55). The helper virus AdNG163R-2 can be obtained from Philip Ng
- Hybond-XL Membrane (GE Healthcare, cat. no. RPN 303S)
- UltraPure glycerol (Invitrogen, cat. no. 15514-029)
- pAdFTC (see ref. 24) (plasmid obtainable from Anja Ehrhardt, Max von Pettenkofer-Institute or Mark A. Kay, Stanford University)
- pHM5 (see refs. 24,59) (plasmid obtainable from Anja Ehrhardt, Max von Pettenkofer-Institute, Mark A. Kay, Stanford University or Hiroyuki Mizuguchi, Division of Biological Chemistry and Biologicals, National Institute of Health Sciences)
- Proteinase K (Qiagen, cat. no. 19133)
- PrimeIt II Random labeling kit (Stratagene, cat. no. 300385)
- Qiaquick nucleotide removal kit (Qiagen, cat. no. 28304)
- TaqMan universal PCR master mix (Applied Biosystems, cat. no. 4304437)
- LightCycler FastStart DNA Master^{plus} SYBR Green I (Roche, cat. no. 03515885001)
- Taq DNA Polymersae (New England Biolabs, cat. no. M0320)

EQUIPMENT

- 250-ml storage bottle, sterile (Corning, cat. no. CORN430281)
- 500-ml centrifuge tubes, sterile (Corning, cat. no. CORN431123)
- Tissue culture dishes, 60-mm and 150-mm in diameter (Falcon, cat. nos. FALC353004 and FALC353025)
- Sterile conical tubes, 15 and 50 ml (Falcon, cat. nos. FALC352070 and FALC352096)
- Dialysis tubing: Spectra/Por Membrane, MWCO: 50,000; flat width: 28 mm; diameter: 18 mm; volume/length: 2.5 ml cm^{-1}; length: 5 m or 16 feet (Spectrum Laboratories Inc./VWR)
- Dialysis closure: Spectra/Por Closures, 35 mm (Spectrum Laboratories Inc., cat. no. 132736)
- Slide-A-Lyzer dialysis cassettes (Pierce, cat. no. 66381)
- Clinical centrifuge (Hettich, Rotanta 460)
- 500-ml bucket rotor 46/46 R, 460/460 R (Hettich, art. no. HETT5624)
- Spinner flask, 3,000 ml (Bellco, cat. no. 1965-61030)
- One or five position magnetic stirrer, Bell-ennium (Bellco, cat. no. 7785-D2015)
- SW41 ultracentrifuge rotor (Beckman Coulter)
- Ultracentrifuge (Beckman Coulter)
- Ultra Clear Ultracentrifuge tubes (Beckman Coulter, cat. no. 344059)
- DNA gel apparatus and power supplies
- 37 °C bacteria incubator
- 37 °C, 5% CO_2 humidified tissue culture incubator
- 37 °C orbital shaker
- Electroporator (Bio-Rad) or similar apparatus

- Spectrophotometer
- Taqman 7500 fast real-time PCR system (Applied Biosystems)
- Light-Cycler 2.0 (Roche)
- UV Stratalinker 1800 (Stratagene)
- Phosphoimager FLA-3000 (Fujifilm)

REAGENT SETUP

Cell-culture conditions for 116 cells Growth medium: MEM (high glucose), 2 mM glutamine, 10% FBS, 40 μg ml^{-1} hygromycin B[55]. ▲ CRITICAL General culture conditions are 37 °C in a humidified atmosphere (5% CO_2). For 60- and 150-mm cell culture plates, we use 5 and 25 ml of growth medium, respectively. We observed that without antibiotics, 116 cells show better growth in tissue culture plates and in suspension in spinner culture flasks. In addition, we tested FBS from various companies and found that FBS from Sigma results in best growth of 116 cells. We routinely split these cells 1:2, 1:3, 1:4 or 1:5. It is important not to overgrow 116 cells, and we usually split at a confluence of 95%. After receiving this cell line, passage until passage 3 or 4 before long-term storage in a liquid nitrogen tank. When starting adenovirus production, these 'low passage' cells are used for transfection.

Amplification of the helper virus AdNG163R-2 Before starting the HC-AdV virus amplification protocol (Step 24), the helper virus needs to be produced[55]. This methodology is described in detail in **Box 1**.

Biosafety and containment guidance All cloning steps and cell culture work involved in helper virus and HC-AdV production and subsequent purification should be performed in accordance with BL2 guidelines.

Buffers

- Denaturation buffer: 1.5 M NaCl, 0.5 M NaOH (can be stored at room temperature (15–26 °C) for several months).
- Neutralization buffer: 0.5 M Tris-HCl (pH 7.5), 1.5 M NaCl (can be stored at room temperature for several months).
- 2× SSC: 3 M NaCl, 0.3 M sodium citrate (pH 7.0) (can be stored at room temperature for several months).
- Phosphate buffer: 1 M Na_2HPO_4, 1 M NaH_2PO_4 (pH 7.5) (can be stored at room temperature for several months).
- Church buffer: 1% BSA, 1 mM EDTA (pH 8.0), 0.5 M phosphate buffer, 7% sodium dodecyl sulfate (SDS) (prepare freshly from respective stock solutions and BSA powder).
- Proteinase K–SDS solution: proteinase K (0.5 mg ml^{-1}), 10 mM Tris-HCl (pH 7.5), 0.5% SDS, 10 mM EDTA (pH 8.0) (buffer without proteinase K can be stored at room temperature for several months. Proteinase K should be freshly added).
- HEPES-buffered saline: 140 mM NaCl, 1.5 M Na_2HPO_4, 40 mM HEPES (can be stored at 4 °C in a dry and ventilated place for several months).
- Cesium chloride solutions: these solutions are based on the following formula: 137.48–138.11/CsCl density = g CsCl + (100 − (×g CsCl)) ml H_2O. Three cesium chloride solutions are required, which are prepared using the following recipe:
  - 1.5 g cm^{-3} : 45.41 g CsCl + 54.50 ml H_2O
  - 1.35 g cm^{-3} : 35.18 g CsCl + 64.22 ml H_2O
  - 1.25 g cm^{-3} : 26.99 g CsCl + 73.01 ml H_2O
  - All three solutions should be sterile-filtered. Cesium chloride solutions can be stored for several months at 4 °C.
- Lysis buffer: 10 mM Tris-HCl (pH 7.5), 10 mM EDTA (pH 8.0), 0.5% SDS (can be stored at room temperature for several months).
- Tris–EDTA (TE) buffer: 10 mM Tris-HCl (pH 7.5), 10 mM EDTA (pH 8.0). Can be stored at room temperature for several months.

EQUIPMENT SETUP

Preparation and handling of glassware We use Bomix diluted in water to disinfect glassware. Rinse spinner flask with Bomix solution and incubate for 20 min until all the adenovirus from the previous preparation is destroyed. Rinse five times with water to remove Bomix residues. This step is followed by adding 2 liters of E-Toxa clean solution (0.5% diluted in water). Incubate for 20 min to destroy all endotoxins. Rinse spinner flask five times with water. Treat dialysis bottle by performing the same procedure. Finally, glassware needs to be autoclaved. ▲ CRITICAL Bleach can also be used to destroy remaining virus in the spinner flask. Other reagents may result in inefficient cell growth.

PROCEDURE

Cloning of HC-AdV constructs based on pAdFTC ● TIMING ~2 weeks

1| Clone the complete transgene expression cassette including promoter and polyadenylation signal into the shuttle vector pHM5 (ref. 59) (see molecular cloning manuals[62] for details on cloning techniques and protocols and **Fig. 2a**). Purify plasmid using standard kits for plasmid midi preparations according to the manufacturer's instructions or other appropriate protocols. Amplify the pHM5 plasmids with insert on kanamycin-containing LB plates or in LB medium with kanamycin.

2| Prepare a plasmid DNA mini preparation of pAdFTC (**Fig. 2b**) using alkaline lysis including phenol–chloroform extraction followed by ethanol precipitation[62] (**Box 2**).

▲ CRITICAL STEP Never vortex or vigorously pipette the large adenoviral plasmid pAdFTC. For short-term storage, keep large plasmids at 4 °C. Repeated freeze–thaw cycles should be avoided. For the cloning procedure, avoid any column purification for the plasmid pAdFTC. This will result in fragmentation of DNA and subsequently to false clones.

3| Digest 10 μg of the vector pAdFTC from Step 2 and 15 μg of the shuttle vector pHM5 containing the gene of interest from Step 1 with the restriction enzyme I-*Ceu*I (10 U) for 3 h at 37 °C. Set up digests in a total volume of 50 μl.

4| Perform a phenol–chloroform extraction and ethanol precipitation (**Box 2**).

5| Digest I-*Ceu*I-digested pAdFTC and pHM5-based shuttle vectors from Step 4 for at least 3 h or overnight with the restriction enzyme PI-*Sce*I (10 U) at 37 °C in a total volume of 50 μl. Subsequently, perform a second phenol–chloroform extraction followed by ethanol precipitation (**Box 2**). Dissolve DNA in an appropriate volume of dH_2O (~25 μl).

▲ CRITICAL STEP I-*Ceu*I and PI-*Sce*I change the mobility of DNA on an agarose gel, and therefore, a phenol–chloroform extraction and ethanol precipitation (**Box 2**) is required before running an agarose gel.

6| Separate DNA fragments of digested pHM5 plasmid containing your gene of interest (from Step 5) on a preparative agarose gel[62] and gel-purify[62] the DNA fragment to be inserted into pAdFTC (length of linearized backbone DNA fragment of pHM5 is 2.8 kb).

7| Dephosphorylate digested pAdFTC (from Step 5) with CIP (10 U) for 1 h at 37 °C in a total volume of 25 μl. Subsequently, purify DNA by phenol–chloroform extraction and ethanol precipitation (**Box 2**).

PROTOCOL

BOX 1 | AMPLIFICATION AND TITRATION OF THE HELPER VIRUS AdNG163R-2 ● TIMING ~3 WEEKS

Preamplification of the helper virus AdNG163R-2

1. Use human embryonic kidney cells (293 cells) for amplification of the helper virus AdNG163R-2 (see ref. 55). Three serial passages using 60-mm (one in total), 100-mm (two in total) and 150-mm (six in total) tissue culture dishes are required for preamplification. Start preamplification procedure with infection of a confluent (3×10^6 cells) 60-mm tissue culture dish either with purified AdNG163R-2 helper virus (5 TU per cell) or, if you received virus lysate, with 500 µl of lysate, which was treated by three freeze–thaw cycles in liquid nitrogen and a 37 °C water bath.
2. Forty-eight hours after infection, a cytopathic effect (CPE) should be observed because of helper virus replication (cells are rounded up and loosely or completely detached from the tissue culture dish).
▲ CRITICAL STEP For an effective amplification and high viral titers, CPE should be completed by 48 h. If it takes longer than 2 d for complete CPE, proceed with Step 3 of this box. After that, take complete cell–virus suspension and repeat Steps 1 and 2 described in this box.
3. Harvest cells and supernatant (= passage P1) by flushing off infected cells with the medium covering the cells from the surface of the tissue culture dish using a pipette.
■ PAUSE POINT Cell–virus suspension can be stored at −80 °C for several days before continuation of the amplification procedure.
4. For the second passage, infect 293 cells of two confluent 100-mm tissue culture dishes (9×10^6 cells per dish) with one half of the helper virus-containing cell–virus suspension, respectively (~1.5 ml; produced in Step 3 of this box). Forty-eight hours after infection, a cytopathic effect (CPE) should be observed because of helper virus replication (cells are rounded up and loosely or completely detached from the tissue culture dish). Harvest cells and supernatant (= passage 2) by flushing off infected cells as described in Step 3 described in this box.
▲ CRITICAL STEP For an effective amplification and high viral titer, CPE should be completed after 48 h. If it takes longer than 2 d for complete CPE, take complete cell–virus suspension from Step 4 and repeat Steps 1 and 2 of this box.
■ PAUSE POINT Cell–virus suspension (~20 ml) can be stored at −80 °C for several days before continuation of the amplification procedure.
5. For the next step, six confluent 150-mm tissue culture dishes (2×10^7 cells per dish) are needed. Make sure you further maintain 293 cells because 30 confluent 150-mm tissue culture dishes (2×10^7 cells per dish) are required for large-scale amplification (see below).
6. When cells grown in 150-mm tissue culture dishes reach 90–95% confluence, release viral particles from cells obtained in Step 4 described in this box (~20 ml) by freezing (liquid nitrogen) and thawing (37 °C water bath) four times. For the third passage, each of the six confluent 150-mm tissue culture dishes (2×10^7 cells per dish) should be infected with 3 ml of the helper virus-containing lysate.
7. Harvest cells and supernatant in three 50-ml conical tubes (~120 ml) after 48 h as described in Step 3 within this box.
▲ CRITICAL STEP To evaluate whether the helper virus preamplification was successful, a quantitative real-time PCR (qPCR) specific for helper virus can be performed (see Step 73B(i-ix)).
■ PAUSE POINT Cell–virus suspension (~120 ml) can be stored at −80 °C for several days before continuation of the procedure.

Large-scale amplification and purification of helper virus AdNG163R-2

8. Prepare 30 confluent 150-mm tissue culture dishes (2×10^7 cells per dish) with 90–95% confluence. Release viral particles from cell–virus suspension (~120 ml, obtained in Step 7 of this box) by freezing in liquid nitrogen and thawing in a 37 °C water bath three times. Each of the 30 confluent 150-mm dishes should be infected with 4 ml of the helper virus-containing lysate.
9. Harvest cells and supernatant in two 500-ml centrifuge tubes (~600 ml in total) after 48 h as described in Step 3 (see above).
10. Centrifuge for 10 min at 890*g* with a clinical centrifuge.
11. Remove and discard the remaining medium.
12. Resuspend pellets in 28 ml of DPBS by pipetting up and down 8–10 times to get a single-cell suspension.
13. Freeze resuspended virus in liquid nitrogen for 5 min. Make sure that the suspension is completely frozen. Store at −80 °C until starting purification with caesium chloride gradients and dialysis (Steps 57–72). Virus–cell suspension from one spinner culture flasks will be split on six tubes of one SW41 rotor (see Step 63).
14. For purification of the helper virus AdNG163R-2, perform CsCl gradients as described in detail in Steps 57–72.

Titration of the helper virus AdNG163R-2

15. We first determine the physical titer of the helper virus AdNG163R-2 (for details, see Step 73A).
16. To calculate the optical particle units (OPU), use the following formula:

$$\text{OPU ml}^{-1} = (\text{absorbance at 260 nm}) \times (\text{dilution factor}) \times (1.1 \times 10^{12})$$

The OPU ml^{-1} equals the physical titer, which is expressed in viral particles per ml (vp ml^{-1}). It usually ranges between 5×10^{11} and 2×10^{12} vp ml^{-1}.
17. In addition, perform a plaque-forming assay to determine the transducing units of the final vector preparation. Therefore, serially dilute the final vector preparation (1:10 dilutions) and infect 293 human embryonic kidney cells in six-well plates at a confluence of 90%.
18. Three hours later, we perform an agarose overlay and count plaque-forming units after 7–10 d as described earlier[65]. The final titer usually ranges between 4×10^7 and 8×10^7 TU μl^{-1}. The total volume is approximately 1.0–1.5 ml. Alternatively, other methods described in Step 73 can be applied.

8| Perform an analytic gel electrophoresis[62] to check whether the digests of dephosporylated pAdFTC plasmid (from Step 7) and the pHM5 shuttle vector (from Step 6) are completed and the sizes of the expected fragments are correct; digested pAdFTC runs at 31 kb and digested pHM5 backbone runs at 2.8 kb. The size of the second band excised from the pHM5 shuttle vector depends on the length of the transgene expression cassette.

BOX 2 | PHENOL–CHLOROFORM EXTRACTION OF RESTRICTION ENZYME DIGESTS FOLLOWED BY ETHANOL PRECIPITATION ● TIMING 30 MIN

1. Add dH_2O to the DNA solution up to a total volume of 100 µl.
2. Add 100 µl of phenol:chloroform:isoamyl alcohol and mix gently by inverting several times.
3. After centrifugation for 2 min at high speed (15,000*g*) in a microcentrifuge, transfer supernatant to a new tube.
4. Add 20 µl of sodium acetate (pH 5, 3 M) to supernatant and 400 µl of EtOH (>99.8%; stored at −20 °C). Mix suspension vigorously.
5. To pellet DNA, centrifuge samples for 10 min at high speed (15,000*g*) in a microcentrifuge.
6. After removal of the supernatant, add 300 µl of 70% EtOH and centrifuge for 2 min at high speed (15,000*g*).
7. Remove supernatant and air-dry DNA pellet.

▲ CRITICAL STEP Do not dry DNA pellet for a long time, as it will be harder to get DNA in solution.

8. Dissolve pellet in 10–20 µl of dH_2O.

9| Set up ligation[62] (we ligate in a total volume of 20 µl with 2- to 6-µl vector, 8- to 12-µl insert and 400 U of T4 DNA ligase). Ligate at 16 °C overnight. A schematic overview of the cloning procedure is provided in **Figure 3a**.

10| Perform a phenol–chloroform extraction (**Box 2**) and digest the ligation reaction with the restriction enzyme *Swa*I (10 U) for 2 h at 25 °C in a total volume of 20 µl. To concentrate and purify ligated DNA, perform a second phenol–chloroform extraction (**Box 2**).

11| Transform 1 µl of the *Swa*I digested ligation product by electroporation[62] into 40 µl of DH10B electrocompetent cells and spread transformation mix on ampicillin-containing LB plates (50 µg ml^{-1} ampicillin). Incubate plates for 16–24 h at 37 °C.
? TROUBLESHOOTING

12| Select 5–10 clones and prepare plasmid DNA mini preparations as described in Step 2. Digest plasmids with I-*Ceu*I and PI-*Sce*I as described in Steps 3–5. Check the size of DNA fragments by gel electrophoresis as described in Step 8.
A representative gel is shown in **Figure 3b**.
? TROUBLESHOOTING

13| Amplify bacterial culture consisting of cells with the correct clone in ampicillin-containing LB (50 µg ml^{-1} ampicillin) and perform a midi-/maxi-plasmid preparation. At this point, you may use commercially available columns for plasmid purification according to the manufacturer's instructions.
■ PAUSE POINT Plasmid DNA of the HC-AdV can be stored at −20 °C for several months.

Linearize the HC-AdV production plasmid by restriction enzyme digest ● TIMING ~5 h

14| Digest 20 µg of the pAdFTC-based adenoviral production plasmid (from Step 13) in a total volume of 100 µl using the restriction enzyme *Not*I (20 U) at 37 °C for 2 h.

15| Add 90 µl of phenol:chloroform:isoamyl alcohol (24:24:1 vol/vol) and mix by inverting the tube several times.

16| Centrifuge for 2 min at high speed (15,000*g*) in a bench-top centrifuge at room temperature.

17| Carefully collect supernatant by pipetting and transfer into a new tube.

18| Repeat phenol–chloroform extraction (Steps 15–17).

19| Add 50 µl of sodium acetate (pH 5.0; 3 M) and 1 ml of precooled EtOH (>99.8% stored at −20 °C). Mix by inverting the tube several times.

20| Centrifuge samples for 10 min at high speed (15,000*g*) at room temperature. Carefully remove the supernatant by pipetting.

21| Add 500 µl of 70% EtOH to the DNA pellet obtained, invert the tube three times and centrifuge for 2 min at high speed (15,000*g*) at room temperature.

22| Remove the supernatant by pipetting and briefly air-dry the DNA pellet. Resuspend pellet in ~50 µl of TE buffer.
▲ CRITICAL STEP If you air-dry the DNA pellet too long, it will be difficult to resuspend the linearized DNA fragments.
■ PAUSE POINT Linearized DNA can be stored for several days at 4 °C or at −20 °C for several weeks.

23| Check digest by gel electrophoresis as described in Step 8. You should detect a 9-kb fragment for the plasmid backbone and, depending on the size of your transgene expression cassette, a second DNA fragment (size: 28–36 kb). Before proceeding with the protocol, make sure that you have amplified the helper virus AdNG163R-2 (see also **Box 1**).
? TROUBLESHOOTING

PROTOCOL

Transfection of 116 producer cells with the linearized HC-AdV DNA construct ● TIMING ~2 d

24| The day before transfection, seed low passage (<passage 10) 116 cells (0.8×10^6) into a 60-mm tissue culture dish. Cells should reach 50–80% confluence the next day.

25| At this point, linearized HC-AdV DNA from Step 22 can be transfected into 116 cells using Superfect transfection (option A) or calcium phosphate transfection (option B). Transfection efficiencies for large linear constructs are comparable for both transfection methods. However, reagents for calcium phosphate transfections are cheaper.

(A) Superfect transfection

(i) Mix 5 μg of *Not*I-digested DNA (from Step 22) with OPTI-MEM to a total volume of 150 μl.
(ii) Add 30 μl of Superfect reagent and mix by pipetting up and down three times.
(iii) Incubate for 5–10 min at room temperature.
(iv) Add 1 ml of 116-cell medium (MEM, 10% FBS) and mix by pipetting up and down three times.
(v) Remove the media from the 60-mm tissue culture dish (from Step 24) and immediately add the complete DNA mixture (from Step 25A(iv)).
▲ CRITICAL STEP Transfection using Superfect should be carried out according to the manufacturer's instructions. However, leave out the washing step with PBS because the experience shows that 116 cells change morphology and are only loosely attached to the tissue culture dish if too many media changes are performed.
(vi) Incubate for 2–3 h at standard conditions in the tissue culture incubator.
(vii) Remove the media containing the Superfect–DNA complexes and replace it with prewarmed (37 °C) complete MEM (10% FBS).

(B) Calcium phosphate transfection

(i) Prewarm 2 M $CaCl_2$ and 2× HEPES-buffered saline to room temperature and mix thoroughly. For each transfection, prepare two sterile tubes.
(ii) Mix 12 μg of *Not*I-digested DNA (from Step 22) and 37 μl of 2 M $CaCl_2$ and add sterile water to a final volume of 300 μl into tube 1. Transfer 300 μl of 2× HEPES-buffered saline into tube 2.
▲ CRITICAL STEP The pH of the 2× HEPES-buffered saline is very critical and should be at 7.05.
(iii) Slowly add the DNA solution from tube 1 dropwise to the HEPES-buffered saline in tube 2 while vortexing.
(iv) Incubate the combined solution at room temperature for 30 min.
(v) Vortex, then immediately add the solution dropwise to the cells (from Step 24).
(vi) Swirl the plate briefly for distribution of DNA complexes and incubate at 37 °C and 5% CO_2 until infection with helper virus (see Step 26).
(vii) Change the media (10% FBS) after 6 h.
? TROUBLESHOOTING

Infection with helper virus ● TIMING 1 h + 2 d

26| At 16–18 h post-transfection, infect cells with the helper virus AdNG163R-2 (see also **Box 1**) applying 5 transducing units (TU) per cell: carefully remove the medium and add fresh medium (MEM, 5% FBS) with the appropriate amount of helper virus (a 60-mm tissue culture dish at a confluence of 80–100% contains ~3.2×10^6 cells, and therefore one needs to add ~1.6×10^7 TU of the helper virus).

27| Make sure that the virus is equally distributed on the tissue culture dish by gently moving the dishes every 20 min during the first hour after infection.

28| Harvest cells and supernatant (= passage P0) 48 h post-infection by flushing off the cells using a pipette from the surface of the tissue culture dish using the cell culture medium of this plate. Freeze at −80 °C.
▲ CRITICAL STEP Two days after infection, a cytopathic effect (CPE) should be observed because of virus replication (cells are rounded up and loosely or completely detached from the tissue culture dish). For an efficient amplification, CPE is observable 48 h post-infection.
■ PAUSE POINT Lysate can be stored at −80 °C for at least several days before continuation of the amplification procedure.

Viral preamplification steps using adherent 116 cells ● TIMING ~12 d

29| Three serial passaging steps are required (passages P1–P3) as described in the following steps. Make sure that tissue culture dishes with 116 cells are available for Steps 31, 33 and 36. We use one-third (~1 ml) of the lysate from passage P0 (Step 28) to infect one 60-mm dish of 116 cells at a confluence of 90–95%. To break up cells and release the virus from passage P0 (Step 28), freeze (in liquid nitrogen) and thaw (in 37 °C water bath) several times. If the lysate from passage P0 was stored at −80 °C, conduct three freeze–thaw cycles. If freshly harvested virus from passage P0 is used, perform four freeze–thaw cycles.
▲ CRITICAL STEP It is not necessary to spin down and remove cellular debris after freeze–thaw cycles.
? TROUBLESHOOTING

30| Mix fresh media (MEM, 5% FBS) with one-third of the lysate from Step 29 to a final volume of 3 ml and add the helper virus; at this stage, coinfect with the helper virus applying 2 TU per cell (a 60-mm tissue culture dish at a confluence of 80–100% contains $\sim 3.2 \times 10^6$ cells, and therefore one needs to add $\sim 6.4 \times 10^6$ TU of the helper virus).
? TROUBLESHOOTING

31| Remove the medium from a 60-mm dish with 116 cells (90–95% confluence; from Step 29) and infect with the viral mixture (from Step 30).
? TROUBLESHOOTING

32| Harvest cells and supernatant 48 h after infection by completely detaching cells from the tissue culture dish and thorough aspiration of the cell–medium suspension, and freeze at −80 °C. This viral suspension is called passage P1.
■ **PAUSE POINT** Cell–virus suspension from passage P1 can be stored at −80 °C for several days before continuing.
? TROUBLESHOOTING

33| Use one-third of the lysate from passage P1 (from Step 32) to infect a 60-mm dish of 116 cells at a confluence of 90–95% by repeating Steps 29–32 to obtain passage P2.
■ **PAUSE POINT** Cell–virus suspension from passage P2 can be stored at −80 °C for several days before continuing.
? TROUBLESHOOTING

34| Use two-thirds of the cell–virus suspension from passage P2 (obtained at Step 33) to infect a 150-mm dish of 116 cells at a confluence of 90–95%. To break up cells and release the virus from passage P2 (Step 33), freeze (in liquid nitrogen) and thaw (in 37 °C water bath) several times (see also Step 29).
? TROUBLESHOOTING

35| Mix fresh media (MEM, 5% FBS) with two-thirds of the lysate from Step 34 to a final volume of 20 ml and add the helper virus. Coinfect with the helper virus using 2 TU per cell (a 150-mm tissue culture dish at a confluence of 80–100% contains $\sim 2 \times 10^7$ cells, and therefore one needs to add $\sim 4 \times 10^7$ TU of the helper virus).
? TROUBLESHOOTING

36| Remove the medium from a 150-mm dish of 116 cells (90–95% confluence) and infect with the viral mixture.
? TROUBLESHOOTING

37| Harvest cells and supernatant 48 h after infection as described in Step 32 and freeze at −80 °C. This cell–virus suspension is called passage P3.
▲ **CRITICAL STEP** Some vectors may not amplify sufficiently until finishing passage P3, and they may require additional passages. At this point, primary amplification of HC-AdV containing a beta-galactosidase or green fluorescent protein (GFP) coding sequence can easily be evaluated using beta-galactosidase or GFP readout systems, respectively. As not every HC-AdV contains a marker gene, one may alternatively monitor the status of viral amplification by infection of HeLa cells with aliquots of the viral lysates (passages P0–P3) and subsequent Southern blot analysis or qPCR (see also Step 73).
■ **PAUSE POINT** Cell–virus suspension from passage P3 can be stored at −80 °C for several days before continuation of the amplification procedure.
? TROUBLESHOOTING

Amplification of 116 cells in suspension using a spinner culture system ● **TIMING 5 d**
38| Add 900 ml of prewarmed (37 °C) fresh MEM (10% FBS) with hygromycin B (100 μg ml^{-1}) into the spinner culture flask.
? TROUBLESHOOTING

39| Remove medium from individual 150-mm tissue culture dishes with 116 cells and flush off cells with 10 ml of fresh media (MEM, 10% FBS with 100 μg ml^{-1} hygromycin B). Adherent 116 cells are easy to detach. No trypsin is required. In fact, trypsin may negatively affect growth of suspension cells. Immediately after adding the media, pipette up and down several times to get a homogeneous cell suspension. Subsequently, transfer cells directly into the spinner flask, which contains already 900 ml of fresh medium (MEM, 10% FBS) with hygromycin B (100 μg ml^{-1}).
▲ **CRITICAL STEP** One needs ten 150-mm tissue culture dishes with 116 cells at a confluence of 95–100% to set up a 3-liter suspension culture in a spinner flask (**Fig. 4a**). Detach cells from each single 150-mm dish one after the other. If you wait too long after removing the media and adding the fresh media, cells will become harder to detach.
? TROUBLESHOOTING

40| Incubate spinner flask with the final volume of 1 liter on a magnetic stirrer in a tissue culture incubator for 24 h at 37 °C and 5% CO_2. During the amplification procedure, the magnetic stirrer is adjusted to 70 r.p.m. Rotation avoids attachment of cells to glass surfaces and optimal growth.
? TROUBLESHOOTING

PROTOCOL

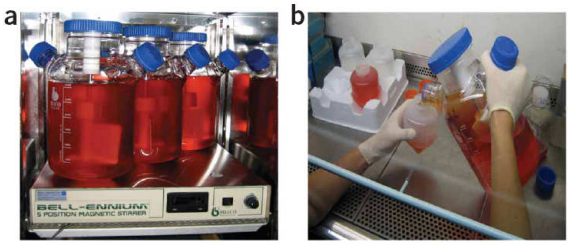

Figure 4 | Amplification of high-capacity adenoviral vectors (HC-AdV) in spinner flasks. (**a**) Producer cells, 116 cells (see ref. 55), grow in suspension and as adherent cells. Cells are amplified in 3 liters of medium using spinner flasks. The Bell-Ennium 5 position magnetic stirrer allows amplification of cells in five 3-liter spinner culture flasks simultaneously. (**b**) Ninety-six hours after setting up the spinner, culture cells are harvested for infection with the HC-AdV and coinfection with the helper virus. Forty-eight hours post-infection cells are harvested using 500-ml centrifuge tubes. Infected cells are resuspended in 28 ml of DPBS. This suspension is used for purification using CsCl gradients.

41| 24 h after setting up the spinner culture, add 500 ml of fresh media (MEM, 10% FBS) supplemented with hygromycin B (100 μg ml^{-1}).
? TROUBLESHOOTING

42| *Optional*: monitor cell growth in spinner culture flask. Each day you may remove an aliquot (1 ml), perform a Trypan blue staining and count cells to monitor cell viability (see **Box 3**). The density of cells usually ranges between 2 × 10^5 and 5 × 10^5 cells per ml.
? TROUBLESHOOTING

43| 48 h after setting up the spinner culture, add 500 ml of fresh media (10% FBS) with hygromycin B (100 μg ml^{-1}).
? TROUBLESHOOTING

44| 72 h after setting up the spinner culture, add 1,000 ml of media (10% FBS) supplemented with hygromycin B, resulting in a total volume of 3-liter cell suspension. After 24 h, continue with the infection procedure (Step 46).
? TROUBLESHOOTING

45| *Optional*: one day before infection, we plate an aliquot (2 ml) of 116 cells grown in suspension in a 60-mm tissue culture dish. About 6 h later, these cells should be adherent, and the next day the dish should have a confluence of approximately 30–50%. With this procedure, one can examine whether cells in the spinner culture are viable and have grown to sufficient amounts.
? TROUBLESHOOTING

Infection of 116 cells grown in suspension and HC-AdV amplification ● TIMING ~2 d

46| Harvest 116 suspension cells from Step 44 (we use 500-ml centrifuge tubes). Centrifuge for 10 min at 500*g* in a clinical centrifuge at room temperature (**Fig. 4b**). The supernatant can be discarded. Keep the emptied spinner culture flask under the tissue culture hood.

47| Resuspend all the cells in MEM with 5% FBS (no hygromycin) by pipetting up and down about 8–10 times to get a single-cell suspension. The amount of fresh resuspension medium depends on whether one uses the lysate from Step 37 (130-ml resuspension medium) or a purified viral stock from Step 72 (150-ml resuspension medium). The total volume of the initial infection should be 150 ml.

48| *Infection of 116 cells grown in suspension*: you may use the virus/cell suspension from Step 37 or purified virus from Step 72.
(A) Infection of 116 suspension cells with lysate (primary amplification) ● TIMING ~1.5 h

(i) To break up cells and to release the virus from cell–virus suspension of passage P3 (Step 37), perform three freeze (in liquid nitrogen) and thaw (in 37 °C water bath) cycles. If the freshly harvested virus from passage P3 is used, perform four freeze–thaw cycles.

BOX 3 | COUNTING OF EUKARYOTIC CELLS TO MONITOR CELL VIABILITY AND CELL DENSITY ● TIMING 10 MIN

1. Aseptically, take 0.1 ml of suspension cells and add 0.1 ml of Trypan blue solution (0.4%, wt/vol).
2. Incubate for 5 min at room temperature and subsequently deliver them to a hemacytometer.
▲ CRITICAL STEP Before counting the cells, vortex cell supension to obtain single-cell solution because cells in suspension partially grow in cell aggregates.
3. Count a total of at least 100 cells and determine the percentage of cells, which are not viable and therefore blue. There should be only a limited percentage of blue cells present (<15%).
4. To ascertain the density of the cells per ml, count the cells in four squares of a standard hemacytometer and calculate the average amount of cells. The cell density is determined by the following formula: cell ml^{-1} = average of counted cells × 2 × 10^4 ml^{-1}.

(ii) Transfer cells from Step 47 to a 250-ml storage bottle and put in a sterile magnetic stir bar.
(iii) Coinfect cells with the virus within the lysate from Step A(i) and the helper virus (2 TU per cell). Assuming a density of 3×10^5 cells per ml, the total amount of cells in a 3-liter spinner flask is 9×10^8 cells. Thus, one needs to add 1.8×10^9 TU of the helper virus AdNG163R-2.

(B) Infection of 116 suspension cells with purified virus stock (reamplification of HC-AdV) ● TIMING ~20 min

(i) Transfer cells from Step 47 to a 250-ml storage bottle and put in a sterile magnetic stir bar.
(ii) Infect cells with 100 viral particles per cell (vp, physical titer as determined in Step 73 (option A) by measuring the absorbance at 260 nm) of formerly purified HC-AdV (Step 72) and coinfect with the helper virus (2 TU per cell). Assuming a density of 3×10^5 cells per ml, the total amount of cells in a 3-liter spinner flask is 9×10^8 cells. Thus, one needs to add ~9×10^{10} vp of the purified HC-AdV and 1.8×10^9 TU of the helper virus AdNG163R-2.

49| Stir the 250-ml storage bottle containing the cell–virus mixture in the tissue culture incubator set at 37 °C and 5% CO_2 for 2 h at 60 r.p.m. on a magnetic stirrer. Make sure that the storage bottle is not completely closed.

50| Transfer the total volume of 150 ml from the storage bottle into the spinner culture flask and add 1,850 ml of prewarmed (37 °C) and fresh media (MEM + 5% FBS, no hygromycin B, 2 liters in total).

51| Incubate for 48 h in the tissue culture incubator at 37 °C and 5% CO_2. Stir at 70 r.p.m.

52| Harvest cells by centrifugation for 10 min at 890*g* at room temperature (we use 500-ml centrifuge tubes and spin them in a clinical centrifuge).

53| Remove the remaining medium.

54| Resuspend pellets (from 2 liters) in 28 ml of DPBS by pipetting up and down 8–10 times to get single-cell suspensions.

55| Freeze resuspended cell–virus suspension in liquid nitrogen for 5 min. Make sure that the suspension is completely frozen. Store at −80 °C until starting the purification using cesium chloride gradients (Steps 57–60). Virus–cell suspension from one spinner culture flask will be split in six tubes (Step 63) of one SW41 rotor.

56| *Optional*: to monitor HC-AdV amplification, one may keep an aliquot for further investigation. When establishing the protocol, each large-scale amplification step of an HC-AdV containing a marker gene coding sequence (beta-galactosidase or GFP) may be monitored by removing an aliquot (**Fig. 5**). As not every HC-AdV contains a marker gene, one may alternatively monitor viral amplification by infection of HeLa cells with collected aliquots and subsequent qPCR or Southern blot analysis (see also Step 73B,D).
■ PAUSE POINT Frozen virus–cell suspension can be stored at −80 °C for several weeks until purification.

Purification of HC-AdV ● TIMING 2 d

57| Before starting the purification procedure, prepare cesium chloride solutions (see REAGENT SETUP).

58| To prepare viral lysate from Step 55 (frozen cell–virus suspension resuspended in DPBS) for cesium chloride gradients, thaw cell–virus suspension in a 37 °C water bath.

59| Shake the tube intermittently to avoid local heating, which could reduce viral titer.

60| Freeze in liquid nitrogen for 5 min. Make sure that the solution is completely frozen.

61| Repeat freeze–thaw cycle two times (Steps 58–60) to disrupt cellular

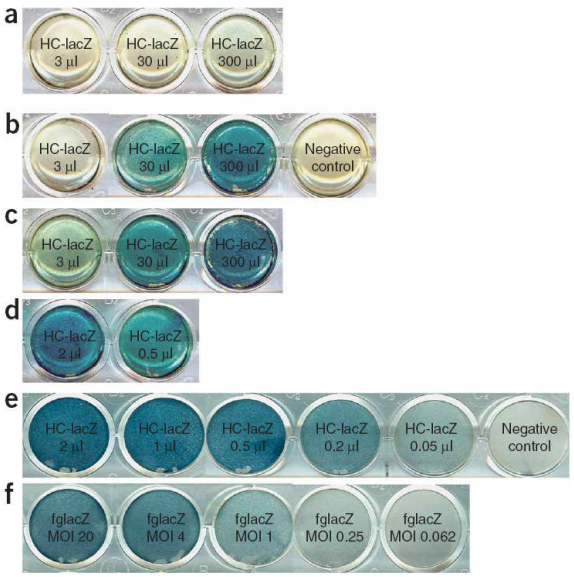

Figure 5 | Monitoring adenoviral amplification steps during large-scale production. In this example, the amplified HC-AdV expresses beta-galactosidase under the control of a cytomegalovirus promoter[55]. HeLa cells were seeded in a 12-well plate. At 90% confluence, cells were infected with an aliquot of the viral progeny of each amplification stage. Twenty-four hours post-infection, cells were stained for beta-galactosidase expression. Infection volumes are indicated. (**a**) Twenty-four hours after infection of the 3-liter suspension, culture with HC-AdV and helper virus (Step 51). (**b**) Forty-eight hours after infection of the suspension culture (Step 51). (**c**) Harvested cell suspension resuspended in 28 ml of DPBS (Step 54). (**d**) Purified virus after CsCl gradient und dialysis (Step 72). (**e**) Reamplified virus from CsCl-purified stock (Step 72). (**f**) Standard curve. HeLa cells were infected with defined multiplicities of infection (MOIs) using a first-generation virus containing the same beta-galactosidase expression cassette (fglacZ) as the analyzed HC-AdV (**Fig. 5a–e**).

PROTOCOL

membranes and to release viral particles from cells. In total, four freezing and thawing steps are required (freezing step for storage included).

62| After the last thawing step, centrifuge at 500*g* for 8 min at room temperature and collect the supernatant containing the HC-AdV. Collect the supernatant in a 50-ml conical tube. The pellet containing cell debris can be discarded.
■ **PAUSE POINT** The collected supernatant can be stored for several hours at 4 °C.

63| During the freeze–thaw cycles (Steps 58–60), prepare cesium chloride (CsCl) step gradients in six UltraClear centrifuge tubes; carefully and slowly pipette CsCl solutions into UltraClear centrifuge tubes in the following order: 0.5 ml of 1.5 g cm^{-3} CsCl solution, 3 ml of 1.35 g cm^{-3} CsCl solution and 3.5 ml of 1.25 g cm^{-3} CsCl solution (**Fig. 6a**).
▲ **CRITICAL STEP** To avoid disruption of the phase interface, reduce the distance between the pipette and solution to a minimum. Disruption of phases leads to more diffuse viral bands (see Step 66).

64| Carefully overlay ~4.5 ml of cleared vector supernatant from Step 62 on top of 1.25 g ml^{-1} CsCl layer. To avoid imbalance, add ~0.5 ml of DPBS on top of cleared vector supernatant until reaching the top of the tube.

65| Centrifuge the gradients in an ultracentrifuge at 12 °C for 1.5 h at 226,000*g* (35,000 r.p.m.) to separate packed viral particles from unpacked particles and remained cellular fragments.
▲ **CRITICAL STEP** Set slow acceleration and deceleration to avoid disruption of the gradient.

66| Take out the UltraClear centrifuge tubes with tweezers. You will see a diffuse band of cell debris as a top layer. Below you will find two white bands. The lower band equals the HC-AdV, and the upper band contains empty particles. When the physical titer (see Step 73A) of the upper band is determined by measuring the absorbance at 260 nm, the values indicate the presence of protein but absence of DNA. The gradient after centrifugation is schematically shown in **Figure 6a**.
? TROUBLESHOOTING

67| Collect the lower bands of each gradient (about 1 ml each tube) after carefully removing the layers of cell debris and empty particles with a 1-ml pipette. Collect and transfer virus with a clean pipette tip into a sterile 50-ml conical tube.
? TROUBLESHOOTING

68| Add 1.35 g ml^{-1} CsCl solution up to a volume of 24 ml. Mix carefully by pipetting up and down. Transfer 12 ml to two UltraClear centrifuge tubes, respectively, and fill them with 1.35 g ml^{-1} CsCl solution to the top.
▲ **CRITICAL STEP** Never centrifuge more than ~3 ml of virus (from Step 67) in one tube because this will result in a diffuse virus band.
? TROUBLESHOOTING

69| Centrifuge overnight (18–20 h) at 226,000*g* (35,000 r.p.m.) at 12 °C in an ultracentrifuge (slow acceleration and deceleration).
? TROUBLESHOOTING

70| Retrieve the HC-AdV (see also **Fig. 6**). You may see two bands of which the lower band should be collected as described in Step 67. The upper band equals residues of empty particles.
? TROUBLESHOOTING

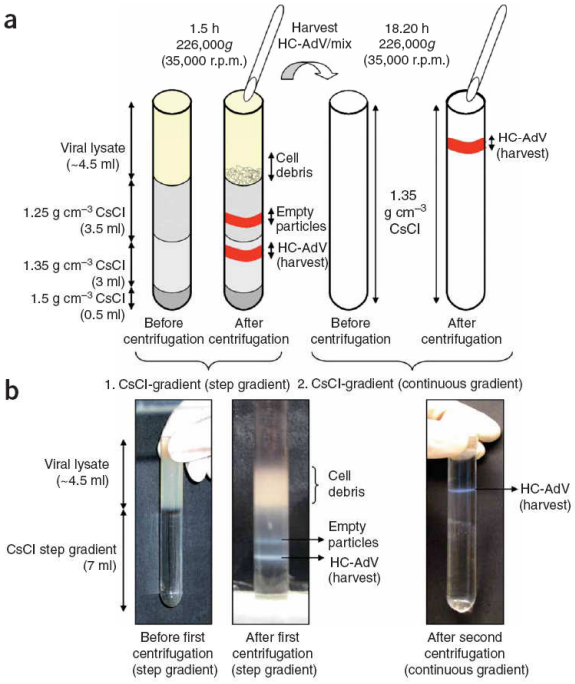

Figure 6 | Flowchart of CsCl purification of HC-AdV. For both centrifugation steps, centrifuge tubes are shown before and after centrifugation. The cesium chloride steps are indicated as well as the respective centrifugation parameters. (**a**) Schematic diagram of CsCl gradients. After three freeze–thaw cycles, the viral lysate is carefully loaded onto the top of the CsCl gradient. After centrifugation at 226,000*g* (35,000 r.p.m., 1.5 h, 12 °C), the band containing the HC-AdV is harvested from the top with a 1-ml pipette (around 1 ml per centrifuge tube). Empty particles (without viral genome) concentrate in the 1.25 g cm^{-3} CsCl phase, whereas complete HC vector particles concentrate in the 1.35 g cm^{-3} CsCl phase. In the continuous CsCl gradients, the HC-AdV particles concentrate in the upper part of the tube. Note that the density of empty particles that are eventually present in the preparation is lower than the density of packed particles. Therefore, empty particles are concentrating above the complete particles. Be sure to harvest the complete particles in a volume as small as possible to concentrate them. (**b**) Photographs of the collection tubes before (left picture) and after the step gradient centrifugation (middle picture) and after the continuous gradient centrifugation (right picture). The particle bands (empty and complete) appear white with a light blue shadow. After the first centrifugation, the collected virus is mixed with 1.35 g cm^{-3} CsCl solution and centrifuged at 226,000*g* (35,000 r.p.m.) overnight at 12 °C. The HC-AdV is visible in the upper part of the tube after second centrifugation (right picture), collected and subsequently dialyzed.

Dialysis of virus for buffer exchange ● TIMING 2 d

71| One can either dialyze collected virus from Step 70 in purchased ready-to-use dialysis cassettes (option A) or dialysis tubing closed with dialysis closures (option B). The latter option may be cheaper in the long-term run.

(A) Dialysis cassettes

(i) Fill dialysis cassettes according to the manufacturer's instructions.
▲ CRITICAL STEP Avoid any air bubbles in the dialysis cassette.

(ii) Dialyze at 4 °C in 500-ml dialysis buffer (10 mM Tris-HCl (pH 7.5), 10% glycerol, 1 mM MgCl2 in deionized H_2O) with slow stirring. Exchange dialysis buffer twice after 60 min and 120 min.

(iii) Third dialysis step should be performed overnight in 500 ml of dialysis buffer at 4 °C with slow stirring.

(iv) Retrieve virus from dialysis cassette.

(B) Dialysis tubing

(i) Cut off dialysis tubing (a strip of about 8 cm in length).

(ii) Wash dialysis tubing three times with sterile and deionized H_2O.

(iii) Close dialysis tubing on one side with a dialysis closure.

(iv) Transfer collected virus into dialysis tubing using a 1-ml pipette.

(v) Close dialysis tubing on the other side with a dialysis closure. Before closure, make sure that all air bubbles are removed.

(vi) Dialyze in 1,000 ml of dialysis buffer (10 mM Tris-HCl (pH 7.5), 10% glycerol and 1 mM MgCl2 in deionized H_2O) at 4 °C with slow stirring for 2 h.

(vii) Remove dialysis buffer and dialyze overnight in 2,000 ml of dialysis buffer at 4 °C with slow stirring. Alternatively, one can use sucrose buffer for dialysis. This sucrose-based dialysis buffer (140 mM NaCl, 5 mM $Na_2HPO_4 \cdot 2H_2O$, 1.5 mM KH_2PO_4 and 730 mM (= 5%) sucrose (pH 7.8)) was shown to avoid aggregation of viral particles. For the whole procedure, please refer to the protocol in ref. 63.

(viii) Collect virus using a 1-ml pipette.

72| Make multiple aliquots (25–50 µl or larger) and store at −80 °C. To titer the virus preparation, additionally make three aliquots of 25 µl. After storage of the HC-AdV at −80 °C, minimize the numbers of freeze–thaws because this may result in the reduction of infectious units[64]. Storage or shipping of adenoviral vectors on dry ice will negatively impact the activity of the virus due to pH changes after exposure to CO_2 (see refs. 45,65).

■ PAUSE POINT Virus can be stored at −80 °C.

Characterization and titration of final vector preparations ● TIMING 1–5 d

73| There are numerous ways to titrate the HC-AdV preparations and to determine the helper virus contamination: measuring the physical titer of final HC-AdV preparations (option A), characterization of HC-AdV preparations and helper virus contamination levels by qPCR (option B), measuring infectious units of the HC-AdV in the final vector preparation by qPCR (option C), quantification of infectious units by Southern blot analysis (option D) and physical and infectious titer standardized by adenovirus reference material (option E). The method of choice, however costly, is the titer determination by qPCR (option B). We routinely perform options A, C and D.

? TROUBLESHOOTING

(A) Measuring the physical titer of final HC-AdV preparations by optical density ● TIMING 1 h

(i) Dilute 25 µl of the final vector preparation from Step 72 with 475 µl of dilution buffer.

(ii) Gently shake for 20 min at room temperature. Centrifuge at room temperature in a microcentrifuge at 15,000*g* for 2 min. Subsequently, measure the absorbance of the supernatant at 260 nm (A260).

(iii) Use the following formula to calculate the optical particle units (OPU): OPU ml^{-1} = (absorbance at 260 nm) × (dilution factor) × (1.1×10^{12}) × (36)/(size of HC-AdV in kb).

(iv) As the A260 values are usually low, we measure four times using 100 µl of the diluted virus.

(v) The OPU equals the number of viral particles, and the final concentration is expressed in viral particles per ml (vp ml^{-1}).

(B) Measuring the physical titer of final HC-AdV preparations and helper virus contamination levels by qPCR ● TIMING 4 h

(i) Incubate 20 µl of purified virus from Step 72 for 2 h with 200 µl of proteinase K–SDS solution at 56 °C.

(ii) Precipitate viral DNA by adding 20 µl of 3 M sodium acetate (pH 5) and 600 µl of precooled EtOH (>99.8%; stored at −20 °C).

(iii) Centrifuge for 8 min at full speed (15,000*g*) at room temperature in a microcentrifuge and discard the supernatant by pipetting.

(iv) Add 600 µl of 70% ethanol and mix gently by inverting the tube several times. After centrifugation at 15,000*g* at room temperature for 5 min, remove the supernatant by pipetting.

(v) Air-dry pellet briefly and resuspend in 25 µl of sterilized dH_2O. Use 5 µl for qPCRs.
■ PAUSE POINT DNA can be stored at −20 °C for up to 1 month. However, for optimal PCR results, it is recommended to use DNA as fresh as possible.

(vi) For precise determination of the total number of HC-AdV and contaminating helper virus genomes present by qPCR, generate three serial dilutions (10^{-3}, 10^{-4} and 10^{-5}) of purified HC-AdV DNA obtained in Step B(v).

PROTOCOL

(vii) For generation of a standard curve for qPCR, 10^2–10^8 genome copies of a purified wild-type adenovirus serotype 5 preparation or any first-generation virus with known physical titer can be assayed. To prepare adenoviral DNA, perform Step B(i–v). Alternatively, a standard plasmid with the appropriate adenoviral sequence (L3) (see ref. 66) or the gene of interest contained in the HC-AdV can be used. However, the following steps describe the determination of the physical titer using wild-type adenovirus serotype 5.

(viii) To determine the physical titer of HC-AdV in final vector preparations, we perform qPCR using the LightCycler Systems (Applied Biosystems). The following primers can be used for every HC-AdV: Ad5ITRfw1-24 5′-CAT CAT CAA TAA TAT ACC TTA TTT-3′ (400 nM) and 436Rev 5′-ACG CCA CTT TGA CCC GGA ACG-3′ (400 nM). These primers amplify the ITR/packaging signal region with the LightCycler FastStart DNAMaster^{Plus} SYBR Green I kit. The program is set as follows: Preincubation at 95 °C for 10 min, amplification in 45 cycles at 95 °C for 10 s, 55 °C for 5 s and 72 °C for 30 s. On the basis of the standard curve (Step B(vii)), the total number of adenoviral genomes in your final vector preparation can be calculated. The amount of helper virus as determined in Step B(ix) needs to be subtracted.

(ix) qPCR for helper virus contamination is carried out by the Taqman 7500 Fast Real-Time PCR System (Applied Biosystems) amplifying a 235-bp area of the adenoviral late gene 3 (L3). Using the oligonucleotides L3 forward 5′-AGA AGC TTA GCA TCC GTT ACT CGA GTT GG-3′ (400 nM) and L3 reverse 5′-ATA AGC TTG CAT GTT GGT ATG CAG GAT GG-3′ (400 nM) together with an L3-specific probe 5′-Fam-CCA CCC GTG TGT ACC TGG TGG ACA-Tamra-3′ (300 nM) (Ella Biotech), the PCR is performed with the following program: AmpErase UNG reaction at 50 °C for 2 min, preincubation/activation at 95 °C for 10 min, amplification and data collection during 40 cycles (95 °C for 15 s and 60 °C for 1 min). Universal PCR Mastermix was used for Taqman qPCR. On the basis of the standard curve (Step B(vii)), the total number of helper virus genomes in your final vector preparation can be calculated.

(x) Owing to the back-recombination of E1 sequences contained in the genome of the 116 producer cell line, it is important to rule out whether replication-competent adenovirus is present in the HC-AdV preparation and the helper virus stock[66]. Purified virus can be analyzed by qPCR using the following primers, which specifically detect E1: E1-Adenovirus Forward 5′-GGG TGA GGA GTT TGT GTT AGA TTA TG-3′ (400 nM); E1-Adenovirus Reverse 5′-TCC TCC GGT GAT AAT GACAAG A-3′ (400 nM); E1-Adenovirus probe TET-5-AGC ACC CCG GGC ACG GTT G-3-TAMRA (300 nM).
▲ CRITICAL STEP These oligonucleotides will also detect chromosomal DNA from 293 cells in which the left arm of the adenoviral DNA, including E1, is stably integrated. Thus, these primer sets should be used only for final vector preparations.

(C) Measuring total particles and infectious units of the HC-AdV in the final vector preparation by qPCR ● TIMING **4 d**

(i) Seed 293 cells in four 60-mm tissue culture dishes. For infection, cells should reach 90% confluence.

(ii) To determine infectious units, infect cells of one tissue culture dish with 0.4 µl of CsCl-purified virus and a second tissue culture dish with 2 µl of CsCl-purified virus from Step 72. Harvest cells after 3 h with trypsin. For trypsinisation, remove medium, add enough trypsin to cover the whole plate (15 ml) and incubate at 37 °C and 5% CO_2 for 5 min. Flush off the cells with the trypsin covering the plate using a pipette. Pellet the cells by centrifugation at 890*g* for 3 min at room temperature. Resuspend pellet in 200 µl of DPBS. Wash the cells thoroughly with DPBS to remove free (noninfective) vector particles by centrifugation at 890*g* for 3 min at room temperature. Discard the supernatant and resuspend pellet in 200 µl of DPBS.
▲ CRITICAL STEP At least two different volumes of CsCl-purified virus should be used for infection used after qPCR and to be within the range of the standard curve (for generation of a standard curve, see also Step B(vii)). For determination of the infectious titer, it is crucial to remove all noninfective viral particles from the cell surfaces and the medium by trypsin treatment and thorough washing.

(iii) For determination of the number of total particles (physical titer), harvest 293 noninfected cells from Step C(i) without trypsin by flushing off the cells with the medium covering the cells using a pipette. Pellet the cells by centrifugation at 890*g* for 3 min at room temperature. Resuspend pellet in 200 µl of DPBS. Add 0.4 µl of CsCl-purified HC-AdV preparation directly to the pelleted cells.

(iv) Repeat Step C(iii) with the last tissue culture dish from Step C(i), but infect harvested cells with 2 µl of CsCl-purified HC-AdV.

(v) Isolate genomic DNA from cells in Steps C(ii–iv) (for a detailed protocol, see **Box 4**).
■ PAUSE POINT Genomic DNA can be stored at −20 °C for up to 1 month. However, for optimal PCR results, it is recommended to use DNA as fresh as possible.

(vi) To determine total particles and infectious particles, analyze serial dilutions of genomic DNA of infected 293 cells from Step C(ii), Step C(iii) and Step C(iv) by qPCR using specific primer (see Step B(viii)) for the detection of the adenoviral ITR (for qPCR setup, see Steps B(vi–ix)).

(D) Quantification of infectious units by Southern blot analysis ● TIMING **5 d**

(i) Seed HeLa cells in six 60-mm tissue culture dishes (0.8×10^6 cells per dish).

(ii) The next day, infect four dishes with multiplicity of infection (MOI) of 33, 11, 3.7 and 1.2 of a first-generation adenoviral vector for which the viral titer was determined by a plaque-forming assay (see **Box 1** (C)).

(iii) Infect one tissue culture dish from Step D(i) with 0.4 µl and the last tissue culture dish with 2 µl of the CsCl-purified HC-AdV from Step 72. Incubate all six dishes for 3 h in a tissue culture incubator (37 °C; 5% CO_2).

BOX 4 | ISOLATION OF GENOMIC DNA FROM CELL PELLETS ● TIMING 2 D

1. Resuspend cell pellet in 200 µl of DPBS and vortex for 3 s.
2. Add 200 µl of proteinase K–SDS solution.
3. Vortex suspension for 3 s and incubate 12–16 h at 55 °C while gently shaking.
4. Add 2 µl of RNAse A and incubate for 30 min at 37 °C.
5. To perform a phenol–chloroform extraction, add 350 µl of phenol:chloroform:isoamyl alcohol.
6. After centrifugation for 2 min at high speed (15,000*g*) in a microcentrifuge, transfer the supernatant to a new tube. Repeat phenol–chloroform extraction as described above (Steps 5 and 6 described in this box).
7. Add 50 µl of sodium acetate (pH 5, 3 M) to the supernatant and 1 ml of precooled EtOH (>99.8%; stored at −20 °C). Mix suspension vigorously.
8. To pellet genomic DNA, centrifuge samples for 10 min at high speed (15,000*g*).
9. After removal of the supernatant, add 500 µl of 70% EtOH and centrifuge for 2 min at high speed (15,000*g*). Remove the supernatant and add 500 µl of 70% EtOH.
10. Shake for ~30 min at room temperature.
11. After centrifugation at high speed (15,000*g*) for 2 min, remove the supernatant and air-dry DNA pellet.
▲ CRITICAL STEP Do not dry DNA pellet for a long time, as it will be harder to get genomic DNA in solution.
12. Resuspend the DNA pellet in 120 µl of TE buffer and shake the samples. If you encounter difficulties in getting the DNA into solution, incubate for ~1 h at 37 °C while shaking. If the DNA solution still appears viscous, shake the samples for several hours at 37 °C, or you may incubate samples at 55 °C for ~1 h.

(iv) Harvest cells by trypsin treatment (see Step C(ii)) and centrifuge them at 10,600*g* with a microcentrifuge for 2 min at 4 °C. Freeze cell pellets at −20 °C.
■ PAUSE POINT Cell pellets can be stored at −20 °C for several weeks.

(v) Thaw cell pellets and isolate genomic DNA (see **Box 4**). Digest 15 µg of DNA with *Hin*dIII to generate DNA fragments[62]. For specific detection of your gene of interest, you may also use other restriction enzymes.

(vi) For Southern blot analysis[62], prepare a 0.8% agarose gel[62] and load purified and digested genomic DNA from Step D(v). Perfom gel electrophoresis to separate DNA fragments.

(vii) Treat the gel with 200 ml of 0.125 N HCl for 30 min and subsequently with 200 ml of denaturation buffer (30 min). Transfer DNA from agarose gel to an alkaline membrane by capillary transfer in denaturation buffer (24 h)[62].

(viii) After transfer, incubate the membrane in neutralization buffer for 1 min at room temperature and cross-link three times by UV light irradiation at a dose of 1.5 J cm^{-2} (using UV Stratalinker 1800) to fix DNA to the membrane[62].
■ PAUSE POINT Cross-linked membrane can be stored at room temperature at a dry place for several weeks.

(ix) To generate a probe for Southern blot hybridization, which can be used for any HC-AdV preparation, PCR-amplify the 5′-ITR and the packaging signal for hybridization using the following primers: Ad5ITRfw1-24 5′-CAT CAT CAA TAA TAT ACC TTA TTT-3′ and 436Rev 5′-ACG CCA CTT TGA CCC GGA ACG-3′. PCR conditions: 95 °C for 15 s, 55 °C for 30 s, and 72 °C for 30 s, 35 cycles using Taq DNA Polymerase from New England Biolabs.

(x) Incubate the membrane in 2× SSC (25 ml) for 1 min at room temperature and subsequently prehybridize for 2 h at 62 °C in church buffer.

(xi) Label the probe generated in Step D(ix) with radioactive nucleotide derivate [α^{32}P]dCTP or [α-^{32}P]dATP using the PrimeIt II Random labeling kit according to the manufacturer's instructions.

(xii) Hybridize blots with [α-^{32}P]dCTP- or [α-^{32}P]dATP-labeled probe from Step D(ix) diluted in church buffer for 16–24 h at 62 °C (see ref. 62).

(xiii) Detect probe binding using Phosphoimager FLA-3000. Compare intensities of signals from samples (from infected cells from Step D(iii)) and from the standard samples (from infected cells from Step D(ii)) to estimate infectious titer. An example of a Southern blot analysis is shown in **Figure 7**.

(E) Physical and infectious titer standardized by adenovirus reference material ● TIMING 4 d

(i) For accurate measurements and production of clinical-grade HC-AdV, the adenoviral reference material (ARM) may be used in combination with Step A, B and D. The ARM is distributed by ATCC (cat. no. VR-1516) and is fully characterized regarding particle concentration and the amount of infectious units per volume. The advantage of this method is that adenoviral preparations produced in different laboratories can be directly compared also with respect to future clinical trials. This method is described in detail elsewhere[67].

(ii) To determine the physical and infectious titer of the HC-AdV, the adenovirus reference material might be used instead of the first-generation vector (see Step B(vii) and Step D(ii)).

(iii) Comparison of the intensities of bands specific for ARM or HC-AdV DNA indicates the relative infectivity. This method was described in more detail earlier[67].

PROTOCOL

● TIMING

The whole procedure takes ~5 weeks. An flow diagram overview is provided in **Figure 1**. However, preparations including amplification of the helper virus and the amplification of 116 cells are necessary and need to be completed during cloning and before starting the generation and amplification of HC-AdV. The following list will give an overview for the duration of the most important steps. Detailed timing is provided in the step-by-step procedure.

Box 1, amplification of the helper virus AdNG163R-2: ~2 weeks

Steps 1–13, cloning of the production plasmid of HC-AdV : ~2 weeks

Steps 14–23, linearization of HC-AdV production plasmid for transfection: ~5 h

Steps 24–37, transfection of linearized HC-AdV production plasmid and preamplification of HC-AdV in adherent 116 cells: ~14 d

Steps 38–45, amplification of 116 cells in suspension culture for infection with HC-AdV and helper virus AdNG163R-2: 5 d

Steps 46–50, infection of 116 cells in suspension with HC-AdV and helper virus AdNG163R-2: 3 h

Step 51, large-scale amplification of HC-AdV in spinner flask: 2 d

Steps 52–56, harvesting infected cells from spinner flask: 30 min

Steps 57–72, purification of HC-AdV: 3 d total

Step 73, Characterization and titration of final vector preparations: 1 h to 5 d, depending on the method of choice

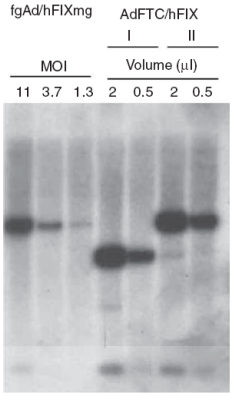

Figure 7 | Transducing units in final vector preparations as determined by Southern blot analysis. HeLa cells were seeded in 60-mm tissue culture dishes and transduced with the respective volumes of the final vector preparations. A standard curve was generated by infection with defined multiplicities of infection (MOIs) of cells with a first-generation adenoviral vector containing in part identical DNA sequences. Three hours postinfection, cells were harvested, genomic DNA isolated and samples were subjected to Southern blot analyses. To create a standard curve, the first-generation adenovirus fgAd/hFIXmg[24], which expresses the human coagulation factor IX (hFIX), was used for infection of HeLa cells. The Southern blot analysis shown here was performed to analyze two different HC-AdV preparations (I and II) with two different FIX expression cassettes.

? TROUBLESHOOTING

Too many or no colonies after transformation into DH10B cells (Step 11)

If you observe too many colonies on ampicillin-containing LB plates, either the I-*Ceu*I digest or the PI-*Sce*I digest of the vector pAdFTC or the *Swa*I digest of the ligation reaction was not complete.

If you have a low number of colonies or no colonies, check the competency of your competent DH10B cells. In addition, check the quality of DNA used for transformation and transformation conditions.

No insert detected in the plasmid pAdFTC derivate after ligation and transformantion (Step 12)

If you have difficulties cloning your gene of interest from the shuttle vector pHM5 into the adenoviral plasmid pAdFTC, make sure that all your materials for ligation (insert and vector) are freshly prepared on the same day and/or increase the amount of insert when setting up the ligation reaction. Alternatively, do not gel-purify the insert (Step 6), but purify I-*Ceu*I- and PI-*Sce*I-digested pHM5 shuttle plasmid by phenol–chloroform extraction followed by ethanol precipitation. Use this DNA for the ligation reaction (pHM5 contains a kanamycin and pAdFTC, an ampicillin resistance gene; therefore, religated pHM5 shuttle plasmid are unable to grow (Step 11)).

Incomplete release of the bacterial backbone from the HC-Ad production plasmid detected by agarose gel electrophoresis (Step 23)

Check the performance of your *Not*I enzyme and extend the time of *Not*I digestion and/or use more units of *Not*I. Make sure that precipitated DNA is resuspended completely.

Transfection efficiency of linearized vector is low (Steps 25A and B)

Check all reagents used for transfection. Make sure that the quality of DNA transfected into 116 cells is optimal. For quality control, transfect a plasmid expressing a marker gene (e.g., GFP or beta-galactosidase). Transfection efficiencies should range from 40% to 80%.

Insufficient viral preamplification steps using adherent 116 cells are not sufficient (Steps 29–37)

Some vectors may not be amplified sufficiently after finishing P3, and therefore, they may require additional passages. One may also increase the volume of the lysate used for infection: instead of one-third, one may use two-thirds of the cell–virus suspension for an additional amplification step (repeat Steps 34–37).

When establishing the protocol, it is best to start with amplifying an HC-AdV expressing a marker gene. If a marker gene is integrated in your HC-AdV genome (e.g., GFP or beta-galactosidase), amplification can be easily monitored at each step during pre- and large-scale amplification.

If you encounter difficulties amplifying HC-AdVs without a marker gene after establishing the protocol, simultaneously amplify an HC-AdV containing any marker gene. At each step, check amplification of the HC-AdV with the marker gene similar to the experiment depicted in **Figure 5**.

Make sure that your HC-AdV production plasmid contains all important components for virus amplification by restriction enzyme digest. To confirm that all DNA sequences essential for viral amplification are correct, you may also analyze by DNA sequencing whether the adenoviral 5′-ITR and packaging signal (using primer pDYAL21180 5′-ATG GCC TGG GCA TGG ACC GCA-3′) as well as the 3′-ITR (using primer pDYAL3858 5′-CGT GTG AGA TGG ACA TCC AGT-3′) are complete and not mutated.

Check the quality of the helper virus AdNG163R-2. Make sure by performing a plaque-forming assay (see **Box 1**) that infectious titer is not reduced.

The 116 production cell line must be free of mycoplasma, as the presence of mycoplasma contamination in the helper cell line may dramatically lower the adenovirus yields.

No or inefficient amplification of 116 cells grown in suspension (Steps 38–45)

Check for contamination, viability and growth (see **Box 3**) of 116 cells on each day after setting up the spinner flask (Step 38). Make sure that FBS was added to the tissue culture medium, no antibiotics were added and that the magnetic stirrer works properly. To compensate low growth rates, incubate for 48 h instead of 24 h after adding 1 liter of media in Step 44.
The 116 production cell line must be free of mycoplasma, as the presence of mycoplasma contamination in the helper cell lines may dramatically lower the adenovirus yields.

Only thin or no band visible in CsCl step gradient (Steps 66–70)

If the band visible in the CsCl step gradients consisting of packed viral particles (lower band) is thin and the titer of the CsCl-purified HC-AdV preparation as determined in Step 73 is low, the pre- and large-scale amplification was not optimal. Reamplify purified virus in 3-liter suspension culture of 116 cells (Step 38–56) using purified, low-titer HC-AdV preparation for infection (Step 48(B)). After reamplification, the band is usually much stronger.

If there was no band visible for packed viral particles after the CsCl step gradient, check virus amplification after each amplification step. You may monitor viral amplification during preamplification in adherent 116 cells and in 116 cells grown in suspension by removing an aliquot at each step (see also **Fig. 5**).

The quality of the linearized adenoviral genome for transfection (Step 23) and transfection efficiencies are also critical for achieving high final vector titers during preamplification. In addition, check the quality of the helper virus preparation by plaque-forming assay (see **Box 1**).

Titer in final vector preparation is low or no HC-AdV is detected after titration (Step 73)

Check all reagents and methods used for measuring the viral titer and repeat the procedures. If you obtain the same result with two different methods (titer of final vector preparation is low), the pre- and large-scale amplification was not optimal. Reamplify purified virus in 3-liter suspension culture of 116 cells (Step 48B). After reamplification, the band is usually much stronger.

Other reasons for low-titer HC-AdV preparations could be problems occuring during dialysis procedure in general. Therefore, repeat large-scale amplification and collect an aliquot after the second ultracentrifuge purification step (Step 70). Check if your HC-AdV is present before starting dialysis using one detection method (Step 73).

ANTICIPATED RESULTS

Average yields for an HC-AdV preparation from a 3-liter suspension culture are 1–2 ml, with an infectious titer of 5×10^6 to 5×10^7 TU μl^{-1} or, if determined as physical titer, 5×10^7 to 2×10^8 vp μl^{-1}. The contamination with helper-virus ranges between 0.02% and 0.2% (see refs. 55,67). Notably, when using the cell–virus suspension from Step 37 for initial large-scale amplification, the titer might vary dependent on preamplification steps.

ACKNOWLEDGMENTS This work was supported by DFG grants SFB455 and SPP1230 and the Wilhelm Sander Stiftung to A.E. We thank Philip Ng for helpful discussions and advice.

Published online at http://www.natureprotocols.com/
Reprints and permissions information is available online at http://npg.nature.com/reprintsandpermissions/

1. Luo, J. *et al.* A protocol for rapid generation of recombinant adenoviruses using the AdEasy system. *Nat. Protoc.* **2**, 1236–1247 (2007).
2. Yang, Y., Ertl, H.C. & Wilson, J.M. MHC class I-restricted cytotoxic T lymphocytes to viral antigens destroy hepatocytes in mice infected with E1-deleted recombinant adenoviruses. *Immunity* **1**, 433–442 (1994).
3. Hardy, S., Kitamura, M., Harris-Stansil, T., Dai, Y. & Phipps, M.L. Construction of adenovirus vectors through Cre-lox recombination. *J. Virol.* **71**, 1842–1849 (1997).
4. Hartigan-O'Connor, D., Amalfitano, A. & Chamberlain, J.S. Improved production of gutted adenovirus in cells expressing adenovirus preterminal protein and DNA polymerase. *J. Virol.* **73**, 7835–7841 (1999).
5. Fisher, K.J., Choi, H., Burda, J., Chen, S.J. & Wilson, J.M. Recombinant adenovirus deleted of all viral genes for gene therapy of cystic fibrosis. *Virology* **217**, 11–22 (1996).
6. Parks, R.J. *et al.* A helper-dependent adenovirus vector system: removal of helper virus by Cre-mediated excision of the viral packaging signal. *Proc. Natl. Acad. Sci. USA* **93**, 13565–13570 (1996).
7. Zhang, Y. & Bergelson, J.M. Adenovirus receptors. *J. Virol.* **79**, 12125–12131 (2005).
8. Benihoud, K., Yeh, P. & Perricaudet, M. Adenovirus vectors for gene delivery. *Curr. Opin. Biotechnol.* **10**, 440–447 (1999).

PROTOCOL

9. Kozarsky, K.F. & Wilson, J.M. Gene therapy: adenovirus vectors. *Curr. Opin. Genet. Dev.* **3**, 499–503 (1993).
10. Wickham, T.J., Roelvink, P.W., Brough, D.E. & Kovesdi, I. Adenovirus targeted to heparan-containing receptors increases its gene delivery efficiency to multiple cell types. *Nat. Biotechnol.* **14**, 1570–1573 (1996).
11. Kawano, R. *et al.* Transduction of full-length dystrophin to multiple skeletal muscles improves motor performance and life span in utrophin/dystrophin double knockout mice. *Mol. Ther.* **16**, 825–831 (2008).
12. Deol, J.R. *et al.* Successful compensation for dystrophin deficiency by a helper-dependent adenovirus expressing full-length utrophin. *Mol. Ther.* **15**, 1767–1774 (2007).
13. Gilbert, R. *et al.* Prolonged dystrophin expression and functional correction of mdx mouse muscle following gene transfer with a helper-dependent (gutted) adenovirus-encoding murine dystrophin. *Hum. Mol. Genet.* **12**, 1287–1299 (2003).
14. Brown, B.D. *et al.* Helper-dependent adenoviral vectors mediate therapeutic factor VIII expression for several months with minimal accompanying toxicity in a canine model of severe hemophilia A. *Blood* **103**, 804–810 (2004).
15. McCormack, W.M. Jr. *et al.* Helper-dependent adenoviral gene therapy mediates long-term correction of the clotting defect in the canine hemophilia A model. *J. Thromb. Haemost.* **4**, 1218–1225 (2006).
16. Cerullo, V. *et al.* Correction of murine hemophilia A and immunological differences of factor VIII variants delivered by helper-dependent adenoviral vectors. *Mol. Ther.* **15**, 2080–2087 (2007).
17. Koeberl, D.D. *et al.* Efficacy of helper-dependent adenovirus vector-mediated gene therapy in murine glycogen storage disease type Ia. *Mol. Ther.* **15**, 1253–1258 (2007).
18. Oka, K. *et al.* Sustained phenotypic correction in a mouse model of hypoalphalipoproteinemia with a helper-dependent adenovirus vector. *Gene. Ther.* **14**, 191–202 (2007).
19. Toietta, G. *et al.* Lifelong elimination of hyperbilirubinemia in the Gunn rat with a single injection of helper-dependent adenoviral vector. *Proc. Natl. Acad. Sci. USA* **102**, 3930–3935 (2005).
20. Mian, A. *et al.* Long-term correction of ornithine transcarbamylase deficiency by WPRE-mediated overexpression using a helper-dependent adenovirus. *Mol. Ther.* **10**, 492–499 (2004).
21. Nomura, S. *et al.* Low-density lipoprotein receptor gene therapy using helper-dependent adenovirus produces long-term protection against atherosclerosis in a mouse model of familial hypercholesterolemia. *Gene. Ther.* **11**, 1540–1548 (2004).
22. Brunetti-Pierri, N. *et al.* Sustained phenotypic correction of canine hemophilia B after systemic administration of helper-dependent adenoviral vector. *Hum. Gene. Ther.* **16**, 811–820 (2005).
23. Ehrhardt, A. *et al.* A gene-deleted adenoviral vector results in phenotypic correction of canine hemophilia B without liver toxicity or thrombocytopenia. *Blood* **102**, 2403–2411 (2003).
24. Ehrhardt, A. & Kay, M.A. A new adenoviral helper-dependent vector results in long-term therapeutic levels of human coagulation factor IX at low doses *in vivo*. *Blood* **99**, 3923–3930 (2002).
25. Lamartina, S. *et al.* Helper-dependent adenovirus for the gene therapy of proliferative retinopathies: stable gene transfer, regulated gene expression and therapeutic efficacy. *J. Gene. Med.* **9**, 862–874 (2007).
26. Butti, E. *et al.* IL4 gene delivery to the CNS recruits regulatory T cells and induces clinical recovery in mouse models of multiple sclerosis. *Gene. Ther.* **15**, 504–515 (2008).
27. Brunetti-Pierri, N. *et al.* Pseudo-hydrodynamic delivery of helper-dependent adenoviral vectors into non-human primates for liver-directed gene therapy. *Mol. Ther.* **15**, 732–740 (2007).
28. Jager, L. & Ehrhardt, A. Emerging adenoviral vectors for stable correction of genetic disorders. *Curr. Gene. Ther.* **7**, 272–283 (2007).
29. Soifer, H. *et al.* A novel, helper-dependent, adenovirus-retrovirus hybrid vector: stable transduction by a two-stage mechanism. *Mol. Ther.* **5**, 599–608 (2002).
30. Picard-Maureau, M. *et al.* Foamy virus-adenovirus hybrid vectors. *Gene. Ther.* **11**, 722–728 (2004).
31. Yant, S.R. *et al.* Iransposition from a gutless adeno-transposon vector stabilizes transgene expression *in vivo*. *Nat. Biotechnol.* **20**, 999–1005 (2002).
32. Ehrhardt, A. *et al.* Somatic integration from an adenoviral hybrid vector into a hot spot in mouse liver results in persistent transgene expression levels *in vivo*. *Mol. Ther.* **15**, 146–156 (2007).
33. Lieber, A., Steinwaerder, D.S., Carlson, C.A. & Kay, M.A. Integrating adenovirus-adeno-associated virus hybrid vectors devoid of all viral genes. *J. Virol.* **73**, 9314–9324 (1999).
34. Recchia, A., Perani, L., Sartori, D., Olgiati, C. & Mavilio, F. Site-specific integration of functional transgenes into the human genome by adeno/AAV hybrid vectors. *Mol. Ther.* **10**, 660–670 (2004).
35. Kreppel, F. & Kochanek, S. Long-term transgene expression in proliferating cells mediated by episomally maintained high-capacity adenovirus vectors. *J. Virol.* **78**, 9–22 (2004).
36. Dorigo, O. *et al.* Development of a novel helper-dependent adenovirus–Epstein–Barr virus hybrid system for the stable transformation of mammalian cells. *J Virol* **78**, 6556–6566 (2004).
37. Suzuki, K. *et al.* Highly efficient transient gene expression and gene targeting in primate embryonic stem cells with helper-dependent adenoviral vectors. *Proc. Natl. Acad. Sci. USA* **105**, 13781–13786 (2008).
38. Ohbayashi, F. *et al.* Correction of chromosomal mutation and random integration in embryonic stem cells with helper-dependent adenoviral vectors. *Proc. Natl. Acad. Sci. USA* **102**, 13628–13633 (2005).
39. Cregan, S.P. *et al.* Helper-dependent adenovirus vectors: their use as a gene delivery system to neurons. *Gene. Ther.* **7**, 1200–1209 (2000).
40. Wang, H., Cao, H., Wohlfahrt, M., Kiem, H.P. & Lieber, A. Tightly regulated gene expression in human hematopoietic stem cells after transduction with helper-dependent Ad5/35 vectors. *Exp. Hematol.* **36**, 823–831 (2008).
41. Balamotis, M.A., Huang, K. & Mitani, K. Efficient delivery and stable gene expression in a hematopoietic cell line using a chimeric serotype 35 fiber pseudotyped helper-dependent adenoviral vector. *Virology* **324**, 229–237 (2004).
42. Cerullo, V. *et al.* Toll-like receptor 9 triggers an innate immune response to helper-dependent adenoviral vectors. *Mol. Ther.* **15**, 378–385 (2007).
43. Zhu, J., Huang, X. & Yang, Y. Innate immune response to adenoviral vectors is mediated by both Toll-like receptor-dependent and -independent pathways. *J. Virol.* **81**, 3170–3180 (2007).
44. Koehler, D.R. *et al.* Aerosol delivery of an enhanced helper-dependent adenovirus formulation to rabbit lung using an intratracheal catheter. *J. Gene. Med.* **7**, 1409–1420 (2005).
45. Croyle, M.A., Yu, Q.C. & Wilson, J.M. Development of a rapid method for the PEGylation of adenoviruses with enhanced transduction and improved stability under harsh storage conditions. *Hum. Gene. Ther.* **11**, 1713–1722 (2000).
46. Ruzsics, Z. *et al.* Transposon-assisted cloning and traceless mutagenesis of adenoviruses: Development of a novel vector based on species D. *J. Virol.* **80**, 8100–8113 (2006).
47. Umana, P. *et al.* Efficient FLPe recombinase enables scalable production of helper-dependent adenoviral vectors with negligible helper-virus contamination. *Nat. Biotechnol.* **19**, 582–585 (2001).
48. Ng, P., Beauchamp, C., Evelegh, C., Parks, R. & Graham, F.L. Development of a FLP/frt system for generating helper-dependent adenoviral vectors. *Mol. Ther.* **3**, 809–815 (2001).
49. Meneses-Acosta, A. *et al.* Development of a suspension serum-free helper-dependent adenovirus production system and assessment of co-infection conditions. *J. Virol. Methods* **148**, 106–114 (2008).
50. Zhou, H. *et al.* A Cre-expressing cell line and an E1/E2a double-deleted virus for preparation of helper-dependent adenovirus vector. *Mol. Ther.* **3**, 613–622 (2001).
51. Barjot, C., Hartigan-O'Connor, D., Salvatori, G., Scott, J.M. & Chamberlain, J.S. Gutted adenoviral vector growth using E1/E2b/E3-deleted helper viruses. *J. Gene. Med.* **4**, 480–489 (2002).
52. Ng, P., Parks, R.J. & Graham, F.L. Preparation of helper-dependent adenoviral vectors. *Methods Mol. Med.* **69**, 371–388 (2002).
53. Sandig, V. *et al.* Optimization of the helper-dependent adenovirus system for production and potency *in vivo*. *Proc. Natl. Acad. Sci. USA* **97**, 1002–1007 (2000).
54. Rauschhuber, C., Xu, H., Salazar, F.H., Marion, P.L. & Ehrhardt, A. Exploring gene-deleted adenoviral vectors for delivery of short hairpin RNAs and reduction of hepatitis B virus infection in mice. *J. Gene. Med.* **10**, 878–889 (2008).
55. Palmer, D. & Ng, P. Improved system for helper-dependent adenoviral vector production. *Mol. Ther.* **8**, 846–852 (2003).
56. Hillgenberg, M., Schnieders, F., Loser, P. & Strauss, M. System for efficient helper-dependent minimal adenovirus construction and rescue. *Hum. Gene. Ther.* **12**, 643–657 (2001).
57. Shi, C.X., Graham, F.L. & Hitt, M.M. A convenient plasmid system for construction of helper-dependent adenoviral vectors and its application for analysis of the breast-cancer-specific mammaglobin promoter. *J. Gene. Med.* **8**, 442–451 (2006).
58. Toietta, G. *et al.* Generation of helper-dependent adenoviral vectors by homologous recombination. *Mol. Ther.* **5**, 204–210 (2002).
59. Mizuguchi, H. & Kay, M.A. Efficient construction of a recombinant adenovirus vector by an improved *in vitro* ligation method. *Hum. Gene. Ther.* **9**, 2577–2583 (1998).
60. Parks, R.J. & Graham, F.L. A helper-dependent system for adenovirus vector production helps define a lower limit for efficient DNA packaging. *J. Virol.* **71**, 3293–3298 (1997).
61. Bett, A.J., Prevec, L. & Graham, F.L. Packaging capacity and stability of human adenovirus type 5 vectors. *J. Virol.* **67**, 5911–5921 (1993).
62. Sambrook, J. & Russell, D.W. *Molecular Cloning: A Laboratory Manual* (Cold Spring Harbor Laboratory Press, Cold Spring Harbor, New York, 2001).
63. Offringa, R., Kwappenberg, K., Rabelink, M., Rea, D. & Hoeben, R. Adenoviral transduction of dendritic cells. *Methods Mol. Med.* **109**, 83–96 (2005).
64. Ugai, H. *et al.* Stability of a recombinant adenoviral vector: optimization of conditions for storage, transport and delivery. *Jpn. J. Cancer. Res.* **93**, 598–603 (2002).
65. Nyberg-Hoffman, C. & Aguilar-Cordova, E. Instability of adenoviral vectors during transport and its implication for clinical studies. *Nat. Med.* **5**, 955–957 (1999).
66. Puntel, M. *et al.* Quantification of high-capacity helper-dependent adenoviral vector genomes *in vitro* and *in vivo*, using quantitative TaqMan real-time polymerase chain reaction. *Hum. Gene. Ther.* **17**, 531–544 (2006).
67. Palmer, D.J. & Ng, P. Physical and infectious titers of helper-dependent adenoviral vectors: a method of direct comparison to the adenovirus reference material. *Mol. Ther.* **10**, 792–798 (2004).
68. Haase, S.B. & Calos, M.P. Replication control of autonomously replicating human sequences. *Nucleic Acids. Res.* **19**, 5053–5058 (1991).

Hyperactive Sleeping Beauty Transposase Enables Persistent Phenotypic Correction in Mice and a Canine Model for Hemophilia B

Martin A Hausl[1], Wenli Zhang[1], Nadine Müther[1], Christina Rauschhuber[1], Helen G Franck[2], Elizabeth P Merricks[2], Timothy C Nichols[2], Mark A Kay[3,4] and Anja Ehrhardt[1]

[1]Max von Pettenkofer-Institut, Department of Virology, Ludwig-Maximilians-Universität Munich, Munich, Germany; [2]Department of Pathology and Laboratory Medicine, University of North Carolina, Chapel Hill, North Carolina, USA; [3]Department of Pediatrics, School of Medicine, Stanford University, Stanford, California, USA; [4]Department of Genetics, School of Medicine, Stanford University, Stanford, California, USA

Sleeping Beauty (SB) transposase enables somatic integration of exogenous DNA in mammalian cells, but potency as a gene transfer vector especially in large mammals has been lacking. Herein, we show that hyperactive transposase system delivered by high-capacity adenoviral vectors (HC-AdVs) can result in somatic integration of a canine factor IX (cFIX) expression-cassette in canine liver, facilitating stabilized transgene expression and persistent haemostatic correction of canine hemophilia B with negligible toxicity. We observed stabilized cFIX expression levels during rapid cell cycling in mice and phenotypic correction of the bleeding diathesis in hemophilia B dogs for up to 960 days. In contrast, systemic administration of an inactive transposase system resulted in rapid loss of transgene expression and transient phenotypic correction. Notably, in dogs a higher viral dose of the active SB transposase system resulted into transient phenotypic correction accompanied by transient increase of liver enzymes. Molecular analysis of liver samples revealed SB-mediated integration and provide evidence that transgene expression was derived mainly from integrated vector forms. Demonstrating that a viral vector system can deliver clinically relevant levels of a therapeutic protein in a large animal model of human disease paves a new path toward the possible cure of genetic diseases.

Received 2 February 2010; accepted 13 July 2010; published online 17 August 2010. doi:10.1038/mt.2010.169

INTRODUCTION

Hemophilia B is an X-linked inherited blood clotting disorder caused by mutations in the coagulation factor IX (*FIX*) gene. This genetic disease has a prevalence of about 1 in 30,000 Caucasian males. Current standard therapies for hemophilia B are based on protein infusion treatments utilizing recombinant proteins or plasma-derived blood components. However, limitations of this treatment option are the potential development of inhibitors, the inconvenience of repeated injections of the coagulation factor concentrates, and the expenses of replacement factor production.

As an alternative treatment strategy for hemophilia B, a plethora of liver-based gene therapy approaches have been proposed. Preclinical studies in murine and canine models for hemophilia B involving gene delivery vehicles based on retrovirus, lentivirus, adeno-associated virus (AAV), and recombinant adenovirus were performed. Moloney murine leukemia virus-based retroviral vectors for example, which integrate into the host genome, were utilized in hemophilia dogs.[1] Furthermore, lentiviral vectors have been shown to be sufficient in mice but efficacy in hemophilia B dogs remains to be shown.[2,3] To date the longest duration of canine FIX (cFIX) expression (8 years) in hemophilia B dogs was demonstrated after a single liver-directed injection of a recombinant AAV based on serotype 2 vector (AAV2).[4] In that particular study it is claimed that extrachromosomal AAV vector genomes were responsible for long-term expression of cFIX. Unfortunately, in the context of a clinical trial in hemophilia patients, this AAV-based approach resulted in transient phenotypic correction (2 months) of the bleeding diathesis[5] most likely due to an adaptive immune response directed against the incoming viral capsid.

In the present study, we utilized an integrating adenoviral hybrid-vector system for somatic integration and long-term phenotypic correction of the bleeding disorder. Various generations of recombinant adenoviral vectors were used in the past for the treatment of hemophilia B. The early generation vectors deleted for the early-transcribed adenoviral genes *E1* and *E3* resulted in therapeutic cFIX levels in mice and hemophilia B dogs. However, cFIX levels in mouse serum although in a therapeutic range significantly decreased over time and plasma cFIX levels of treated animals declined to undetectable levels 2 months postinjection.[6] It became clear that synthesized viral antigens expressed from the early generation recombinant adenoviral genomes induced immune responses that are at least in part responsible for destruction of transduced cells. The primary immune effector cells in this process are major histocompatibility complex class I-restricted cytotoxic T-lymphocytes.[7–9] Further deletion of the E2a, E2b, or E4 regions, while appearing safer, still resulted in some toxicity.[10–12]

Correspondence: *Anja Ehrhardt, Max von Pettenkofer-Institut, Department of Virology, Ludwig-Maximilians-Universität München, Pettenkofer Street 9A, 80336 Munich, Germany. E-mail: ehrhardt@mvp.uni-muenchen.de*

The newest generation of adenoviral vectors is deleted for all viral coding sequences allowing for packaging of up to 36 kb of foreign DNA.[13,14] These vectors are commonly referred to as "gutted," gene-deleted, helper-dependent, or high-capacity adenoviral vectors (HC-AdVs). It was demonstrated that hepatic transduction utilizing HC-AdV is not accompanied by chronic toxicity due to the absence of viral gene expression.[15,16] However, even HC-AdVs exhibit some dose-dependent toxicity related to the incoming viral particles (vps).[17] It was shown that systemic cytokines including the early indicator of inflammation interleukin-6 as mediators of the innate immune responses were activated[17,18] and an attenuated adaptive immune response was observed due to an infiltration of adenovirus-specific cytotoxic T-lymphocytes.[19]

Nonetheless, none of the currently available gene transfer vehicles for gene therapeutic applications is flawless and, to date, HC-AdV still represents one of the most promising gene delivery vehicles. This type of vector has been shown to result in long-term transgene expression and phenotypic correction in various species and animal models. We and others have shown that after a single injection a HC-AdV can be maintained life-long in mice and for up to 2 years in rats.[16,20–23] In dogs and nonhuman primates, HC-AdV liver transduction also led to long-term transgene expression.[15,16] To date, the longest period of transgene expression (up to 964 days) was observed by Brunetti-Pierri and colleagues using a HC-AdV for hepatic transduction of baboons.[16,24] With respect to canine hemophilia B, there are currently two studies utilizing HC-AdV based on human adenovirus serotype 5. Our previous study demonstrated that, at a nontoxic dose, transient phenotypic correction can be achieved for several weeks after systemic administration of HC-AdV into hemophilia B dogs.[25] Another study observed long-term phenotypic correction at a higher dose which in turn was associated with transient liver toxicity.[26]

With a very few exceptions (*e.g.*, in embryonic stem cells)[27] adenoviral vectors are believed to integrate into host chromosomes at low frequencies.[28,29] To prolong the therapeutic effect after liver-based adenoviral gene transfer and to stabilize persistence of the therapeutic DNA at a lower dose, we hypothesized that somatic integration of the transgene from the episomal adenoviral vector genome into the host genome may stabilize and prolong the therapeutic effect. To test this hypothesis, we evaluated an improved version of our previously described adenovirus/Sleeping Beauty (SB) transposase hybrid-vector system[30] for the first time in a canine model for hemophilia B. For high integration efficiencies into genomic DNA, the hybrid-vector technology utilized in the present study was based on a hyperactive version of the SB transposase (HSB5). This transposable element was originally generated from inactive copies of an ancestral Tc1/mariner-like transposon in fish[31] and the mechanism for SB-mediated somatic integration is schematically shown in **Figure 1a**. By performing a mutational analysis screen the hyperactive mutant HSB5 was identified displaying tenfold higher integration efficiencies compared to wild-type SB.[32] Herein, we show that this integrating viral vector system results in significantly stabilized transgene expression in rapidly dividing hepatocytes in mice. Furthermore, we demonstrate for the first time efficacy of a SB transposase system in a large animal exemplified by long-term phenotypic correction in a canine model for hemophilia B.

RESULTS

A two-component system for transposon mobilization from HC-AdVs

To achieve stabilized transgene expression, we used an improved version of the "two-vector-system" presented in our previous study.[30] This system relies on cotransduction of one cell with two HC-AdVs. The first vector represents the transposon donor-vector (HC-AdV-TcFIX) which contains a transposon encoding the canine coagulation factor IX (cFIX)[25] under the control of the liver-specific human α-1-antitrypsin promoter (hAAT) flanked by FRT recognition sites for Flp-mediated recombination (**Figure 1b**). The second vector (HC-AdV-HSB5) encodes Flp recombinase and the hyperactive SB transposase mutant HSB5 (**Figure 1b**), which displays tenfold increased integration efficiencies in comparison to the wild-type transposase.[32] The mechanism of transposition from the adenoviral vector depends on two steps (**Figure 1c**). After both vectors cotransduce a target cell, Flp recombinase first mediates circularization of the transposon from the adenoviral vector genome. This step was necessary because adenoviral vector genomes predominantly exist as linear DNA molecule and we showed in the past that transposition mainly works from circular substrates.[30] In a second step, the excised circle serves as a substrate for SB transposase-mediated somatic integration.

As a negative control for the integration machinery a derivate of the second vector (HC-AdV-mSB) containing an inactive version of SB transposase (mSB) was generated (**Figure 1b**). HC-AdVs were produced according to a previously described protocol for large-scale production of HC-AdV in spinner flasks.[33,34] Final vector preparations were analyzed for helper virus contamination levels and the amount of transducing units per volume of the HC-AdV was determined (for details see **Supplementary Materials and Methods** section).

Stable transgene expression in mice after a single injection of the adenovirus/SB transposase hybrid-vector system

To address the question whether the new version of the adenoviral hybrid-vector system results into stable transgene expression levels *in vivo*, C57Bl/6 mice were coinjected at a ratio of 3:1 with the vectors HC-AdV-TcFIX and HC-AdV-HSB5, respectively. As a negative control for HSB5-mediated somatic integration, mice were treated with HC-AdV-mSB instead of HC-AdV-HSB5. In two independent experiments, animals were injected with 3×10^{10} and 1×10^{10} vps, respectively, or with a twofold higher dose. Animal injections, the viral dose, and the vector combinations, which were used, are summarized in **Table 1**. To demonstrate HSB5-mediated integration of the transgene expression-cassette from the adenoviral vector genome into the host chromosomal DNA, we intraperitoneally injected carbon tetrachloride (CCl_4) 5–7 weeks after vector administration. CCl_4 causes liver damage and therefore in treated liver tissue rapid cell cycling takes place to reconstitute normal liver size. As a consequence episomal vector forms are lost due to cell division whereas integrated transposons are maintained. To analyze stability of canine FIX expression, cFIX serum levels were measured periodically by enzyme-linked immunosorbent assay (ELISA) (**Figure 2a**). For mice treated with the functional SB transposase system, plasma cFIX levels maintained stable in a

Table 1 Summary of animal injections

				Vector 1			Vector 2		
Animal	Species	Gender	Weight	Type	TU/kg	vps/kg	Type	TU/kg	vps/kg
M1	C57Bl/6 mouse	Female	~25 g	HC-AdV-TcFIX	6.0×10^{10}	1.2×10^{12}	HC-AdV-HSB5	2.0×10^{10}	4.0×10^{11}
M2–M4	C57Bl/6 mice	Female	~25 g	HC-AdV-TcFIX	6.0×10^{10}	1.2×10^{12}	HC-AdV-mSB	2.0×10^{10}	4.0×10^{11}
M5–M6	C57Bl/6 mice	Female	~25 g	HC-AdV-TcFIX	1.2×10^{11}	2.4×10^{12}	HC-AdV-HSB5	4.0×10^{10}	8.0×10^{11}
M7–M8	C57Bl/6 mice	Female	~25 g	HC-AdV-TcFIX	1.2×10^{11}	2.4×10^{12}	HC-AdV-mSB	4.0×10^{10}	8.0×10^{11}
D1	Hemophilia B dog	Female	16.3 kg	HC-AdV-TcFIX	3.1×10^{10}	6.2×10^{11}	HC-AdV-HSB5	1.6×10^{10}	3.2×10^{11}
D2	Hemophilia B dog	Female	13.7 kg	HC-AdV-TcFIX	7.7×10^{10}	1.5×10^{12}	HC-AdV-HSB5	3.9×10^{10}	7.8×10^{11}
D3	Hemophilia B dog	Female	16.7 kg	HC-AdV-TcFIX	3.4×10^{10}	7.0×10^{11}	HC-AdV-mSB	1.7×10^{10}	3.4×10^{11}

Abbreviations: HC-AdV, high-capacity adenoviral vector; HSB5, hyperactive Sleeping Beauty transposase; mSB, inactive transposase system; TU, transducing units; vps, viral particles.
Mice (M1–M8) and hemophilia B dogs (D1–D3) were injected either with the hyperactive (M1, M5, M6, D2) or the inactive SB (M2–M4, M7, M8, D3) Sleeping Beauty (SB) transposase system. For injections into mice, two independent experiments are shown (M1–M4 and M5–M8).

physiological range (cFIX levels of 2,000–10,000 ng/ml) even after injection of CCl_4, whereas in mice transduced with vector encoding the inactive mSB, serum cFIX levels significantly dropped after CCl_4 administration to concentrations <150 ng/ml (mice M2–M4) or undetectable levels (mice M7 and M8).

As additional control, we analyzed the expression from episomal HC-AdV-TcFIX without Flp-mediated excision of the transposon. Therefore, mice were injected with the HC-AdV-TcFIX and HC-AdV-luciferase (see also **Supplementary Materials and Methods** section), a HC-AdV encoding for firefly luciferase replacing the vector HC-AdV-HSB5 in our experimental setup. Before injection of CCl_4 similar serum, cFIX levels were detected in both groups. However, after a single injection of the liver toxin CCl_4 expression levels rapidly decreased within the next 3 weeks (from serum cFIX levels of 1,300 to levels of 120 ng/ml) (**Supplementary Figure S1**). In sharp contrast, transgene expression levels from untreated mice remained stable.

To directly compare stability of transgene expression from episomal HC-AdV, HC-AdVs from which the transgene is excised, and HC-AdVs from which the transgene is excised and subsequently integrated into the host genome, we determined the loss rate of transgene expression for all systems with and without induction of rapid cell cycling in murine liver. We found that our integrating HC-AdV system utilizing HSB5 for somatic integration is superior in cycling cells compared to episomal HC-AdVs (**Figure 2b**). Moreover, we observed that the loss rate of transgene expression was independent of excision of the transposon from the adenoviral vector (**Figure 2b**). In conclusion, these results demonstrate that our system is clearly superior in rapidly dividing cells compared to conventionally used HC-AdVs, suggesting that this system may be useful for stable transduction of dividing cells (*e.g.*, stem cells).

We also performed limited toxicity studies by monitoring alanine aminotransferase (ALT) levels in mouse serum samples of treated mice to detect acute toxicity associated with administration of HC-AdVs. As a negative control, mice were injected with Dulbecco's phosphate-buffered saline (PBS), the solvent for the HC-AdVs for injections. One day postinjection comparable ALT levels were measured in mice which received the HSB5 or the mSB vector system (**Figure 2c**). Although ALT levels in HSB5- and mSB-treated mice were slightly elevated compared to the control group treated with Dulbecco's PBS, we would like to emphasize that ALT levels remained in the normal range for all treated mice (20–80 IU/l).

Phenotypic correction after intravenous injection of the adenovirus/SB tranposase hybrid-vector system into hemophilia B dogs

After verifying that this improved version of the transposase system works efficiently in mice, we addressed the question whether transposition enables phenotypic correction in a preclinical animal model for hemophilia B. Therefore, we intravenously injected three hemophilia B dogs carrying a missense mutation in the catalytic domain of the genomic cFIX coding sequence.[35] All dogs (D1, D2, and D3) were coinjected with the canine factor IX (cFIX) transposon donor vector and the transposase delivery vector at a 2:1 ratio. Virus injections, the viral dose, and the vector combinations, which were used in hemophilia B dogs, are summarized in **Table 1**. D1 received a total dose of 9.4×10^{11} vps/kg of the HSB5 system and D2 a 2.6-fold increased dose (2.4×10^{12} vps/kg). As a control, dog D3 was injected with the inactive version of the transposase system at a total dose of 1.2×10^{12} vps/kg, which was equivalent to the virus dose applied in dog D1.

For dog D1, which received the HSB5-based hybrid-vector system, the whole blood clotting time was shortened to 18.5 minutes and stabilized for the total length of the study (960 days) (**Figure 3a**). This clearly demonstrated that phenotypic correction of the coagulation factor IX deficiency occurred and suggested that in contrast to our historical study utilizing a comparable dose of the cFIX encoding vector,[25] stabilization of transgene expression occurred. In sharp contrast, systemic administration of the inactive transposase system (mSB) in dog D3 at a similar viral dose resulted in transient phenotypic correction for <16 days (**Figure 3c**). Surprisingly, dog D2, which also was treated with the HSB5-system but with an increased dose showed only transient phenotypic correction (**Figure 3b**). This may indicate that toxic side effects associated with the incoming viral proteins or a robust immunological response against incoming vps or against one of the transgene products may have occurred.

In order to monitor transgene expression, cFIX levels in canine plasma samples were monitored. We detected supra-physiological plasma cFIX levels of up to 40,000 ng/ml (normal

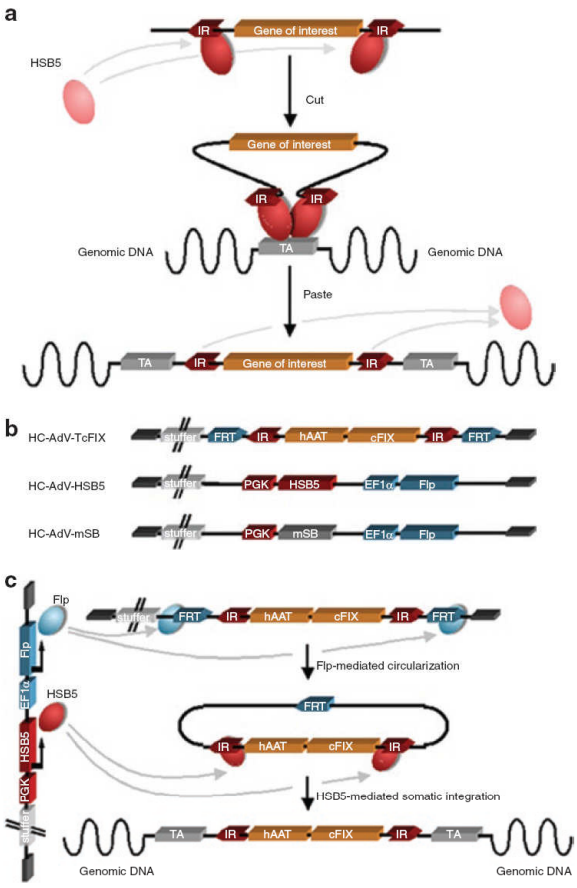

Figure 1 Mechanism of Sleeping Beauty (SB) transposition and the high-capacity adenoviral vector (HC-AdV) system for delivery. (**a**) Depicted is a two-component system in which a gene of interest flanked by transposon-derived inverted repeats (IRs) is mobilized by the transposase protein provided in trans. For gene transfer experiments, the transposon is usually excised from a plasmid and integrated into a genomic target site (TA). This mechanism is commonly referred to as "cut-and-paste" mechanism. (**b**) HC-AdV-TcFIX represents the transposon-donor vector from which the transposon is mobilized. The transposon[15] flanked by inverted repeats (IRs) and FRT sites for Flp-mediated excision. It expresses canine coagulation factor IX (cFIX) under control of the liver-specific human α-1-antitrypsin promoter (hAAT) including two liver-specific enhancers (HCR, hepatocyte control region; ApoE: apolipoprotein E). The HC-AdV-HSB5 contains a transgene expression-cassette for the hyperactive Sleeping Beauty (SB) transposase HSB5 under the control of the phosphoglycerate kinase promoter (PGK) and an expression-cassette for the Flp recombinase driven by the elongation factor-1-α promoter (EF1α). The control vector HC-AdV-mSB contains the mutated and inactive version of SB (mSB). All HC-AdVs include 22-kb stuffer DNA derived from human chromosomal DNA to optimize packaging of viral vectors. (**c**) For somatic integration cells are simultaneously infected with HC-AdV-TcFIX and HC-AdV-HSB5. Expressed Flp-recombinase recognizes FRT sites and mediates circularization and therefore transposon mobilization from the HC-AdV, which is essential for HSB5 functionality. Inverted repeats (IRs) of circularized intermediates are recognized by expressed hyperactive SB protein provided in trans, mediating somatic integration of the transposon into the cellular genome. HC-AdV, high-capacity adenoviral vector; HSB5, hyperactive Sleeping Beauty transposase; mSB, inactive transposase system.

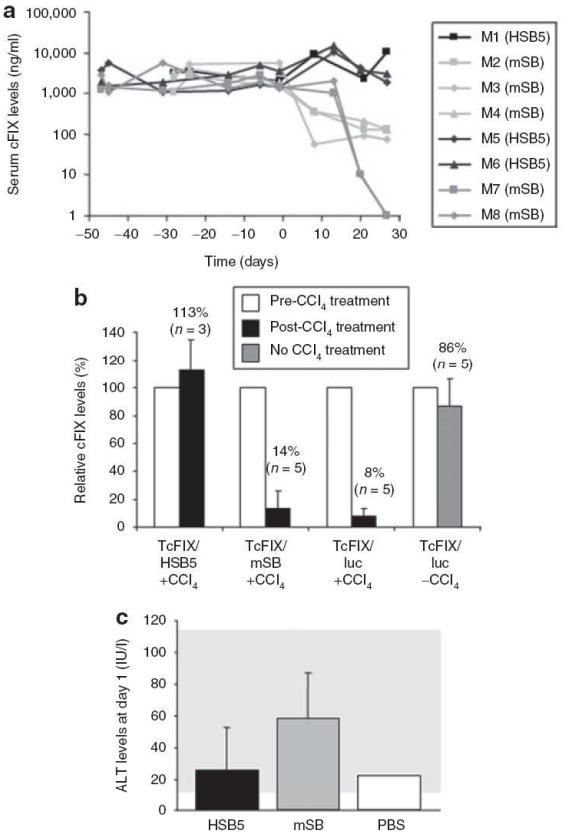

Figure 2 Stability of expression levels in mice treated with adenovirus-transposase hybrid-vectors and acute toxicity related with vectors. C57Bl/6 mice were coinjected with HC-AdV-TcFIX and HC-AdV-HSB5 at a ratio of 3:1 with a total number of 8×10^{10} viral particles (mouse M1) or 4×10^{10} viral particles (mice M5 and M6). Mice of the control groups were treated with HC-AdV-mSB instead of HC-AdV-HSB5 (8×10^{10} viral particles: mice M2–M4; 4×10^{10} viral particles: mice M7 and M8). Four to seven weeks after vector administration rapid hepatocyte proliferation was induced at day 0 by intraperitonal injection of carbon tetrachloride (CCl_4) to analyze stability of transgene expression and somatic integration. (**a**) Canine FIX expression levels were measured periodically by ELISA. (**b**) Relative transgene expression levels in mice after delivery of HC-AdV-TcFIX with either HC-AdV-HSB5 (TcFIX/HSB5 + CCl_4), HC-AdV-mSB (TcFIX/mSB + CCl_4) or the irrelevant vector HC-AdV-luciferase (TcFIX/Luc + CCl_4) as a control for persistence of the canine FIX-expressing vector without excision of the transgene by Flp recombination. To analyze persistence of transgene expression without CCl_4 treatment (TcFIX/luc –CCl_4), another control group solely received the vector HC-AdV-TcFIX and HC-AdV-luciferase. A total of 8×10^8 transducing units were injected at a ratio of 3:1 (transposon TcFIX vector: HSB5, mSB, or Luc vector). Mice were treated with CCl_4 and serum levels of cFIX before CCl_4 treatment (white bar) were defined as 100% for each group. Black bar, post-CCl_4 treatment; gray bar: no CCl_4 treatment. Serum cFIX levels were determined 3 weeks after CCl_4 treatment for all groups. (**c**) Alanine transaminase (ALT) levels in serum samples of mice 1 day postinjection were measured to detect acute liver toxicity related with HC-AdV administration. Serum samples of mice injected with Dulbecco's phosphate-buffered saline (DPBS), the solvent for intravenous application of HC-AdVs were used as a negative control. cFIX, canine factor IX; ELISA, enzyme-linked immunosorbent assay; HC-AdV, high-capacity adenoviral vector; HSB5, hyperactive Sleeping Beauty transposase; mSB, inactive transposase system; PBS, phosphate-buffered saline.

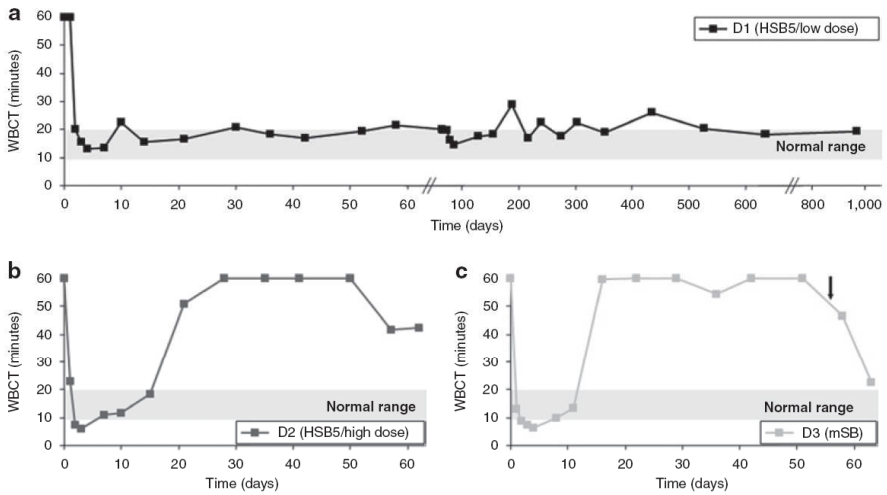

Figure 3 Whole blood clotting time (WBCT) as indicator for phenotypic correction in treated hemophilia B dogs. The whole blood clotting time (WBCT) is an indicator for a functional coagulation cascade and therefore for a sufficient replacement of the inactive factor IX in hemophilia B dogs. The WBCT for untreated hemophilia B dogs is longer than 60 minutes. After injection of HC-AdVs the WBCT was measured periodically for (**a**) D1 (HSB5/low dose), (**b**) D2 (HSB5/high dose), and (**c**) D3 (mSB). The black arrow indicates a bleeding episode, which was treated by cFIX administration. cFIX, canine factor IX; HC-AdV, high-capacity adenoviral vector; HSB5, hyperactive Sleeping Beauty transposase; mSB, inactive transposase system.

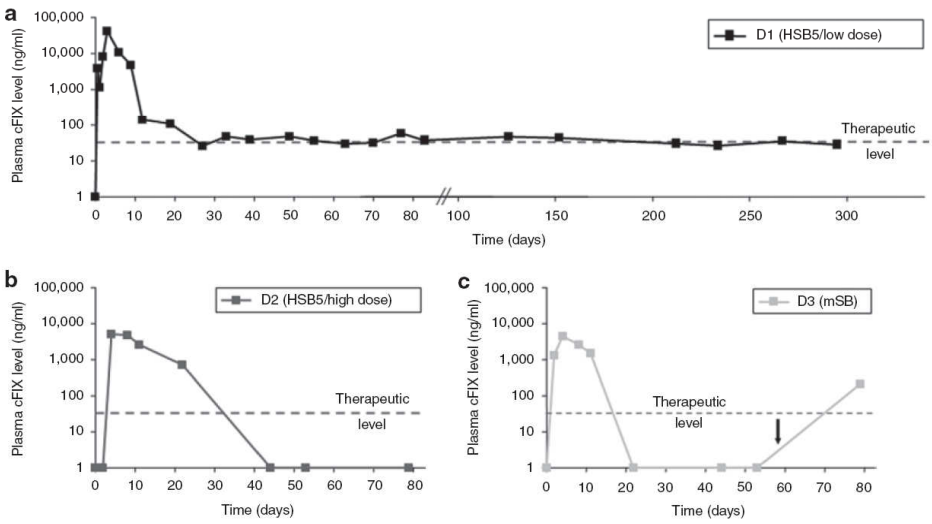

Figure 4 Expression levels of canine factor IX in treated hemophilia B dogs. The expression level of canine factor IX (cFIX), which is encoded by the transposon, was measured by ELISA. Normal cFIX plasma levels of healthy dogs are between 500 and 12,000 ng/ml. Notably, 50 ng/ml are sufficient for effective coagulation (therapeutic level). Plasma levels of cFIX were measured in hemophilia B dog (**a**) D1 (HSB5/low dose), (**b**) D2 (HSB5/high dose), and (**c**) D3 (mSB). The black arrow indicates the administration of cFIX after a bleeding episode. ELISA, enzyme-linked immunosorbent assay; HSB5, hyperactive Sleeping Beauty transposase; mSB, inactive transposase system.

cFIX level = 5,000 ng/ml) for dog D1 3–9 days postinjection (Figure 4a). During days 9 and 27 postinjection, we observed a rapid decline of cFIX plasma levels. However, after 4 weeks, plasma cFIX levels stabilized within a therapeutic range (60 ng/ml) for up to 295 days (latest time point analyzed by cFIX ELISA). For dogs D2 and D3 we observed physiological cFIX plasma levels 5–10 days postinjection which declined to undetectable levels 40 and 20 days postinjection for dogs D2 and D3, respectively (Figure 4b,c).

Laboratory measurements and toxicity profile in hemophilia B dogs

To investigate whether vector related toxicity occurred, we performed a plethora of laboratory measurements. We monitored

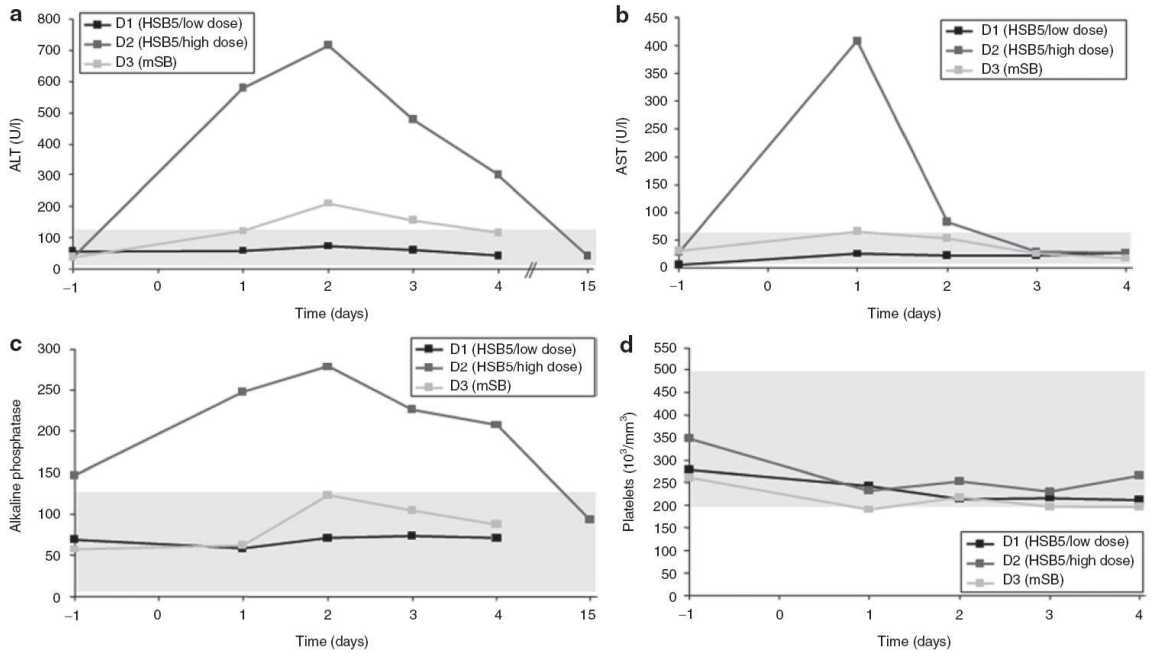

Figure 5 Acute toxicity profile of treated hemophilia B dogs. Plasma samples of dogs D1 (HSB5/low dose), D2 (HSB5/high dose), and D3 (mSB) were collected at indicated time points and analyzed for markers related with acute liver toxicity. (**a**) Alanine aminotransferase levels (ALT; normal range 12–118 U/l) were measured as well as (**b**) aspartate aminotransferase levels (AST; normal range 15–66 U/l), and (**c**) alkaline phosphatase levels (normal range 5–131 U/l). In addition (**d**) the number of platelets (normal range 200,000–500,000 per mm^3) were quantified for all three dogs. HSB5, hyperactive Sleeping Beauty transposase; mSB, inactive transposase system.

aspartate aminotransferase (normal range, 12–118 U/l) and ALT (normal range, 15–66 U/l) levels in plasma of dogs D1, D2, and D3. We found that ALT and aspartate aminotransferase levels were elevated in dog D2, whereas transaminase levels for dogs D1 and D3 remained in a normal range (Figure 5a,b). Quantification of alkaline phosphatase levels revealed that this parameter was increased in dog D2, whereas levels stayed in a normal range for dogs D1 and D3 (Figure 5c). In concordance with these results, we also observed the most significant drop of platelets in dog D2 (Figure 5d). Furthermore, all other monitored parameters remained in a normal range for dogs D1 and D3. All laboratory measurements for treated dogs D1, D2, and D3 are summarized in **Supplementary Table S1**.

Lack of antibodies against cFIX and detection of low levels for neutralizing antiadenoviral antibodies

To further investigate the potential reasons for transient phenotypic correction in dogs D2 and D3 and the rapid decrease of cFIX plasma levels in dog D1 during the first weeks postinjection, we searched for anti-cFIX inhibitors and measured neutralizing antiadenoviral antibody levels. The Bethesda inhibitor assay was used to detect anti-cFIX inhibitors in dog plasma before and after injection, but no antibodies against the transgene-encoded product were detected in either dog (data not shown). Thus, the decrease in cFIX transgene expression was not caused by a humoral immune response directed against the recombinant cFIX protein.

For analysis of the humoral immune response directed against the adenoviral vector, we examined dog serum at various time points for the presence of antiadenoviral neutralizing antibodies. For this purpose, we used a neutralization assay, measuring the inhibitory effect of antiadenoviral antibodies contained in canine serum samples by infection of 293 cells with an adenoviral vector encoding a reporter gene. Neutralizing antibodies for dog D1 were monitored until the end of the experiment (960 days postinjection) and for dogs D2 and D3 up to 80 days postinjection (latest time points measured). Highest levels were measured 2–3 weeks post-treatment (Figure 6). Although the biological relevance of this finding is not clear at the time, injection of HC-AdVs at a similar dose resulted in comparable or even higher levels of neutralizing antibodies in a previous study,[25] indicating that these levels are normal for the injected vector dose.

Molecular analysis of transgene persistence and detection of transposition events in canine liver

To demonstrate that the cFIX transposon underwent transposition in canine liver and to analyze the fate of transduced vector DNA, we performed detailed molecular analyses of liver-derived canine genomic DNA. First, we addressed the question whether episomal vector forms were maintained in liver cells or whether they were lost over time. Therefore, we performed semiquantitative PCR analysis of liver genomic DNA isolated from dog D1 960 days postinjection specifically detecting vector genome sequences contained in adenoviral vector genomes (amplified regions are depicted

in **Supplementary Figure S2**). We observed that episomal vector forms either containing the cFIX transposon (HC-AdV-TcFIX and the excised circular cFIX transposase substrate) or the hyperactive transposase (HC-AdV-HSB5) were below 0.01 and 0.0002 genome copy numbers per cell, respectively (**Figure 7a**). These results indicated that episomal vector genome numbers were strongly reduced over time. In contrast, 0.01 copy numbers per cell of the cFIX transposon were maintained in canine liver (**Figure 7a**) suggesting that cFIX expression was mainly derived from integrated transposons. However, more detailed studies need to be performed and at the time we cannot exclude whether transgene expression from episomal vector genomes may also contribute to measurable cFIX expression levels and phenotypic correction in dog D1. Similar tendencies for the vector status were obtained in mice (**Figure 7a**). In addition canine genomic DNA was analyzed for excised and episomal circular intermediates, but no evidence for the excised transposons could be shown (**Supplementary Figure S3**).

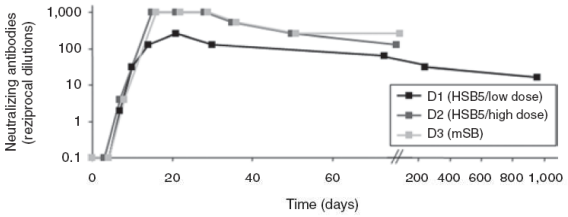

Figure 6 Neutralizing antibodies directed against adenoviral vectors in treated hemophilia B dogs. As an indicator for the adaptive immune response challenged by the HC-AdVs, neutralizing antibodies directed against the vector were measured. Therefore, the highest dilution of canine serum was determined, which is able to inhibit 50% transduction efficiencies of a reporter virus in 293 cells. The neutralizing-antibody titer was defined as the reciprocal of this dilution. HC-AdV, high-capacity adenoviral vector.

To determine sites of insertion after transposition, we applied a PCR-based assay, which detects chromosomal DNA linked to the integrated transposon inverted repeats (IRs). We identified transposition events with intact IR and integration into a target site-dinucleotide in genomic DNA of canine liver cells derived from dog D1 (**Figure 7b**; detailed blast results are depicted in **Supplementary Figure S4**).

DISCUSSION

This study evaluated for the first time efficacy of the SB transposase system in a large animal model. Herein, a hyperactive

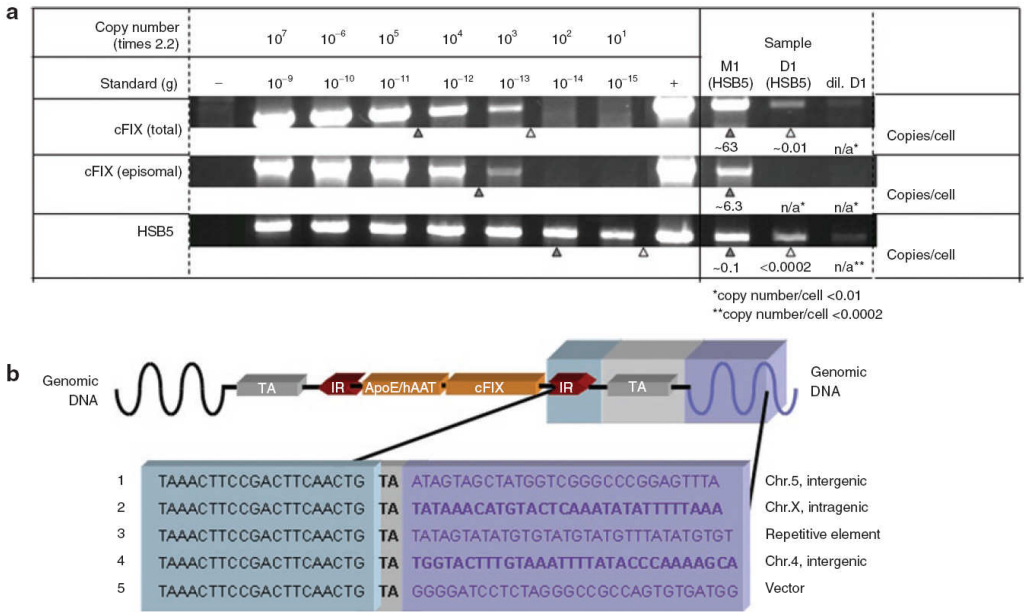

Figure 7 Molecular status of vector genomes and detection of transposition events in transduced liver cells. Hyperactive Sleeping Beauty transposase (HSB5)-transduced liver samples of mouse M1 (28 days post-CCl_4 treatment) and dog D1 (960 days postinjection) were analyzed regarding episomal HC-AdV genomes and canine factor IX (cFIX) transposon integrated into the host genome. (**a**) Fate of vector genomes in transduced canine and murine liver was analyzed by PCR. Top, total number of coagulation factor IX transgenes; middle, detection of intact and episomal transposase donor-vector genomes (high-capacity adenoviral vector HC-AdV-TcFIX); bottom, PCR specifically detecting Sleeping Beauty transposase encoding sequences. D1, liver genomic DNA from dog D1 (500 ng); dil. D1, liver genomic DNA from dog D1 (10 ng); M1, liver genomic DNA from mouse M1 (10 ng). Serial DNA standard dilutions ranged from 1 ng (10^{-9} g; 2.2 × 10^7 genome copies) to 1 fg (10^{-15} g; 22 genome copies) were analyzed and spiked with 50-ng genomic DNA derived from 293 cells to simulate canine genomic DNA in samples. Genomic DNA obtained from HeLa cells, infected with the corresponding viral vectors was used as positive control (+) whereas DNA from noninfected HeLa cells served as negative control (–). Vector genome copies are presented as copy numbers per liver cell (copy number/cell). (**b**) Identification of sites of insertion in canine liver cell genomes after HSB5-mediated transposition. Genomic regions containing the transposon were isolated, sequenced, and blasted against the canine genome database. Five integration events are depicted and the corresponding chromosomal regions are mentioned. HC-AdV, high-capacity adenoviral vector.

transposon-based vector system for somatic integration was delivered into hemophilia B dogs by a HC-AdV. We found that one dog (D1) showed long-term phenotypic correction (**Figure 3a**) of the clotting disorder (3 years) and persistent expression of cFIX (**Figure 4a**) which was mainly derived from integrated transgenes (**Figure 7a**). Furthermore, there was no measurable acute liver toxicity (**Figure 5a–d**).

However, application of a twofold higher viral dose (2.4×10^{12} vps/kg body weight) showed transient albeit complete correction of the hereditary genetic disease in canines (**Figure 3b**). Therefore, increasing the viral dose resulted in transient liver toxicity (**Figure 5a–d**) and may present one potential reason for the strong decrease of plasma cFIX levels observed in dog D2. A similar or even higher dose as compared to dog D2 was used in previous studies for phenotypic correction of canine hemophilia.[26,36,37] In concordance with our present study, these studies also measured transient hepatotoxicity after systemic administration of the HC-AdV at a viral vector load of $1–3 \times 10^{12}$ vps/kg body weight. These dose-dependent toxic effects are supported by our historical data in hemophilia B dogs showing that a lower dose of 0.9×10^{11} vps/kg resulted in undetectable liver toxicity and no thrombocytopenia.[25]

As speculated already in other studies performed in canines, our data emphasize that only a small therapeutic window for HC-AdV may exist. This dose threshold effect, for which a linear increase in viral vector dose does not correlate with protein expression, was also shown in mice.[38] However, the minimal dose in mice for achieving long-term transgene expression seems to be lower compared to canines. This underscores the species-dependent differences after systemic administration of adenoviral vectors and that direct extrapolation across species may not be possible.

In the present study, we explored for the first time a hyperactive SB transposase for somatic integration from an adenoviral vector. We believe that utilizing HSB5 with a tenfold higher transposition activity *in vitro* in comparison to wild-type SB which was used in our previous study[25] was probably a critical factor for achieving stabilized transgene expression in a large animal model. However, the actual integration efficiency of the HSB5-based system and the grade of improvement in comparison to our previously described two-vector system utilizing wild-type SB transposase[30] needs to be investigated in more detail. To further optimize our integrating vector system it may be interesting to explore a novel SB transposase mutant with 100-fold increased integration efficiencies (SB100×).[39] In fact, utilizing SB100× may allow further decreasing the viral vector dose for achieving sufficient integration and stabilized transgene expression, although a minimal dose which yet remains to be determined will still be required for cotransduction of cells with both vectors. Another approach for reducing the effective viral vector dose may be the use of hyperactive cFIX variants as shown by Brunetti-Pierri *et al.*, who delivered a hyperactive human FIX expression-cassette using an adenoviral vector resulting in an improved therapeutic effect.[40] Moreover, with respect to targeting liver cells, our approach could be optimized by utilizing more efficient routes of administration. For instance, the recently introduced pseudo-hydrodynamic balloon catheter injection method was shown to increase liver-transduction efficiency.[24]

Taking a closer look at the antiadenoviral neutralizing-antibody levels (**Figure 6**) for all treated dogs, an increase was observed 2 weeks after administration. During this time period, plasma cFIX levels decreased to low or even undetectable levels for all dogs. Because no significant anti-cFIX inhibitor levels were detected, this increase in antiadenoviral neutralizing-antibody levels could suggest that a robust adaptive immune response against the administrated viral vector capsids or cells presenting viral capsid proteins occurred. In particular the cellular immune response might be one major reason for the subsequent clearance of transduced cells and therefore the rapid decline in cFIX antigen levels. However, in the present study, we only analyzed antiadenoviral neutralizing-antibody levels in hemophilia B dogs and it is important to emphasize that not only the humoral immune response but also the innate immune system may play an important role.

Another safety issue of our hybrid-vector system may be the presence of HSB5 and Flp recombinase encoding DNA sequences in our vectors. Besides the fact, that for the SB transposase system overproduction inhibition could occur, which might potentially be the reason for transient effects in dog D2, high levels of SB transposase and/or Flp recombinase might result in genotoxicity or other adverse effects. Furthermore, at the time it is not known whether long-term expression *in vivo* of either SB transposase and/or Flp recombinase causes any side effects such as unwanted recombination of host genomic DNA which might even occur at low expression rates. However, our results indicated that episomal vector genomes were strongly reduced over time or even completely cleared from the organ. This could be shown for the vector encoding HSB5 as well as for cFIX (**Figure 7a**). These results are in concordance with previous data showing low frequencies of adenoviral vectors for homologous or heterologous integration events in transduced hepatocytes in mice.[28,29]

Regarding the safety for SB transposase-mediated integration, it is established that SB transposase mediates somatic integration into target site-dinucleotides.[31] Up to now no insertional mutagenesis is known for gene therapy studies utilizing SB transposases and a recent study revealed that SB shows a random integration pattern with a small bias toward genes.[41] Moreover, integration preferences were not significantly influenced by transcriptional activity. Although the dog-specific genomic sequence database from National Center for Biotechnology Information (NCBI) is not complete,[42,43] we have begun to analyze insertion sites after SB-mediated somatic integration from the adenoviral vector into the canine genome (**Figure 7b**). We realize that the number of insertion sites my not be representative at this point, but our genome-wide screen for sites of transposition events from the adenoviral vector in murine liver cells revealed a random integration pattern without any preferences for integration into transcriptionally active sites (data not shown).

The combination of the SB transposase system with gutless adenovirus showed significantly stabilized transgene expression during rapid cell cycling (**Figure 2a**). Furthermore, we showed that in the presence of cell division our novel vector system was superior to conventionally utilized and episomally maintained HC-AdVs (**Figure 2b**). However, we are aware of the fact that hepatocytes are in most cases quiescent cells and therefore, stable

liver-transduction for the treatment of hemophilia B may not be the perfect setup and model disease for our novel vector system. Moreover, it was also demonstrated that a single injection of an HC-AdV without integration machinery can result in long-term expression and phenotypic correction.[16,20–23] However, for instance for stable transduction of stem cells, progenitor cells or any other cell type which may undergo extensive cell division, our system may be a very valuable tool.

It is of note that in a previously published study, we found that HC-AdV genomes seem to be more stable during cell division compared to nonviral DNA.[44] However, within the present study we found that after injection of HC-AdV-TcFIX alone and subsequent CCl_4 treatment for induction of cell cycling transgene expression levels rapidly declined. This loss in transgene expression was as extensive as in mice which received the mSB encoding vector. Although this is somewhat different to our previously published study it is important to point out that in contrast to our newly performed experiment our previous study utilized partial hepatectomy for induction of cell cycling resulting into 2–3 cell divisions of each hepatocyte. In contrast, treatment with CCl_4 is harsher and results into extensive liver necrosis and subsequently also more cell divisions. This in turn may lead to a more extensive loss of episomal vector genomes. This is on concordance with our previous study in which we also observed a dramatic loss of transgene expression and vector genome copies after CCl_4 treatment.[45]

It is of note, that adenoviral vectors were utilized in the past to deliver other than SB-based integration machineries derived from retrotransposons, retrovirus, AAV, and bacteriophage-derived integrase phiC31 (reviewed in ref. 46). At the time, none of the currently available systems for somatic integration may be perfect with respect to genotoxicity and SB-mediated integration may represent a valuable alternative, however, site-specific integration into a single and "safe" genomic locus may be the ideal option. Towards this goal, SB fusion proteins exploring zinc-fingers for site-specific DNA binding[32,45] and zinc-finger nucleases in the context of viral vectors[46] are currently being explored.

Last but not least, one important challenge which needs to be addressed in the future is the complexity of the design of this adenovirus/SB transposase hybrid-vector system. To increase integration efficiency the ratio between transposons and SB transposase proteins should be optimized including the ratio between vectors and the promotors driving the transcription of SB transposase and Flp recombinase. Moreover, utilizing an inducible system for expression of the integration machinery might reduce genotoxic and immunogenic side effects and may decrease an overproduction inhibition effect. Finally, we believe that exploring a "one-vector-strategy" including all components for somatic integration (therapeutic DNA and the respective recombinase) in one vector genome is an option to overcome the necessity of cotransduction of one cell with two vectors.

In summary, this study provides for the first time novel insights into efficacy of adenoviral hybrid-vectors for somatic integration and the SB system in a larger animal model. For stable transduction and treatment of tissues with a high-cell turn-over rate, our system represents a valuable tool for treatment. For instance, treatment of diseases affecting the skin or *ex vivo* correction of hematopoietic stem cells may be feasible utilizing our vector system. We believe that with further improvements this system may even pave the way toward clinical applications.

MATERIALS AND METHODS

Generation of HC-AdVs. See **Supplementary Materials and Methods** section for detailed description of cloning procedures for generation of adenoviral production plasmids and HC-AdV amplification, purification, and titration.

Animal studies. C57Bl/6 mice were kept and treated according to the guidelines of the Ludwig Maximilians University of Munich (Munich, Germany). All mice were tail vein injected using a total volume of 200 µl. Viral vector preparations were diluted in Dulbecco's PBS. Rapid cell cycling of murine liver cells was induced by intraperitoneal administration of 50 µl CCl_4 (Sigma-Aldrich, Taufkirchen, Germany) solution (1:1 dilution in mineral oil).

Inbred hemophilia B dogs were from the University of North Carolina at Chapel Hill (Chapel Hill, NC). These hemophilia B dogs carry a missense mutation in the catalytic domain of the FIX-coding sequence resulting in undetectable FIX activity.[35] Dog studies were performed under the guidelines of the University of North Carolina. For vector administration, dogs were sedated with Domitor (750 µg/m^2 body surface area) and the vector dilution (~18.5 ml) followed by ~10 ml PBS for vector wash was infused by peripheral vein injection at 0.5 ml/minute into the right foreleg. During injection heart rate, blood pressure, and temperature were monitored. Routine laboratory measurements before and after adenoviral administration were performed as described earlier.[25,47]

Measurement of ALT serum levels in mice. For quantification of ALT levels in murine serum, we followed the instructions of the ALT detection kit (Randox, Crumlin, UK) as described earlier.[45] We applied 15 µl of murine serum for each reaction.

Blood analysis after adenoviral-mediated gene transfer into hemophilia B dogs. Blood samples were obtained periodically from hemophilia B dogs and the whole blood clotting time was determined as previously described.[25,47] A Bethesda inhibitor assay was used to detect anti-canine FIX inhibitors in dog serum. In brief, dog plasma samples were mixed with pooled normal canine plasma and incubated at 37 °C. The anti-canine FIX inhibitor titer was calculated from the residual FIX activity of each sample.

ELISA. The cFIX ELISA measuring cFIX levels in murine serum and canine plasma was performed.[48] Briefly, to coat ELISA plates, the polyclonal rabbit anti-cFIX primary antibody (RACIX-IG; Affinity Biologicals, Ancaster, ON, Canada) was diluted 1:500 for dog and 1:200 for mouse samples. After incubation with samples obtained from treated animals the sheep horseradish peroxidase–conjugated secondary antibody (SACIX-HRP; Affinity Biologicals) was diluted 1:1,000 and 1:200 for mouse and canine samples, respectively. For generation of a standard curve, dilutions of pooled dog plasma with a normal range of 5–11.5 µg/ml cFIX antigen were used.

Detection of neutralizing antiadenoviral antibodies. The principle of this test was to analyze at which dilution the canine serum potentially containing antiadenoviral antibodies is able to inhibit 50% of the transduction of a reporter virus. Two hundred and ninety three cells were cultured in Dulbecco's modified Eagle's medium supplemented with 10% fetal bovine serum. One day before performing the assay, 293 cells were seeded into 96-well tissue culture plates containing 100 µl medium. To destroy heat-sensitive complement components, dog serum was incubated at 56 °C for 40 minutes. Serum samples were diluted in twofold steps in Dulbecco's modified Eagle's medium with 10% heat-inactivated fetal bovine serum in a total volume of 50 µl. We added 50 µl of the lacZ-expressing reporter virus Ad-RSV/lacZ[6] diluted with Dulbecco's modified Eagle's medium containing 10% heat-inactivated fetal bovine serum (final concentration of 1×10^9 plaque-forming units/ml). After incubation of 1 hour at 37 °C,

the serum-virus mixture was applied to 293 cells with 80% confluency. After 24 hours, cells were fixed with 0.5% glutaraldehyde, washed with PBS, and stained in PBS-containing 3 mmol/l potassium ferricyanide, 3 mmol/l potassium ferrocyanide, 2 mmol/l $MgCl_2$, and 1 mg/ml 5-bromo-4-chloro-3-indolyl-β-D-galactopyranoside (X-gal). As a negative control serum samples derived from untreated dogs and PBS were used. The neutralizing antiadenovirus antibody titer was defined as the reciprocal of the highest dilution of serum at which the infectivity of the reporter virus was decreased by 50%.

Molecular characterization of vector genomes by PCR. To analyze whether adenoviral vector genomes were maintained in murine and canine liver and to determine the amount of the integrated cFIX encoding transposons, we isolated genomic DNA from liver tissue (~100 mg). PCR analysis was performed using GoTaq polymerase (Promega, Mannheim, Germany). For mouse samples 10 ng and for canine samples 500 and 10 ng (dil. D1) of isolated genomic DNA were subjected to PCR.

Semiquantitative PCRs for detection of total number of canine coagulation factor IX (cFIX) encoding DNA were run with 45 cycles at 95 °C for 45 seconds, 53 °C for 45 seconds, and 72 °C for 60 seconds using oligonucleotides ApoE for (5′- CCC AGA GAC TGT CTG ACT CA -3′) and cFIXshort.rev (5′-GAG ACA CAC CTC ATT ACA TA-3′). This PCR amplifies a 998-bp DNA fragment spanning the liver-specific hAAT promoter and the first part of the cFIX complementary DNA. Therefore, it detects episomal versions of the cFIX transgene (excised circles after Flp-recombinase recombination and complete adenoviral vector genomes of HC-AdV-TcFIX) as well as integrated copies of the cFIX encoding transposon.

To address the question whether episomal HC-AdV-TcFIX genomes (Figure 2b) were present, a touchdown-PCR specific for a 1,455-bp fragment of HC-AdV-TcFIX was run with 35 cycles at 95 °C for 45 seconds, 65 °C for 45 seconds, 72 °C for 90 seconds, decreasing the annealing temperature each cycle for 0.3 °C and utilizing the oligonucleotides pICeu (5′-TAA CTA TAA CGG TCC TAA GGT AGC -3′) and pApoE/hAAT-3 (5′- AGA TCA GGG GGA TCA TTC ACT GTC CCA GGT CA-3′).

For detection of HC-AdV-HSB5 a touchdown-PCR was performed with 35 cycles at 95 °C for 45 seconds, 65 °C for 45 seconds, 72 °C for 80 seconds, decreasing the annealing temperature at each cycle for 0.3 °C and using the oligonucleotides PGK-Pro_5_ *Bgl*II (5′- AGA TCT ACC GGG TAG GGG AGG CGC-3′) and HSB5'1,000 (5′-GCT CCC AAG GAT GAA CCA GAC TTG-3′) amplifying a 585 bp region.

Circular intermediates were detected by touchdown-PCR (product: 700 bp). Thirty-five cycles at 95 °C for 45 seconds, 65 °C for 45 seconds, 72 °C for 50 seconds, decreasing annealing temperature each cycle for 0.3 °C were performed and the oligonucleotides fwFRTcyclization (5′-CCA AGC TGT TTA AAG GCA CA-3′) and rev1FRTcyclization (5′-GTA GGT CAC GGT CTC GAA GC-3′) were used.

For calculation of genome copy numbers per cell we performed serial DNA standard dilutions of plasmids pHC-AdV-TcFIX and pHC-AdV-HSB5 ranging from 1 ng (10^{-9}g; 2.2×10^7 copies) to 1 fg (10^{-15}g; 22 copies). Dilutions were spiked with genomic DNA derived from HeLa cells. For calculation of genome copy numbers per cell, we took into account that one copy of a diploid canine and mouse genome contains 5 billion and 5.7 billion bp, respectively.

Analysis of sites of insertion after transposon-mediated somatic integration in canine liver cells. Genomic DNA isolated from canine liver cells was used to determine sites of insertion by the BD GenomeWalkerTM Kit from BD Biosciences Clontech (Heidelberg, Germany). Therefore four genomic DNA libraries were produced with restriction enzyme nucleases that create blunt-ended DNA fragments (*Stu*I, *EcoRV*, *Pvu*II, and *Ssp*I) and a linker was ligated to the DNA fragments. Subsequently a two-step PCR was performed in which one primer binds to the IR of the IR and the other primer binds to the linker (primer pair for first PCR: IR-specific primer 1, 5′-cct taa gac agg gaa tct tta ctc gga-3′ and adopter primer 1, 5′-gta ata cga ctc act ata ggg c-3′; primer pair for the nested PCR: IR-specific primer 2, 5′-ggc taa ggt gta tgt aaa ctt ccg act -3′ and adopter primer 2, 5′-act ata ggg cac gcg tgg t-3′). PCR products were subcloned using the Zero Blunt TOPO PCR cloning kit (Invitrogen, Karlsruhe, Germany) and analyzed by sequencing. Sequencing results were blasted against a dog-specific genomic sequence data base from NCBI (http://www.ncbi.nlm.nih.gov/projects/genome/guide/dog/).

SUPPLEMENTARY MATERIAL

Figure S1. Expression levels from episomal HC-AdVs.
Figure S2. PCR setups for specific detection of total cFIX and episomal HC-AdVs.
Figure S3. Detection of circular intermediates in transduced canine liver cells.
Figure S4. Detailed description of integration sites after SB-mediated transposition into genomic DNA of canine liver cells.
Table S1. Laboratory measurements of dogs D1 (HSB5), D2 (HSB5, high dose), and D3 (mSB).
Materials and Methods.

ACKNOWLEDGMENTS

The authors thank Philip Ng for providing the producer cell line 116 and the helper virus AdNG163R-2. This work was supported in part by DFG grants SFB 455 and SPP 1230, the Wilhelm Sander-Foundation, EU Framework Programme 7 (Persistent Transgenesis), the Friedrich-Baur-Foundation (A.E.) and the National Institutes of Health NHLBI HL064274 (M.A.K). W.Z. was supported by a fellowship from the Chinese Scholarship Council in cooperation with Northwestern A&F University (Yangling, China).

REFERENCES

1. Kay, MA, Rothenberg, S, Landen, CN, Bellinger, DA, Leland, F, Toman, C *et al.* (1993). *In vivo* gene therapy of hemophilia B: sustained partial correction in factor IX-deficient dogs. *Science* **262**: 117–119.
2. Brown, BD, Cantore, A, Annoni, A, Sergi, LS, Lombardo, A, Della Valle, P *et al.* (2007). A microRNA-regulated lentiviral vector mediates stable correction of hemophilia B mice. *Blood* **110**: 4144–4152.
3. Vandendriessche, T, Thorrez, L, Acosta-Sanchez, A, Petrus, I, Wang, L, Ma, L *et al.* (2007). Efficacy and safety of adeno-associated viral vectors based on serotype 8 and 9 vs. lentiviral vectors for hemophilia B gene therapy. *J Thromb Haemost* **5**: 16–24.
4. Niemeyer, GP, Herzog, RW, Mount, J, Arruda, VR, Tillson, DM, Hathcock, J *et al.* (2009). Long-term correction of inhibitor-prone hemophilia B dogs treated with liver-directed AAV2-mediated factor IX gene therapy. *Blood* **113**: 797–806.
5. Manno, CS, Pierce, GF, Arruda, VR, Glader, B, Ragni, M, Rasko, JJ *et al.* (2006). Successful transduction of liver in hemophilia by AAV-Factor IX and limitations imposed by the host immune response. *Nat Med* **12**: 342–347.
6. Kay, MA, Landen, CN, Rothenberg, SR, Taylor, LA, Leland, F, Wiehle, S *et al.* (1994). *In vivo* hepatic gene therapy: complete albeit transient correction of factor IX deficiency in hemophilia B dogs. *Proc Natl Acad Sci USA* **91**: 2353–2357.
7. Yang, Y, Ertl, HC and Wilson, JM (1994). MHC class I-restricted cytotoxic T lymphocytes to viral antigens destroy hepatocytes in mice infected with E1-deleted recombinant adenoviruses. *Immunity* **1**: 433–442.
8. Yang, Y, Xiang, Z, Ertl, HC and Wilson, JM (1995). Upregulation of class I major histocompatibility complex antigens by interferon gamma is necessary for T-cell-mediated elimination of recombinant adenovirus-infected hepatocytes in vivo. *Proc Natl Acad Sci USA* **92**: 7257–7261.
9. Yang, Y, Li, Q, Ertl, HC and Wilson, JM (1995). Cellular and humoral immune responses to viral antigens create barriers to lung-directed gene therapy with recombinant adenoviruses. *J Virol* **69**: 2004–2015.
10. Amalfitano, A, Hauser, MA, Hu, H, Serra, D, Begy, CR and Chamberlain, JS (1998). Production and characterization of improved adenovirus vectors with the E1, E2b, and E3 genes deleted. *J Virol* **72**: 926–933.
11. Andrews, JL, Kadan, MJ, Gorziglia, MI, Kaleko, M and Connelly, S (2001). Generation and characterization of E1/E2a/E3/E4-deficient adenoviral vectors encoding human factor VIII. *Mol Ther* **3**: 329–336.
12. Gorziglia, MI, Kadan, MJ, Yei, S, Lim, J, Lee, GM, Luthra, R *et al.* (1996). Elimination of both E1 and E2 from adenovirus vectors further improves prospects for *in vivo* human gene therapy. *J Virol* **70**: 4173–4178.
13. Parks, RJ, Chen, L, Anton, M, Sankar, U, Rudnicki, MA and Graham, FL (1996). A helper-dependent adenovirus vector system: removal of helper virus by Cre-mediated excision of the viral packaging signal. *Proc Natl Acad Sci USA* **93**: 13565–13570.
14. Parks, RJ and Graham, FL (1997). A helper-dependent system for adenovirus vector production helps define a lower limit for efficient DNA packaging. *J Virol* **71**: 3293–3298.
15. Brunetti-Pierri, N, Stapleton, GE, Palmer, DJ, Zuo, Y, Mane, VP, Finegold, MJ *et al.* (2007). Pseudo-hydrodynamic delivery of helper-dependent adenoviral vectors into non-human primates for liver-directed gene therapy. *Mol Ther* **15**: 732–740.

16. Morral, N, Parks, RJ, Zhou, H, Langston, C, Schiedner, G, Quinones, J *et al.* (1998). High doses of a helper-dependent adenoviral vector yield supraphysiological levels of α1-antitrypsin with negligible toxicity. *Hum Gene Ther* **9**: 2709–2716.
17. Brunetti-Pierri, N, Palmer, DJ, Beaudet, AL, Carey, KD, Finegold, M and Ng, P (2004). Acute toxicity after high-dose systemic injection of helper-dependent adenoviral vectors into nonhuman primates. *Hum Gene Ther* **15**: 35–46.
18. Mane, VP, Toietta, G, McCormack, WM, Conde, I, Clarke, C, Palmer, D *et al.* (2006). Modulation of TNFα, a determinant of acute toxicity associated with systemic delivery of first-generation and helper-dependent adenoviral vectors. *Gene Ther* **13**: 1272–1280.
19. Muruve, DA, Cotter, MJ, Zaiss, AK, White, LR, Liu, Q, Chan, T *et al.* (2004). Helper-dependent adenovirus vectors elicit intact innate but attenuated adaptive host immune responses in vivo. *J Virol* **78**: 5966–5972.
20. Ehrhardt, A and Kay, MA (2002). A new adenoviral helper-dependent vector results in long-term therapeutic levels of human coagulation factor IX at low doses in vivo. *Blood* **99**: 3923–3930.
21. Kim, IH, Józkowicz, A, Piedra, PA, Oka, K and Chan, L (2001). Lifetime correction of genetic deficiency in mice with a single injection of helper-dependent adenoviral vector. *Proc Natl Acad Sci USA* **98**: 13282–13287.
22. Schiedner, G, Morral, N, Parks, RJ, Wu, Y, Koopmans, SC, Langston, C *et al.* (1998). Genomic DNA transfer with a high-capacity adenovirus vector results in improved *in vivo* gene expression and decreased toxicity. *Nat Genet* **18**: 180–183.
23. Toietta, G, Mane, VP, Norona, WS, Finegold, MJ, Ng, P, McDonagh, AF *et al.* (2005). Lifelong elimination of hyperbilirubinemia in the Gunn rat with a single injection of helper-dependent adenoviral vector. *Proc Natl Acad Sci USA* **102**: 3930–3935.
24. Brunetti-Pierri, N, Stapleton, GE, Law, M, Breinholt, J, Palmer, DJ, Zuo, Y *et al.* (2009). Efficient, long-term hepatic gene transfer using clinically relevant HDAd doses by balloon occlusion catheter delivery in nonhuman primates. *Mol Ther* **17**: 327–333.
25. Ehrhardt, A, Xu, H, Dillow, AM, Bellinger, DA, Nichols, TC and Kay, MA (2003). A gene-deleted adenoviral vector results in phenotypic correction of canine hemophilia B without liver toxicity or thrombocytopenia. *Blood* **102**: 2403–2411.
26. Brunetti-Pierri, N, Nichols, TC, McCorquodale, S, Merricks, E, Palmer, DJ, Beaudet, AL *et al.* (2005). Sustained phenotypic correction of canine hemophilia B after systemic administration of helper-dependent adenoviral vector. *Hum Gene Ther* **16**: 811–820.
27. Ohbayashi, F, Balamotis, MA, Kishimoto, A, Aizawa, E, Diaz, A, Hasty, P *et al.* (2005). Correction of chromosomal mutation and random integration in embryonic stem cells with helper-dependent adenoviral vectors. *Proc Natl Acad Sci USA* **102**: 13628–13633.
28. Harui, A, Suzuki, S, Kochanek, S and Mitani, K (1999). Frequency and stability of chromosomal integration of adenovirus vectors. *J Virol* **73**: 6141–6146.
29. Stephen, SL, Sivanandam, VG and Kochanek, S (2008). Homologous and heterologous recombination between adenovirus vector DNA and chromosomal DNA. *J Gene Med* **10**: 1176–1189.
30. Yant, SR, Ehrhardt, A, Mikkelsen, JG, Meuse, L, Pham, T and Kay, MA (2002). Transposition from a gutless adeno-transposon vector stabilizes transgene expression in vivo. *Nat Biotechnol* **20**: 999–1005.
31. Ivics, Z, Hackett, PB, Plasterk, RH and Izsvák, Z (1997). Molecular reconstruction of Sleeping Beauty, a Tc1-like transposon from fish, and its transposition in human cells. *Cell* **91**: 501–510.
32. Yant, SR, Huang, Y, Akache, B and Kay, MA (2007). Site-directed transposon integration in human cells. *Nucleic Acids Res* **35**: e50.
33. Jager, L, Hausl, MA, Rauschhuber, C, Wolf, NM, Kay, MA and Ehrhardt, A (2009). A rapid protocol for construction and production of high-capacity adenoviral vectors. *Nat Protoc* **4**: 547–564.
34. Palmer, D and Ng, P (2003). Improved system for helper-dependent adenoviral vector production. *Mol Ther* **8**: 846–852.
35. Evans, JP, Brinkhous, KM, Brayer, GD, Reisner, HM and High, KA (1989). Canine hemophilia B resulting from a point mutation with unusual consequences. *Proc Natl Acad Sci USA* **86**: 10095–10099.
36. Brown, BD, Shi, CX, Powell, S, Hurlbut, D, Graham, FL and Lillicrap, D (2004). Helper-dependent adenoviral vectors mediate therapeutic factor VIII expression for several months with minimal accompanying toxicity in a canine model of severe hemophilia A. *Blood* **103**: 804–810.
37. McCormack, WM Jr, Seiler, MP, Bertin, TK, Ubhayakar, K, Palmer, DJ, Ng, P *et al.* (2006). Helper-dependent adenoviral gene therapy mediates long-term correction of the clotting defect in the canine hemophilia A model. *J Thromb Haemost* **4**: 1218–1225.
38. Bristol, JA, Shirley, P, Idamakanti, N, Kaleko, M and Connelly, S (2000). *In vivo* dose threshold effect of adenovirus-mediated factor VIII gene therapy in hemophiliac mice. *Mol Ther* **2**: 223–232.
39. Mátés, L, Chuah, MK, Belay, E, Jerchow, B, Manoj, N, Acosta-Sanchez, A *et al.* (2009). Molecular evolution of a novel hyperactive Sleeping Beauty transposase enables robust stable gene transfer in vertebrates. *Nat Genet* **41**: 753–761.
40. Brunetti-Pierri, N, Grove, NC, Zuo, Y, Edwards, R, Palmer, D, Cerullo, V *et al.* (2009). Bioengineered factor IX molecules with increased catalytic activity improve the therapeutic index of gene therapy vectors for hemophilia B. *Hum Gene Ther* **20**: 479–485.
41. Yant, SR, Wu, X, Huang, Y, Garrison, B, Burgess, SM and Kay, MA (2005). High-resolution genome-wide mapping of transposon integration in mammals. *Mol Cell Biol* **25**: 2085–2094.
42. Kirkness, EF, Bafna, V, Halpern, AL, Levy, S, Remington, K, Rusch, DB *et al.* (2003). The dog genome: survey sequencing and comparative analysis. *Science* **301**: 1898–1903.
43. Lindblad-Toh, K, Wade, CM, Mikkelsen, TS, Karlsson, EK, Jaffe, DB, Kamal, M *et al.* (2005). Genome sequence, comparative analysis and haplotype structure of the domestic dog. *Nature* **438**: 803–819.
44. Ehrhardt, A, Xu, H and Kay, MA (2003). Episomal persistence of recombinant adenoviral vector genomes during the cell cycle in vivo. *J Virol* **77**: 7689–7695.
45. Jager, L and Ehrhardt, A (2009). Persistence of high-capacity adenoviral vectors as replication-defective monomeric genomes *in vitro* and in murine liver. *Hum Gene Ther* **20**: 883–896.
46. Jager, L and Ehrhardt, A (2007). Emerging adenoviral vectors for stable correction of genetic disorders. *Curr Gene Ther* **7**: 272–283.
47. Snyder, RO, Miao, C, Meuse, L, Tubb, J, Donahue, BA, Lin, HF *et al.* (1999). Correction of hemophilia B in canine and murine models using recombinant adeno-associated viral vectors. *Nat Med* **5**: 64–70.
48. Xu, L, Gao, C, Sands, MS, Cai, SR, Nichols, TC, Bellinger, DA *et al.* (2003). Neonatal or hepatocyte growth factor-potentiated adult gene therapy with a retroviral vector results in therapeutic levels of canine factor IX for hemophilia B. *Blood* **101**: 3924–3932.

3.8 Supplements

3.8.1 Supplementary Figures

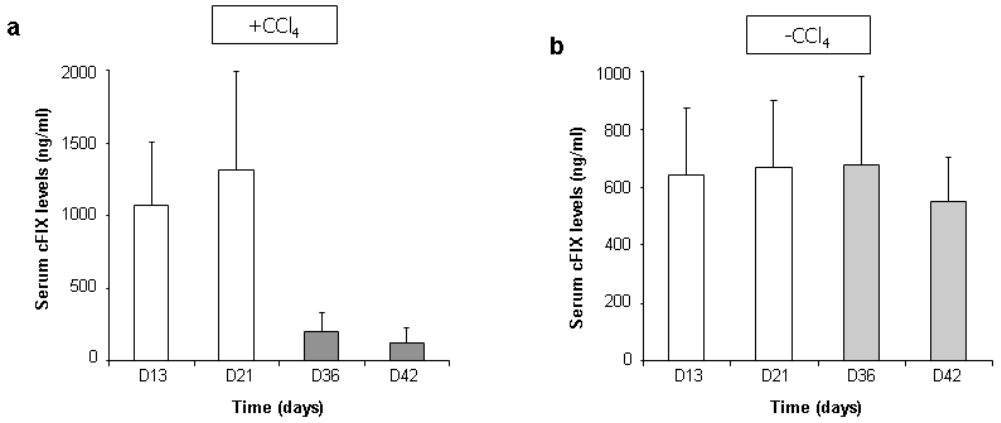

Supplementary Figure 3.1: Expression levels from episomal HC-AdVs. C57Bl/6 mice were co-injected with HC-AdV-TcFIX and HC-AdV-luciferase (n=10) at a ratio of 3: 1 (transposon TcFIX vector: luciferase vector) with a total number of $8x10^8$ transducing units. Three weeks after vector administration (on day 21 virus post-injection) one group (n=5) was injected with carbon tetrachloride ($+CCl_4$) to induce hepatocyte proliferation. (a) Stability of transgene expression was monitored by performing an ELISA two and three weeks post CCl_4 treatment (days 36 and 42). (b) The control group (n=5) was not treated with CCl_4 ($-CCl_4$).

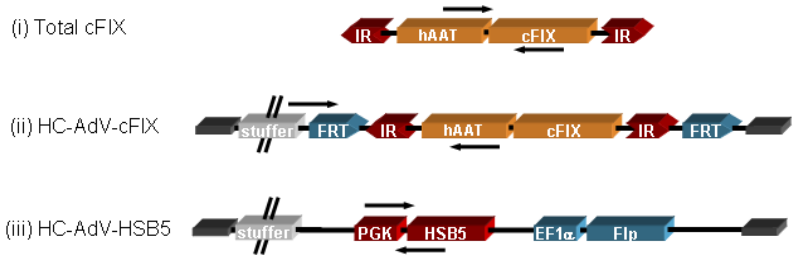

Supplementary Figure 3.2: PCR setups for specific detection of total cFIX and episomal HC-AdVs. Primers are presented as horizontal arrows. (i) For detection of all DNA sequences encoding the cFIX expression cassette, primer binding sites in the liver-specific hAAT-promotor and the cFIX encoding sequence were chosen. Therefore, interferences with the genomic cFIX encoding sequence were avoid and only transposon encoded expression cassettes were detected independent of the molecular status of the transposon (HC-AdV, circular intermediate or integrated transposon). (ii) Primer-set for amplification of the intact episomal HC-AdV-TcFIX genome without excision of the transposon. (iii) Primer-set specifically detecting Sleeping Beauty Transposase encoding sequences.

Supplementary Figure 3.3: Detection of circular intermediates in transduced canine liver cells. Additional PCR analysis to detect specifically episomal circular intermediates after Flp-mediated recombination was performed. (a) Primer binding site are depicted. (b) Two dilutions of liver genomic DNA from D1 (D1: 500 ng; D1 dil.: 10 ng) were analyzed. As a positive control (+) genomic DNA obtained from Hela cells infected with the corresponding viral vectors was used, whereas DNA from non-infected Hela cells served as negative control (–).

1 Canis familiaris chromosome 5 genomic contig, Accession number: NW_876312, intergenic
(27874 bp at 5' side: similar to Olfactory receptor 6M1; 36562 bp at 3' side: similar to Zinc finger protein 202)

2 Canis familiaris chromosome X genomic contig, Accession number: NW_879562.1, Exon, similar to Synaptophysin
(Major synaptic vesicle protein p38)

3 Repetitive element, many hits in the canine genome

4 Canis familiaris chromosome 4 genomic contig, Accession number: NW_876311.1, intergenic, low sequence homology (82 %)

5 HC-AdV DNA sequence (integration of the excised circle into HC-AdV DNA)

Supplementary Figure 3.4: Detailed description of integration sites after SB-mediated transposition into genomic DNA of canine liver cells.

3.8.2 Supplementary Tables

Day	WBC	HCT	HGB	CPK	Tot Bili	Amyl	Urea N	Creat	BUN/ Creat	Total Prot.	Alb	Glu	Chol	Ca+	P	Na+	K+	Chl	Alb/ Glob	Glob	Lip	Tri-glyc	GGTP	Mg+
Normal	6.0-17.0	37-55	12.0-18.0	59-895	.1-.3	290-1125	6.0-25	.5-1.6	4.0-27	5.0-7.4	2.7-4.4	70-136	92-324	8.9-11.4	2.5-6.0	139-154	3.6-5.5	102-120	.8-2.0	1.6-3.6	77-695	29-291	1.0-12	1.5-2.5
	(a)	(b)	(c)	(d)	(e)	(f)	(g)	(h)	(i)	(j)	(k)	(l)	(m)	(n)	(o)	(p)	(q)	(r)	(s)	(t)	(u)	(v)	(w)	(x)
D1																								
pre*	8,5	49,1	15,6	171	0,1	592	9	0,6	15	5,9	3,7	106	222	10,9	0.2L	151	4	112	1,7	2,2	400	42	<5	1,5
1	10	40,5	13,5	133	0,1	745	12	0,5	24	6	3,3	112	231	10,4	8.4H	148	4,2	112	1,2	2,7	547	37	<5	1.2L
2	7,3	43,7	14,6	228	0,2	530	10	0,5	20	6,2	3,2	97	212	10,4	6	148	4,3	112	1,1	3	441	27L	<5	1,5
3	8,4	47,5	15,3	214	0,1	583	13	0.4L	33H	6	3,6	111	247	10,3	8.1H	145	4,7	108	1,5	2,4	397	48	<5	1,6
4	7,3	44,9	15,2	135	2.0H	564	26H	0,8	33H	6	3,6	137	257	10,7	9.4H	159H	5,4	118	1,5	2,4	419	145	<5	1,7
7	8,6	47	15,6	245	0,2	675	13	0,7	19	6,3	3,4	101	248	10,8	7.8H	154	5,3	114	1,2	2,9	414	49	<5	1.4L
D2																								
pre*	6,8	39,4	13,3	233	0,1	457	8	0,5	16	5,8	2,9	92	263	10,5	7.5H	146	3,9	111	1	2,9	309	48	<5	1,5
1	6,5	40,9	13,5	338	0,2	541	10	0.4L	25	5,3	2,7	111	214	9,5	7.5H	145	3,8	115	1	2,6	456	69	6	1.3L
2	4.7L	41,8	13,9	243	0,1	439	16	0,5	32H	6,1	3,1	103	266	10,1	6.9H	148	4	115	1	3	509	76	8	1,7
3	4.9L	42,9	14,3	172	0,1	444	24	0,7	34H	5,9	2,9	106	272	10,4	7.9H	151	3,9	116	1	3	651	171	7	1,7
4	n.d.	n.d.	n.d.	247	0,1	453	14	0,5	28H	5,4	2,7	98	244	10	7.1H	145	4,4	111	1	2,7	615	76	6	1,5
7	8,2	38,9	13	352	0,2	593	16	0,6	27	5,7	3	110	250	10,4	7.8H	142	4,6	107	1,1	2,7	576	75	5	1,6
10	10,7	46,2	15	275	0,1	536	8	0,5	16	6,1	3	95	223	10,1	7.5H	146	4,5	110	1	3,1	396	59	6	1,6
15	7	39,3	13	214	0,2	693	11	0,7	16	5,1	2,9	105	223	10,6	7.0H	143	4,7	113	1,3	2,2	147	29	<5	1,5
D3																								
pre*	10,4	45,2	15,5	163	0,2	513	16	0,7	23	6,4	3,2	98	222	10,5	5,5	147	3,8	114	1	3,2	272	42	<5	1,5
1	6	35.2L	12,2	80	0,3	527	8	0,5	16	4.6L	2.4L	93	140	8.7L	4,6	152	4	121H	1,1	2,2	151	32	<5	1.1L
2	6,9	43,6	14,7	89	0,2	499	24	0,8	30H	5,4	2,7	101	157	9,5	4,8	149	4,3	112	1	2,7	227	140	5	1,7
3	4.5L	38,6	13,2	116	0,2	519	16	0,6	27	5,4	2.6L	99	157	9,5	5,7	146	4,2	116	0,9	2,8	338	60	5	1.4L
4	4.7L	40,8	13,5	115	0,2	524	25	0,6	42H	5,6	2,8	109	178	9,8	5,6	145	3,8	116	1	2,8	385	71	<5	1.4L

Supplementary Table 1.1: Laboratory measurements of dogs D1 (HSB5), D2 (HSB5, high dose) and D3 (mSB). Samples were collected periodically. (a) white blood count [103/mm3], (b) hematocrit [%], (c) hemoglobin [g/dL], (d) creatin phosphokinase [U/L], (e) total bilirubin [mg/dL], (f) amylase [U/L], (g) urea N [mg/dL], (h) creatinine [mg/dL], (i) Blood urea nitrogen (BUN)/creatinine, (j) total protein [g/L], (k) albumin [g/dL], (l) glutamine [mg/dL], (m) cholesterol [mg/dL], (n) calcium [mg/dL], (o) phosphate [mg/dL], (p) natrium [mEq/L], (q) potassium [mEq/L], (r) chloride [mEq/L], (s) albumin globulin ratio, (t) globulin [g/dL], (u) lipsosome [U/L], (v) triglyceride [mg/dL], (w) gamma glutamyltransferase [U/L], (x) magnesium [mEq/L], H: higher than normal range, L: lower than normal range. * Samples were collected 4 or 5 days before any treatment.

3.8.3 Supplementary Methods

1. Generation of high-capacity adenoviral vector DNA constructs

To generate the plasmids pFTC-HSB5-Flp and pFTC-mSB-Flp for production of high-capacity adenoviral vectors HC-AdV-HSB5 and HC-AdV-mSB (**Figure 1b**), we first ligated the blunted *Eco*RI/*Bam*HI fragment from pCMV-mSB and pCMV-HSB5[1,2] encoding either mSB or HSB5 into the *Pme*I site of pPGK-ΔTP[3,4]. The blunt-ended ClaI/NotI fragment, containing the PGK-promoter and HSB5 or mSB, was then cloned into T4-DNA polymerase treated *Sma*I/*Bsm*I digested plasmid pHD-SB-Flp-Δ*Not*I[3,4], generating the plasmids pHD-HSB5-Flp-ΔNotI (encoding HSB5 under the control of the PGK promoter and Flp under the control of the EF1-alpha promoter) and pHD-mSB-Flp-Δ*Not*I (encoding mSB under the control of the PGK promoter and Flp under the control of the EF1-alpha promoter). Flp recombinase and HSB5 or mSB expression cassettes were released by *Pac*I/*Pme*I digest, blunted and cloned into the *Pme*I site of pHM5*Pme*I derived from plasmid pHM5[5]. Therefore the plasmids pHM5*Pme*I-Flp-HSB5 and pHM5*Pme*I-Flp-mSB were constructed. I-*Ceu*I and PI-*Sce*I fragments from pHM5*Pme*I-Flp-HSB5 and pHM5*Pme*I-Flp-mSB were ligated into the I-*Ceu*I and PI-*Sce*I digested adenoviral production plasmid pAdFTC-I/S/P[6,7].

For construction of the adenoviral production plasmid pFTC-TcFIX-FRT2 we ligated the FRT sites from pBS-P/P-FRT2 as blunt-ended *Pac*I/*Pme*I fragment into the *Xba*I and *Bam*HI sites of the kanamycin resistant plasmid pHM5[5,8] therefore generating the plasmid pHM5-FRT2. Subsequently we cloned the blunted *Xba*I/*Spe*I attB fragment from pCR-attB[9] into the *Sna*BI site of pHM5-FRT2 resulting into the plasmid pHM5-attB-FRT2. Next, the *Pac*I restriction enzyme recognition site within the multiple cloning site was deleted from the plasmid pT_{MCS} (containing inverted repeats for SB-mediated transposition[1]) by *Pac*I restriction enzyme digest, cleavage sites blunted by fill-in reaction and construct re-ligation. The *Not*I site from the resulting plasmid was replaced by a linker from New England Biolabs (NEB) for the restriction enzyme endonuclease *Pme*I generating the plasmid pT_{MCS}-Δ*Pac*I-*Pme*I. The blunted *Kpn*I/*Pst*I fragment from pT_{MCS}-Δ*Pac*I-*Pme*I was ligated into the *Not*I site of pHM5-attB-FRT2 to create the plasmid pHM5-attB-T_{MCS}-FRT2. The *Msc*I fragment from pAAV-cFIX16 (kindly provided by K. Chu and K. A. High, Department of Pediatrics and Pathology, University of Pennsylvania and Children's Hospital of Philadelphia) with a canine factor IX (cFIX) transgene driven by the liver specific apolipoprotein E enhancer and the human alpha-1-antitrypsin (ApoE/hAAT)-promoter was ligated by blunt-end ligation into the *Pme*I site of pHM5-attB-T_{MCS}-FRT2. The I-*Ceu*I/PI-*Sce*I fragment from this shuttle vector

containing the canine FIX expression cassette flanked by SB transposase recognition sites (IR) and Flp recombinase recognition sites (FRT) was ligated into the I-*Ceu*I and PI-*Sce*I digested adenoviral production plasmid pAdFTC-I/S/P as described previously[6,7].

The vector HC-AdV-luciferase is also based on the adenoviral production plasmid pAdFTC-I/S/P and contains a luciferase expression cassette under the control of the liver-specific human alpha-1-antitrypsin promoter (hAAT) including two liver specific enhancers (HCR: hepatocyte control region; ApoE: Apolipoprotein E).

Further details about the cloning strategies and shuttle vectors used for cloning can be obtained upon request.

2. Production of high-capacity adenoviral vectors

Large-scale HC-AdV production was performed in adenoviral producer cell line 116 as described earlier[7,10]. Therefore 116 cells were cultured in minimal essential medium (MEM) supplemented with 10% fetal bovine serum (FBS) and 100 μg/ml hygromycin B. For production of HC-AdV the bacterial backbone was released from the plasmids pFTC-TcFIX-FRT2, pFTC-HSB5-Flp and pFTC-mSB-Flp by *Not*I digest and DNA was transfected into a 6 cm tissue culture dish with 116 cells. Preamplification of HC-AdV vectors was performed in 3 serial passaging steps using adherent 116 cells as described earlier[7,10].

Large-scale HC-AdV production was performed in 116 cells as described earlier[7,10]. In brief, 10 confluent 15 cm tissue culture dishes of 116 cells were transferred into 1 l of MEM supplemented with 10% FBS and 100 μg/ml hygromycin B. The following days, the same growth medium was added to a final volume of 3 l (500 ml on days 2 and 3, 1000 ml on day 4). At day 5, 3 litres of 116 cells (3-4x10^5 cells/ml) were harvested by centrifugation, resuspended in 5% volume medium, and co-infected with 100% of the crude lysate from one 15 cm dish of serial passaging step 3 and AdNG163R-2 helper virus[9] at one infectious unit per cell. Virus infection was performed at 37°C on a magnetic stir plate for 2 hrs, after which medium (MEM supplemented with 5% FBS) was added to a final volume of 2 l. Co-infected cells were harvested 48 hrs later for lysis and HC-AdV virions were purified by a CsCl step gradient and an subsequent overnight ultracentrifugation in a continuous CsCl gradient. In an alternative simplified protocol, purified HC-AdV virus (obtained by the method described above) instead of crude lysate was used as inoculum at a dose of 100 infectious units per cell for co-infection of 3 liters of 116 cells.

3. Titration of adenoviral vector preparations

We determined the physical and the infectious titer of adenoviral vector preparations. The physical titer represents the concentration of vector genomes per ml in a preparation of HC-AdV and is expressed in viral particle (vp) numbers. It was routinely obtained by measuring the absorbance at 260 nm (OD_{260}). Viral DNA was released from virions obtained from CsCl gradients in TE buffer with 0.1% SDS. The OD_{260} was measured to determine the viral titer which is expressed in viral particles (vps) per ml according to the following formula: vps/ml = (absorbance at 260 nm) x (dilution factor) x (1.1×10^{12}) x (36 kb)/(size of adenoviral genome in kb). The amount of transducing units (TUs) within a final vector preparation was determined by Southern blot analysis as described earlier[6,7]. Only vector preparations with high titers (> 4×10^7 TUs/µl) were used for animal experiments. Detection for helper-virus contaminations was performed as described earlier.

3.8.4 Supplementary reference list

1. Yant SR, Meuse L, Chiu W *et al.* (2000). Somatic integration and long-term transgene expression in normal and haemophilic mice using a DNA transposon system. *Nat.Genet.* **25**:35-41.

2. Yant SR, Huang Y, Akache B, Kay MA (2007). Site-directed transposon integration in human cells. *Nucleic Acids Res.* **35**:e50.

3. Yant SR, Ehrhardt A, Mikkelsen JG *et al.* (2002). Transposition from a gutless adeno-transposon vector stabilizes transgene expression in vivo. *Nat.Biotechnol.* **20**:999-1005.

4. Ehrhardt A, Yant SR, Giering JC *et al.* (2007). Somatic integration from an adenoviral hybrid vector into a hot spot in mouse liver results in persistent transgene expression levels in vivo. *Mol.Ther*. **15**:146-156.

5. Mizuguchi H, Kay MA (1998). Efficient construction of a recombinant adenovirus vector by an improved in vitro ligation method. *Hum.Gene Ther*. **9**:2577-2583.

6. Ehrhardt A, Kay MA (2002). A new adenoviral helper-dependent vector results in long-term therapeutic levels of human coagulation factor IX at low doses in vivo. *Blood* **99**:3923-3930.

7. Jager L, Hausl MA, Rauschhuber C *et al.* (2009). A rapid protocol for construction and production of high-capacity adenoviral vectors. *Nat.Protoc.* **4**:547-564.

8. Mizuguchi H, Kay MA (1999). A simple method for constructing E1- and E1/E4-deleted recombinant adenoviral vectors. *Hum.Gene Ther.* **10**:2013-2017.

9. Groth AC, Olivares EC, Thyagarajan B, Calos MP (2000). A phage integrase directs efficient site-specific integration in human cells. *Proc.Natl.Acad.Sci.U.S.A* **97**:5995-6000.

10. Palmer D, Ng P (2003). Improved system for helper-dependent adenoviral vector production. *Mol.Ther.* **8**:846-852.

4. BAC cloning techniques for advanced engineering of high-capacity adenoviral vectors

High-capacity adenoviral vectors (HCA) are powerful tools for a broad range of applications but modification of capsids provided by a helper-virus and the design of complex cargo sequences remain challenging. Herein, we established platforms based on a traceless bacterial artificial chromosome (BAC) cloning strategy and newly invented a recombination pipeline for complex manipulations. We used these tools to design a panel of capsid-modified helper-viruses and to construct the complex vector HCA-2indsys containing four transgene expression cassettes. The latter vector included two complex systems for mifepristone-induced expression in hepatocytes and doxycycline-dependent expression in oct4-expressing cells for selective and inducible expression of reporters in hepatocytes and induced pluripotent stem cells. Therefore, our novel adenovirus pipeline allows selective genetic manipulation of mammalian cells in therapy and cell marking such as visualisation of differentiation and dedifferentiation processes.

4.1. Introduction

Adenoviral vectors are attractive tools for efficient DNA transfer into a broad variety of cycling and resting cells in vitro and in vivo[1]. Up to now 56 human adenoviruses were isolated but historically, most vectors are based on the human adenovirus serotype 5 with a distinct tropism and a high sero-prevalence strongly limiting the usage of these vectors[2,3,4]. For construction of early generation vectors the early region E1 encoding the essential factors for initiation of virus replication or in addition the early regions E2, E3 or E4 were replaced by the genetic cargo sequence[5,6]. In contrast, newest generation of adenoviral vectors called high-capacity adenoviral vectors (HCA) or helper-dependent adenoviral vectors are devoid of all viral coding sequences[7,8,9]. The production is dependent on a helper-virus (HV), which provides viral capsid proteins *in trans* for efficient capsid assembly and release of viral particles, but packaging of helper-virus genome is inhibited due to recombinase-mediated excision of the packaging signal (Fig. 1.8). This enables packaging of HCA genomes containing cargo sequences flanked by minimal 5' and 3' sequences of the adenoviral genome with a maximized capacity for cargo sequences (up to 36 kb) and reduced vector-related toxicity and immune responses[10,11]. Thus, HCAs represent attractive tools for gene and cell therapy as well as for vaccination approaches and basic research applications[12,13]. Due to their

large genome they offer new perspectives regarding applications for transfer of complex expression systems like inducible systems or transgenes under control of endogenous regulation sequences[10,14]. In addition, a limited amount of capsid-modulations was exploited utilizing early generation adenoviral vectors revealing significant improvements in transduction efficiency for specific cell types, in vivo targeting and in escape from neutralizing anti-adenoviral antibodies[15,16,17]. However, up to now the full potential of HCA was not accessible due to the major challenge of cloning and modulating the HCA and HV genomes.

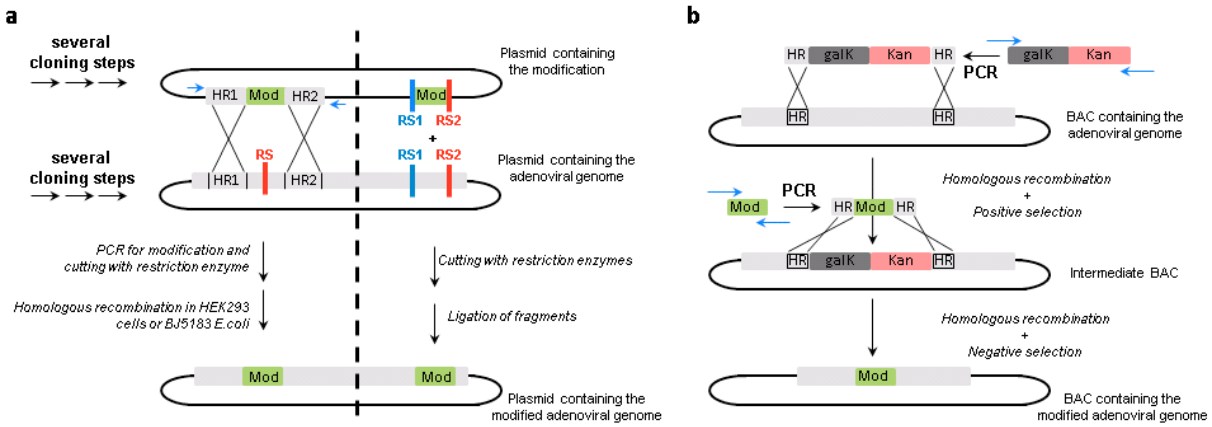

Figure 4.1: Cloning strategies for manipulation of adenoviral genomes. (a) Currently used cloning methods are either based on homologous recombination in HEK293 cells or BJ5183 E. coli bacteria (left) or on rare restriction enzymes and ligation of fragments (right). For both strategies, plasmids have to be generated in several steps, which contain the modification flanked by long homologous regions (HR1 and HR2) or flanked by restriction enzyme binding sites (RS1 and RS2). In addition, plasmids containing the adenoviral genome have to be manipulated inserting a unique restriction enzyme binding site (RS) between the homologous regions (left) or respective rare restriction enzymes binding site within the region of the adenoviral genome, which should be modified (right). **(b)** Cloning technology utilizing bacterial artificial chromosomes (BACs) is based on homologous recombination of homologous regions (HRs) created by PCR (indicated by blue arrows). This allows traceless manipulation of a BAC containing the adenoviral genome in a 2-step process. First a cassette with positive selection marker kanamycin resistance (Kan) and negative selection marker galactokinase (galK) is amplified by PCR generating flanking HRs and introduced into the BAC by homologous recombination and positive selection for kanamycin resistance. Subsequently, the sequence containing the modification (Mod) flanked by HRs is amplified by PCR and replaces the galK-Kan cassette by homologous recombination. Negative selection against galactokinase enables isolation of the BAC containing the modified adenoviral genome.

Currently used methods for genetic manipulation of adenoviruses are based on either rare endonucleases or homologous recombination in mammalian cells or bacteria of E. coli strain BJ5183, which constitutively express λ recombinases (Figure 4.1a)[18,19,20]. However, these methods are highly work-intensive and time-consuming. Moreover, generation is dependent on complex constructions of intermediate clones containing either respective endonuclease binding sites or long homologous sequences (>200 bp)[21]. Therefore, design of HCA genomes is significantly limited in complexity and size of the cargo sequence whereas modulations of the HV genome are restricted to a certain region, which is defined by the homologous regions or the endonuclease binding sites within the intermediate clones.

Recently, an elegant method was established allowing traceless modification of bacterial artificial chromosomes (BACs). Herein, modifications were incorporated by two successive homologous recombinations, which are high efficiency due to the usage of a positive selection marker like zamycin resistance (Kan), ampicillin resistance or zeocin resistance in combination with galactokinase (galK) as a negative selection marker (Figure 4.1b)[22]. In this system recombinases are encoded endogenously by bacteria of E. coli strain SW102, which express high levels upon heat-induction. In contrast to previous methods small homologous regions (<50 bp) are sufficient for efficient recombination, which can be generated by PCR utilizing adequate primers. Therefore, time-consuming and challenging construction of intermediate clones containing the modified sequence flanked by long homologies or endonuclease binding sites and especially vectors with the adenoviral genome with endonuclease binding sites incorporated at the target region is not necessary.

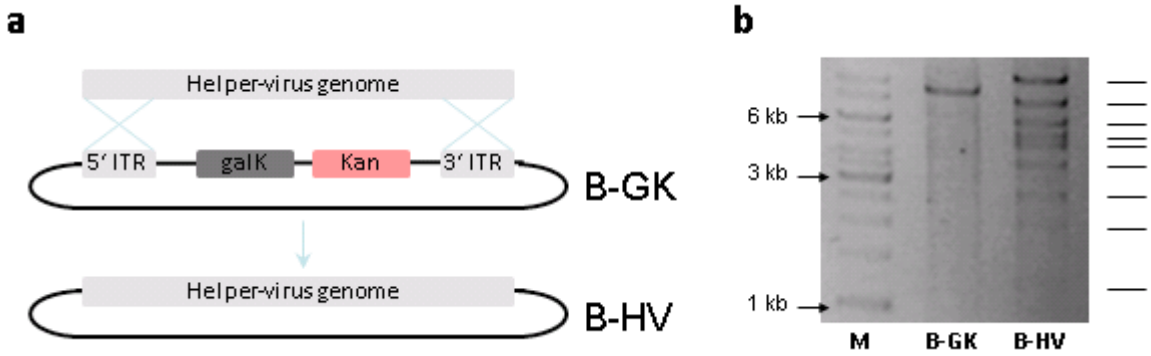

Figure 4.2: Generation of a BAC containing the helper-virus genome. (a) SW102 bacteria with the BAC B-GK, which contains 5' and 3' ITRs of the human adenovirus 5 genome separated by the galK-Kan cassette, were transduced with helper-virus genomes isolated from purified particles. After homologous recombination and negative selection against galK the helper-virus BAC B-HV was isolated. **(b)** B-HV was verified by digest with the restriction enzyme EcoRV (expected pattern is depicted on the right). M: 1 kb ladder (PEQLAB Biotechnologie GMBH, Erlangen, Germany);

4.2. Results

To utilize this technology for manipulation of HCA vectors, we established BAC platforms for the helper-virus genome and the HCA genome allowing arbitrary genetic modifications. For generation of a master BAC clone containing the helper-virus genome, DNA was isolated from purified HV particles and transformed into SW102 bacteria with the BAC B-GK, which contained the 5' and 3' ends of the adenovirus genome separated by a galK-Kan cassette (Fig. 4.2a). After induction of recombination and negative selection against galK a positive clone was isolated. Integrity of generated B-HV was verified by restriction enzyme digest (Fig. 4.2b) and reconstitution of the helper-virus in 293 cells. Notably, this method can be performed for genomes isolated from any adenoviral serotype[23].

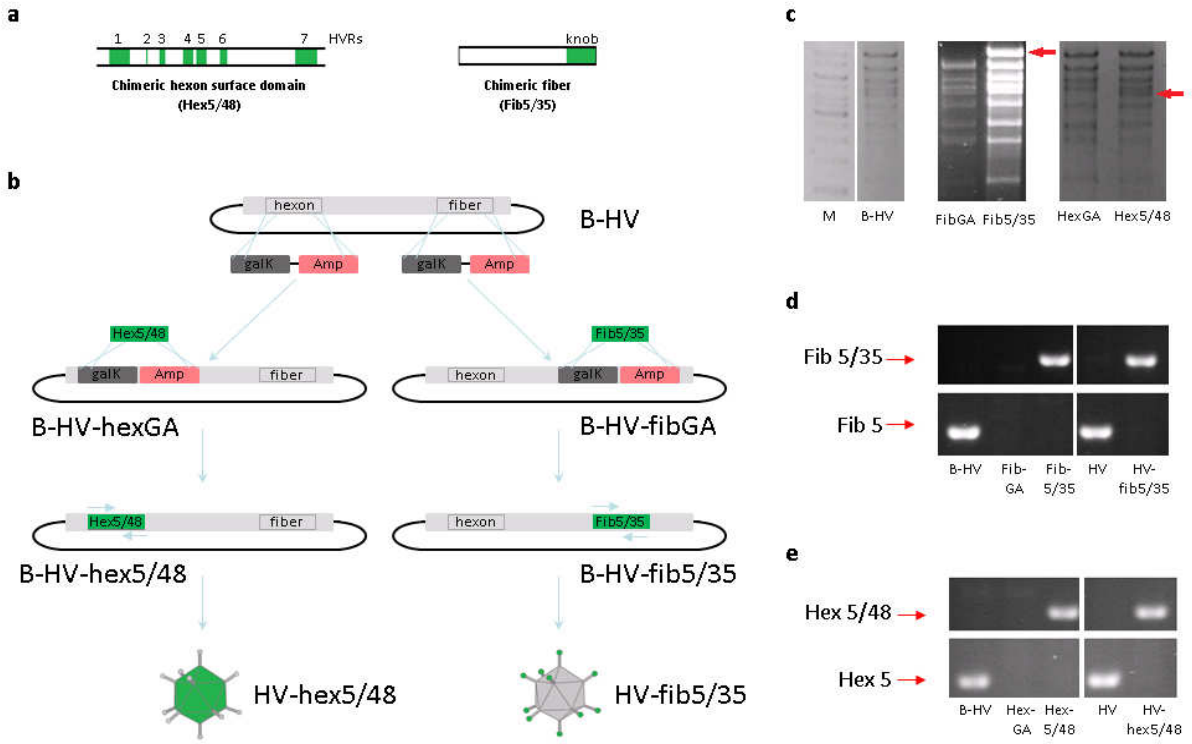

Figure 4.3: Generation of capsid-modified helper-viruses HV-hex5/48 and HV-fib5/35. (a) Genetic sequences encoding modified capsid proteins hex5/48 and fib5/35 are depicted schematically. Hex5/48 is based on the human adenovirus 5 hexon with hypervariable regions (HVRs) precisely exchanged with respective sequences of human adenovirus 48. Fib5/35 consists of the human adenovirus 5 fiber shaft fused with the human adenovirus 35 fiber knob. **(b)** For generation of capsid-modified helper-virus genomes, the galk-Amp cassette was inserted into the hexon and the fiber region, respectively, and subsequently replaced by modified sequences. Capsid-modified HVs were generated by transfection of HEK293 cells with modified HV genomes excised from the respective BACs. **(c)** Before transfection BACs were tested for integrity of the helper-virus genome by EcoRV digests. The red arrows point out the characteristic DNA fragments containing the genetic modification, which are absent in the intermediate clones. **(d)** Fiber-modification fib5/35 was verified for the BAC B-HV-fib5/35 and for the respective helper-virus HV-fib5/35 by specific PCRs. In addition, contamination with unmodified HV-genomes or HV-particles was excluded by PCRs specific for the unmodified fiber. **(e)** Verification of hexon-modification hex5/48 and proof for the absence of contamination with unmodified HV genomes was performed for B-HV-hex5/48 and HV-hex5/48 with specific PCRs.

For proof-of-principle the helper-virus BAC was utilized to incorporate fiber chimera fib5/35 and hexon chimera hex5/48 (Fig. 4.3a, b). Adenoviral vectors with the fib5/35 modification contain fiber knob domains of human adenovirus 35 allow transduction of cells, which are not accessible for vectors with unmodified fibers like hematopoietic stem cells[15]. In contrast, in hex5/48 modified vectors hypervariable regions of the major capsid protein hexon presented on the capsid surface were precisely exchanged by respective sequences of human adenovirus 48[16]. Therefore theses vectors escape from the majority of neutralizing, anti-adenoviral antibodies generated after contact with adenovirus 5 based capsids and interaction with coagulation factor X is inhibited resulting in detargeting the vector from the liver[24]. For generation of these HV genomes a galK-Amp cassette was introduced replacing the fiber encoding gene of the HV-BAC or the region containing the hypervariable regions in the hexon gene, respectively. Subsequently, modified sequences were amplified by PCR and directly incorporated into the helper-virus BACs by homologous recombination replacing the galK-Amp cassette. After negative selection isolated clones were tested for integrity of helper-virus genome by digest with restriction enzyme EcoRV (Fig. 4.3c) and reconstitution of respective viruses. In addition, introduced modifications were verified for BACs and respective helper-viruses by PCRs specific for modified sequences, whereas contaminations with unmodified HV genome were excluded by PCRs specific for unmodified fiber and hexon genes (Fig. 4.3d, e).

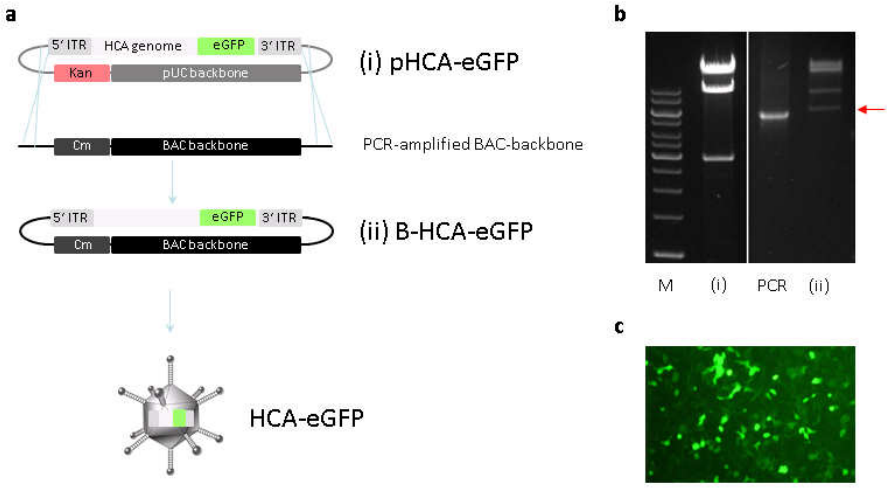

Figure 4.4: Generation of BAC B-HCA-eGPF containing the HCA genome with an eGPF-expression cassette by backbone-exchange. (a) SW102 bacteria with plasmid pHCA-eGFP containing x-chromosomal stuffer DNA and an eGFP expression cassette were transfected with a PCR-product containing the backbone of a BAC flanked by sequences, which are homologous to sequences next to the 5' and 3' ends of the HCA genome. After recombination B-HCA-eGFP clones were isolated by selection for positive selection marker chloramphenicol resistance (Cm), which is part of the BAC-backbone. The respective vector HCA-eGFP was generated by co-transduction of 116 cells with helper-virus particles and HCA genomes excised from B-HCA-eGFP. **(b)** Purity of the PCR-product, which is essential for the cloning procedure, was checked and B-HCA-eGFP was verified by PmeI-digest (specific fragment is marked by the red arrow). **(c)** Column-purified HCA-eGFP was tested by analysis for eGFP-expression in HEK293 cells (10x magnification).

Access to the BAC platform for HCA genomes was provided utilizing an alternative method, which works reverse to the isolation of specific regions from a BAC library[25]. Therefore plasmid pHCA-eGFP encoding a HCA genome with an eGFP expression cassette[26] was transformed into SW102 bacteria. Subsequently, the backbone of a BAC including the gene for chloramphenicol resistance (Cm) was amplified by PCR with adequate primers generating regions homologous to sequences next to the HCA genome. After transformation and homologous recombination positive clones were isolated by selection for chloramphenicol resistance (Fig. Fig. 4.4a). HCA-BAC was verified by digest with restriction enzymes (Fig. 4.4b) and generation of respective high-capacity adenovirus HCA-eGFP.

To exploit full potential of HCAs a recombination pipeline was established enabling smooth combination of sequences to design complex expression systems. This pipeline is based on iterative BAC cloning steps successively incorporating sequences coupled with alternating positive selection markers into the same BAC (Fig. 4.5a). In detail, a PCR product is generated containing a positive selection marker and the first sequence of interest and transformed into bacteria with the BAC, which should be modified. In sharp contrast to the standard procedure, transformed bacteria are grown in liquid culture and directly used to generate competent cells, which are used for the next cloning step. The second PCR product contains another positive selection marker and the second sequence of interest flanked by sequences, which are homolog to 5'- and 3'- sequences of the first selection marker. Homologous recombination and selection for the second selection marker enables efficient site-directed incorporation of the second sequence of interest into the BAC. This process could be repeated for fast combination of sequences within a single BAC. In addition, DNA could be isolated from liquid culture and utilized as template for PCR amplification. Therefore, sequences combined by iterative homologous recombinations could be amplified by PCR and incorporated into another BAC. Combinations of sequences with alternating positive selection markers, which are necessary for the recombination pipeline, are either present in adequate plasmids or generated by subcloning, overlapping PCR or ligation of PCR-amplified sequences. Furthermore, iterative PCRs can be used to generate small sequences like minimal polyadenylation signals, minimal internal ribosomal entry sites (IRES) or minimal pA-signal sequences attached to amplified template sequences (Fig. 4.5b). Therefore, the recombination pipeline enables design of complex systems by smooth modulation of BACs utilizing repetitive cloning steps without isolation of intermediates.

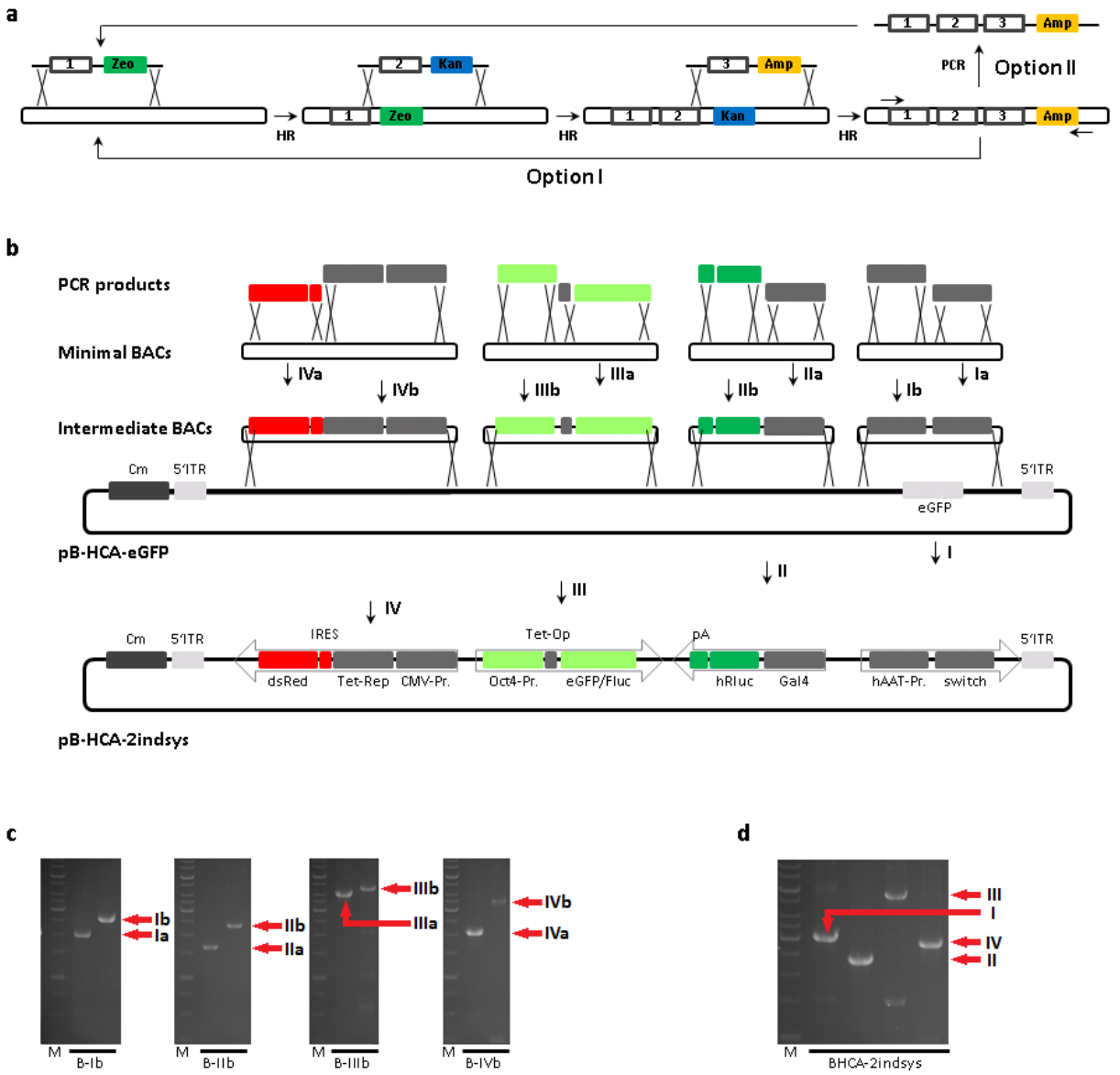

Figure 4.5: Generation of B-HCA-2indsys utilizing the novel recombination pipeline. (a) Principle of the recombination pipeline for combination of sequences. A PCR product containing the first sequence (1) coupled with positive selection marker cin resistance (Zeo) is introduced into a BAC by homologous recombination in SW102 bacteria (HR) and bacteria are grown in liquid culture under selection for zeocin resistance. Next, the generated BAC is used for introduction of a PCR product containing the second sequence (2) coupled to positive selection marker kanamycin resistance (Kan), replacing the zeocin resistance selection marker. The next step for introduction of the third sequence is similar to the second step, but the third sequence is coupled to ampicillin resistance and kanamycin resistance is replaced. For further proceeding either the generated BAC could be used as target BAC for the next cloning step (Option I) or the combined sequences coupled with the last selection marker could be amplified by PCR for insertion into another BAC (Option II). **(b)** The novel recombination pipeline was used to generate four intermediate BACs containing expression cassettes depicted at the bottom (positive selection markers are not shown). For each intermediate BAC two sequences were combined, respectively (steps Ia – IVb). Furthermore, additional sequences were generated by extension of the respective PCR products (IIb: pA-signal, IIIa: Tet-Operator, IVa: IRES). Subsequently, expression cassettes encoded by the intermediate BACs were amplified by PCR incorporated into the BAC B-HCA-eGFP resulting in B-HCA-2indsys (steps I – IV). DNA isolated from liquid cultures of intermediate clones B-Ib – B-IVb **(c)** and the final BAC BHCA-2indsys **(d)** were analysed for inserted sequences by specific PCRs.

We used this method to generate a complex high-capacity adenoviral vector for transient cell marking to track differentiation or dedifferentiation processes. Therefore, two independent inducible and tissue-specific expression systems were incorporated into the HCA genome resulting in the vector HCA-2indsys. One system consists of the switch protein under control of a liver-specific promoter construct containing the apolipoprotein E (ApoE) enhancer element in combination with the human α_1-antitrypsin (hAAT) promoter[27] and the Renilla luciferase under control of the Gal4-promoter[28]. Therefore, transduced hepatocytes express the switch protein and upon administration of mifepristone this protein is activated mediating specific transcription of the Gal4-promoter controlled Renilla luciferase. The second system was realized by two expression cassettes encoding the Tet-suppressor protein under control of the CMV-promotor as well as an eGFP/Firefly luciferase fusion protein under control of the endogenous oct-4 promoter[29] and four Tet-operator sequences[30]. Thus, after transduction of cells expressing the stem cell-specific transcription factor oct4 this factor can bind to the oct4-promoter. However, transcription is blocked by binding of highly expressed Tet-suppressor proteins to the Tet-operator sequences. Only in presence of doxycycline, which interacts with the Tet-suppressor protein and therefore inhibits binding to Tet-operator sequences, the fusion protein eGFP/FLuc is transcribed efficiently. In addition, fluorescence marker dsRed was coupled to constitutive expression of Tet-repressors via an internal ribosomal entry site (IRES) enabling detection of transduction rates. For generation of the BAC encoding the final vector genome HCA-2indsys, expression cassettes encoding components of both expression systems were constructed in parallel by successive homologous recombinations in BACs and verified by specific PCRs (Fig. 4.5c). Subsequently, expression cassettes were incorporated in serial cloning steps into the BAC B-HCA-eGFP replacing the eGFP expression cassette. Generated BAC B-HCA-2indsys was isolated and verified by PCRs specific for inserted sequences (Fig. 4.5d).

Standard purification process for helper-viruses and high-capacity adenoviral vectors consists of two sequential CsCl-gradients for separation of viral particles from cellular debris and empty viral particles followed by a dialysis step to transfer isolated capsids into a physiological buffer[31]. Although this method is very robust, amplification of high amounts of viral particles are necessary and the procedure is work-intensive as well as time-consuming[5,8].

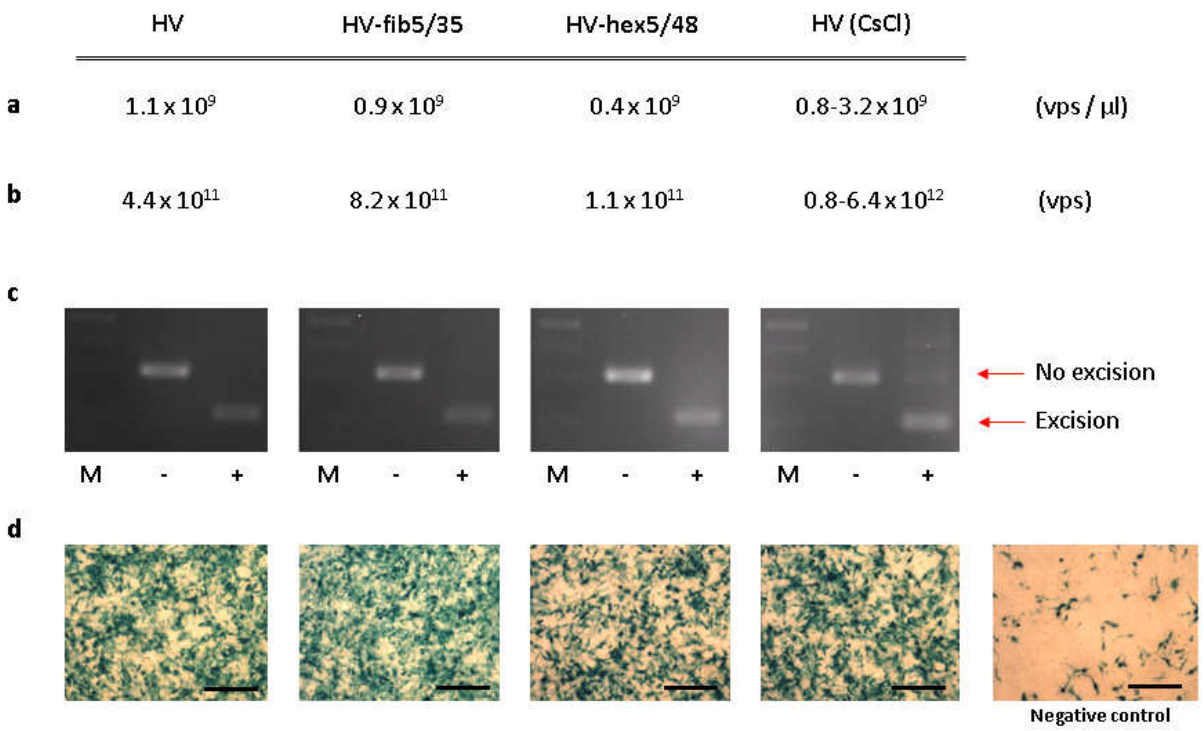

Figure 4.6: Characterization of column-purified helper-viruses. Mean values for physical titers **(a)** and total yields **(b)** were determined for preparations of unmodified helper-virus (HV) and capsid-modified helper-viruses HV-fib5/35 and HV-hex5/48, which were purified with an ion-exchange column. As a reference, the range of titers and total yields for preparations of CsCl-purified HVs are depicted. **(c)** Cre-mediated excision of the packaging signal of column-purified helper-viruses was tested by a PCR specifically amplifying a region containing the packaging signal. For analysis, DNA was used, which was extracted from HEK293 cells (-) and 116 producer cells expressing Cre-recombinase (+) transduced with respective helper-viruses. **(d)** Functionality of helper-viruses was tested by production of HCAs encoding a LacZ expression cassette. Generated HCAs were tested for LacZ-expression after transduction of HEK293 cells. (scale bars: 200 µm)

In contrast, an alternative purification procedure for small-scale production of first-generation adenoviral vectors is based on ion-exchange columns (Vivapure AdenoPACK 20, Sartorius, Göttingen). Although empty viral particles were not separated from packaged capsids, this method requires only 3-6 hours and it is accessible to all laboratories. Therefore, we applied this system to BAC-derived helper-viruses HV, HV-fib5/35 and HV-hex5/48 as well as to the vector HCA-eGFP. Vector preparations were performed utilizing columns for purification of vector particles obtained from amplification with 0.5-1.0 x 10^9 HEK293 cells. Physical titers determined for unmodified HV and HV-fib5/35 were similar to vector preparations obtained by standard purification process, although total yields are significantly lower due to the lower number of cells used for the last amplification step (Fig. 4.6a, b). Even for HV-hex5/48 0.4 x 10^9 vps/µl were obtained, although ion-exchange is impaired due to reduced number of positively charged amino acids displayed on the capsid surface[32]. Functionality of the helper-viruses was verified by testing excision of the packaging signal in cells expressing Cre recombinase (Fig. 2c). Furthermore, we used these helper-viruses to verify suitability for

generation of high-capacity adenoviral vectors encoding a LacZ expression cassette, respectively (Fig. 2d). For HCA-eGFP preparations the physical titers as well as the total vector yields were slightly reduced in comparison with HV preparations or CsCl-purified high-capacity adenoviral vectors (data not shown). Nevertheless, the vector was proven to be functional as shown by detection of by eGFP-expression in transduced HEK293 cells (Fig. 4.4c). In conclusion, column-purification is an attractive option to gain purified HCA amounts sufficient for quantitative in vitro studies and preliminary in vivo studies. Furthermore, it has been shown to be suitable for purification of fiber-modified adenoviral vectors and also hexon-modified adenoviral vectors could be purified despite decreasing vector yields.

4.3. Discussion

In summary, BAC platforms enable smooth design of arbitrary helper-viruses utilizing traceless cloning strategies. Therefore, the BAC cloning technology is a suitable method for rapid generation of adenoviral genomes containing a variety of mutations at a single site within the adenoviral genome. This allows screening of a relatively high number of mutated capsid-proteins in the viral context, which is essential to ensure, that capsids can be formed by incorporation of the mutated protein. Furthermore, a newly invented recombination pipeline was demonstrated to allow complex modulations for high-capacity adenoviral genomes. However, utilization of the recombination pipeline is limited by the size of the PCR product, which could be generated specifically. With respect to this issue, amplification of PCR products of up to 10 kb were shown to be specific utilizing the proof-reading polymerase PRECISOR (BioCat, Heidelberg) (data not shown). Nevertheless, larger sequences such as the dystrophin gene used for treatment of patients with muscular dystrophy[33] could be splitted in two fragments and sequentially incorporated into the target BAC. Additionally, even PCR products generated by a proof-reading polymerase may contain mutations. Therefore, either incorporated sequences should be verified by sequencing or respective functionalities should be tested. Furthermore, incorporation of sequences with homologies to the target BAC larger than 50 bp appeared to be challenging due to unspecific recombination events. Especially with respect to sequences often used in expression cassette such as polyadenylation signals and some promoter- or enhancer-elements, careful planning of the construction procedure is essential to avoid problems caused by this restriction. In contrast, two homologous regions of

more than 500 bp, which were part of the same BAC, were stable even after heat-induction of recombinases (data not shown).

With respect to purification of small-scale preparations of HCAs, ion-exchange columns represent an attractive alternative accessible to any researcher. With respect to the purity of column-purified HCA it is of note that the ratio of infectious units to physical units is about 1:20 for regular HCA preparation purified by CsCl-gradients, indicating a high number of packaged but non-infectious adenoviral particles. Moreover, several other research groups used vector preparations with even worse ratios (1:100 or less)[34]. Therefore, unpackaged particles contained in column-purified HCA preparations probably have no substantial negative effect on the quality. Regarding purification of capsid-modified adenoviral vectors, modulation of surface domains of the hexon protein might affect the total charge of the capsid surface and in consequence alter binding properties. This could result in reduction of the titer as well as the total vector yield and therefore, column-purification might not be suitable for screening of hexon-modified adenoviral vectors. However, columns could be optimized for any capsid-modification and in addition column-purification might be adopted easily to higher numbers of vector particles[32]. Therefore, ion-exchange columns might provide an attractive alternative for the production of sufficient amounts of HCAs for clinical studies.

In summary, the new tools for generation of HCA vectors presented in this study and the option to cross-package any HCA genomes into capsids provided by any helper-virus allow to exploit the full potential of high-capacity adenoviral vectors. This was demonstrated by generation of HCA-2indsys enabling simultaneous delivery of two independent inducible and cell line specific expression systems and generation of two capsid-modified helper-viruses providing additional features for the delivery in cell culture and in vivo. Therefore new resources are opened for current approaches in gene therapy or vaccination as well as for new areas like stem cell technology, tissue engineering or basic research.

4.4. Material and Methods:

4.4.1. Generation of bacterial artificial chromosomes

Detailed description of the general cloning procedure utilized for modulation of bacterial artificial chromosomes by homologous recombination is provided in previous

publications.[22,35] In brief, expression of λ recombinases in SW102 bacteria containing the target BAC listed in Table 4.1 was heat-shock induced by incubation at 42°C for 15 min and subsequently, bacteria were used for preparation of electro-competent cells. Sequence, which should be introduced, flanked by regions homolog to the target site within the target BAC were amplified by PCR (primers are listed in Table 4.1) and competent cells were transformed with about 1.5 µg of purified PCR-product. For isolation of single clones bacteria were selected on agar-plates containing the respective selection marker. For recombination pipeline cloning steps, transformed bacteria were grown in liquid culture containing the respective selection marker(s).

4.4.2. Quantitative PCRs, qualitative PCRs and sequencing

For all PCRs high-fidelity KOD Hot Start DNA Polymerase (Novagen, Darmstadt) was used except for amplification of the BAC-backbone, which was performed with the PRECISOR polymerase (Biocat, Heidelberg). Primers and templates for respective PCRs are depicted in Table 4.1. For quantitative PCRs 35 cycles were performed and for qualitative PCRs 25 cycles were used. For each PCR annealing temperature was 60°C and for elongation recommended time was chosen. For verification of sequences vector genomes were sequenced by Eurofins MWG Operon (Ebersberg, Germany) utilizing adequate primers listed in Table 4.1.

4.4.3. Cell culture

Human embryonic kidney HEK293 cells were cultured in Dulbecco's modified Eagle's medium supplemented with 10 % fetal bovine serum (PAA Laboratories) and producer 116 cells were grown in modified Eagle's medium supplemented with 10 % fetal bovine serum (PAA Laboratories) and hygromycin B (100 µg / ml).

4.4.4. Reconstitution and amplification of unmodified and capsid-modified helper-viruses

For generation and amplification of unmodified and capsid-modified helper-viruses previously published protocols were used[5,8]. In brief, helper-virus genomes were excised from respective BACs by *PacI*-digest and transfected into HEK293 cells utilizing transfection

reagent Fugene 6 (Roche, Penzberg). 10-20 days post transfection cytopathic effect occurred and cells were harvested. Subsequently virus particles were released by three consecutive freeze-thaw steps and for further amplification increasing numbers of HEK293 cells were infected. Final amplification step was performed with 8 x 10^7 HEK293 cells for small-scale preparations and 4 x 10^8 HEK293 cells for large-scale preparations.

4.4.5. Production of high-capacity adenoviral vectors

Production of HCAs was performed in producer cell line 116 as described earlier[7,10]. In detail, HCA genome was released from the BAC and DNA was transfected into a 6 cm tissue culture dish with 116 cells. After 24 hrs cells are co-infected the helper-virus and harvested 72 hrs after transfection. HCA capsids were released by repeated freeze-thaw steps and used for three further amplification steps. For small-scale production finally 8 x 10^7 116 producer cells were used. In contrast, for large-scale amplification 10 confluent 15 cm tissue culture dishes of 116 cells were transferred into 1 l of medium placed in a bioreactor (3l). Cells were grown for five days increasing the volume up to 3 litres. At day 5, cells were harvested by centrifugation, resuspended in 150 ml medium, and co-infected with 100% of the lysate derived from 8 x 10^7 116 producer cells and AdNG163R-2 helper virus[9] (one infectious unit per cell). Virus infection was performed at 37°C on a magnetic stir plate for 2 h. Subsequently, medium (MEM supplemented with 5% FBS) was added to a final volume of 2 l. Co-infected cells were harvested 48 hrs later for unmodified and fiber-modified helper-virus and 96 hrs later for hexon-modified helper-virus. Cells were lysed and released HCAs were purified.

4.4.6. Purification of adenoviral particles with an ion-exchange column and with CsCl gradients

Purification of Small-scale adenoviral vector preparations was performed with ion-exchange columns (Sartorius, Göttingen) according to manufacturer's instructions. To reduce the volume of cell lysate (80 ml) to the volume recommended by the manual, cells were harvested by centrifugation before lysis and resuspended in 20 ml of the supernatant. Large-scale amplified HCAs were purified by two successive caesium chloride (CsCl) gradients according to a manual described previously[7,10]. For application in vitro and in vivo toxic CsCl solutions

with virus were exchanged with a physiological buffer by dialysis. Final vector aliquots were stored at -80°C until usage.

4.4.7. Determination of physical titers of hexon-modified helper-viruses

Determination of physical titers of adenoviral vector preparations was described in detail elsewhere[8]. Briefly, 5 µl of the vector preparation was diluted with 95 µl TE buffer supplemented with 0.1 % sodium dodecylsulfate. Vector capsids were lysed for 30 min at 37 °C and subsequently OD_{260} was determined. The mean value of five measurements was used for calculation of the physical titer.

4.4.8. Detection of Cre-mediated excision of the packaging signal

HEK293 cells and 116 producer cells were seeded in 6-well plates. At 90% confluency, cells were infected with the helper-virus, which should be analyzed (MOI 3). 36 hrs post transduction DNA was extracted from harvested cells, purified with phenol-chloroform and precipitated with isopropanol. DNA samples solved in water were used as templates for PCR analysis (primers listed in Table 4.1).

4.4.9. LacZ-Staining

HEK293 cells were seeded in 6-well plates and transduced with the capsid-modified HCA containing the lacZ expression cassette, which should be analyzed. 48 hrs post transduction cells were washed with Dulbecco's PBS (1x) and fixed with glutaraldehyd (0.8 %). After 10 min cells were washed with Dulbecco's PBS (1x) and stained with the staining solution (1 mg / ml X-Gal, 10 mM $FeK_4(CN)_6$, 10 mM $FeK_3(CN)_6$, 2 mM $MgCl_2$) for 10 h.

4.4.10. Fluorescence microscopy

HEK293 cells were seeded in 6-well plates and transduced with the HCA containing the eGFP expression cassette. 48 hrs post transduction eGFP expression was detected with an inverse fluorescence microscope (Leica DM IRB).

Primer name	*Primer sequence*	*PCR template*	*Target BAC*
Generation of B-HV-fib5/35			
B-HV-fibGA-5	CCCCGTGTATCCATATGACACGGGCTATGCATCAAGCTTGGTACC	pT-GA	B-HV
B-HV-fibGA-3	GGCAATGTATGAAAAAGTGTAAGAGGATGTGGCGCGAATTGGGCCCTCTAGATGC	pT-GA	B-HV
B-HV-fib5/35-5	ATGAAGCGCGCAAGACCGTCTGAAGATACCTTCAACCCCGTGTATCCATATGACACGG	pAd5GFP/F35	B-HV-fibGA
B-HV-fib5/35-3	GCTATGTGGTGGTGGGGCTATACTACTGAGGGCGAATTGGGCCCTCTAG	pAd5GFP/F35	B-HV-fibGA
Generation of B-HV-hex5/48			
B-HV-hexGA-5	TACAACGCCCTGGCTCCCAAGGGTGCCCCAACTCAAGCTATGCATCAAGC	pT-GA	B-HV
B-HV-hexGA-3	TTCCATGGCAAAATTATTTCCAACTCTTATGAATTGGGCCCTCTAGATGC	pT-GA	B-HV
B-HV-hex5/48-5	GGCGTGCTGGACAGGGGCCCTACTTTTAAGCCCTACTCTGGCACTGCCTA	pMA-hex5/48	B-HV-hexGA
B-HV-hex5/48-3	AGGTTGGCATTTAGATTGATTTCCATGGCAAAATTATTTCCAACTCTTAT	pMA-hex5/48	B-HV-hexGA
Generation of B-HCA-eGFP			
B-bb-5	AAGGTATATTATTGATGATGTTTAAACTACGGCGGCCGCACGGGCCATCG	pB-TA	pHCA-eGFP
B-bb-3	TCCAATTCGCCCTATAGTGAGTCGTATTACGCGACACACTTGCATCGGAT	pB-TA	pHCA-eGFP
Generation of B-HCA-2ind*sys*: intermediate clones			
B-Ia-5	GTTTAAACGGCCGCCAGTGTGCTGGAATTCGGTCTGACAGTTACCAATGC	pSwitch	B-Zeo
B-Ia-3	GAAGTGTGATGTTGCAAGTGTGGCGATCGCTCCGGAGGATCCTTAGGAGC	pSwitch	B-Zeo
B-Ib-5	GTTTAAACGGCCGCCAGTGTGCTGGAATTCGCATCAGGAAATTGTAAGCG	pFTC-TcFIX-FRT2	B-Ia
B-Ib-3	AGTCCATGGTGGACCGGTAGCTTGGTGGCCAGATCAGGGGGATCATTCAC	pFTC-TcFIX-FRT2	B-Ia
B-IIa-5	AATTCGCCCTTTCAGAAGAACTCGTCAAGAGTCAGTCCTGCTCCTCGGCC	pGene/V5-His B	B-Kan
B-IIa-3	TGTCGAGTTTAAACATGCATCCTTAATTAACCGAGCTCTTACGCGGGTCG	pGene/V5-His B	B-Kan
B-IIb-5	AGTCCTGCTCCTCGGCCACGAAGTGCATTACCAATGCTTAATCAGTGAGG	phRL-CMV	B-IIa
B-IIb-3	AACGGTTCTTTTTTTCTCTTCACAGGCCACCATGGCTTCCAAGGTGTACG	phRL-CMV	B-IIa
B-IIIa-5/1	TCCCTATCAGTGATAGAGATCGTCGACGAGCATGGTGAGCAAGGGCGAGG	pEPito-[EGFP::Luc]	(extension PCR)
B-IIIa-5/2	AGAGCTCTCCCTATCAGTGATAGAGATCTCCCTATCAGTGATAGAGATCG	(PCR B-IIIa-1)	(extension PCR)
B-IIIa-5/3	CGTGTACGGTGGGAGGTCTATATAAGCAGAGCTCTCCCTATCAGTGATAG	(PCR B-IIIa-2)	(extension PCR)
B-IIIa-5/4	TGTCGAGTTTAAACATGCATCCTTAATTAACGTGTACGGTGGGAGGTC	(PCR B-IIIa-2)	B-Zeo
B-IIIa-3	AGTCCTGCTCCTCGGCCACGAAGTGCATTACCAATGCTTAATCAGTGAGG	pEPito-[EGFP::Luc]	B-Zeo
B-IIIb-5	GTTAACCGGGCTGCATCCGATGCAAGTGTGTCAGAAGAACTCGTCAAGAA	T-oct4-pr-rev	B-IIIa
B-IIIb-3	TTATATAGACCTCCCACCGTACACGCCATCGAGAAGGCAAAATCTGAAGC	T-oct4-pr-rev	B-IIIa
B-IVa-preI-5	AAGTGACGATTTGAGGAAGTTGTGGGTTTATTATCATGTCTGCTCGAAGC	MK pO6-SVT	(PCR I for overlapping PCR)
B-IVa-preI-3/1	CTCCTAATATTTATAATTTCTTCTTCCAGAAATGGCCTCCTCCGAGGACG	MK pO6-SVT	(PCR I for overlapping PCR)
B-IVa-preI-3/2	TCAGCCCTGCTGAGTCAGATCAGCTCCTAATATTTATAATTTCTTCTTCC	(extension PCR)	(PCR I for overlapping PCR)
B-IVa-preII-5	CCGGAATTGCCAGCTGGGGCG	T-Kan	(PCR II for overlapping PCR)
B-IVa-preII-3	CGCTTAATGCGCCGCTACAGGGCGCGTGGGTATGCATCAAGCTTGGTACC	T-Kan	(PCR II for overlapping PCR)
B-IVa-5	AAGTGACGATTTGAGGAAGTTGTGGGTTTATTATCATGTCTGCTCGAAGC	(overlapping PCR)	B-HCA-eGFP
B-IVa-3	CGCTTAATGCGCCGCTACAGGGCGCGTGGGTATGCATCAAGCTTGGTACC	(overlapping PCR)	B-HCA-eGFP
B-IVb-5	CATTTCTGGAAGAAGAAATTATAAATATTAATAAGATCTGAATTCCCGGG	pCI-dsRed	B-IVa
B-IVb-3	CAGGGCGCGTGGGCGCTTAATGCGCCGCTAGTCAGTCCTGCTCCTCGGCC	pCI-dsRed	B-IVa
Generation of B-HCA-2ind*sys*: final clone			
B-HCA-I-5	TAGGCGTTTTGCGCTGCTTCGCGATCGCTCAGAAGAACTCGTCAAGAAGG	B-Ib	B-HCA-eGFP
B-HCA-I-3	GAAGGCACAGTCGAGGCTGATCAGCGGGTTAGGAGCTGATCTGACTCAGC	B-Ib	B-HCA-eGFP
B-HCA-II-5	GTGAGATCATGCACGTCACCAATCTCTTTACCAATGCTTAATCAGTGAGG	B-IIb	B-HCA-I
B-HCA-II-3	CTAAAGGGCGAATTCTGCAGATATCCATCACTCTTACGCGGGTCGAAGCG	B-IIb	B-HCA-I
B-HCA-III-5	GTCACTTCCCAGATCCGCGCTTTCTCTGTCAGAAGAACTCGTCAAGAAGG	B-IIIb	B-HCA-II
B-HCA-III-3	TAAAATCGATAAGGATCCAGGTGGCACTTTATTCGAAGCTTGAGCTCGAG	B-IIIb	B-HCA-II
B-HCA-IV-5	GAACGTCACACCGTCAGCAGCAGCGGCGATCGCCTCCCCAATCCAGGTCC	B-IVb	B-HCA-III
B-HCA-IV-3	TCCAGGTTCCCCAAAAGCACCCCTATTTGTAGGAACTTCGGATCCGGCGC	B-IVb	B-HCA-III
Exision-PCR			
pack-sig-5	GGAAGTGTGATGTTGCAAGTGTGG		
pack-sig-3	CTTCCATCAAACGAGTTGGTGCTC		
Control PCRs / sequencing primers			
Co-I-5	TAGGGCCCGTAGGCTCAGAGGCACACAGGAGT		
Co-I-3	TGTAGCGGTCACGCTGCGCG		
Co-II-5	CCTCCCACACCTCCCCCTGAA		
Co-II-3	AGATCAGGGGGATCATTCACTGTCCCAGGTCA		
Co-III-5	GGGTGCTTTTGGGGAACCTGG		
Co-III-3	TCTAGAGCGGCCGCTTCGAGC		
Co-IV-5	CGATCGCCTCCCCAATCCAGG		
Co-IV-3	GTGTTTCTCAGCTTGCCATCC		
Co-Ia-5	CACCATGGACTCCCAGCAGCC		
Co-Ia-3	TGTGATGTTGCAAGTGTGGCG		
Co-Ib-5	TATCGAGATTTTCAGGAGCTAAGGA		
Co-Ib-3	AAGTCGGCAAATATCGCATGC		
Co-IIa-5	ACCGTTAGTATTACTGCTAGC		
Co-IIa-3	ACCCGCTGTATCAACACCGCC		
Co-IIb-5	GTTCATCCATAGTTGCCTGACTCC		
Co-IIb-3	TGCTATTCTGCTCAACCTTCC		
Co-IIIa-5	TATCGAGATTTTCAGGAGCTAAGGAGTTTAAACGGCCGCCAGTGTGCTGG		
Co-IIIa-3	CGTGTACGGTGGGAGGTCTATATAAGCAGAGCTCTCCCTATCAGTGATAG		
Co-IIIb-5	CCGGTGAACAGCTCCTCGCCC		
Co-IIIb-3	CAGCACCCTGATGCGACCACG		
Co-IVa-5	GCGGCCGCCTACAGGAACAGGTGGTGGCG		
Co-IVa-3	CGAGGAGCAGGACTGAC		
Co-IVb-5	CGCCTCCCCAATCCAGGTCC		
Co-IVb-3	ATGGCCTCCTCCGAGGACGTC		

Table 4.1: Primers, plasmids and BACs used for generation and analysis of BACs described in this study. In each line, materials used for one cloning step are described: primers and template DNA used for generation of the PCR-product as well as the BAC, which should be modified. The BACs B-Kan, B-Zeo and pB-TA5 as well as plasmids pT-GA, pMA-hex5/48, pFTC-TcFIX-FRT2, phRL-CMV, T-oct4-pr-rev, T-Kan and pCI-dsRed were constructed in the laboratory of Anja Ehrhardt. Plasmids pAd5GFP/F35 and pHCA-eGFP were provided by Dmitry Shayakhmetov, pSwitch and pGene/V5-HisB were derived from the Kit Gene Switch (Invitrogen), pEpito-[eGFP/FLuc] from Rudolf Haase and MKp06-SVT from Zsolt Ruzsics.

4.5. References

1. **Kay, M. A.** (2011). "State-of-the-art gene-based therapies: the road ahead." Nat Rev Genet **12**(5): 316-328.
2. **Sullivan, D. E., S. Dash, et al.** (1997). "Liver-directed gene transfer in non-human primates." Hum Gene Ther **8**(10): 1195-1206.
3. **Shiver, J. W. and E. A. Emini** (2004). "Recent advances in the development of HIV-1 vaccines using replication-incompetent adenovirus vectors." Annu Rev Med **55**: 355-372.
4. **Benihoud, K., P. Yeh, et al.** (1999). "Adenovirus vectors for gene delivery." Curr Opin Biotechnol **10**(5): 440-447.
5. **Luo, J., Z. L. Deng, et al.** (2007). "A protocol for rapid generation of recombinant adenoviruses using the AdEasy system." Nat Protoc **2**(5): 1236-1247.
6. **Lusky, M., M. Christ, et al.** (1998). "In vitro and in vivo biology of recombinant adenovirus vectors with E1, E1/E2A, or E1/E4 deleted." J Virol **72**(3): 2022-2032.
7. **Parks, R. J., L. Chen, et al.** (1996). "A helper-dependent adenovirus vector system: removal of helper virus by Cre-mediated excision of the viral packaging signal." Proc Natl Acad Sci U S A **93**(24): 13565-13570.
8. **Jager, L., M. A. Hausl, et al.** (2009). "A rapid protocol for construction and production of high-capacity adenoviral vectors." Nat Protoc **4**(4): 547-564.
9. **Palmer, D. and P. Ng** (2003). "Improved system for helper-dependent adenoviral vector production." Mol Ther **8**(5): 846-852.
10. **Morral, N., R. J. Parks, et al.** (1998). "High doses of a helper-dependent adenoviral vector yield supraphysiological levels of alpha1-antitrypsin with negligible toxicity." Hum Gene Ther **9**(18): 2709-2716.
11. **Muruve, D. A., M. J. Cotter, et al.** (2004). "Helper-dependent adenovirus vectors elicit intact innate but attenuated adaptive host immune responses in vivo." J Virol **78**(11): 5966-5972.
12. **Ehrhardt, A., H. Xu, et al.** (2003). "A gene-deleted adenoviral vector results in phenotypic correction of canine hemophilia B without liver toxicity or thrombocytopenia." Blood **102**(7): 2403-2411.
13. **Weaver, E. A., P. N. Nehete, et al.** (2009). "Comparison of replication-competent, first generation, and helper-dependent adenoviral vaccines." PLoS One **4**(3): e5059.

14. **Puntel, M., A. K. Muhammad, et al.** (2010). "A novel bicistronic high-capacity gutless adenovirus vector that drives constitutive expression of herpes simplex virus type 1 thymidine kinase and tet-inducible expression of Flt3L for glioma therapeutics." J Virol **84**(12): 6007-6017.

15. **Shayakhmetov, D. M., T. Papayannopoulou, et al.** (2000). "Efficient gene transfer into human CD34(+) cells by a retargeted adenovirus vector." J Virol **74**(6): 2567-2583.

16. **Roberts, D. M., A. Nanda, et al.** (2006). "Hexon-chimaeric adenovirus serotype 5 vectors circumvent pre-existing anti-vector immunity." Nature **441**(7090): 239-243.

17. **Terashima, T., K. Oka, et al.** (2009). "DRG-targeted helper-dependent adenoviruses mediate selective gene delivery for therapeutic rescue of sensory neuronopathies in mice." J Clin Invest **119**(7): 2100-2112.

18. **Chartier, C., E. Degryse, et al.** (1996). "Efficient generation of recombinant adenovirus vectors by homologous recombination in Escherichia coli." J Virol **70**(7): 4805-4810.

19. **McGrory, W. J., D. S. Bautista, et al.** (1988). "A simple technique for the rescue of early region I mutations into infectious human adenovirus type 5." Virology **163**(2): 614-617.

20. **Mizuguchi, H. and M. A. Kay** (1998). "Efficient construction of a recombinant adenovirus vector by an improved in vitro ligation method." Hum Gene Ther **9**(17): 2577-2583.

21. **Degryse, E.** (1996). "In vivo intermolecular recombination in Escherichia coli: application to plasmid constructions." Gene **170**(1): 45-50.

22. **Warming, S., N. Costantino, et al.** (2005). "Simple and highly efficient BAC recombineering using galK selection." Nucleic Acids Res **33**(4): e36.

23. **Ruzsics, Z., M. Wagner, et al.** (2006). "Transposon-assisted cloning and traceless mutagenesis of adenoviruses: Development of a novel vector based on species D." J Virol **80**(16): 8100-8113.

24. **Waddington, S. N., J. H. McVey, et al.** (2008). "Adenovirus serotype 5 hexon mediates liver gene transfer." Cell **132**(3): 397-409.

25. **Lee, E. C., D. Yu, et al.** (2001). "A highly efficient Escherichia coli-based chromosome engineering system adapted for recombinogenic targeting and subcloning of BAC DNA." Genomics **73**(1): 56-65.

26. **Shayakhmetov, D. M., Z. Y. Li, et al.** (2004). "Genome size and structure determine efficiency of postinternalization steps and gene transfer of capsid-modified adenovirus vectors in a cell-type-specific manner." J Virol **78**(18): 10009-10022.

27. **Ehrhardt, A. and M. A. Kay** (2002). "A new adenoviral helper-dependent vector results in long-term therapeutic levels of human coagulation factor IX at low doses in vivo." Blood **99**(11): 3923-3930.

28. **Osterwalder, T., K. S. Yoon, et al.** (2001). "A conditional tissue-specific transgene expression system using inducible GAL4." Proc Natl Acad Sci U S A **98**(22): 12596-12601.

29. **Nordhoff, V., K. Hubner, et al.** (2001). "Comparative analysis of human, bovine, and murine Oct-4 upstream promoter sequences." Mamm Genome **12**(4): 309-317.

30. **Mohr, C. A., J. Arapovic, et al.** (2010). "A spread-deficient cytomegalovirus for assessment of first-target cells in vaccination." J Virol **84**(15): 7730-7742.

31. **Kanegae, Y., M. Makimura, et al.** (1994). "A simple and efficient method for purification of infectious recombinant adenovirus." Jpn J Med Sci Biol **47**(3): 157-166.

32. **Konz, J. O., R. C. Livingood, et al.** (2005). "Serotype specificity of adenovirus purification using anion-exchange chromatography." Hum Gene Ther **16**(11): 1346-1353.

33. **Kawano, R., M. Ishizaki, et al.** (2008). "Transduction of full-length dystrophin to multiple skeletal muscles improves motor performance and life span in utrophin/dystrophin double knockout mice." Mol Ther **16**(5): 825-831.

34. **Alba, R., A. C. Bradshaw, et al.** (2009). "Identification of coagulation factor (F)X binding sites on the adenovirus serotype 5 hexon: effect of mutagenesis on FX interactions and gene transfer." Blood **114**(5): 965-971.

35. **Sharan, S. K., L. C. Thomason, et al.** (2009). "Recombineering: a homologous recombination-based method of genetic engineering." Nat Protoc **4**(2): 206-223.

5. Hexon-modified helper-viruses showed significantly altered tropisms in vivo

High-capacity adenoviral vectors (HCAs) resemble a potential tool to face challenges in gene therapy and vaccination. Nevertheless usage of this vector type for in vivo applications is restricted to liver tissue due to binding of coagulation factor X (FX). Furthermore, efficiency of repeated administrations is hampered due to recognition of the capsid surface by neutralizing antibodies.

In this study we modified the hexon containing hypervariable regions (HVRs) as the most abundant capsid component, which resemble most of the immunogenic sites of the vector capsid and which mediate FX-binding. Therefore, chimeric hexon gene regions were synthesized with coding sequences of HVRs precisely exchanged with respective sequences of human adenovirus serotype 12, 41, 44, 48 and 50. In parallel, a cloning system based on type II endonucleases was used to generate chimeric hexon genes replacing complete hexon surface domains with respective sequences from human adenoviruses 4, 7, 12, 13 and 41. After demonstrating that all chimeric proteins trimerize in presence of adenoviral 100K-protein they were incorporated by homologous recombination into a bacterial artificial chromosome containing the genome of the helper-virus, which provides the capsid proteins during HCA amplification. Although reconstitution of respective viruses was challenging, helper-viruses HV-HVR12 and HV-HVR48 containing precisely exchanged hypervariable regions from serotypes 12 and 48 as well as HV-SD4 and -SD12 with hexon surface domains replaced by sequences from serotype 4 and 12 were successfully generated.

Replication rates of hexon-modified helper-viruses appeared to be lower than for unmodified vectors but physical titers as well as infectious titers of final vector preparations were comparable to unmodified helper-viruses. In vitro FX-binding assays and bioluminescence measurements after intravenous application in vivo showed that transduction of liver tissue with HV-SD4 is inefficient compared to the conventionally used adenovirus serotype 5, although in vitro transduction efficiency is significantly enhanced in presence of FX. Based on these observations we concluded, that the strength of FX-binding might be a key player for efficient transduction of liver tissue in vivo. In contrast, for HV-HVR12 an impressive increase of luciferase activity from liver tissue and transduction of peripheral tissue was observed. More than 30-fold increased transduction rates in vitro in the absence of FX under

serum-free conditions suggested a new interaction directly mediating attachment of the viral capsid to an unkown cell surface marker. Surprisingly, bioluminescence measurements for HV-SD12 revealed no transduction of liver tissue even though some luciferase activity in peripheral tissue could be detected. Although this was in line with in vitro FX binding analysis, both vectors HV-SD12 and HV-HVR12 contain identical hypervariable regions and therefore, similar distributions and transduction efficiencies were expected with respect to our current knowledge. Thus, we concluded, that the hypervariable regions within the hexon are not exclusively responsible for the distinct in vivo tropism of adenovirus and that precise exchanges of hypervariable regions might have a stronger impact on structure of the capsid surface than expected. In summary, this study showed potency of capsid modifications to alter in vivo tropism opening new options for a broad variety of applications.

5.1. Introduction

Transfer of DNA into cells is an essential tool in biotechnology and molecular medicine. Due to low transduction rates of naked DNA for various cell types and inefficient in vivo delivery, vectors based on replication-deficient viruses are utilized as transfer vehicles.[1,2] These so called vectors package DNA and transport it into cells using virus-specific entry pathways. A multitude of vector types with type-specific features based on different viruses e.g. lenti- and retroviruses, herpes simplex virus 1, adeno-associated viruses or adenoviruses were utilized in the past to face the various challenges regarding cellular gene transfer.[2,3]

Vectors based on adenoviruses are an attractive option for gene transfer into dividing and non-dividing cells in vitro as well as in vivo.[4] Therefore they are potent tools for basic research as well as for gene therapy or vaccination approaches.[5] The adenovirus capsid is 70-90 nm in diameter and consists of a protein shell and a virus core with the viral double-strand DNA genome, which is 36 kb in length. Independently of the cell cycle status, cell entry is initiated by interaction of the viral fiber knob with the Coxsackie virus and adenovirus receptor (CAR).[6] Subsequently RGD motifs of the penton proteins bind to α_V integrins inducing endosomal uptake.[7] Virus capsids can escape from endosomes by partial disassembly and are transported along the microtubuli to the nucleus.[8] After docking to the nuclear pore complexes, capsids disassemble and viral DNA is imported into the nucleus where it persists episomally.[9]

Most adenoviral vectors are based on human adenovirus 5 (hAd5) and for construction of first generation vectors the E1 region encoding major key players for initiation of virus replication was deleted enabling insertion of a transgene expression cassette up to 5 kb in size.[10] Nevertheless, these vectors showed leaky expression of viral proteins mediated by cellular transcription factors.[11] Therefore, intravenous administration in animals and humans resulted in high liver toxicity and formation of a strong anti-adenoviral immune response inhibiting repeated treatments.[12,13] Further deletions of E2, E3 and E4, encoding factors, responsible for efficient virus replication and modulation of the cellular status as well as the intracellular immune responses, enhanced the packaging capacity of vectors for transgenic sequences.[14] Despite reduced toxicity and immunogenicity of second generation vectors these issues remain challenging. In addition, vector yields often are significantly reduced, although proteins encoded by deleted genes are provided by production cell lines *in trans*.

In contrast, newest generation of adenoviral vectors called high-capacity adenoviral vectors (HCA), helper-dependent adenoviral vectors or gutted adenoviral vectors are devoid of all viral coding regions.[15,16] Only the inverted terminal repeats (ITRs) located at the left and the right termini of the adenoviral genome and the packaging signal (ψ) are maintained within the HCA genome. Generation of these vectors depend on a helper-virus providing capsid proteins and mediating efficient capsid assembly and release (Fig. 1.8). The majority of helper-viruses contain a packaging signal flanked by loxP-sites and for production of HCAs a producer cell line is utilized, which is derived from HEK 293 cells which constitutively express Cre recombinase.[17,18] For generation of HCAs, producer cells are transduced with the HCA genome and co-infected with the helper-virus. The helper-virus provides capsid proteins *in trans* whereas packaging of helper-virus genome is inhibited due to Cre-mediated excision of the packaging signal. As a consequence only HCA genomes are packaged, which are 28-36 kb in size.[19] Therefore, transport of cargo DNA is enabled allowing delivery of complex expression systems[20] or transgenes under control of large endogenous regulatory sequences. Importantly, due to the lack of viral genes HCA-related toxicity is strongly reduced in comparison to first-generation adenoviral vectors[21] and adaptive immune response directed against the vector is significantly diminished.[22] Several studies to these features demonstrated, that HCAs show better performance in gene therapeutic approaches and vaccination studies.[23,24]

Nevertheless, researchers utilizing HCAs for in vivo approaches are still facing substantial challenges. One of the remaining obstacles is the inhibition of repeated administrations by

neutralizing anti-adenoviral antibody formation after first treatment with adenoviral vectors or infection with wild-type hAd5.[25] Most of these antibodies are directed against the major capsid protein hexon comprising more than 90 % of the whole capsid surface.[26] In detail, recognized targets within in the hexon are mainly unstructured sequences called hypervariable regions (HVRs), which are serotype-specific and located at the capsid surface (Fig. 1.6c).[27] Another severe restriction of HCAs which are predominantly based on hAd5 is the liver-tropism shown after intravenous injection.[28,29] Recent studies demonstrated that targeting to liver cells is mediated by interaction of surface structures formed by HVRs of hexon trimers with coagulation factor X (FX), which is present in blood at high concentrations (Fig. 1.6a, b).[30,31,32] Capsid-bound FX molecules interact with heparin-sulfate proteoglycans (HSPGs) on cellular surface of hepatocytes mediating attachment of the vector capsids to target cells and endosomal uptake.[33] Therefore, in a multitude of attempts capsid-modifications were evaluated for their potential to retarget adenoviral vectors from the liver to other organs or cell types.

Initial approaches were based on the modulation of the fiber protein and respective interaction with CAR. Fiber chimeras were created by exchanging the fiber knob with respective domains of other adenovirus serotypes, variation of the fiber shaft length or incorporation of peptides into variable loops of the fiber knob to mediate specific interactions with cell surface markers.[34,35,36,37] Other studies were based on bridging fiber proteins to specific receptors by bispecific antibody variants.[38] Although for many modifications strongly enhanced cellular uptake was shown in vitro and also detargeting from the liver was observed to small extend, retarting effects to specific tissues in vivo were marginal.[39] Similar results were seen for incorporation of ligands into the minor capsid protein pIX present on the capsid surface[40], whereas mutation of the RGD-motif in the major capsid protein penton generally impairs uptake of adenoviral capsids in most cell types except for some cancer cell lines.[41] Analysis of fiber- and penton-modifications showed low or no effect with respect to masking against neutralizing antibodies.[42] In further studies adenoviral vectors were generated based on other human and non-human adenovirus serotypes, which successful escaped anti-adenovirus 5 antibodies.[43,44] Nevertheless, little is known about genomic organization including the position of the packaging signal, biodistribution after administration, vector-related toxicity and immune responses as well as the oncogenic potential of non-human serotypes. Furthermore, until now only for hAd 1, 2 and 6 adenoviral vectors were adopted to the high-capacity adenoviral vectors system, because respective cloning procedures remain challenging

even though a new cloning system was established which might provide a suitable technology.[45]

Other attempts to modify the adenovirus capsid surface included modulation or complete exchange of the hexon protein with respective sequences of other adenovirus serotypes. Realization of this idea appeared to be challenging due to the major role of hexons for the protein interaction network providing capsid stability.[46] In detail, the adenovirus protein shell consists of 240 copies of hexon trimers. Besides mediating trimerization, hexon trimers bind to neighboring trimers, penton pentamers located at the capsid vertices, and protein networks consisting of minor capsid protein pIIIa, pVIII and pIX providing substantial portions for total capsid stability.[47] All interactions are mediated by structural domains of the hexon not displayed on the capsid surface, except for two interactions within hexon trimers anchored in surface domains DE1 and FG1.[48]

In an attempt to genetically modify the hexon composition in the adenovirus protein shell, first approaches were based on replacement of the complete hexon encoding sequence with corresponding sequences from other human adenoviruses. However, alteration did not result in virus capsid formation and virus reconstitution except for exchanges with hexons of hAd1, hAd2 and hAd6, which all belong to serotype class C, and hexons derived from serotypes 3 and 12.[49,50,51] Chimeras within the serotype class C resulted in viruses with similar growth kinetics and high potential to escape anti-adenovirus 5 antibodies and all vectors mediated transduction of liver tissue. In contrast, chimeric adenoviruses with hexons 3 and 12 exhibited strongly reduced replication rates and yields of final preparations were more than ten-fold lower in comparison to unmodified vectors based on hAd5. In a recent study first generation adenoviral vectors were developed containing a modified hexon gene with precisely exchanged HVRs from hAd48.[52] Yields of vector preparations were similar to unmodified vectors and in vivo studies demonstrated highly efficient escape from neutralizing anti-human adenovirus serotype 5 antibodies. In addition, in vitro studies showed abrogation of FX-binding and biodistribution analysis in mice after intravenous administration revealed low transduction rates of liver cells.[32] These data emphasize the impact of hexon-mediated factor X binding on the biodistribution after intravenous injection, underlining importance of hexon-modulation for any approach to improve in vivo targeting.

In this study we modified the surface domains of hexon protein from the adenoviral helper-virus providing the capsid proteins for high-capacity adenoviral vectors. We either exchanged sequences of the hypervariable regions precisely or the entire hexon surface domains

including all HVRs were replaced with equivalent sequences derived from other human adenovirus serotypes.[48] Subsequently hexon variants were incorporated into the helper-virus genome utilizing a BAC technology which was established recently in our laboratory. Successfully reconstituted helper-viruses were analyzed in vitro with respect to binding of FX and in vivo biodistribution after intravenous injection in mice was analysed.

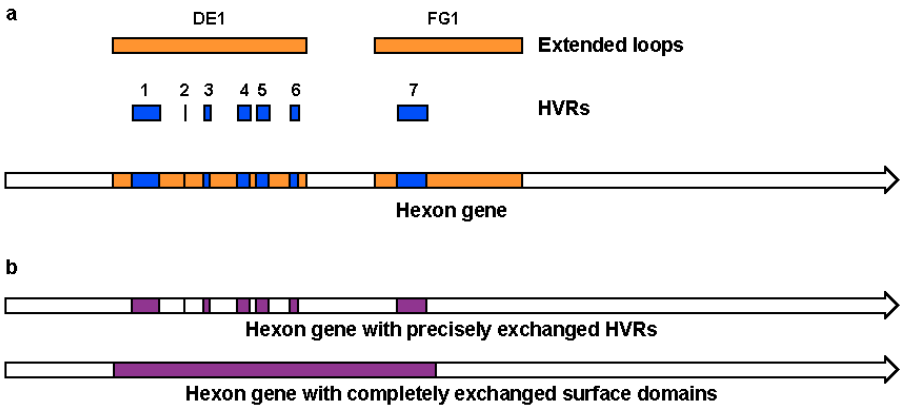

Figure 5.1: Principle for construction of modified hexon genes. (a) The solvent-exposed surface of human adenovirus serotype 5 hexon proteins is mainly part of two extended loops DE1 and FG1, which contain 7 hypervariable regions (HVRs) representing main target sites for anti-hAd5 antibodies and binding sites for coagulation factor X. Respective gene sequences are depicted in orange (extended loops) and blue (HVRs) within the hexon gene shown as white arrow. **(b)** Modified hexon genes either contain HVRs of another adenovirus serotype precisely replacing original HVRs or complete surface domains are exchanged containing solvent-exposed parts of the DE1- and FG1-loop, which include all HVRs.

5.2. Results

5.2.1. Design and construction of chimeric hexon genes

An essential step to exploit full potential of high-capacity adenoviral vectors is modification of the capsid by modulation of the helper-virus genome. This could enable specific targeting to organs or cell types as well as repeated administration without eliciting a severe immune response. Previously, genetically modified adenoviruses were generated encoding a hexon chimera with hypervariable regions (HVRs) precisely replaced with respective regions of hAd48.[52] This vector showed efficient amplification, successful escape from neutralizing antibodies and abrogation from factor X resulting in detargeting from the liver. Herein, we synthesized similar chimeras based on gene region of hAd5 encoding the HVRs precisely replacing HVRs with the respective sequence of another human adenovirus serotype (Fig.

5.1b). To evaluate the reconstitution procedure we utilized hAd48 as a positive control and hAd12, because in a previous attempt a larger portion of this particular hexon protein was successfully exchanged.[49] Furthermore, serotype 44 and 50 were chosen due to low seroprevalences and distinct FX-binding properties, which are even for hAd50 compared to hAd5 or not detectable for hAd44.[32,53,54] Additionally, hAd41 mainly infecting the gastrointestinal tract was included to evaluate the role of HVRs of hexon proteins for serotype-specific biodistribution.[55]

HVR-specific sequences of each serotype were determined utilizing sequence alignments of amino acid sequences. Due to this analysis all HVRs are located in domains DE1 (HVRs 1-6) and FG1 (HVR 7), which contain the complete region presented on the capsid surface (Fig. 5.1a) as shown by X-ray christallographic measurements.[48] Furthermore, structural analysis enabled prediction of secondary structure elements within the hexon protein. Protein sequence alignment revealed close proximity or even overlapping amino acids of these structural elements and HVRs. Therefore, exchanges of HVRs with respective sequences of other serotypes might interfere with correct formation of secondary structures. In our new approach we enlarged exchanged sequences in a second setup, including surface domains located within domains DE1 and FG1 as well as the connecting domain DE2, which is highly conserved. We hypothized that with this strategy disrupture of secondary structure motifs is avoided and alterations in tertiary structure are minimalized resulting in maintenance of trimere stability and capsid integrity. Therefore, we constructed respective hexon chimeras with serotypes from adenovirus subgroups A-F (Fig. 5.1b). Utilizing respective sequences from hAd4 (E), hAd7 (B), hAd12 (A), hAd13 (D) and hAd41 (F), plasmids were generated allowing analysis of chimeric hexon proteins expressed in mammalian cells. For smooth contruction of respective plasmids we created a master vector (pCI-M) containing highly conserved N-terminal and C-terminal regions derived from the hAd5 hexon gene (Fig. 5.2a). Hexon sequences were separated by endonuclease type II (AarI and BspQI) binding sites, which bind sequence dependent but cut sequence independent at defined distances from binding sites. This feature enabled traceless insertion of PCR products with hexon surface regions of various adenovirus serotypes into the master vector by ligation of sticky ends, created by AarI and BspQI (Fig. 5.2a). Constructed expression vectors pCI-hex5-SD4, -SD7, -SD12, -SD13 and -SD41 for respective hexon chimeras were proven by modification-specific PCRs (Fig. 5.2b) and restriction digests (data not shown).

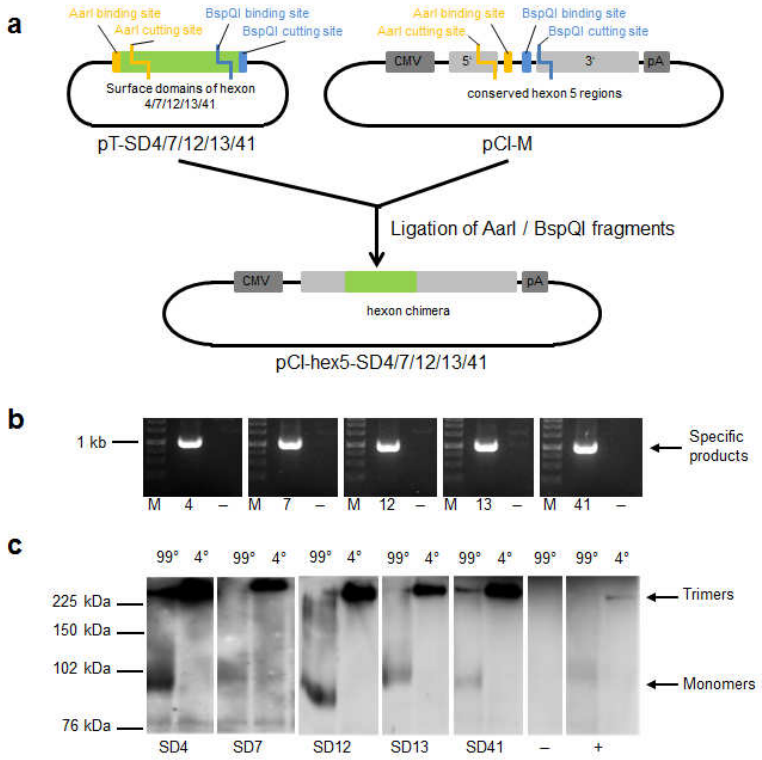

Figure 5.2: Construction of chimeric hexon genes and trimerisation of respective proteins. (a) For generation of chimeric hexon genes, plasmids pT-SD4, -SD7, -SD12, -SD13 and -SD41 were used, which were generated by incorporation of PCR products into vector pCR-BluntII-Topo. Amplified sequences contain surface domains (SD) of hexon genes from respective wild-type adenovirus serotypes flanked by binding sites for type II endonuclease AarI and BspQI, which cut within the SD sequences. Furthermore, plasmid pCI-M was used, which contains a mammalian expression cassette encoding conserved 5' and 3' regions of the hAd5 hexon gene. Sequences were separated by binding site AarI and BspQI, which cut within conserved regions. Ligation of fragments created by AarI / BspQI double digest resulted in mammalian expression vectors for the respective hexon chimera. **(b)** Plasmids were analyzed by PCRs specific for the respective hexon chimeric gene. As negative control (-), the plasmid encoding unmodified hexon gene was used. **(c)** HEK293 cells were co-transfected with mammalian expression plasmids for hexon chimeras and adenoviral chaperone 100K-protein. Cells were harvested after 48 h and boiled (99°C) as well as cooled (4°C) lysates were analyzed for expression and trimerization of chimeric hexon proteins. Plasmid encoding unmodified hexon gene was used as positive control (+) whereas cells transfected only with plasmid encoding 100K-protein served as negative control (-). M: 1 kb ladder (PEQLAB Biotechnologie GMBH, Erlangen, Germany);

5.2.2. Trimerisation of chimeric hexon proteins with exchanged hexon surface regions

Modified hexon proteins were analyzed for their potential to form viral capsids. Initial steps during capsid assembly are interaction of cytosolic hexon protein with adenoviral 100K-protein providing solubility of hexon proteins and enabling nuclear import as well as trimerization of hexon proteins.[56] To evaluate ability of novel hexon chimeras to perform these steps, HEK 293 cells were co-transfected with plasmid pCI-100K-pr encoding the adenoviral 100K-protein and the mammalian expression plasmids encoding respective hexon chimera. Cells were harvested 48 h after transfection and lysates were either boiled or cooled before analysis by Western blot. For detection a polyclonal antibody was utilized, which recognizes unmodified hexon proteins as well as chimeras. As a positive control unmodified hexon proteins were analyzed and as a negative control HEK293cells were transfected with the plasmid pCI-100K-pr. For heated samples derived from modified hexons a dominant band

was detected at about 100 kDa, respectively, matching the size of unmodified hexon monomers (Fig. 5.2c). Visualization of this band indicated solubility mediated by efficient interaction between hexon chimeras and the adenoviral 100K-protein. In contrast, for all cooled samples hexon trimers with a molecular weight of 330 kDa were detected (Fig. 5.2c). Therefore all chimeras were proven to be able to trimerize. Notably, boiled samples derived from cells transfected with pCI-SD4 and pCI-SD41 contained small amounts of trimers indicating a high heat-stability of modified hexon trimers. Furthermore, due to the fact that trimerization mainly takes place in the nucleus, the absence of monomers in all cooled samples indicated efficient nuclear import of hexon chimeras as well as high stability of trimers at 37°C.[56]

5.2.3. Construction of BACs encoding hexon-modified helper-virus genomes

Next, sequences encoding surface domains of one serotype as well as synthesized sequences containing precise HVR exchanges were incorporated into the helper-virus genome replacing endogenous hexon gene sequence (Fig. 5.3a). Therefore, we utilized our recently generated bacterial artificial chromosome pB-HV containing the genome derived from helper-virus AdNG163R-2[18], which can be used for HCA production. In brief, the cloning procedure involved following steps. First, the region of the hexon gene encoding the surface domains within DE1 and FG1 was replaced by prokaryotic double selection marker galK-Amp, containing negative selection marker galactokinase and positive selection marker ampicillin. Subsequently, chimeric hexon gene fragments were PCR-amplified and incorporated into the intermediate BAC replacing galK-Amp, respectively. This resulted in helper-virus BACs pB-HV-HVR12, -HVR41, -HVR44, -HVR48, -HVR50, -SD4, -SD7, -SD12, -SD13 and -SD41. In addition, revertant BAC pB-HV-HVR5/5 containing the unmodified hexon gene was constructed by incorporation of HVR regions amplified from unmodified adenovirus into intermediate BAC to proof stability and reliability of the BAC cloning procedures.

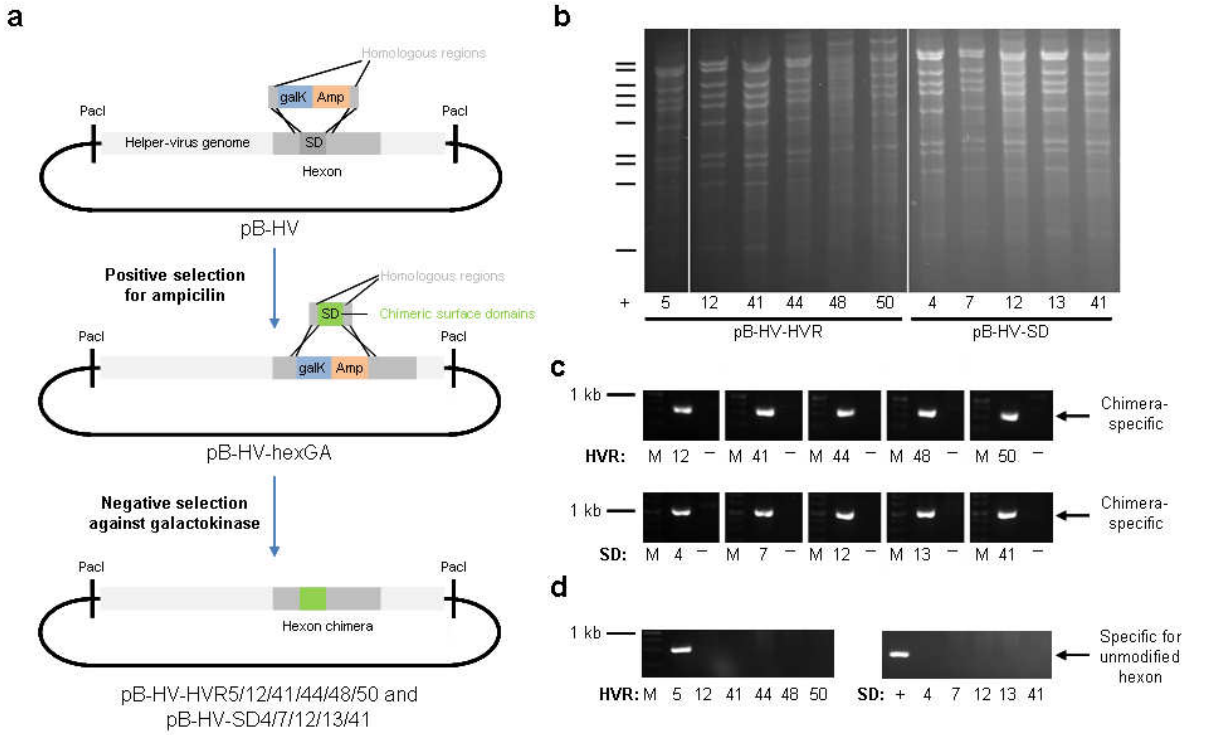

Figure 5.3: Incorporation of chimeric hexon genes into helper-virus genomes embedded in bacterial artificial chromosomes. (a) Hexon-modified helper-virus genomes were generated by traceless modulation of a bacterial chromosome (BAC) utilizing homologous recombination. Positive-negative selection marker cassette galactokinase-ampicillin (galK-Amp) was incorporated into BAC pB-HV containing the helper-virus genome replacing the region encoding surface domains of hexon gene. Intermediate clone pB-HV-hexGA was isolated after selection for ampicillin. Subsequently PCR-amplified chimeric hexon sequences replaced selection cassette and final BACs were obtained upon selection against galactokinase. **(b)** Integrity of hexon-chimeric helper-virus BACs was verified by restriction digests with EcoRV. **(c)** Incorporation of chimeric hexon sequences was verified by specific PCRs and pB-HV was used as negative control. **(d)** Contaminations with unmodified helper-virus BACs were excluded by PCR specific for surface domains of original hexon from serotype 5. Unmodified pB-HV as well as revertant BAC pB-HVR5 were used as a positive control. M: 1 kb ladder (PEQLAB Biotechnologie GMBH, Erlangen, Germany);

Previous attempts demonstrated low efficiencies for reconstitution of hexon-modified adenoviruses. Therefore, a reporter cassette containing eGFP/Firefly luciferase fusion protein was incorporated into the E3 region of each hexon-modified helper-virus genome, replacing non-coding stuffer DNA.[18] This allows visualization of eGFP expression during reconstitution and in vitro experiments. In addition, non-invasive bioluminescence imaging based on Firefly luciferase could be used for in vivo analysis. Final constructs were analyzed by restriction enzyme digests resulting in a specific pattern of fragments of respective viral genomes (Fig. 5.3b). Furthermore, incorporated hexon modifications were verified by PCRs specific for respective modifications (Fig. 5.3c) and in parallel contaminations with unmodified helper-virus BACs were excluded by PCR analysis with primers specific for the unmodified hexon gene (Fig. 5.3d).

5.2.4. Low reconstitution efficiency for hexon-modified helper-viruses

To reconstitute hexon-modified helper-viruses HV-HVR12 – 50 and HV-SD4 – 41, genomes were excised from respective helper-virus BACs by PacI digest. Subsequently HEK293 cells were transfected with linear DNA and after cytopathic effect was observed cells were harvested and used for further amplification steps. In initial experiments no hexon-modified helper-virus could be generated including the positive control HV-HVR48, a hexon modification which was reconstituted before. To overcome this hurdle, reconstitution was repeated utilizing three different HEK293 cell lines derived from American tissue culture collection (ATCC) and two other sources with significantly different features such as amplification rates. Additionally, we used various transfection reagents previously used for virus reconstitutions as well as different amounts of DNA purified by column preparation, phenol-chloroform extraction or alkaline lysis and successive isopropanol precipitation. After a multitude of attempts positive control HV-HVR48 as well as three new hexon-modified helper-viruses HV-HVR12, HV-SD4 and HV-SD12 could be amplified. This demonstrated feasibility of both approaches, namely exchanging hypervariable regions precisely as well as replacement of complete surface domains. However, reconstitution remained challenging, because no stable protocol could be established and no clear bottleneck could be identified for the reconstitution procedure.

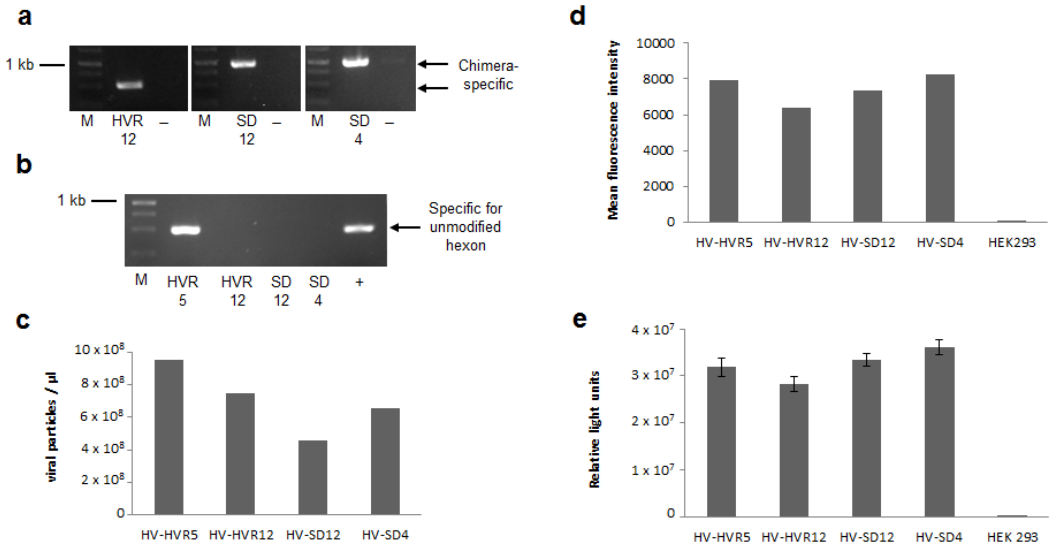

Figure 5.4: Characterization of final preparations for reconstituted hexon-modified helper-viruses. Vector genomes derived from purified viral particles of final vector preparations of HV-HVR12, HV-SD12 and HV-SD4 were analyzed by PCRs **(a)** specific for respective hexon-modification to verify chimeric hexon genes and **(b)** specific for unmodified hexon gene to detect contamination. For these vector preparations **(c)** physical titers (viral particles per µl) were determined. Functionality of reporter gene eGFP-FLuc was tested by infection of HEK293 cells with respective helper-viruses (1 µl /well) and analyzed **(d)** by flow cytometry for eGFP expression or **(e)** by luciferase assay for Firefly luciferase activity. M: 1 kb ladder (PEQLAB Biotechnologie GMBH, Erlangen, Germany);

In separated approaches utilizing identical conditions only one helper-virus was generated again whereas all other reconstitutions failed including the positive control. We hypothezised that purity of BAC-DNA used for transfection and the transfection efficiency could play a key role. This was indicated by relation between transduction efficiency and the success rate in generation of helper-viruses. In single reconstitution experiments we observed, that high transfection rates, as indicated by increased number of eGFP-positive cells, resulted in successful formation of infectious particles but during amplification cytopathic effect of HEK293 cells was delayed (72-96 h post-infection). Nevertheless, hexon-modified helper-viruses could be amplified and purified according to the standard procedure for unmodified adenoviral vectors. Final vector preparations were analyzed by PCR specific for hexon-modifications to verify hexon-modifications and by PCR specific for unmodified hexon genes to exclude contaminations with unmodified adenoviral vectors (Fig. 5.4a, b). In addition, sequencing results for PCR-amplified HVR regions revealed 100 % identity with expected sequence demonstrating sequence conservation during BAC cloning as well as stability of vector genomes during amplification. Physical titers of vector preparations for modified and unmodified helper-viruses were in similar ranges and comparable to previous preparations (Fig. 5.4c). Furthermore 48 h after infection with respective helper-viruses HEK293 cells were analyzed by flow cytometry and luciferase assay demonstrating functionality or eGFP-Firefly luciferase reporter cassettes in the E3 region of each vector (Fig. 5.4d, e). These data also verified similar transduction efficiencies for identical numbers of unmodified and hexon-modified virus particles indicating comparable stability of novel and unmodified viral capsids.

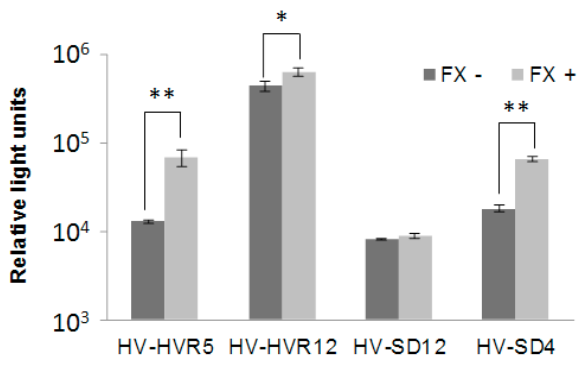

Figure 5.5: Analysis of FX-binding in vitro for hexon-modified helper-viruses. SKOV3 cells were incubated for 3h with hexon-modified helper-viruses (1000 viral particles / cell) in absence or presence of coagulation factor X (FX) in serum-free conditions. 48 h post infection cells were analyzed for Firefly luciferase activity. * P > 0.05; ** P > 0.005; Experiments were performed by Raul Alba in the laboratory of Andrew H. Baker (British Heart Foundation Glasgow, Cardiovascular Research Centre);

5.2.5. FX-binding analysis of hexon-modified helper-viruses

Previous studies demonstrated stringent dependence of in vivo biodistribution on interaction of hexon surface domains with coagulation factor X (FX).[32] Thus, we investigated FX-mediated uptake of hexon-modified adenoviruses in vitro. This assay is based on SKOV3 cells, which are transduced by unmodified adenoviral vectors with very low efficiency due to low cellular expression levels of CAR. In contrast, transduction efficiency of unmodified virus increases dramatically in the presence of FX, which mediates initial attachment of the viral capsid to heparin-sulfate proteoglycans expressed at high levels on the cell surface of SKOV3 cells.[32] Herein, generated hexon-modified helper-viruses were used to infected SKOV3 cells with 1000 viral particles / cell in absence or presence of FX and 48 hrs post-infection Firefly luciferase expression was measured (Fig. 5.5). For HV-HVR12 strongly enhanced uptake was observed in absence of FX, suggesting that a new interaction site mediating efficient attachment to the cell surface and successive uptake is involved. In addition uptake was significantly increased in presence of factor X. In contrast, transduction efficiency in absence of FX for HV-SD12 as well as HV-SD4 was as low as detected for unmodified vectors. In addition, presence of FX did not result in an increase of expression for HV-SD12 but for HV-SD4. This indicated efficient binding of hAd4 hexon surface domains to FX comparable to unmodified vectors, whereas no interaction with domains from hAd12 was observed.

5.2.6. Biodistribution of intravenously injected hexon-modified helper-viruses in mice

For further evaluation of hexon-modified helper-viruses and to gain insight into the in vivo biodistribution in vivo studies were performed. All vectors were injected intravenously into one C57Bl/6 mouse at a high dose (1×10^{11} viral particles) and two mice at a low dose (3.3×10^{10} viral particles). Twenty days post-infection first in vivo bioluminescence measurements were performed (Fig. 5.6). To evaluate the degree of vector clearance luciferase activity was detected a second time after 40 days (Fig. 5.6). In concordance with increased transduction efficiency in FX-binding assays, mice infected with HV-HVRs12 showed a dramatic increase in luciferase activity in liver tissue in comparison to the unmodified helper-virus (Fig. 5.6). Notably, pictures with optimized signal-to-noise ratios and analysis of extracted organs (data not shown) indicated that luciferase was mainly expressed from liver tissue, although low transduction rates for other organs near to the liver could not be excluded.

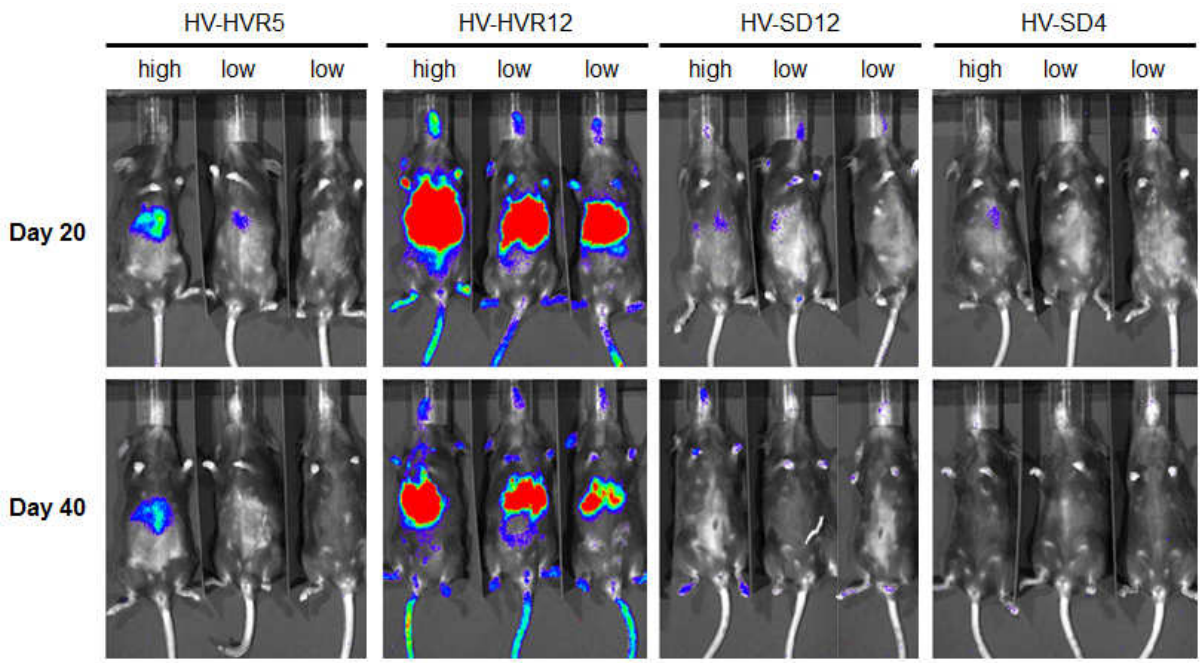

Figure 5.6: In vivo biodistribution of hexon-modified helper-viruses in mice after intravenous injection. In vivo biodistribution of hexon-modified adenoviral vectors in C57Bl/6 mice was analyzed utilizing a bioluminometer. For each vector one mouse was tail-vein injected with a high dose (1 x 10^{11} vps) and two mice with a low dose (3.3 x 10^{10} vps). **(a)** 20 days and **(b)** 40 days after treatment 200 µl of D-luciferin (20 mg/ml) were injected intraperitoneal. 10 minutes after injection bioluminometric measurements were performed. Experiments were performed with the help of Wenli Zhang in the laboratory of Anja Ehrhardt.

In addition, low bioluminescence signals were also seen in the snoot, the feet and the tail underlining hypothesis of an alternative entry pathway. Comparison of luciferase activity between measurements revealed stronger decrease of bioluminescence measured for the liver than for signals derived from periphery tissue indicating variation in expression silencing or vector clearance. In contrast, for HV-SD12, which also showed lack of FX binding in vitro very low bioluminescence signals were detected in the liver after 20 days. Furthermore weak luciferase activity was observed in peripheral tissues like the snoot and the feet for HV-SD12, which was similar to HV-HVR12. In addition, signal derived from the liver was decreased to undetectable levels after 40 days for HV-SD12, but luciferase expression in peripheral regions was stable or even increased for the mouse treated with the high virus dose. In contrast to FX-binding assay results, in vivo analysis of HV-SD4 infected mice exhibited low or not detectable transduction rates for liver cells after 20 days and 40 days, respectively, even though strong liver transduction efficiency was expected based on the results of the FX binding assay. These data demonstrated that modifications of hexon surface domains have high potential to alter transduction efficiency in vitro and in vivo and severely influence the in vivo biodistribution of adenoviruses.

5.3. Discussion

High-capacity adenoviral vectors resemble veritable tools for gene therapy and vaccination approaches. Major obstacles for current applications are the targeting to the liver after intravenous injection as well as immunogenicity of the viral capsid shell. In this study we exploited potential of adenoviral capsid surface modulations, which have been shown to escape from the humoral immune response and to affect the biodistribution in vivo. Therefore, we altered sequences encoding surface domains of major capsid protein hexon in the context of the helper-virus genome, which provides capsid proteins for HCA vectors. In detail, either hypervariable regions or complete surface domains were exchanged precisely with respective sequences of other human adenovirus serotypes utilizing a recently established BAC cloning technique. Even though reconstitution was challenging, helper-viruses with precisely exchanged HVRs from hAd12 and hAd48 were generated as well as chimeras with surface domains derived from hAd4 and hAd12. Final vector preparation yields were comparable to preparations of unmodified helper-viruses underlining suitability for generation of HCAs. Analysis of novel helper-viruses HV-HVRs12, HV-SD12 and HV-SD4 revealed strong impact of modifications on in vitro transduction efficiency for CAR negative cells and tremendous effects on in vivo biodistribution after intravenous injection.

The rational for the design of hexon-modifications was based on conservation of structural features and interactions. Alignment of amino acid sequences of various human adenovirus serotypes showed high conservation of all domains of the hexon base indicating importance of structural integrity for these parts of the hexon.[48] In addition, high definition structural analysis revealed numerous interactions of hexon monomers with all proteins of the capsid shell except for the fiber protein and this interaction network was assumed to provide the capsid stability. All interaction sites are located within the conserved hexon basement, which build up the scaffold for viral capsid shell[46], emphasizing importance for conservation of these protein regions. Therefore, it is highly likely that any alterations of these parts of the hexon protein affect structural integrity of the whole capsid. In concordance with this assumption and in previous attempts, which aimed for generation of adenoviruses with completely exchanged hexons or with hexon chimeras containing large exchanges, no stable capsids were formed and therefore no virus replication was observed. The molecular design applied in this study was based on exchanging hypervariable regions precisely or replacing only the hexon surface domains. Therefore, no interactions of hexons with other capsid proteins were affected and only two regions with trimerization elements located in domains

DE1 and FG1 of unmodified hexons were deleted. A previous study demonstrated efficient capsid formation by precise exchanges of hypervariable regions with respective sequences of hAd48. However, for this design secondary structures predicted by crystal structure of hexon monomers[47,48] might be affected and severe effects on tertiary structure of the hexon surface domains cannot be excluded. Therefore, in this study the alternative design of hexon chimeras included exchange of main parts of the domains DE1 and FG1. Althought this approach was predicted to be even more challenging than the precise replacement of HVRs[52] (personal communication with J. Bruder), HV-SD4 and -SD12 could be generated successfully and hexon-modifications were verified by sequencing.

However, formation of intact capsids remains as a major challenge for generation of hexon-modified adenoviruses. Although numerous reconstitution experiments with varying conditions were evaluated in this study, no stable protocol could be established. Even though a clear bottleneck of the procedure was not identified, purity of linearized viral genome DNA utilized for transduction of adenovirus producer cells as well as high transfection efficiencies seemed to be critical factors. However, several viral vectors with exchanged hypervariable regions as well as with completely replaced surface domains were reconstituted, indicating that the size of sequence modifications does not significantly influence the reconstitution efficiency. In concordance with this assumption, complete trimerisation of protein chimeras in cell culture (Fig. 5.1c) demonstrated, that steric hindrance did not inhibit early assembly steps and that hexon trimer stability was not significantly reduced. Furthermore, serotype-specific HVR sequences are similar in size in comparison with the original sequence derived from hAd5. Therefore, steric hindrance causing inhibition of interactions between hexon trimers and neighboring hexon trimers or other proteins of the capsid shell is unlikely.

Amplification of successfully reconstituted hexon-modified adenoviruses revealed prolonged replication rates. This fact as well as the low success rate for reconstitution of hexon-modified viruses indicated, that capsid assembly is impaired, potentially being caused by variation of the kinetics for formation of hexon trimers. However, repeated freeze-thaw cycles performed during virus purification did not result in decrease of final vector yields, indicating high stability of hexon-modified adenoviruses. Furthermore, kinetics of eGFP expression seems to be similar for hexon-modified and unmodified vectors. Therefore, intracellular processes like escape from endosomes, transport along the microtubule, attachment to the nuclear pore or disassembly of the capsids for genome release are comparable to unmodified vectors.

Although replication cycles of modified vectors were prolonged and optimal time points for harvesting cells to obtain maximum numbers of packaged viral particles were not determined, titers of final vector preparations as well as total yields were comparable to preparations of unmodified vectors. Therefore, generation of HCAs utilizing these novel hexon-modified helper-viruses should result in comparable titers and yields. In addition, sequencing results obtained for modified regions of viral genomes derived from purified particles of the final vector preparation revealed no mutations within the chimeric hexon sequences during amplification in cell culture demonstrating high stability of the modified vector genome. Furthermore, prolonged replication time even might have a positive effect on helper-virus contamination in HCA preparations, because it was previously shown, that the expression level of Cre-recombinase is the limiting factor for efficient excision of packaging signal.[17] Therefore the delay in capsid formation and packaging of the helper-virus genomes prolongs incubation time with the recombinases, which in turn might result in reduction of the number of packaged helper-virus genomes. This phenomenon was also observed for phiC31 integrase-mediated excision of the packaging signal.[57]

Comparison of transduction rates for CAR-negative cells in presence and absence of coagulation factor X in cell culture and in vivo biodistribution after intravenous injections revealed surprising data, which are not in line with current knowledge and hypotheses. First, mice injected intravenously with HV-SD4 did not show strong liver tropism, although addition of FX showed significant increase of virus uptake in CAR-negative SKOV3 cells. However, concentrations of FX used in cell culture are higher than levels of circulating FX in vivo and proximity of virus and target cells as well as the lack of the blood stream enables cellular uptake in cell culture even for capsids weakly interacting with FX. Furthermore, intravenously injected viruses interact with other blood components such as erythrocytes reducing the number transduced target cells.[58] Therefore, we hypothesized that liver tropism mediated by FX depends on the strength of FX interaction with hexon surface domains. Upon this assumption HV-SD4 capsids might have a higher dissociation constant for FX-binding than unmodified hAd5-based capsids resulting in enhanced FX-mediated uptake for CAR-negative cells in vitro but no efficient transduction of liver cells in vivo. Based on this hypothesis, observation of FX-mediated uptake in the FX-binding assay in cell culture would be insufficient to predict in vivo liver tropism after intravenous administration. In contrast, more precise FX-binding assays in vitro would be a good indicator for strong FX ablation resulting in reduced transduction rates in the liver tissue in mice. As previously observed for

adenoviral vectors with HVRs precisely exchanged with HVRs of hAd48, the fate of HV-SD4 after tail vain injection into mice could not be determined due to the lack of expression of sufficient amounts of Firefly luciferase. This might be caused by macrophage mediated vector clearance or binding to erythrocytes and successive elimination.

The second issue raised by in vivo analysis was the generation of new binding sites of the virus capsid for cell surface markers of circulating proteins by modification of hexon proteins. Injection of HV-HVR12 resulted in expression of Firefly luciferase in liver cells with a 500-fold increase in maximum signal strength in comparison to the maximum signal derived after infection with unmodified helper-virus. Liver tropism could be verified by bioluminometric measurement of extracted organs, although signals derived from isolated organs decreased rapidly during preparation. In addition, bioluminescence was detected in periphery tissue. Low signal strength might be caused by low numbers of infected cells or insufficient distribution of the Firefly luciferase substrate D-luciferin. Therefore it could not be excluded, that transduction efficiency for cell types located in the periphery is high, but signal intensity is low due to low amounts of D-luciferin. In contrast, also the possibility should be considered, that the signal could be detected only due to the localization at the body surface of the mice. Therefore transduction rate might be low for cells in the periphery, but bioluminescence signals were still detectable due to the missing absorption of signal by other tissue of the body. Strong signals derived from the liver and weak signals in periphery tissue might be caused by one or two new binding sites generated by hexon-modifications. This is underlined by results of the FX-binding assay showing 40-fold increased transduction efficiency for HV-HVR12 in comparison to unmodified vector in absence of FX, which is in line with the increase of the liver signal in vivo. The fact, that transduction is increased in cell culture experiments also indicates, that HV-HVR12 capsids directly interact with a yet unknown cellular surface component.

For FX-binding experiments with HV-SD12 no enhanced uptake into CAR-negative cells in absence or in presence of FX was noticed. As expected from these data, in vivo experiments revealed low signals derived from liver tissue after days post-injection, which declined to undetectable levels at day 40. Transduction of liver cells detected after 20 days might have occurred due to unspecific uptake of viral particles from the blood as it was seen for liver-ablated adenoviral vectors in previous studies.[59] Furthermore, low bioluminescence signals from peripheral tissue were observed. These signals persisted for at least 40 days, what might be caused by low induction of the immune response or by slow accumulation of expressed

Firefly luciferase. Moreover, comparison of bioluminescence pictures from HV-HVR12 and HV-SD12 after 40 days supports the hypothesis, that HV-HVR12 capsids have novel cellular surface attachment sites. One of these sites might be specific for hAd12 derived sequences mediating the transduction of peripheral tissue whereas a second binding site specific for HV-HVR12 might enhance the transduction efficiency in general resulting in strong signals for cells in the periphery and hepatocytes. With respect to the usage of the novel hexon-modified helper-viruses in future approaches, dissociation constants for interaction with coagulation factor X should be determined to illuminate details of association between FX-binding and in vivo liver tropism. Furthermore, new interaction partners and respective affinities should be identified to shed light on the mechanisms determining in vivo biodistributions.

Based on the assumption that factor X binding motifs are located in the hypervariable regions and that this interaction mediates transduction of liver tissue after intravenous injections, both vectors HV-HVRs12 and HV-SD12 were expected to behave similarly. However, due to dramatic differences in bioluminescence signal strength obtained from liver tissue, impact of exchanged hexon sequences seems to be less predictable than assumed. This might have occurred due to structural alterations, which were not considered during design of helper-virus modifications utilizing precise excision of HVRs. Although conserved regions within the surface domains were not exchanged by generation of these hexon chimeras, replacements of some hypervariable regions might have disrupted structural elements essential for formation of the known tertiary structure of the surface domains. Therefore, new unexpected binding sites might have been generated just by chance, in addition to interaction sites encoded by the incorporated sequences from the respective adenovirus serotype. In contrast, structural integrity of complete domains used for exchanges of surface domains is more likely to be stable than that of chimeric domains generated by HVR-replacements. Furthermore, altered interaction with other domains might affect stability of capsids with completely exchanged surface domains but should not affect capsid surface regions containing binding sites e.g. the FX binding site. Therefore, effects on biodistribution by replacement of complete surface domains might be more predictable based on the in vivo distribution of respective wild-type adenoviruses.

Nevertheless, biodistribution of novel adenoviral vectors generated in this study have to be evaluated in more detail e.g. by tracking bioluminescence signal locations and strength more frequently as well as by analysis of DNA isolated from extracted organs to reveal vector fate independent from expression of reporter genes. Furthermore, analysis of alanin-

aminotransferase (ALT) levels, released by hepatocytes when toxicity occurs, have to be analyzed to explore differences in vector associated toxicity and innate immune responses. In addition, efficacy of capsid-modified adenoviral vectors depends on the amount of neutralizing antibodies directed against the modified capsid and the number of vector-specific cytotoxic T cells. Therefore, these essential factors should be analyzed periodically after injection. In combination with monitored expression levels of delivered transgenes, time courses for components of the immune system will reveal advantages and limitations of respective vectors.

Moreover, in vivo experiments with macrophage-depleted mice utilizing clodronate liposomes should be performed to evaluate the role of uptake by macrophages in the liver (Kupffer cells). For unmodified adenoviral vectors main portion of the administered virus particles are cleared by Kupffer cells and in correlation with the uptake of adenoviruses, the immune response is triggered. Therefore, it might be interesting to determine the impact of hexon-modification on the uptake, especially for HV-HVR12. In addition, experiments utilizing mice with CAR-expressing erythrocytes simulating the situation in humans as well as with warfarin-treated mice inhibiting FX-mediated liver tropims might illuminate new features of the vectors with hexon-modified capsids. Also, evaluation of hexon-modified adenoviral vectors in other mouse strains such as Balb/c-mice or in other species such as Syrian hamsters might provide novel insights in in vivo performance of these viral vectors.

With respect to gene therapeutic approaches multiple applications of HCAs transporting identical expression cassettes might provide an option to increase expression levels of delivered transgenes or siRNAs. With respect to correction of liver-associated genetic defects, HCA generated with HV-HVR12 holds great promises due to observed increase in liver transduction. For retargeting of HCAs from the liver to other tissues or cell types HV-SD4 and HV-SD12 might be used due to low signals obtained from the liver after intravenous administration. Both helper-virus variants could be used as a basis for incorporation of fiber mutants with high affinity for tissue-specific markers. This should result in efficient retargeting of the respective HCA in combination with shielding the vector capsids against anti-adenovirus 5 antibodies. For vaccination approaches repeated intramuscular injections of HCAs encoding one or several antigens might be an option to boost the immune response enhancing strength and diversity of antigen-specific antibodies and cytotoxic T cells. Therefore, evasion from neutralizing anti-adenovirus 5 antibodies as well as cross-reactivity

of antibodies specific for the modified vectors, should be determined to optimize sequential administrations and therefore to minimize the anti-adenoviral immune responses.

To sum it up, we investigated three new hexon-modified helper-viruses for generation of HCAs. The new features of the novel HVs revealed in this study clearly demonstrated potency for modification of hexons to enable modulation of the adenovirus tropism after intravenous administration. Furthermore, experimental data raised questions regarding the strict relation of FX-binding and the in vivo liver tropism (HV-SD4) and the structural integrity of hexon surface domains modulated by precise exchanges of hypervariable regions (HV-HVR12). In summary, this study underlines the key role for modulation of most prominent capsid surface domains to generate HCAs with specific targeting and immune-modulatory features, although design and generation remain challenging.

5.4. Materials and Methods

5.4.1. Construction of plasmids for expression in mammalian cells

For generation of plasmids encoding hexon chimeras with completely exchanged surface regions, a master clone was constructed. Therefore conserved 5' and 3' sequences were amplified by PCR and subcloned into the vector pCR-BluntII-Topo (Invitrogen) generating vectors pT-hex5-5' with *AarI* and *BglII* binding sites at the 3' end and pT-hex5-3' with *BglII* and *BspQI* binding sites at the 5' end (primers: Table 1.1a). Both vectors were cut with *BglII* and *NotI* and fragments were ligated resulting in pT-M. Subsequently conserved hexon regions were excised from pT-M with restriction enzymes *SpeI* and *NotI* and cloned into mammalian expression vector pCI (Promega) which was cut with *XbaI* and *NotI*. Constructed vector pCI-M contained conserved 5' and 3' regions of hAd5 hexon separated by restriction enzyme binding sites *AarI*, *BglII* and *BspQI*. Recognition sites for endonucleases type II *AarI* and *BspQI* are directed towards the conserved hexon sequences. Subsequently, digests with *AarI* and *BspQI* enabled cutting in the conserved regions generating sticky ends and excision of binding sites. For generation of hexon chimeras, sequences of hexon genes encoded by viral genomes of respective adenovirus serotypes were amplified by PCR. PCR products encode *AarI* binding sites at the 5' end and *BspQI* binding sites at the 3' end, with respective cutting sites in the amplified hexon-specific region (primers: Table 1.1b).

a	**Generation of master clone pCI-M**	
	hAd5-hex-5-5	ATGGCTACCCCTTCGATGATG
	hAd5-hex-5-3	AGATCTCACCTGCAGGGCTTAAAAGTAGGGCCCCT
	hAd5-hex-3-5	AGATCTGCTCTTCTGCCATGGAAATCAATCTAAAT
	hAd5-hex-3-3	TTATGTTGTGGCGTTGCCGGC
b	**Generation and analysis of T-SD clones and analysis of pB-HV-SD BAC-clones**	
	hAd4-SD-5	AGATCTCACCTGCAGTTTAAGCCCTACTCCGGCACT
	hAd4-SD-3	AGATCTGCTCTTCTGGCAAAAGGATTGCCTAC
	hAd7-SD-5	AGATCTCACCTGCAGTTTAAGCCATATTCCGGCACA
	hAd7-SD-3	AGATCTTCGCTTCTGGCCTGGTTGTTGCCTAT
	hAd12-SD-5	AGATCTCACCTGCAGTTTAAGCCCTATTCCGGAACC
	hAd12-SD-3	AGATCTGCTCTTCTGGCGGCTATATTCCCAATCC
	hAd13-SD-5	AGATCTCACCTGCAGTTTAAGCCCTACTCGGGCACGGCT
	hAd13-SD-3	AGATCTGCTCTTCTGGCAAAGATGTTGCCCTTCC
	hAd41-SD-5	AGATCTCACCTGCAGTTTAAGCCCTACTCCGGAACCGCC
	hAd41-SD-3	AGATCTGCTCTTCTGGCAAAAATGTTCCCAGATTC
c	**Generation of pCI-100K-pr**	
	hAd5-100Kpr-5	CACTCTAGAATGGAGTCAGTCGAGAAGAAGG
	hAd5-100Kpr-3	CACGCGGCCGCCTACGGTTGGGTCGGCGAACGG
d	**Sequencing modified regions of hexon chimera and generation of pB-HV-SD BAC-clones**	
	Seq-hex-SD-5	GATAACCGTGTGCTGGACATG
	Seq-hex-SD-3	TTGTCGGGCAAATACAGCGCT
e	**Generation of intermediate BAC pB-HV-hexGA**	
	B-HV-hexGA-5	TACAACGCCCTGGCTCCCAAGGGTGCCCCAACTCAAGCTATGCATCAAGC
	B-HV-hexGA-3	TTCCATGGCAAAATTATTTCCAACTCTTATGAATTGGGCCCTCTAGATGC
f	**Generation of pB-HV-HVR BAC-clones**	
	B-HV-HVR-5	GGCGTGCTGGACAGGGGCCCTACTTTTAAGCCCTACTCTGGCACTGCCTA
	B-HV-HVR-3	AGGTTGGCATTTAGATTGATTTCCATGGCAAAATTATTTCCAACTCTTAT
g	**Analysis of pB-HV-HVR BAC-clones**	
	HVR5-for	CTACTGAGGCGACCGCAGGCAATGG
	HVR5-rev	TGACCTGTTTTAGGTTTTACCTTGG
	HVR12-for	ATTCAGCTAACAATGCAGCAAACAC
	HVR12-rev	TTGCTTCACTGACAGTGTTGTCGGC
	HVR41-for	CGCCTTGCCAAGCACTCCTAATGAG
	HVR41-rev	GCATAATTGTCGTCTGCAGTCCAGG
	HVR44-for	GACATTCCACAAAATGGTGTTCAGG
	HVR44-rev	TTTGATATTGCATTATCCACTTCCC
	HVR48-for	ATATTCCCAGTACTGGCACAGGTGG
	HVR48-rev	GATTGTGTTCAGATACTGCAGTGTC
	HVR50-for	GACCTAAGATCACAAATGACTGGCC
	HVR50-rev	CTTTCCAAGTAGTGGTTTCATCACC

Table 5.1: Primers used for cloning procedures and analysis.

Amplified sequences were subcloned into the plasmid pCR-BluntII-Topo resulting in vectors pT-hex5-SD4, -SD7, -SD12, -SD13 and -SD41. After excising inserts with *AarI* and *BspQI*, fragments were subcloned into the master plasmid pCI-M digested with *AarI* and *BspQI* resulting in mammalian expression plasmids encoding for hexon chimera. To construct plasmid pCI-100K-pr vector pCI was linearized with *SmaI* and dephosphorylated with alkaline phosphatase. In parallel, the gene encoding adenoviral 100K-protein was PCR-amplified utilizing viral genomic DNA isolated from purified hAd5 particles as template (primers: Table 1.1c). Purified PCR product was phosphorylated with T4 polynucleotide kinase and blunt-end ligated with *SmaI*-cutted pCI vector (T4 DNA Ligase) resulting in vector pCI-100K-pr.

5.4.2. Synthesis of sequences encoding chimeric hexon surface domains

For synthesis of chimeric hexon surface domains sequences of HVRs located within the human adenovirus serotype 5 hexon gene sequence at positions 403-495 (HVR1), 562-582 (HVR2), 634-657 (HVR3), 742-783 (HVR4), 802-843 (HVR5), 913-945 (HVR6) and 1255-1353 (HVR7) were precisely exchanged with respective sequences of human adenovirus serotype 12, 41, 44, 48 and 50. Sequences synthesis was performed by GeneArt, Invitrogen (Regensburg, Germany) and for delivery sequences were incorporated into a standard vector.

5.4.3. Construction of BACs encoding for hexon-modified helper-virus genomes

For incorporation of hexon chimeric sequences into the adenoviral helper-virus genome we utilized cloning techniques based on bacterial artificial chromosomes described elsewhere in detail.[60] In brief, recently described bacterial artificial chromosome pB-HV was transformed into SW102 E.coli and in parallel a galK-Amp cassette was PCR-amplified with additional sequences at 5' and 3' ends homologous to hexon gene sequences upstream and downstream of HVRs encoding sequences (primers: Table 1.1e). 1.5 µg of respective PCR products was transformed into SW102 containing pB-HV and after heat-shock activated homologous recombination and selection for the ampicillin intermediate clone pB-HV-hexGA was isolated. Subsequently, chimeric hexon sequences generated by synthesis or regions of respective adenoviral genomes coding for the surface domains of the hexon were PCR-amplified utilizing primers (primers: Table 1.1d, f). Purified PCR products were used for

BAC cloning replacing the galk-Amp sequence with chimeric hexon sequences by homologous recombination and single clones were isolated by negative selection against galK. Next, all hexon-modified helper-virus BACs were modulated replacing the stuffer DNA in the E3 region[18] by a reporter gene expression cassette encoding a eGFP-Firefly luciferase fusion protein under the control of the CMV-enhancer/EF1α promoter derived from pEPito-[hCMV/EF1P]-[EGFP::Luc]-ΔMARS.[61] For this cloning step primers dE3-GFP/FLuc-5 (5-AACACATCGAATACGTTGTCCTGCCTTACCAATGCTTAATCAGTGAGGC-3) and dE3-GFP/FLuc-3 (5-CAGCCAGAAAGTGAGGGAGCCACGGTTACATAACTTACGGTA AATGGCCC-3) were utilized. Positive clones were purified and used for reconstitution of respective hexon-modified adenoviral helper-viruses.

5.4.4. Quantitative and qualitative PCRs

All PCRs were performed utilizing high-fidelity KOD Hot Start DNA Polymerase (Novagen), which generates blunt ends. All used primers and templates for respective PCRs are listed in Supplementary Table 1. For quantitative PCRs 35 cycles were performed with an annealing temperature of 60° and an elongation time of 25 seconds per kb, whereas for PCRs for verification of modifications 25 cycles were used. Specific primers for control PCRs to verify hexon chimeras with precisely exchanged hypervariable regions were designed to bind to sequences of HVR5 and HVR7 of respective hexon genes (primers: Table 1.1g). Replacements of the complete surface domains were determined by primers used for generation of respective plasmids for expression in mammalian cells (primers: Table 1.1b).

5.4.5. Cell culture

Human embryonic kidney HEK293 cells were cultured in Dulbecco's modified Eagle's medium supplemented with 10 % fetal bovine serum (PAA Laboratories) and human ovarian carcinoma SKOV3 cells were cultured in RPMI 1640 media (Invitrogen) supplemented with 2 mM L-glutamine (Invitrogen), 10 % fetal calf serum (PAA Laboratories) and 1 mM sodium pyruvate.

5.4.6. Reconstitution, amplification and purification of hexon-modified helper-viruses

Helper-viruses were generated and amplified according to protocols published previously. [62,63] In brief, respective helper-virus BAC DNA was digested with *PacI* and transfected into HEK293 cells with Fugene 6 (Roche). After cytopathic effect occured 10-20 days post transfection, cells were harvested and virus particles were released by three consecutive freeze-thaw steps. Helper-virus was amplified by infection of increasing numbers of HEK293 cells. For the final amplification step 4 x 10^8 HEK293 cells were infected and generated helper-virus particles were purified by two successive caesium chloride (CsCl) gradients. For application in vitro and in vivo toxic CsCl solutions with virus were exchanged with a physiological buffer by dialysis and vector aliquots were stored at -80°C until usage.

5.4.7. Determination of physical titers of hexon-modified helper-viruses and sequencing

Detailed procedures to determine physical titers of an adenoviral vector preparation were described elsewhere.[62] In brief, for determination of number of packaged viral particles (physical titer) we diluted 5 µl of the vector preparation with 95 µl TE buffer supplemented with 0.1 % sodium dodecylsulfate. After shaking for 30 min at 37 °C OD_{260} was measured 5 times and mean value was used to calculate the physical titer. Sequencing for verification of modified hexon regions was performed by Eurofins MWG Operon (Ebersberg, Germany) utilizing sequencing primers (primers: Table 1.1d).

5.4.8. Western Blot analysis

HEK 293 cells were seeded in 60 mm dishes and co-transfected at 60% confluence with mammalian expression plasmids pCI-100K-pr encoding adenoviral 100K-protein and pCI-hex5-SD4, -SD7, -SD12, -SD13 and -SD41 for expression of the chimeric hexon protein, respectively. 72 hrs post-transfection, cells were harvested in 200 µl lysis buffer (50 nM Tris-HCl pH 8.0, 150 nM NaCl, 1 % NP-40) and incubated for 30 min on ice. For western blot analysis 5 µl loading dye (5x) was added to 15 µl cell lysate, respectively, and subsequently boiled at 95°C for 5 min or cooled at 4°C. Proteins were separated by SDS-PAGE utilizing a 10% SDS-polyacrylamid gel and transferred by semi-dry blotting on a methanol-activated PVDF membrane. The membrane was treated over night with blocking buffer (20 mM Tris pH 7.5, 500 mM NaCl, 5% milk powder) and after 3 washing steps with TBST (20 mM Tris

pH 7.5, 500 mM NaCl, 0.05% Tween, 0.2 % Triton-X100), the membrane was incubated for 1 hr with the polyclonal anti-adenovirus antibody PA1-7201 (Dianova, final concentration 1:500) diluted in blocking buffer. Subsequently, the membrane was washed 3 times and incubated with the monoclonal peroxidase-conjugated rabbit anti-goat antibody (Jackson ImmunoResearch Laboratories Inc., final dilution 1:10000) diluted with blocking buffer. For protein detection blots were washed three times, ECL reagent (GE Healthcare) was added and peroxidase activity detected according to manufacturers' instructions.

5.4.9. Flow cytometric analysis

HEK 293 cells were seeded in 6-well plates and infected with unmodified or hexon-modified helper-virus (1 µl/well). After 48 hrs incubation at 37°C cells, were washed with DPBS and treated with trypsin. Detached cells were harvested and resuspended in DPBS supplemented with 0.1% FBS. Subsequently, each sample was analyzed for eGFP expression by flow cytometer FACS Canto II and data derived from 20,000 detected events were used for evaluation, respectively.

5.4.10. Luciferase assay

Quantification of Firefly luciferase expression was performed utilizing the Dual-Luciferase^{R} Reporter Assay System kit (Promega). In detail, HEK 293 cells seeded in 6-well plates were infected with unmodified or hexon-modified helper-virus (1 µl/well). 48 hrs post-infection, cells were washed with DPBS and harvested in 500 µl passive lysis buffer provided by the kit. 5 µl of the cell lysate were mixed with 35 µl luciferase assay reagent II, respectively, and subsequently Firefly luciferase activity was measured for 5 seconds at 492 nm utilizing a luminometer (Microlumat Plus LB 96V, Berthold).

5.4.11. In vitro analysis of FX-mediated transduction

FX binding assay was performed in a 96-well format with 5 x 10^4 SKOV3 cells/well. Cells were infected with unmodified or modified helper-viruses (1000 vps/cell) in serum-free medium in absence or presence of FX (Haematological Technologies) with a final concentration of 1 IU/ml. After 3 hrs incubation at 37 °C infected cells were washed with

DPBS and subsequently maintained in full medium for 48 hrs. Next, cells were harvested and transduction efficiency was quantified by detection of Firefly luciferase activity.

5.4.12. In vivo biodistribution studies

Female C57Bl/6 mice were kept and treated according to the guidelines of the Ludwig Maximilians University of Munich (Munich, Germany). Viral vectors were diluted in DPBS and injected intravenously via tail vein using a total volume of 250 µl. For biodistribution measurements 250 µl D-luciferin diluted with DPBS (20 mg/ml) was administered intraperitoneally. Ten minutes post-injection bioluminescence imaging was performed detecting luciferase activity by the CCD camera (1 min exposure time) and recorded images were evaluated using the Xenogen IVIS Imaging System 200 Software.

5.5. References

1. **Lechardeur, D., A. S. Verkman, et al.** (2005). "Intracellular routing of plasmid DNA during non-viral gene transfer." Adv Drug Deliv Rev **57**(5): 755-767.
2. **O'Connor, T. P. and R. G. Crystal** (2006). "Genetic medicines: treatment strategies for hereditary disorders." Nat Rev Genet **7**(4): 261-276.
3. **Gonin, P. and C. Gaillard** (2004). "Gene transfer vector biodistribution: pivotal safety studies in clinical gene therapy development." Gene Ther **11 Suppl 1**: S98-S108.
4. **Chardonnet, Y. and S. Dales** (1970). "Early events in the interaction of adenoviruses with HeLa cells. I. Penetration of type 5 and intracellular release of the DNA genome." Virology **40**(3): 462-477.
5. **Graham, F. L. and L. Prevec** (1992). "Adenovirus-based expression vectors and recombinant vaccines." Biotechnology **20**: 363-390.
6. **Bergelson, J. M., J. A. Cunningham, et al.** (1997). "Isolation of a common receptor for Coxsackie B viruses and adenoviruses 2 and 5." Science **275**(5304): 1320-1323.
7. **Wickham, T. J., P. Mathias, et al.** (1993). "Integrins alpha v beta 3 and alpha v beta 5 promote adenovirus internalization but not virus attachment." Cell **73**(2): 309-319.
8. **Wodrich, H., D. Henaff, et al.** (2010). "A capsid-encoded PPxY-motif facilitates adenovirus entry." PLoS Pathog **6**(3): e1000808.

9. **Trotman, L. C., N. Mosberger, et al.** (2001). "Import of adenovirus DNA involves the nuclear pore complex receptor CAN/Nup214 and histone H1." Nat Cell Biol **3**(12): 1092-1100.

10. **Stow, N. D.** (1981). "Cloning of a DNA fragment from the left-hand terminus of the adenovirus type 2 genome and its use in site-directed mutagenesis." J Virol **37**(1): 171-180.

11. **Yang, Y., F. A. Nunes, et al.** (1994). "Cellular immunity to viral antigens limits E1-deleted adenoviruses for gene therapy." Proc Natl Acad Sci U S A **91**(10): 4407-4411.

12. **Dai, Y., E. M. Schwarz, et al.** (1995). "Cellular and humoral immune responses to adenoviral vectors containing factor IX gene: tolerization of factor IX and vector antigens allows for long-term expression." Proc Natl Acad Sci U S A **92**(5): 1401-1405.

13. **Yang, Y., Q. Li, et al.** (1995). "Cellular and humoral immune responses to viral antigens create barriers to lung-directed gene therapy with recombinant adenoviruses." J Virol **69**(4): 2004-2015.

14. **Lusky, M., M. Christ, et al.** (1998). "In vitro and in vivo biology of recombinant adenovirus vectors with E1, E1/E2A, or E1/E4 deleted." J Virol **72**(3): 2022-2032.

15. **Hardy, S., M. Kitamura, et al.** (1997). "Construction of adenovirus vectors through Cre-lox recombination." J Virol **71**(3): 1842-1849.

16. **Parks, R. J., L. Chen, et al.** (1996). "A helper-dependent adenovirus vector system: removal of helper virus by Cre-mediated excision of the viral packaging signal." Proc Natl Acad Sci U S A **93**(24): 13565-13570.

17. **Ng, P., C. Evelegh, et al.** (2002). "Cre levels limit packaging signal excision efficiency in the Cre/loxP helper-dependent adenoviral vector system." J Virol **76**(9): 4181-4189.

18. **Palmer, D. and P. Ng** (2003). "Improved system for helper-dependent adenoviral vector production." Mol Ther **8**(5): 846-852.

19. **Parks, R. J. and F. L. Graham** (1997). "A helper-dependent system for adenovirus vector production helps define a lower limit for efficient DNA packaging." J Virol **71**(4): 3293-3298.

20. **Puntel, M., A. K. Muhammad, et al.** (2010). "A novel bicistronic high-capacity gutless adenovirus vector that drives constitutive expression of herpes simplex virus type 1 thymidine kinase and tet-inducible expression of Flt3L for glioma therapeutics." J Virol **84**(12): 6007-6017.

21. **Morral, N., R. J. Parks, et al.** (1998). "High doses of a helper-dependent adenoviral vector yield supraphysiological levels of alpha1-antitrypsin with negligible toxicity." Hum Gene Ther **9**(18): 2709-2716.

22. **Muruve, D. A., M. J. Cotter, et al.** (2004). "Helper-dependent adenovirus vectors elicit intact innate but attenuated adaptive host immune responses in vivo." J Virol **78**(11): 5966-5972.

23. **O'Neal, W. K., H. Zhou, et al.** (2000). "Toxicity associated with repeated administration of first-generation adenovirus vectors does not occur with a helper-dependent vector." Mol Med **6**(3): 179-195.

24. **Weaver, E. A., P. N. Nehete, et al.** (2009). "Comparison of replication-competent, first generation, and helper-dependent adenoviral vaccines." PLoS One **4**(3): e5059.

25. **Shiver, J. W. and E. A. Emini** (2004). "Recent advances in the development of HIV-1 vaccines using replication-incompetent adenovirus vectors." Annu Rev Med **55**: 355-372.

26. **Sumida, S. M., D. M. Truitt, et al.** (2005). "Neutralizing antibodies to adenovirus serotype 5 vaccine vectors are directed primarily against the adenovirus hexon protein." J Immunol **174**(11): 7179-7185.

27. **Pichla-Gollon, S. L., M. Drinker, et al.** (2007). "Structure-based identification of a major neutralizing site in an adenovirus hexon." J Virol **81**(4): 1680-1689.

28. **Hiltunen, M. O., M. P. Turunen, et al.** (2000). "Biodistribution of adenoviral vector to nontarget tissues after local in vivo gene transfer to arterial wall using intravascular and periadventitial gene delivery methods." FASEB J **14**(14): 2230-2236.

29. **Sullivan, D. E., S. Dash, et al.** (1997). "Liver-directed gene transfer in non-human primates." Hum Gene Ther **8**(10): 1195-1206.

30. **Kalyuzhniy, O., N. C. Di Paolo, et al.** (2008). "Adenovirus serotype 5 hexon is critical for virus infection of hepatocytes in vivo." Proc Natl Acad Sci U S A **105**(14): 5483-5488.

31. **Parker, A. L., S. N. Waddington, et al.** (2006). "Multiple vitamin K-dependent coagulation zymogens promote adenovirus-mediated gene delivery to hepatocytes." Blood **108**(8): 2554-2561.

32. **Waddington, S. N., J. H. McVey, et al.** (2008). "Adenovirus serotype 5 hexon mediates liver gene transfer." Cell **132**(3): 397-409.

33. **Bradshaw, A. C., A. L. Parker, et al.** (2010). "Requirements for receptor engagement during infection by adenovirus complexed with blood coagulation factor X." PLoS Pathog **6**(10): e1001142.

34. **Shayakhmetov, D. M. and A. Lieber** (2000). "Dependence of adenovirus infectivity on length of the fiber shaft domain." J Virol **74**(22): 10274-10286.

35. **Shayakhmetov, D. M., T. Papayannopoulou, et al.** (2000). "Efficient gene transfer into human CD34(+) cells by a retargeted adenovirus vector." J Virol **74**(6): 2567-2583.

36. **Smith, T. A., N. Idamakanti, et al.** (2003). "Adenovirus serotype 5 fiber shaft influences in vivo gene transfer in mice." Hum Gene Ther **14**(8): 777-787.

37. **Terashima, T., K. Oka, et al.** (2009). "DRG-targeted helper-dependent adenoviruses mediate selective gene delivery for therapeutic rescue of sensory neuronopathies in mice." J Clin Invest **119**(7): 2100-2112.

38. **Nettelbeck, D. M., D. W. Miller, et al.** (2001). "Targeting of adenovirus to endothelial cells by a bispecific single-chain diabody directed against the adenovirus fiber knob domain and human endoglin (CD105)." Mol Ther **3**(6): 882-891.

39. **Nakamura, T., K. Sato, et al.** (2003). "Reduction of natural adenovirus tropism to the liver by both ablation of fiber-coxsackievirus and adenovirus receptor interaction and use of replaceable short fiber." J Virol **77**(4): 2512-2521.

40. **Poulin, K. L., R. M. Lanthier, et al.** (2010). "Retargeting of adenovirus vectors through genetic fusion of a single-chain or single-domain antibody to capsid protein IX." J Virol **84**(19): 10074-10086.

41. **Wickham, T. J., M. E. Carrion, et al.** (1995). "Targeting of adenovirus penton base to new receptors through replacement of its RGD motif with other receptor-specific peptide motifs." Gene Ther **2**(10): 750-756.

42. **Roy, S., D. S. Clawson, et al.** (2005). "Use of chimeric adenoviral vectors to assess capsid neutralization determinants." Virology **333**(2): 207-214.

43. **Vogels, R., D. Zuijdgeest, et al.** (2003). "Replication-deficient human adenovirus type 35 vectors for gene transfer and vaccination: efficient human cell infection and bypass of preexisting adenovirus immunity." J Virol **77**(15): 8263-8271.

44. **Keriel, A., C. Rene, et al.** (2006). "Canine adenovirus vectors for lung-directed gene transfer: efficacy, immune response, and duration of transgene expression using helper-dependent vectors." J Virol **80**(3): 1487-1496.

45. **Parks, R., C. Evelegh, et al.** (1999). "Use of helper-dependent adenoviral vectors of alternative serotypes permits repeat vector administration." Gene Ther **6**(9): 1565-1573.

46. **Fabry, C. M., M. Rosa-Calatrava, et al.** (2005). "A quasi-atomic model of human adenovirus type 5 capsid." Embo J **24**(9): 1645-1654.

47. **Liu, H., L. Jin, et al.** (2010). "Atomic structure of human adenovirus by cryo-EM reveals interactions among protein networks." Science **329**(5995): 1038-1043.

48. **Rux, J. J., P. R. Kuser, et al.** (2003). "Structural and phylogenetic analysis of adenovirus hexons by use of high-resolution x-ray crystallographic, molecular modeling, and sequence-based methods." J Virol **77**(17): 9553-9566.

49. **Youil, R., T. J. Toner, et al.** (2002). "Hexon gene switch strategy for the generation of chimeric recombinant adenovirus." Hum Gene Ther **13**(2): 311-320.

50. **Roy, S., P. S. Shirley, et al.** (1998). "Circumvention of immunity to the adenovirus major coat protein hexon." J Virol **72**(8): 6875-6879.

51. **Wu, H., I. Dmitriev, et al.** (2002). "Construction and characterization of adenovirus serotype 5 packaged by serotype 3 hexon." J Virol **76**(24): 12775-12782.

52. **Roberts, D. M., A. Nanda, et al.** (2006). "Hexon-chimaeric adenovirus serotype 5 vectors circumvent pre-existing anti-vector immunity." Nature **441**(7090): 239-243.

53. **De Jong, J. C., A. G. Wermenbol, et al.** (1999). "Adenoviruses from human immunodeficiency virus-infected individuals, including two strains that represent new candidate serotypes Ad50 and Ad51 of species B1 and D, respectively." J Clin Microbiol **37**(12): 3940-3945.

54. **Abbink, P., A. A. Lemckert, et al.** (2007). "Comparative seroprevalence and immunogenicity of six rare serotype recombinant adenovirus vaccine vectors from subgroups B and D." J Virol **81**(9): 4654-4663.

55. **Willcocks, M. M., M. J. Carter, et al.** (1988). "Restriction enzyme analysis of faecal adenoviruses in Newcastle upon Tyne." Epidemiol Infect **101**(2): 445-458.

56. **Hong, S. S., E. Szolajska, et al.** (2005). "The 100K-chaperone protein from adenovirus serotype 2 (Subgroup C) assists in trimerization and nuclear localization of hexons from subgroups C and B adenoviruses." J Mol Biol **352**(1): 125-138.

57. **Alba, R., P. Hearing, et al.** (2007). "Differential amplification of adenovirus vectors by flanking the packaging signal with attB/attP-PhiC31 sequences: implications for helper-dependent adenovirus production." Virology **367**(1): 51-58.

58. **Carlisle, R. C., Y. Di, et al.** (2009). "Human erythrocytes bind and inactivate type 5 adenovirus by presenting Coxsackie virus-adenovirus receptor and complement receptor 1." Blood **113**(9): 1909-1918.

59. **Alba, R., A. C. Bradshaw, et al.** (2010). "Biodistribution and retargeting of FX-binding ablated adenovirus serotype 5 vectors." Blood **116**(15): 2656-2664.

60. **Warming, S., N. Costantino, et al.** (2005). "Simple and highly efficient BAC recombineering using galK selection." Nucleic Acids Res **33**(4): e36.

61. **Haase, R., O. Argyros, et al.** (2010). "pEPito: a significantly improved non-viral episomal expression vector for mammalian cells." BMC Biotechnol **10**: 20.

62. **Jager, L., M. A. Hausl, et al.** (2009). "A rapid protocol for construction and production of high-capacity adenoviral vectors." Nat Protoc **4**(4): 547-564.

63. **Luo, J., Z. L. Deng, et al.** (2007). "A protocol for rapid generation of recombinant adenoviruses using the AdEasy system." Nat Protoc **2**(5): 1236-1247.

6. Discussion

Gene therapy is an attractive alternative for long-term correction of genetic disorders, which is based on delivery of therapeutic DNA into cells affected by the respective mutated gene. For efficient transport of the therapeutic DNA vectors are used, which are commonly based on recombinant viruses. The viral vector type and associated vector features mainly determine the outcome of a gene therapeutic approach. In this work, I focused on adenoviral vectors, which are generally based on human adenovirus 5 (hAd5). hAd5 is a non-enveloped virus with a double-strand DNA genome, which was shown to transduce a broad range of cell types with high transduction efficiencies in cell culture and after intravenous injection in mice transduction of liver tissue is observed. High-capacity adenoviral vectors (HCAs) are the newest generation of adenoviral vectors with vector genomes devoid of all coding viral sequences. In principle, for generation of HCAs 116 producer cells are co-transduced with a helper-virus (HV) enabling generation of virus capsids and the high-capacity adenoviral vector genome encoding the therapeutic DNA, which is packaged into the virus capsid (Figure 1.7). Therefore, they enable the transfer of therapeutic DNA of up to 36 kb in size. As a major advantage of HCAs compared to earlier generations of recombinant adenoviral vectors, vector-associated toxicity and immunogenicity are low due to the lack of leaky expression of viral proteins. Nevertheless, acute toxicity detected after administration of high doses of HCAs and remaining immune response directed against the incoming viral particle or the transgene product are major obstacles for applications of HCAs, because these features can result in a decreased therapeutic effects. As another limitation, adenoviral vectors are not able to transduce certain cell types utilized for cell-mediated gene therapy such as hematopoietic stem cells and applications for in vivo gene therapies are mainly restricted to diseases affecting the liver. In addition, vector genomes remain episomal in transduced cells and therefore achievement of long-term effects is hampered especially for dividing cells. The aim of this work was to establish novel methods for genetic engineering of HCAs and to evaluate options to improve HCA features with respect to therapeutic applications.

6.1. A rapid protocol for construction and production of high-capacity adenoviral vectors

As a basis for optimization of HCA features a standardized protocol for efficient production of HCAs was established in this thesis. This protocol includes an efficient cloning procedure for incorporation of therapeutic DNA of up to 14 kb into a HCA genome based on rare restriction enzymes (Figure 2.3) and large-scale amplification of HCAs utilizing a spinner-flask system for culturing up to 3 liter of the producer cell line 116, which has been adopted for suspension culture (Figure 2.4). Furthermore, purification of produced HCAs by two CsCl gradients and successive dilution of the vector in physiological buffer by dialysis are described as well as titration methods for determination of the physical titer and the infectious titer of HCA preparations. All steps of the manual are described in detail highlighting critical points and moreover, an extensive trouble shooting guide is supplied. This should allow any scientist to establish this challenging method in a laboratory and therefore, to yield vector preparations with titers of $5 \times 10^6 - 5 \times 10^7$ transducing units per µl and total numbers of $5 \times 10^9 - 1 \times 10^{11}$ transducing units within 3 weeks. In conclusion, the protocol provides a standard, which allows evaluation and comparison of results obtained with HCAs produced and tested by different groups. In addition, amplification based on a spinner-flask has been shown to be an extendable system as a recently presented study demonstrated efficient amplification of adenoviral vectors utilizing a bioreactor with a volume of 200 liters (Cecchini, Virag et al. 2011). Therefore, this protocol provides the opportunity for up-scaling the production under GMP conditions, which might be essential for translation of HCAs into clinical studies. With respect to optimization of HCA-based vector systems this protocol is a prerequisite for introduction of any genetic alteration into HV genomes or HCA genomes.

6.2. Hyperactive Sleeping Beauty transposase enables persistent phenotypic correction in mice and a canine model for hemophilia B

As already mentioned, one major challenge for utilization of HCAs in gene therapeutic approaches is the fact, that HCA genomes remain episomal in the nucleus of transduced cells. Therefore, no long-term effects can be achieved in replicating cells. To face this problem a hybrid vector system was established, which combines somatic integration of transgenic sequences mediated by the Sleeping Beauty transposase (SB) with efficient delivery by HCAs. Evaluation of this system in a murine hemophilia B model revealed efficient

transduction of hepatocytes and integration into host genomes as well as long-term phenotypic correction mediated by stable expression levels of functional transgenic human coagulation factor IX (Yant, Ehrhardt et al. 2002).

In a follow-up study, I improved the system replacing native SB with the hyperactive version HSB5 (Fig. 3.1c), which has been shown to perform 10 times better in cell culture (Yant, Huang et al. 2007). Evaluation in mice demonstrated stable expression of canine coagulation factor IX (cFIX) even after induction of cell cycling by liver toxin CCl_4 (Fig. 3.2a) indicating efficient delivery after intravenous application and high integration rates. In a preclinical study with a canine model for hemophilia B, treatment resulted in phenotypic correction for almost 3 years (Fig. 3.3a) mediated by low but stable serum cFIX expression (Figure 3.4a). However, increase of the total vector dose for treatment of a second hemophilia B dog resulted in reduction of cFIX expression down to undetectable levels (Fig. 3.4b) accompanied by reoccurance of the phenotype (Fig. 3.3b). In contrast to the treatment with a low dose, liver enzymes were strongly increased after intravenous administration (Fig. 3.5a, b) and additionally, high levels of neutralizing anti-adenoviral antibodies appeared 2-5 weeks after treatment (Fig. 3.6), but no formation of anti-cFIX antibodies was observed. This indicated a strong immune response specifically directed against adenoviral vector particles, which might also include generation of cytotoxic T cells specific for transduced cells contributing to the reduction of cFIX levels. In conclusion, the therapeutic window for the adenovirus-SB transposase hybrid vector system is narrow and therefore, utilization of hyperactive HSB5 might have been essential to achieve a long-term effect. Semi-quantitative analysis of DNA extracted from liver cells of the phenotypically corrected dog demonstrated, that sustained expression of cFIX was mainly derived from integrated transposons (Fig. 3.7a) and SB-mediated integration was verified by sequencing of integration sites (Fig. 3.7b). In contrast, the number of episomal vector forms either containing the transposon or encoding the integration machinery was comparably low (Fig. 3.7a), indicating a low probability for severe damages of chromosomal DNA caused by rest activity of the integration machinery.

However, for translation of the system into clinical studies further modifications are necessary to broaden the therapeutic window and to improve the safety profile (reviewed in Hausl, Zhang et al. 2011). Therefore, utilization of the SB100 with 100-fold higher activity in comparison to the original Sleeping Beauty transposase will significantly increase the efficiency of the system (Mates, Chuah et al. 2009). In addition, optimized IRs flanking the transposon have been shown to significantly enhance the number of transposition events

especially for large transposons (Yant, Park et al. 2004; Zayed, Izsvak et al. 2004). Furthermore, higher efficacy of the system could be achieved by combination of the integration machinery and the transposon within a single HCA (one-vector system) circumventing the necessity for co-transduction of a target cell with two vectors. However, to prevent excision of the transposon during HCA amplification, expression of the integration machinery components has to be coupled with a system for inducible expression such as the feed-forward system based on the artificial hormone mifepristone, which was shown to be suitable for clinical studies (Elia and Ulmann 1986; Sharma, Moldt et al. 2008). In addition, temporal restriction of the expression profile might be an option to avoid the overproduction inhibition effect observed for all SB variants (Mates, Chuah et al. 2009) and to reduce potential genotoxicity caused by Flpe recombinase (Branda and Dymecki 2004) and SB transposase variants (Yant, Wu et al. 2005) as well as protein-associated toxicity of the SB transposase itself (Galla, Schambach et al. 2011). Moreover, the one-vector system will allow coupling of circularization of the transposon with the shut-down of Flpe expression and the on-set of the SB transposase expression (Yant, Ehrhardt et al. 2002). In the same approach the excision of the transposon from the circular intermediate could be utilized to stop expression of the SB transposase. Therefore, expression of Flpe recombinase and SB transposase will be reduced to a minimum significantly decreasing toxic side effects and preventing hopping of the transposon within the host genome, which might cause genotoxic effects (Vassiliou, Cooper et al. 2011).

It is of note that for delivery of the SB transposase system, retroviral vectors or AAV vectors might be considered as an option (Müther, Noske et al. 2009). Lentivirus/SB hybrid vectors with a defective lentiviral integrase have been generated resulting in random SB-mediated integration of the therapeutic transgene (Staunstrup et al. 2009). However, further improvements of the integration machinery is limited by the restricted capacity of lentiviral vectors (>10 kb) and furthermore, some transposon sequences have been shown to decrease the vector titer (Vink et al., 2009). Currently, no AAV-based hybrid vector systems are known and generation might be challenging due to strongly limited packaging capacity of AAV vectors (>5kb). In addition, highly structured inverted terminal repeats flanking AAV vector genomes might influence recognition of the inverted repeats flanking the transposon by the transposase (Aurnhammer, Haase et al. 2011). Therefore, adenoviral vectors are the vector of choice for application of this type of hybrid vector systems in vivo and moreover, HCAs

provide sufficient capacity to enable optimizations of the integration machinery and the therapeutic DNA.

Besides vector optimization utilization of other machineries enabling somatic integration also might be an attractive alternative. However, the newest hyperactive version of the Sleeping Beauty transposase (SB100X) has been shown to be most efficient in comparison to other transposon-based integration machineries except for the recently developed hyperactive version of the PiggyBac transposase, which have been shown to mediate even higher rates of somatic integration in cell culture and in vivo (Doherty, Huye et al. 2011; Yusa, Zhou et al. 2011). Additionally, the PiggyBac transposase enables transposition of large cargo sequences with low reduction in efficiency (Li, Turner et al. 2011), whereas size of the optimized SB transposon is limited to transgenic sequences less than 12 kb in size (Alessandra Recchia, personal communication). Furthermore, in contrast to Sleeping Beauty transposons excision of a PiggyBac transposon, which has been integrated in the chromosomal host DNA, is traceless (Yusa, Rad et al. 2009). Therefore, a hybrid vector system based on the PiggyBac transposase might be an attractive alternative with respect to the capacity of 36 kb for HCAs, although the integration profile is biased towards transcriptional active chromosomal regions to a small extend (Huang, Guo et al. 2010). Especially for ex vivo gene therapeutic application traceless excision of the PiggyBac transposon is an important feature, because it allows generation of autologous cells by dedifferentiation, differentiation or trans-differentiation without any permanent alterations of the chromosomal DNA potentially influencing altered cells after retransplantation (Yusa, Rad et al. 2009).

To reduce the genotoxicity, an integration machinery specifically targeting distinct loci within the host genome is a desired goal. One option is the bacterial phiC31 integrase, which preferentially integrates into a hot spot located at chromosomal region 19q13 or in other pseudo-attP sites within the host genome (Chalberg, Portlock et al. 2006). However, serious side-effects such as chromosomal translocations were detected when using when using the phiC31 integrase (Ehrhardt, Xu et al. 2005). As an alternative for more specific targeting within the host genome, DNA binding domains of zinc-finger nucleases were analyzed in the past, which exhibit specific recognition of distinct sequences with a length of 18 bps. Moreover, these domains could be re-designed to bind other sequences enabling targeting of an unique site within the human genome (Porteus 2008). Although design of these domains remains challenging, several zinc-finger binding domains have been constructed to bind to genome regions called “safe harbors”, which have been shown not to be related with any

genotoxic side-effects (Alwin, Gere et al. 2005). Furthermore, a new type of binding domains called transcription activator like effector domains (TALEs) was discovered recently (Boch, Scholze et al. 2009). For the design of TALEs, subdomains binding one distinct base-pair could be rearranged resulting in a DNA binding domain which specifically binds the respective DNA sequence (Miller, Tan et al. 2011). For gene therapeutic approaches zinc-finger nucleases as well as TALEs could be combined with homologous recombination between the host genome DNA and a therapeutic donor sequence, which is provided *in trans* (Wood, Lo et al. 2011). Although a recent study demonstrated efficacy of this system in neonatal mice (Li, Haurigot et al. 2011), application in adults is hampered by the fact, that in differentiated cells double-strand breaks are mainly repaired by non-homologous end joining (Tichy, Pillai et al. 2010). As an alternative for site-specific integration fusion proteins have been generated combining zinc-finger DNA binding domains or artificial DNA-binding domains with proteins mediating somatic integration such as the Sleeping Beauty transposase or the piggyBac transposase (Wilson, Kaminski et al. 2005; Wu, Meir et al. 2006). Nevertheless, design of these fusion proteins appeared to be challenging, because either specificity of DNA-binding or functionality of the integration machinery is often reduced (Yant, Huang et al. 2007).

However, one major disadvantage of approaches utilizing systems for site-directed integration is the low integration efficiency, which is mainly caused by the low number of target sites present in the mammalian genome. In contrast, systems mediating random integration such as the Sleeping Beauty transposase or integration into transcriptional active sites like for lentiviral vectors are more efficient due to high number of target sites within the host genome but insertional mutagenesis might cause genotoxic effects. Nevertheless, a recent report describing a clinical study utilizing regular lenti-viral vectors for ex vivo transduction of cells showed that several months after transplantation of transduced cells no expansion of certain cell clones due to transformation was observed (Mazurier, Gan et al. 2004; Biffi, Bartolomae et al. 2011). In summary, major issues which need to be addressed are whether the safety of random integration machineries is high enough for their use in clinical trials and whether the efficiency of site-directed integration machineries could be increased to obtain sufficient effects in humans.

Moreover, the necessity for somatic integration mediating long-term expression of a transgene has to be considered carefully, because particularly in resting cells episomal persistence might be an option, which is not associated with insertional mutagenesis. This is underlined by

preclinical studies in hemophilia B dogs, which were treated with HCAs (Brunetti-Pierri, Stapleton et al. 2009) or AAV vectors (Niemeyer, Herzog et al. 2009). Both studies demonstrated expression of canine FIX mainly derived from episomal stable vector genomes resulting in therapeutic effect for 6 and 8 years, respectively. Furthermore, DNA replicons for episomal persistence such as vectors based on scaffold/matrix attachment regions (S/MAR) could also present an attractive option (Stehle, Scinteie et al. 2003). These replicons enable replication during the cell cycle and therefore, they provide a potent alternative for integration machineries. However, application of episomal stable and replicating DNA circles has been shown to be hampered by low transduction and establishment efficiencies, although a hybrid vector system utilizing HCA for delivery of DNA replicons may hold great promise (Voigtländer R., Muck-Hausl M.; unpublished data).

Besides improvements regarding the integration machinery of the adenovirus-SB transposase hybrid vector system, the HCA vector could be altered to provide new properties. Several groups discovered modifications of the adenovirus capsid, which enable detargeting from the liver after intravenous injection by ablation from FX-binding. This was achieved by point mutations in the HVRs responsible for FX-binding (Alba, Bradshaw et al. 2009) or exchanges of the HVRs with respective sequences from other serotypes (Roberts, Nanda et al. 2006). Furthermore, combinations with other capsid-modifications like certain published fiber-modifications might allow retargeting of HCAs to other organs (Noureddini and Curiel 2005). This could provide the opportunity to apply the hybrid vector system for in vivo treatment of genetic defects affecting other cell types than hepatocytes. Moreover, several capsid-modifications have been shown to increase the transduction rate of respective HCAs for distinct cell types in cell culture. For instance adenoviral vectors with fiber knobs of the human adenovirus serotype 35 were shown to mediate transduction of hematopoietic stem cells (Yotnda, Onishi et al. 2001). Therefore, the hybrid vector system utilizing HCAs with these modulations might resemble a potent alternative for gene transfer in cell-mediated ex vivo gene therapeutic approaches. Additionally, some capsid-modifications have shown to enable escape from the anti-hAd5 humoral immune response allowing repeated vector administration in vivo and therefore, enhancement of vector potency (Liu, O'Brien et al. 2009). However, to exploit full potential of HCAs more efficient engineering techniques are required enabling rapid modulation of arbitrary capsid components and generation of complex HCAs like the described 1-vector system.

6.3. BAC cloning techniques for advanced engineering of adenoviruses enable selective and complex gene transfer

Current cloning strategies for generation of high-capacity adenoviral vector genomes and manipulation of helper-virus genomes are work-intensive and efficiencies are moderate (Jager, Hausl et al. 2009; Khare, May et al. 2011). To enable easy and rapid genetic manipulations, I established a cloning platform based on bacterial artificial chromosomes (BACs), which enables modifications of the adenoviral genome by homologous recombination (Fig. 4.1). In detail, bacteria of the E.coli strain SW102 expressing λ recombinases upon heat-induction were used to mediate recombination of sequences with at least 25-30 base pairs of homology (Warming, Costantino et al. 2005). These homologous regions flanking the sequences of interest could be generated by PCR using respective primers. For traceless modifications a technique based on a bacterial expression cassette containing a negative and a positive selection marker can be used (Wang, Zhao et al. 2009). This double selection marker is introduced into the target region of the genome region and subsequently replaced by the sequence, which should be introduced (Fig. 3b).

The BAC cloning technology for manipulation of adenoviral vectors established in this thesis provides several advantages compared to methods described previously. These conventional cloning strategies are based on rare restriction enzymes or homologous recombination in the E.coli strain BJ5183 or human embryonic kidney-derived 293 (HEK293) cells (McGrory, Bautista et al. 1988; Bett, Haddara et al. 1994; Chartier, Degryse et al. 1996; Mizuguchi and Kay 1998). For all these methods two intermediate clones have to be generated containing the sequence of interest flanked by either restriction enzyme sites or homologous regions and encoding a modified vector genome with a restriction site at the target region, respectively (Fig. 1.9). In sharp contrast, for the novel BAC-based system no intermediate clones have to be constructed. Furthermore, the new BAC-based method is suitable for traceless modulation of any site within the genome such as an intragenic region, whereas the conventional system for recombination in HEK293 cells is restricted to 5’ and 3’ regions of the genome. Also, previously described cloning methods based on rare restriction enzyme are not suitable for this kind of application.

The BAC cloning platform is easily accessible for complete viral genomes isolated from purified particles (Ruzsics, Wagner et al. 2006) as I exemplified by generation of the BAC containing the helper-virus genome (Figure 4.2). Furthermore, I established an alternative method called backbone-exchange. This method enables the conversion of a plasmid

containing an adenoviral genome into the respective BAC, as demonstrated by generation of a BAC containing a high-capacity adenoviral genome (Fig. 4.4). These construction methods guarantee rapid access for all available vectors to the BAC cloning platform within a single cloning step. Moreover, the backbone-exchange technique includes the option to switch the vector types from first-generation adenoviral vector (FG-AdV) genomes to respective helper-virus genomes or replication-competent oncolytic adenovirus genomes containing modulated E1 regions (Parks, Chen et al. 1996; Nettelbeck, Rivera et al. 2002). In contrast, previous reported construction methods for generation of novel FG-AdVs or adoption of FG-AdVs to HVs afford multiple cloning steps of high complexity (Zhou, Zhou et al. 2010; Khare, May et al. 2011). In this thesis utility of the BAC cloning platform was proven by traceless modification of the generated HV-BAC incorporating established fiber chimera fib5/35 (Yotnda, Onishi et al. 2001), which has been shown to alter tropism in cell culture, or hexon chimera hex5/48 (Roberts, Nanda et al. 2006), which detargets the vector from the liver and enables escape from neutralizing antibodies (Fig. 4.3). This demonstrates, that any known modification of adenoviral genomes could be easily adopted to any BAC-encoded adenoviral genome. Moreover, capsid-modifications could be rapidly merged within one adenoviral genome to combine respective vector properties such as more precise in vivo retargeting and escape from neutralizing antibodies offering the option of repeated vector administrations in vivo.

To exploit the full potential of high-capacity adenoviral vectors, I established a recombination pipeline based on the BAC technology. This allows generation of high-capacity adenoviral genomes containing multiple expression cassettes. In principle, this recombination pipeline is based on iterative homologous recombinations with alternating positive selection markers coupled to the sequences, which should be inserted (Fig. 4.5a). Therefore, after homologous recombination selection in liquid culture for the respective selection marker is possible. This culture can directly be used for insertion of the next sequence coupled with another positive selection marker replacing the previously used positive selection marker. In sharp contrast to established cloning procedures no intermediate clones have to be isolated and as a consequence several sequences could be combined rapidly within a HCA genome with small effort. Full potential of the recombination pipeline could be exploited by construction of several sequence combinations in parallel. Successively generated sequences could be amplified by PCR and combined in a single BAC (Fig. 4.5b). Additionally, the recombination pipeline allows introduction of small sequences like minimal internal ribosomal entry sites

(IRES), protease cleavage sites, minimal polyadenylation signals, microRNA target sites and small operator sequences such as used for the tetracycline-inducible expression system.

In this study, I applied this advanced cloning technology for generation of the BAC BHCA-2indsys containing two independent expression systems. For construction, 8 sequences derived from plasmids or genomic DNA and 3 small sequences generated by PCR were combined within the HCA genome by 12 cloning steps utilizing the recombination pipeline (Fig. 4.5b). One of the incorporated systems mediates cell-type specific expression of the humanized Renilla luciferase in hepatocytes (Ehrhardt, Xu et al. 2003) upon induction by addition of the synthetic hormone mifepristone (Osterwalder, Yoon et al. 2001), whereas the second system enables expression of enhanced green fluorescence protein (eGFP) and Firefly luciferase in cells expressing the stem cell-specific transcription factor oct4 (Nordhoff, Hubner et al. 2001) in presence of the antibiotic drug doxycycline (Mohr, Arapovic et al. 2010). In the future, HCA derived from this BAC might be used in experiments for transient tracking of cells in cell culture during dedifferentiation or differentiation processes. Furthermore, it might provide an option to track the differentiation status of stem cells after transplantation in cell-mediated gene therapeutic approaches (Warlich, Kuehle et al. 2011). In addition, modulated expression systems enabling inducible expression of transcription factors at a certain differentiation status might provide the opportunity to control transdifferentiation in cell culture or even in vivo (Takeuchi and Bruneau 2009; Vierbuchen, Ostermeier et al. 2010).

Construction of BHCA-2indsys demonstrated, that the concept of the recombination pipeline allows efficient combination of sequences within a BAC containing a HCA genome, whereas with currently used cloning methods the effort would be enormous and construction would be very time consuming (Hausl, Zhang et al. 2010; Puntel, Muhammad et al. 2010). Furthermore, corrections or alterations could be incorporated upon demand utilizing the positive-negative selection BAC cloning strategy. Therefore, reporter genes could be incorporated for initial evaluation of a HCA, which subsequently could be replaced by the gene of interest. Additionally, intermediate clones, which were created during generation of a complex HCA genome, could be isolated upon demand to generate a collection of clones, which could be used for construction of HCA genomes required for other studies.

Although the BAC technology combines several advantages in comparison to cloning methods conventionally used for generation of adenoviral vectors, the question might rise, whether even more efficient cloning procedures can be established. However BAC cloning

variants utilizing SacB, rpsL$^+$ or rare restriction enzymes like I-SceI for negative selection were associated with high numbers of false positive clones caused by low selection pressure or sensitivity of the respective sequences for mutations introduced during amplification in growing bacteria (Zhang, Buchholz et al. 1998; Jamsai, Orford et al. 2003; Warming, Costantino et al. 2005; Wang, Zhao et al. 2009). Nevertheless, alternative negative selection markers provide the opportunity to generate intermediate clones for traceless manipulation of two or more regions within a single BAC. In the past, yeast artificial chromosomes (YACs) were used for manipulation of large DNA sequences, but transformation efficiencies in yeast are low (Monaco and Larin 1994) and cloning procedures and isolation of the respective DNA were hampered by rearrangements and a high degree of chimerism. Moreover, inserts incorporated in YACs were shown to be instable, limiting their usefulness for generation of adenoviral vector genomes (Green, Riethman et al. 1991). Regarding applications of commercial kits such as the gateway system (Invitrogen) or the in-fusion cloning method (Clontech) for adenoviral vectors, these cloning strategies are restricted to manipulation of the E1 region within a plasmid containing a first-generation adenoviral vector genome provided by the respective company. In contrast, circular polymerase extension cloning (CPEC) allows combination of various elements with overlapping homologous regions by PCR with a proof-reading polymerase (Quan and Tian 2009; Quan and Tian 2011). However, when using the latter method construction of plasmids is currently limited to a size of about 20 kb and therefore this method is not suitable for design of complete adenoviral vector genomes (Shevchuk, Bryksin et al. 2004). Nevertheless, CPEC might resemble a powerful tool to generate intermediate clones or combine sequences with a positive selection marker essentially for usage in the recombination pipeline. Finally, the most elegant way to generate complex HCAs would be the complete synthesis of the vector genome. Recently it has been demonstrated, that synthesis of DNA sequences of about 24 kb in size could even be used for generation of a functional synthetic bacterial genome (Gibson, Benders et al. 2008). However, costs are still very high and synthesis takes a long time for sequences of 30 kb or larger. In summary, with respect to the options provided by the established BAC cloning method based on positive-negative selection as well as by the newly invented techniques called backbone-exchange and recombination pipeline, valuable tools for modulation of large DNA sequences were established in this thesis.

Beside restrictions set by previously used cloning methods high effort required for large-scale production severely impaired simultaneous production of a multitude of HCAs. Therefore, I

tested commercially available ion-exchange columns (Vivapure AdenoPACK 20, Sartorius, Göttingen) for small-scale HCA-preparations. Although packaged viral vectors are not dissected from empty particles, these HCA preparations had similar titers (Fig. 4.6), which are sufficient to perform extensive cell culture experiments and initial in vivo experiments. Despite the fact that utilization of ion-exchange columns for purification of HCAs was a logical step and success of the application was not surprising, this method simplifies the generation of HCAs, HVs or other adenoviral vectors significantly and provides the opportunity to implement HCAs in the laboratory without expensive equipment such as an ultracentrifuge. Moreover, ion-exchange columns might provide an attractive alternative for up-scaling the production of HCAs to provide vector particle amounts sufficient for clinical studies. In addition, with respect to capsid-modifications, which might affect the total charge of the capsid surface and in consequence alter binding properties, column properties could be adapted to altered capsids for optimized vector yields (Konz, Livingood et al. 2005).

6.4. Hexon-modified helper-viruses showed significantly altered tropism in vivo

Next, I utilized the new cloning platform to investigate further improvements for HCAs. One of the major disadvantages evaluated in previous studies is the robust adaptive immune response, which reduces the effect yielded by a single application of HCAs and also prohibits repeated treatments. Moreover, in vivo therapies utilizing intravenous administration are restricted to liver-associated diseases. Key plaver for all these features is the major capsid protein hexon, which contains the majority of epitopes recognized by neutralizing antibodies and also mediates FX-binding and therefore liver tropism (Fig. 1.6) (Sumida, Truitt et al. 2005). In detail, immunogenic epitopes as well as the FX binding site are located within the hypervariable regions (HVRs), which are part of the solvent-exposed surface domains DE1 and FG1 of the hexon protein (Fig. 5.1a) (Rux, Kuser et al. 2003; Waddington, McVey et al. 2008; Alba, Bradshaw et al. 2009). Previous studies showed that precise exchanges of HVRs with respective sequences of human adenovirus serotype 48 resulted in efficient escape from neutralizing antibodies as well as detargeting from the liver for first-generation adenoviral vectors (Roberts, Nanda et al. 2006). Therefore, I adopted this design for generation of modified helper-virus genomes containing HVRs of human adenovirus serotypes 12, 41, 44 and 50 as well as 48 serving as a positive control (Fig. 5.1c). In addition, crystal structures of all major capsid proteins are known as well as interactions between capsid proteins have been

investigated extensively. Moreover, the detailed structure of the whole adenovirus capsid was published recently (Liu, Jin et al. 2010; Reddy, Natchiar et al. 2010). These publications confirmed that nearly all interaction sites associated with the hexon protein are within hexon domains orientated to the inner part of the capsid and conservation of these domains in all human adenovirus serotypes underlines the importance for the structural integrity of the capsids (Rux, Kuser et al. 2003; Saban, Silvestry et al. 2006). Therefore, I designed hexon chimeras with completely exchanged surface domains derived from respective sequences of human adenoviruses 4, 7, 12, 13 and 41, which are members of the distinct adenovirus serotype subgroups A-F (Fig. 5.1b). Protein analysis of chimeras revealed no inhibition of early capsid assembly steps including interaction with adenoviral chaperon 100K-protein, nuclear import and trimerization of modified hexon proteins (Fig. 5.2).

Subsequently all chimeric hexon sequences were cloned into a helper-virus genome containing an eGFP/Firefly luciferase reporter construct utilizing BAC technology (Fig. 5.3). However, reconstitution of respective hexon-modified HVs appeared to be challenging and the bottleneck could not be identified, although transfection efficiency and purity of transfected DNA seemed to be critical factors. Nevertheless, helper-viruses with precisely exchanged HVRs (HV-HVR12 and positive control HV-HVR48) as well as with completely exchanged hexon surface domains (HV-SD4 and HV-SD12) could be rescued and titers as well as total yields of respective vector preparations were comparable to unmodified HVs (Fig. 5.4). These facts indicate that in principle both designs of hexon chimeras allow generation of fully assembled and stable virus capsid. To circumvent the reconstitution problems, utilization of a stable cell line expressing unmodified hexon proteins might be an option, although homologous recombination between the unmodified and the modified hexon genes is highly likely. Therefore, viral particles with unmodified adenoviral genomes would contaminate the reconstituted hexon-modified virus preparation and due to higher growth rate, unmodified virus outgrows the hexon-modified virus in further amplication steps. As another option, miRNA inhibitors like the p19 protein of the tomato bushy stunt virus might be applied in cis increasing reconstitution efficiency by enhanced production of viral proteins. This has been shown very recently by our group (Rauschhuber C., Häusl M.; manuscript in preparation).

Novel reconstituted capsid-modified HVs were tested in cell culture for FX-binding (Fig. 5.5) and furthermore, vector-specific biodistribution after intravenous injection into mice was analyzed by in vivo bioluminescence measurements (Fig. 5.6). However, obtained results

were not in concordance with the current assumption that FX-mediated uptake of adenoviral vectors in CAR-negative SKOV3 cells correlates with the liver-tropism in vivo (Waddington, McVey et al. 2008; Alba, Bradshaw et al. 2009). In detail, cell culture experiments revealed enhanced uptake of the unmodified helper-virus in presence of FX and transduction of the liver in vivo as reported before. In line with the hypothesis, for HV-SD12 no interaction with FX was seen and in consequence liver-derived bioluminescence signals were not significantly higher than the background. However, transduction of SKOV3 cells by HV-SD4 was increased in presence of FX, whereas in vivo bioluminescence measurements showed no transduction of liver cells in mice. These results indicate that the liver-tropism might depend on the strength of the interaction between hexon HVRs and FX molecules. Due to the fact that the FX-binding assay exhibits a low sensitivity, it is not sufficient to predict liver-tropism in vivo. Therefore, more precise determination of the dissociation constant utilizing surface plasmon resonance or alternative methods might be an option to determine threshold values, which may allow prediction of liver-tropism in vivo. With respect to retargeting of vectors to other tissues this information might be essential for the vector design. For instance novel attachment sites introduced into other capsid proteins such as the fiber knob could mediate interactions specific for a distinct cell type (Terashima, Oka et al. 2009). However, the degree of retargeting will depend on the strength of the novel interaction in comparison to the binding between hexon proteins and FX molecules or any other competing interactions (Martin, Brie et al. 2003; Nicklin, White et al. 2004).

Another issue was raised by different results obtained for HV-HVR12 and HV-SD12. Capsids of both vectors present identical hypervariable regions at the surface and therefore, similar transduction profiles in cell culture and in vivo were expected. However, for SKOV3 cells, transduction efficiency of HV-HVR12 in absence of FX was more than 40-fold increased compared to HV-SD12, which was shown to mediate similar transduction efficiencies as unmodified HVs (Fig. 5.5). Moreover, in presence of FX transduction rates are even increased for HV-HVR12, whereas for HV-SD12 no effect was observed. Furthermore, maximum bioluminescence signals obtained from the liver after intravenous injected HV-HVR12 were about 500-fold higher than for the unmodified HV at identical vector doses, whereas no transduction of liver cells was seen for HV-SD12 (Fig. 5.6). These discrepancies between vectors with identical HVRs indicate an influence of the protein sequences surrounding the HVRs in the context of the capsid surface domains (Waddington, McVey et al. 2008; Alba, Bradshaw et al. 2009). Regarding HV-HVR12, high transduction rates for CAR-negative cells

and strongly increased uptake in liver cells as well as in peripheral tissue implicate, that a new binding site was generated unexpectedly. This indicates that the features of hexon chimeras obtained by precise exchanges of HVRs are less predictable than originally thought and therefore, exchanges of complete hexon surface domains might be more suitable for the rational design because they have the features of the original adenovirus serotype used for the modification of hexon proteins. However, precise exchanges might offer the possibility for modulation of the virus capsid in a random approach generating tissue-specific capsid-modulations by in vivo selection for appropriate vectors as it was shown for AAV capsids (Grimm, Lee et al. 2008; Li, Asokan et al. 2008).

With respect to retargeting, the interaction allowing efficient CAR-and FX-independent cellular uptake of HV-HVR12 should be investigated in more detail. This might be the basis for a set of new adenoviral vectors in case FX-binding could be inhibited without affecting the novel binding site. In detail, highly efficient retargeting might be yielded by combination with hexon-mutations ablating FX-binding (Alba, Bradshaw et al. 2009) and modifications of other capsid proteins such as the fiber protein for retargeting to other cell types (Nicklin, White et al. 2004; Terashima, Oka et al. 2009). Side effects caused by unspecific transduction of other cell types like cells located in peripheral tissue could be prevented on transcriptional level utilizing cell type-specific promoters, enhancers and suitable miRNA target sites (Wolff, Wolff et al. 2009). Moreover, vectors not associated with FX-binding and liver-tropism such as HV-SD12 might serve as scaffold for retargeting vectors, however, transduction efficiency probably will be significantly lower. For ex vivo approaches HV-HVR12 might provide a potent solution to treat certain stem cells. Due to the new binding site, HCAs generated with HV-HVR12 might be able to transducer specific cell types, which could hardly be transduced by HCAs with unmodified capsids. In addition, all HCAs generated with the novel helper-viruses should escape from the majority of neutralizing anti-hAd5 antibodies enabling repeated administrations (Roberts, Nanda et al. 2006). For these reasons novel vectors exploited in this study are an excellent basis for optimization of HCAs regarding ex vivo transduction efficiency and in vivo retargeting in combination with escape from immune responses. Further improvements should focus on reduction of the innate immune responses, which at least in part are responsible for the rapid clearance of vector genomes after in vivo administration. Options for realization might be capsid-modifications enabling evasion from antigen presenting cells such as Kupffer cells (Khare, May et al. 2011) and vector

modulations circumventing intracellular recognition of adenoviral vector components (Ross, Kennedy et al. 2009).

6.5. Perspectives

In summary, I provided a standardized protocol for incorporation of therapeutic DNA into a HCA genome and large-scale production of the respective HCA. Furthermore, I established a new cloning platform based on the BAC technology and I invented novel tools allowing construction of complex or multiple HCA genomes as well as modulation of helper-virus genomes. Moreover, for fast evaluation of HCAs, ion-exchange columns were used successfully for rapid purification of small-scale HCA preparations. For optimization of HCAs, I prove functionality of an improved version of the Sleeping Beauty transposase based integration machinery delivered by HCAs to mediate stable long-term expression of a therapeutic protein in mice and hemophilia B dogs. With respect to the tropism and immunogenicity of HCAs, I constructed novel hexon-modified helper-viruses, which should enable escape from neutralizing antibodies and which demonstrated distinct transduction features in cell culture as well as altered biodistribution after intravenous injection in vivo. With respect to obtained results and the opportunities for further optimizations of HCAs enabled by newly established methods, this work may pave the way towards successful gene therapeutic applications as well as new perspectives are opened for other application fields like basic research, vaccination purposes and cancer therapies utilizing oncolytic adenoviruses.

7. Appendix

7.1. Abbreviations

ψ	packaging signal
[α-^{32}P]dATP	α-^{32}P labeled deoxyadenosintriphosphate
[α-^{32}P]dCTP	α-^{32}P labeled deoxycytosintriphosphate
µg / mg / g	microgram, milligram, gram
µl, ml, l	microliter, milliliter, liter
µm / mm / m	micrometer, millimeter, meter
µM, mM, M	micromolar, millimolar, molar
AAV	adeno-associated virus
AIDS	acquired immunodeficiency syndrome
ALT	alanine aminotransferase
Amp(R)	ampicillin resistance
ApoE	apolipoprotein E (enhancer)
ARM	adenovirus reference material
AST	aspartate aminotransferase
ATCC	American tissue culture collection
BAC	bacterial artificial chromosome
bp / kb	base pair / kilo base pair
BUN	blood urea nitrogen
CAR	cosackievirus and adenovirus receptor
CCl_4	carbon tetrachloride
CD46	cluster of differentiation 46
cDNA	complementary DNA
cFIX	canine coagulation factor IX
CIP	calf intestinal alkaline phosphatase
Cm	chloramphenicol
CPE	cytopathic effect
CPEC	circular polymerase extension cloning
CpG	cytosine phosphatidyl guanine
CR1	complement receptor 1

CsCl	cesium chloride
DBP	DNA-binding protein
DFG	Deutsche Forschungsgemeinschaft
DNA	deoxyribonucleic acid
DPBS	Dulbecco's phosphate buffered saline
dsDNA	double-strand DNA
DSG-2	desmoglein-2
E.coli	Escherichia coli
E1-4	early transcribed (adenoviral) genome region 1-4
EF1α	elongation factor-1-α (promoter)
ELISA	enzyme-linked immunosorbent assay
EtOH	ethanol
EU	European Union
FBS	Fetal bovine serum
FG-AdV	First-generation adenoviral vector
FLuc	Firefly luciferase
FRT	Flp recognition target sequence
FX	coagulation factor X
g	gravity (unit for centrifugation)
galK	galactokinase
GC content	guanine/cytosine content
GFP	green fluorescent protein
Gla	γ-carboxylated glutamic acid domain
GMP	good manufacturing practice
GON	group of nine
hAAT	human α-1-antitrypsin (promoter)
hAd(5)	human adenovirus (5)
HCA	high-capacity adenoviral vector
HC-AdV	high-capacity adenoviral vector
HCR	hepatic control region
HEK293	human embryonic kidney 293 cell line
HIV-1	human immunodeficiency virus 1
HR	homologous region

hRLuc	humanized Renilla luciferase
hrs	hours
HSB5	hyperactive Sleeping Beauty transposase 5
HSPGs	heparan sulfate proteoglycans
HV	helper-virus
HVRs	hypervariable regions
IgkMAR	murine immunoglobulin k locus
IR	inverted repeat (binding site for the Sleeping Beauty transposase)
IRES	internal ribosomal entry site
ITR	inverted terminal repeat
J cm^{-2}	joule per square centimeter
Kan	kanamycin resistance
L1-L5	late transcribed (adenoviral) genome regions 1-5
LacZ	β-galactosidase
LB	Luria Bertani medium
MCS	multiple cloning site
MEM	Minimal essential medium
min	minute
MLP	(adenoviral) major late promoter
MLV	murine leukaemia virus
MOI	multiplicity of injection
mRNA	messenger RNA
mSB	mutated (non-functional) Sleeping Beauty transposase
NCBI	National Center for Biotechnology Information
OPU	optical particle unit
P	passage
pA	polyadenylation signal
PCR	polymerase chain reaction
PGK	phosphoglycokinase promoter
pH	potential hydrogenii
POL	(adenoviral) polymerase
qPCR	quantitative polymerase chain reaction
r.p.m.	rotations per minute

RCA	replication competent adenovirus
RGD loop	loop containing the amino acid sequence arginine-glycin-aspartate
RS	restriction enzyme binding site
S phase	synthesis phase
S/MAR	scaffold/matrix attachment region
SB	Sleeping Beauty transposase
SCID	severe combined immunodeficiency
SD	surface domain
SDS	sodium dodecylsulfate
SFB	Sonderforschungsbereich
siRNA	small inhibitory RNA
SPP	Schwerpunktprogramm
ssDNA	single-strand DNA
ssRNA	single-strand RNA
TALE	transcription activator like effector
TP	terminal protein
tu, TU	transducing units
U	unit
UV	ultraviolet
Vol/vol	volume per volume
vp(s)	viral particle(s)
VSV-G	glycoprotein of vesicular stomatitis virus
WBCT	whole blood clotting time
wt/vol	weight per volume
YAC	yeast artificial chromosome
Zeo	zeocin resistance

7.2. Reference list for the introduction and the discussion

Akusjarvi, G. (1993). "Proteins with transcription regulatory properties encoded by human adenoviruses." Trends Microbiol **1**(5): 163-170.

Alba, R., A. C. Bradshaw, et al. (2009). "Identification of coagulation factor (F)X binding sites on the adenovirus serotype 5 hexon: effect of mutagenesis on FX interactions and gene transfer." Blood **114**(5): 965-971.

Alba, R., P. Hearing, et al. (2007). "Differential amplification of adenovirus vectors by flanking the packaging signal with attB/attP-PhiC31 sequences: implications for helper-dependent adenovirus production." Virology **367**(1): 51-58.

Alwin, S., M. B. Gere, et al. (2005). "Custom zinc-finger nucleases for use in human cells." Mol Ther **12**(4): 610-617.

Antonarakis, S. E. and J. S. Beckmann (2006). "Mendelian disorders deserve more attention." Nat Rev Genet **7**(4): 277-282.

Arbuthnot, P. (2010). "Harnessing RNA interference for the treatment of viral infections." Drug News Perspect **23**(6): 341-350.

Aurnhammer, C., M. Haase, et al. (2011). "Universal Real-Time PCR for the Detection and Quantification of Adeno-Associated Virus Serotype 2-Derived Inverted Terminal Repeat Sequences." Hum Gene Ther.

Bai, M., B. Harfe, et al. (1993). "Mutations that alter an Arg-Gly-Asp (RGD) sequence in the adenovirus type 2 penton base protein abolish its cell-rounding activity and delay virus reproduction in flat cells." J Virol **67**(9): 5198-5205.

Baum, C. (2007). "Insertional mutagenesis in gene therapy and stem cell biology." Curr Opin Hematol **14**(4): 337-342.

Benihoud, K., P. Yeh, et al. (1999). "Adenovirus vectors for gene delivery." Curr Opin Biotechnol **10**(5): 440-447.

Bergelson, J. M., J. A. Cunningham, et al. (1997). "Isolation of a common receptor for Coxsackie B viruses and adenoviruses 2 and 5." Science **275**(5304): 1320-1323.

Berkner, K. L. and P. A. Sharp (1983). "Generation of adenovirus by transfection of plasmids." Nucleic Acids Res **11**(17): 6003-6020.

Bertram, J. S. (2000). "The molecular biology of cancer." Mol Aspects Med **21**(6): 167-223.

Bett, A. J., W. Haddara, et al. (1994). "An efficient and flexible system for construction of adenovirus vectors with insertions or deletions in early regions 1 and 3." Proc Natl Acad Sci U S A **91**(19): 8802-8806.

Biffi, A., C. C. Bartolomae, et al. (2011). "Lentiviral vector common integration sites in preclinical models and a clinical trial reflect a benign integration bias and not oncogenic selection." Blood **117**(20): 5332-5339.

Blaese, R. M., K. W. Culver, et al. (1995). "T lymphocyte-directed gene therapy for ADA-SCID: initial trial results after 4 years." Science **270**(5235): 475-480.

Boch, J., H. Scholze, et al. (2009). "Breaking the code of DNA binding specificity of TAL-type III effectors." Science **326**(5959): 1509-1512.

Bollenbach, T., K. Vetsigian, et al. (2007). "Evolution and multilevel optimization of the genetic code." Genome Res **17**(4): 401-404.

Bos, J. L. (1989). "ras oncogenes in human cancer: a review." Cancer Res **49**(17): 4682-4689.

Bradshaw, A. C., A. L. Parker, et al. (2010). "Requirements for receptor engagement during infection by adenovirus complexed with blood coagulation factor X." PLoS Pathog **6**(10): e1001142.

Branda, C. S. and S. M. Dymecki (2004). "Talking about a revolution: The impact of site-specific recombinases on genetic analyses in mice." Dev Cell **6**(1): 7-28.

Brooks, A. R., R. N. Harkins, et al. (2004). "Transcriptional silencing is associated with extensive methylation of the CMV promoter following adenoviral gene delivery to muscle." J Gene Med **6**(4): 395-404.

Brown, B. D. and L. Naldini (2009). "Exploiting and antagonizing microRNA regulation for therapeutic and experimental applications." Nat Rev Genet **10**(8): 578-585.

Brunetti-Pierri, N., G. E. Stapleton, et al. (2009). "Efficient, long-term hepatic gene transfer using clinically relevant HDAd doses by balloon occlusion catheter delivery in nonhuman primates." Mol Ther **17**(2): 327-333.

Brunetti-Pierri, N., G. E. Stapleton, et al. (2007). "Pseudo-hydrodynamic delivery of helper-dependent adenoviral vectors into non-human primates for liver-directed gene therapy." Mol Ther **15**(4): 732-740.

Burnett, R. M., M. G. Grutter, et al. (1985). "The structure of the adenovirus capsid. I. An envelope model of hexon at 6 A resolution." J Mol Biol **185**(1): 105-123.

Carlisle, R. C., Y. Di, et al. (2009). "Human erythrocytes bind and inactivate type 5 adenovirus by presenting Coxsackie virus-adenovirus receptor and complement receptor 1." Blood **113**(9): 1909-1918.

Castanotto, D. and J. J. Rossi (2009). "The promises and pitfalls of RNA-interference-based therapeutics." Nature **457**(7228): 426-433.

Cavazzana-Calvo, M., S. Hacein-Bey, et al. (2000). "Gene therapy of human severe combined immunodeficiency (SCID)-X1 disease." Science **288**(5466): 669-672.

Cecchini, S., T. Virag, et al. (2011). "Reproducible high yields of recombinant adeno-associated virus produced using invertebrate cells in 0.02- to 200-liter cultures." Hum Gene Ther **22**(8): 1021-1030.

Chalberg, T. W., J. L. Portlock, et al. (2006). "Integration specificity of phage phiC31 integrase in the human genome." J Mol Biol **357**(1): 28-48.

Chartier, C., E. Degryse, et al. (1996). "Efficient generation of recombinant adenovirus vectors by homologous recombination in Escherichia coli." J Virol **70**(7): 4805-4810.

Chatterjee, P. K., M. E. Vayda, et al. (1985). "Interactions among the three adenovirus core proteins." J Virol **55**(2): 379-386.

Chen, H. H., L. M. Mack, et al. (1997). "Persistence in muscle of an adenoviral vector that lacks all viral genes." Proc Natl Acad Sci U S A **94**(5): 1645-1650.

Chiu, C. Y., P. Mathias, et al. (1999). "Structure of adenovirus complexed with its internalization receptor, alphavbeta5 integrin." J Virol **73**(8): 6759-6768.

Chroboczek, J., F. Bieber, et al. (1992). "The sequence of the genome of adenovirus type 5 and its comparison with the genome of adenovirus type 2." Virology **186**(1): 280-285.

Crystal, R. G. (1995). "Transfer of genes to humans: early lessons and obstacles to success." Science **270**(5235): 404-410.

Darras, B. T., B. R. Korf, et al. (1993). "Dystrophinopathies."

Daya, S. and K. I. Berns (2008). "Gene therapy using adeno-associated virus vectors." Clin Microbiol Rev **21**(4): 583-593.

Doherty, J. E., L. Huye, et al. (2011). "Hyperactive piggyBac gene transfer in human cells and in vivo." Hum Gene Ther.

Douglas, C. u. (2002). Adenoviral Vectors for Gene Therapy.

Douglas, K. L. (2008). "Toward development of artificial viruses for gene therapy: a comparative evaluation of viral and non-viral transfection." Biotechnol Prog **24**(4): 871-883.

Dropulic, B. (2011). "Lentiviral vectors: their molecular design, safety, and use in laboratory and preclinical research." Hum Gene Ther **22**(6): 649-657.

Echavarria, M. (2008). "Adenoviruses in immunocompromised hosts." Clin Microbiol Rev **21**(4): 704-715.

Edelstein, M. L., M. R. Abedi, et al. (2004). "Gene therapy clinical trials worldwide 1989-2004-an overview." J Gene Med **6**(6): 597-602.

Ehrhardt, A., R. Haase, et al. (2008). "Episomal vectors for gene therapy." Curr Gene Ther **8**(3): 147-161.

Ehrhardt, A. and M. A. Kay (2002). "A new adenoviral helper-dependent vector results in long-term therapeutic levels of human coagulation factor IX at low doses in vivo." Blood **99**(11): 3923-3930.

Ehrhardt, A., H. Xu, et al. (2003). "A gene-deleted adenoviral vector results in phenotypic correction of canine hemophilia B without liver toxicity or thrombocytopenia." Blood **102**(7): 2403-2411.

Ehrhardt, A., H. Xu, et al. (2005). "A direct comparison of two nonviral gene therapy vectors for somatic integration: in vivo evaluation of the bacteriophage integrase phiC31 and the Sleeping Beauty transposase." Mol Ther **11**(5): 695-706.

Ehrhardt, A., S. R. Yant, et al. (2007). "Somatic integration from an adenoviral hybrid vector into a hot spot in mouse liver results in persistent transgene expression levels in vivo." Mol Ther **15**(1): 146-156.

Elia, D. and A. Ulmann (1986). "[RU 486 (mifepristone): from clinical trials to the perspectives for clinical use]." Contracept Fertil Sex (Paris) **14**(12): 1099-1103.

Engelhardt, J. F., L. Litzky, et al. (1994). "Prolonged transgene expression in cotton rat lung with recombinant adenoviruses defective in E2a." Hum Gene Ther **5**(10): 1217-1229.

Fabry, C. M., M. Rosa-Calatrava, et al. (2005). "A quasi-atomic model of human adenovirus type 5 capsid." Embo J **24**(9): 1645-1654.

Fabry, C. M., M. Rosa-Calatrava, et al. (2009). "The C-terminal domains of adenovirus serotype 5 protein IX assemble into an antiparallel structure on the facets of the capsid." J Virol **83**(2): 1135-1139.

Fairchild, P. J., S. Cartland, et al. (2004). "Embryonic stem cells and the challenge of transplantation tolerance." Trends Immunol **25**(9): 465-470.

Fallaux, F. J., A. Bout, et al. (1998). "New helper cells and matched early region 1-deleted adenovirus vectors prevent generation of replication-competent adenoviruses." Hum Gene Ther **9**(13): 1909-1917.

Fang, B., H. Wang, et al. (1996). "Lack of persistence of E1- recombinant adenoviral vectors containing a temperature-sensitive E2A mutation in immunocompetent mice and hemophilia B dogs." Gene Ther **3**(3): 217-222.

Fisher, K. J., H. Choi, et al. (1996). "Recombinant adenovirus deleted of all viral genes for gene therapy of cystic fibrosis." Virology **217**(1): 11-22.

Flewett, T. H., A. S. Bryden, et al. (1973). "Letter: Virus particles in gastroenteritis." Lancet **2**(7844): 1497.

Flint, J. and T. Shenk (1997). "Viral transactivating proteins." Annu Rev Genet **31**: 177-212.

Fredman, J. N. and J. A. Engler (1993). "Adenovirus precursor to terminal protein interacts with the nuclear matrix in vivo and in vitro." J Virol **67**(6): 3384-3395.

Galla, M., A. Schambach, et al. (2011). "Avoiding cytotoxicity of transposases by dose-controlled mRNA delivery." Nucleic Acids Res **39**(16): 7147-7160.

Gardlik, R., R. Palffy, et al. (2005). "Vectors and delivery systems in gene therapy." Med Sci Monit **11**(4): RA110-121.

Gibson, D. G., G. A. Benders, et al. (2008). "Complete chemical synthesis, assembly, and cloning of a Mycoplasma genitalium genome." Science **319**(5867): 1215-1220.

Gonin, P. and C. Gaillard (2004). "Gene transfer vector biodistribution: pivotal safety studies in clinical gene therapy development." Gene Ther **11 Suppl 1**: S98-S108.

Grable, M. and P. Hearing (1990). "Adenovirus type 5 packaging domain is composed of a repeated element that is functionally redundant." J Virol **64**(5): 2047-2056.

Greber, U. F., P. Webster, et al. (1996). "The role of the adenovirus protease on virus entry into cells." Embo J **15**(8): 1766-1777.

Green, E. D., H. C. Riethman, et al. (1991). "Detection and characterization of chimeric yeast artificial-chromosome clones." Genomics **11**(3): 658-669.

Grimm, D., J. S. Lee, et al. (2008). "In vitro and in vivo gene therapy vector evolution via multispecies interbreeding and retargeting of adeno-associated viruses." J Virol **82**(12): 5887-5911.

Haase, R., O. Argyros, et al. (2010). "pEPito: a significantly improved non-viral episomal expression vector for mammalian cells." BMC Biotechnol **10**: 20.

Hamosh, A., A. F. Scott, et al. (2005). "Online Mendelian Inheritance in Man (OMIM), a knowledgebase of human genes and genetic disorders." Nucleic Acids Res **33**(Database issue): D514-517.

Hardy, S., M. Kitamura, et al. (1997). "Construction of adenovirus vectors through Cre-lox recombination." J Virol **71**(3): 1842-1849.

Hartigan-O'Connor, D., A. Amalfitano, et al. (1999). "Improved production of gutted adenovirus in cells expressing adenovirus preterminal protein and DNA polymerase." J Virol **73**(9): 7835-7841.

Harvey, B. G., J. Maroni, et al. (2002). "Safety of local delivery of low- and intermediate-dose adenovirus gene transfer vectors to individuals with a spectrum of morbid conditions." Hum Gene Ther **13**(1): 15-63.

Hausl, M. A., W. Zhang, et al. (2010). "Hyperactive sleeping beauty transposase enables persistent phenotypic correction in mice and a canine model for hemophilia B." Mol Ther **18**(11): 1896-1906.

Hay, R. T., N. D. Stow, et al. (1984). "Replication of adenovirus mini-chromosomes." J Mol Biol **175**(4): 493-510.

Hearing, P., R. J. Samulski, et al. (1987). "Identification of a repeated sequence element required for efficient encapsidation of the adenovirus type 5 chromosome." J Virol **61**(8): 2555-2558.

Hehir, K. M., D. Armentano, et al. (1996). "Molecular characterization of replication-competent variants of adenovirus vectors and genome modifications to prevent their occurrence." J Virol **70**(12): 8459-8467.

Henning, P., K. M. Andersson, et al. (2005). "Tumor cell targeted gene delivery by adenovirus 5 vectors carrying knobless fibers with antibody-binding domains." Gene Ther **12**(3): 211-224.

Hernandez-Alcoceba, R. (2011). "Recent advances in oncolytic virus design." Clin Transl Oncol **13**(4): 229-239.

Hilleman, M. R. and J. H. Werner (1954). "Recovery of new agent from patients with acute respiratory illness." Proc Soc Exp Biol Med **85**(1): 183-188.

Huang, X., H. Guo, et al. (2010). "Gene transfer efficiency and genome-wide integration profiling of Sleeping Beauty, Tol2, and piggyBac transposons in human primary T cells." Mol Ther **18**(10): 1803-1813.

Jager, L., M. A. Hausl, et al. (2009). "A rapid protocol for construction and production of high-capacity adenoviral vectors." Nat Protoc **4**(4): 547-564.

Jamsai, D., M. Orford, et al. (2003). "Targeted modification of a human beta-globin locus BAC clone using GET Recombination and an I-Scei counterselection cassette." Genomics **82**(1): 68-77.

Jawetz, E. (1959). "The story of shipyard eye." Br Med J **1**(5126): 873-876.

Kalyuzhniy, O., N. C. Di Paolo, et al. (2008). "Adenovirus serotype 5 hexon is critical for virus infection of hepatocytes in vivo." Proc Natl Acad Sci U S A **105**(14): 5483-5488.

Kanegae, Y., M. Makimura, et al. (1994). "A simple and efficient method for purification of infectious recombinant adenovirus." Jpn J Med Sci Biol **47**(3): 157-166.

Katada, H. and M. Komiyama (2011). "Artificial restriction DNA cutters to promote homologous recombination in human cells." Curr Gene Ther **11**(1): 38-45.

Kawano, R., M. Ishizaki, et al. (2008). "Transduction of full-length dystrophin to multiple skeletal muscles improves motor performance and life span in utrophin/dystrophin double knockout mice." Mol Ther **16**(5): 825-831.

Keriel, A., C. Rene, et al. (2006). "Canine adenovirus vectors for lung-directed gene transfer: efficacy, immune response, and duration of transgene expression using helper-dependent vectors." J Virol **80**(3): 1487-1496.

Khare, R., S. M. May, et al. (2011). "Generation of a Kupffer cell-evading adenovirus for systemic and liver-directed gene transfer." Mol Ther **19**(7): 1254-1262.

Knowles, M. R., K. W. Hohneker, et al. (1995). "A controlled study of adenoviral-vector-mediated gene transfer in the nasal epithelium of patients with cystic fibrosis." N Engl J Med **333**(13): 823-831.

Kochanek, S., P. R. Clemens, et al. (1996). "A new adenoviral vector: Replacement of all viral coding sequences with 28 kb of DNA independently expressing both full-length dystrophin and beta-galactosidase." Proc Natl Acad Sci U S A **93**(12): 5731-5736.

Kojaoghlanian, T., P. Flomenberg, et al. (2003). "The impact of adenovirus infection on the immunocompromised host." Rev Med Virol **13**(3): 155-171.

Konkle, B. A., N. C. Josephson, et al. (1993). "Hemophilia B."

Konz, J. O., R. C. Livingood, et al. (2005). "Serotype specificity of adenovirus purification using anion-exchange chromatography." Hum Gene Ther **16**(11): 1346-1353.

Kreppel, F. and S. Kochanek (2008). "Modification of adenovirus gene transfer vectors with synthetic polymers: a scientific review and technical guide." Mol Ther **16**(1): 16-29.

Krougliak, V. and F. L. Graham (1995). "Development of cell lines capable of complementing E1, E4, and protein IX defective adenovirus type 5 mutants." Hum Gene Ther **6**(12): 1575-1586.

Li, H., V. Haurigot, et al. (2011). "In vivo genome editing restores haemostasis in a mouse model of haemophilia." Nature **475**(7355): 217-221.

Li, M. A., D. J. Turner, et al. (2011). "Mobilization of giant piggyBac transposons in the mouse genome." Nucleic Acids Res.

Li, W., A. Asokan, et al. (2008). "Engineering and selection of shuffled AAV genomes: a new strategy for producing targeted biological nanoparticles." Mol Ther **16**(7): 1252-1260.

Lin, A. N. and D. M. Carter (1993). "Epidermolysis bullosa." Annu Rev Med **44**: 189-199.

Liu, H., L. Jin, et al. (2010). "Atomic structure of human adenovirus by cryo-EM reveals interactions among protein networks." Science **329**(5995): 1038-1043.

Liu, J., K. L. O'Brien, et al. (2009). "Immune control of an SIV challenge by a T-cell-based vaccine in rhesus monkeys." Nature **457**(7225): 87-91.

Luo, J., Z. L. Deng, et al. (2007). "A protocol for rapid generation of recombinant adenoviruses using the AdEasy system." Nat Protoc **2**(5): 1236-1247.

Lusky, M., M. Christ, et al. (1998). "In vitro and in vivo biology of recombinant adenovirus vectors with E1, E1/E2A, or E1/E4 deleted." J Virol **72**(3): 2022-2032.

Ma, L., H. A. Bluyssen, et al. (2001). "Rapid determination of adenoviral vector titers by quantitative real-time PCR." J Virol Methods **93**(1-2): 181-188.

Malatack, J. J., D. M. Consolini, et al. (2003). "The status of hematopoietic stem cell transplantation in lysosomal storage disease." Pediatr Neurol **29**(5): 391-403.

Martin, K., A. Brie, et al. (2003). "Simultaneous CAR- and alpha V integrin-binding ablation fails to reduce Ad5 liver tropism." Mol Ther **8**(3): 485-494.

Mates, L., M. K. Chuah, et al. (2009). "Molecular evolution of a novel hyperactive Sleeping Beauty transposase enables robust stable gene transfer in vertebrates." Nat Genet **41**(6): 753-761.

Mathews, M. B. and T. Shenk (1991). "Adenovirus virus-associated RNA and translation control." J Virol **65**(11): 5657-5662.

Mathias, P., T. Wickham, et al. (1994). "Multiple adenovirus serotypes use alpha v integrins for infection." J Virol **68**(10): 6811-6814.

Matthews, D. A. and W. C. Russell (1998). "Adenovirus core protein V is delivered by the invading virus to the nucleus of the infected cell and later in infection is associated with nucleoli." J Gen Virol **79 (Pt 7)**: 1671-1675.

Mazurier, F., O. I. Gan, et al. (2004). "Lentivector-mediated clonal tracking reveals intrinsic heterogeneity in the human hematopoietic stem cell compartment and culture-induced stem cell impairment." Blood **103**(2): 545-552.

McGrory, W. J., D. S. Bautista, et al. (1988). "A simple technique for the rescue of early region I mutations into infectious human adenovirus type 5." Virology **163**(2): 614-617.

Miller, J. C., S. Tan, et al. (2011). "A TALE nuclease architecture for efficient genome editing." Nat Biotechnol **29**(2): 143-148.

Mintzer, M. A. and E. E. Simanek (2009). "Nonviral vectors for gene delivery." Chem Rev **109**(2): 259-302.

Mirza, M. A. and J. Weber (1982). "Structure of adenovirus chromatin." Biochim Biophys Acta **696**(1): 76-86.

Mizuguchi, H. and M. A. Kay (1998). "Efficient construction of a recombinant adenovirus vector by an improved in vitro ligation method." Hum Gene Ther **9**(17): 2577-2583.

Mohr, C. A., J. Arapovic, et al. (2010). "A spread-deficient cytomegalovirus for assessment of first-target cells in vaccination." J Virol **84**(15): 7730-7742.

Monaco, A. P. and Z. Larin (1994). "YACs, BACs, PACs and MACs: artificial chromosomes as research tools." Trends Biotechnol **12**(7): 280-286.

Morral, N., R. J. Parks, et al. (1998). "High doses of a helper-dependent adenoviral vector yield supraphysiological levels of alpha1-antitrypsin with negligible toxicity." Hum Gene Ther **9**(18): 2709-2716.

Muruve, D. A., M. J. Cotter, et al. (2004). "Helper-dependent adenovirus vectors elicit intact innate but attenuated adaptive host immune responses in vivo." J Virol **78**(11): 5966-5972.

Muther, N., N. Noske, et al. (2009). "Viral hybrid vectors for somatic integration - are they the better solution?" Viruses **1**(3): 1295-1324.

Müther, N., N. Noske, et al. (2009). "Viral Hybrid Vectors for Somatic Integration - Are They the Better Solution?" Viruses **1**(3): 1295-1324.

Naldini, L. (2011). "Ex vivo gene transfer and correction for cell-based therapies." Nat Rev Genet **12**(5): 301-315.

Nasz, I. and E. Adam (2001). "Recombinant adenovirus vectors for gene therapy and clinical trials." Acta Microbiol Immunol Hung **48**(3-4): 323-348.

Nettelbeck, D. M., A. A. Rivera, et al. (2002). "Novel oncolytic adenoviruses targeted to melanoma: specific viral replication and cytolysis by expression of E1A mutants from the tyrosinase enhancer/promoter." Cancer Res **62**(16): 4663-4670.

Nevins, J. R. (1987). "Regulation of early adenovirus gene expression." Microbiol Rev **51**(4): 419-430.

Newcomb, W. W., J. W. Boring, et al. (1984). "Ion etching of human adenovirus 2: structure of the core." J Virol **51**(1): 52-56.

Ng, P., C. Beauchamp, et al. (2001). "Development of a FLP/frt system for generating helper-dependent adenoviral vectors." Mol Ther **3**(5 Pt 1): 809-815.

Nicklin, S. A., S. J. White, et al. (2004). "In vitro and in vivo characterisation of endothelial cell selective adenoviral vectors." J Gene Med **6**(3): 300-308.

Niemeyer, G. P., R. W. Herzog, et al. (2009). "Long-term correction of inhibitor-prone hemophilia B dogs treated with liver-directed AAV2-mediated factor IX gene therapy." Blood **113**(4): 797-806.

Nilsson, E. C., R. J. Storm, et al. (2011). "The GD1a glycan is a cellular receptor for adenoviruses causing epidemic keratoconjunctivitis." Nat Med **17**(1): 105-109.

Nordhoff, V., K. Hubner, et al. (2001). "Comparative analysis of human, bovine, and murine Oct-4 upstream promoter sequences." Mamm Genome **12**(4): 309-317.

Norrby, E., J. van der Veen, et al. (1970). "A new serological technique for identification of adenovirus infections." Proc Soc Exp Biol Med **134**(3): 889-895.

Nott, A., S. H. Meislin, et al. (2003). "A quantitative analysis of intron effects on mammalian gene expression." RNA **9**(5): 607-617.

Noureddini, S. C. and D. T. Curiel (2005). "Genetic targeting strategies for adenovirus." Mol Pharm **2**(5): 341-347.

O'Connor, T. P. and R. G. Crystal (2006). "Genetic medicines: treatment strategies for hereditary disorders." Nat Rev Genet **7**(4): 261-276.

Osterwalder, T., K. S. Yoon, et al. (2001). "A conditional tissue-specific transgene expression system using inducible GAL4." Proc Natl Acad Sci U S A **98**(22): 12596-12601.

Palmer, D. and P. Ng (2003). "Improved system for helper-dependent adenoviral vector production." Mol Ther **8**(5): 846-852.

Palmer, D. J. and P. Ng (2005). "Helper-dependent adenoviral vectors for gene therapy." Hum Gene Ther **16**(1): 1-16.

Parker, A. L., S. N. Waddington, et al. (2006). "Multiple vitamin K-dependent coagulation zymogens promote adenovirus-mediated gene delivery to hepatocytes." Blood **108**(8): 2554-2561.

Parks, R. J., L. Chen, et al. (1996). "A helper-dependent adenovirus vector system: removal of helper virus by Cre-mediated excision of the viral packaging signal." Proc Natl Acad Sci U S A **93**(24): 13565-13570.

Pastore, L., N. Morral, et al. (1999). "Use of a liver-specific promoter reduces immune response to the transgene in adenoviral vectors." Hum Gene Ther **10**(11): 1773-1781.

Patterson, S. and W. C. Russell (1983). "Ultrastructural and immunofluorescence studies of early events in adenovirus-HeLa cell interactions." J Gen Virol **64**(Pt 5): 1091-1099.

Perricone, M. A., J. E. Morris, et al. (2001). "Aerosol and lobar administration of a recombinant adenovirus to individuals with cystic fibrosis. II. Transfection efficiency in airway epithelium." Hum Gene Ther **12**(11): 1383-1394.

Pichla-Gollon, S. L., M. Drinker, et al. (2007). "Structure-based identification of a major neutralizing site in an adenovirus hexon." J Virol **81**(4): 1680-1689.

Pluta, K. and M. M. Kacprzak (2009). "Use of HIV as a gene transfer vector." Acta Biochim Pol **56**(4): 531-595.

Porteus, M. (2008). "Design and testing of zinc finger nucleases for use in mammalian cells." Methods Mol Biol **435**: 47-61.

Poulin, K. L., R. M. Lanthier, et al. (2010). "Retargeting of adenovirus vectors through genetic fusion of a single-chain or single-domain antibody to capsid protein IX." J Virol **84**(19): 10074-10086.

Puntel, M., A. K. Muhammad, et al. (2010). "A novel bicistronic high-capacity gutless adenovirus vector that drives constitutive expression of herpes simplex virus type 1 thymidine kinase and tet-inducible expression of Flt3L for glioma therapeutics." J Virol **84**(12): 6007-6017.

Quan, J. and J. Tian (2009). "Circular polymerase extension cloning of complex gene libraries and pathways." PLoS One **4**(7): e6441.

Quan, J. and J. Tian (2011). "Circular polymerase extension cloning for high-throughput cloning of complex and combinatorial DNA libraries." Nat Protoc **6**(2): 242-251.

Ramachandra, M. and R. Padmanabhan (1995). "Expression, nuclear transport, and phosphorylation of adenovirus DNA replication proteins." Curr Top Microbiol Immunol **199 (Pt 2)**: 50-88.

Raper, S. E., N. Chirmule, et al. (2003). "Fatal systemic inflammatory response syndrome in a ornithine transcarbamylase deficient patient following adenoviral gene transfer." Mol Genet Metab **80**(1-2): 148-158.

Reddy, V. S., S. K. Natchiar, et al. (2010). "Crystal structure of human adenovirus at 3.5 A resolution." Science **329**(5995): 1071-1075.

Rekosh, D. (1981). "Analysis of the DNA-terminal protein from different serotypes of human adenovirus." J Virol **40**(1): 329-333.

Roberts, D. M., A. Nanda, et al. (2006). "Hexon-chimaeric adenovirus serotype 5 vectors circumvent pre-existing anti-vector immunity." Nature **441**(7090): 239-243.

Robinson, C. M., G. Singh, et al. (2011). "Computational analysis and identification of an emergent human adenovirus pathogen implicated in a respiratory fatality." Virology **409**(2): 141-147.

Rollier, C. S., A. Reyes-Sandoval, et al. (2011). "Viral vectors as vaccine platforms: deployment in sight." Curr Opin Immunol **23**(3): 377-382.

Ross, P. J., M. A. Kennedy, et al. (2009). "Host cell detection of noncoding stuffer DNA contained in helper-dependent adenovirus vectors leads to epigenetic repression of transgene expression." J Virol **83**(17): 8409-8417.

Russell, W. C. (2009). "Adenoviruses: update on structure and function." J Gen Virol **90**(Pt 1): 1-20.

Rux, J. J., P. R. Kuser, et al. (2003). "Structural and phylogenetic analysis of adenovirus hexons by use of high-resolution x-ray crystallographic, molecular modeling, and sequence-based methods." J Virol **77**(17): 9553-9566.

Ruzsics, Z., M. Wagner, et al. (2006). "Transposon-assisted cloning and traceless mutagenesis of adenoviruses: Development of a novel vector based on species D." J Virol **80**(16): 8100-8113.

Saban, S. D., M. Silvestry, et al. (2006). "Visualization of alpha-helices in a 6-angstrom resolution cryoelectron microscopy structure of adenovirus allows refinement of capsid protein assignments." J Virol **80**(24): 12049-12059.

San Martin, C., J. N. Glasgow, et al. (2008). "Localization of the N-terminus of minor coat protein IIIa in the adenovirus capsid." J Mol Biol **383**(4): 923-934.

Schaack, J. (2005). "Adenovirus vectors deleted for genes essential for viral DNA replication." Front Biosci **10**: 1146-1155.

Schmid, S. I. and P. Hearing (1995). "Selective encapsidation of adenovirus DNA." Curr Top Microbiol Immunol **199 (Pt 1)**: 67-80.

Schmid, S. I. and P. Hearing (1998). "Cellular components interact with adenovirus type 5 minimal DNA packaging domains." J Virol **72**(8): 6339-6347.

Scriver, C. R. and P. J. Waters (1999). "Monogenic traits are not simple: lessons from phenylketonuria." Trends Genet **15**(7): 267-272.

Segura, M. M., R. Alba, et al. (2008). "Advances in helper-dependent adenoviral vector research." Curr Gene Ther **8**(4): 222-235.

Seshidhar Reddy, P., S. Ganesh, et al. (2003). "Development of adenovirus serotype 35 as a gene transfer vector." Virology **311**(2): 384-393.

Setel, P. W., L. Saker, et al. (2004). "Is it time to reassess the categorization of disease burdens in low-income countries?" Am J Public Health **94**(3): 384-388.

Sharma, N., B. Moldt, et al. (2008). "Regulated gene insertion by steroid-induced PhiC31 integrase." Nucleic Acids Res **36**(11): e67.

Shaw, A. R. and E. B. Ziff (1980). "Transcripts from the adenovirus-2 major late promoter yield a single early family of 3' coterminal mRNAs and five late families." Cell **22**(3): 905-916.

Shevchuk, N. A., A. V. Bryksin, et al. (2004). "Construction of long DNA molecules using long PCR-based fusion of several fragments simultaneously." Nucleic Acids Res **32**(2): e19.

Shi, C. X., F. L. Graham, et al. (2006). "A convenient plasmid system for construction of helper-dependent adenoviral vectors and its application for analysis of the breast-cancer-specific mammaglobin promoter." J Gene Med **8**(4): 442-451.

Sliva, K. and B. S. Schnierle (2010). "Selective gene silencing by viral delivery of short hairpin RNA." Virol J **7**: 248.

Smart, J. E. and B. W. Stillman (1982). "Adenovirus terminal protein precursor. Partial amino acid sequence and the site of covalent linkage to virus DNA." J Biol Chem **257**(22): 13499-13506.

Smith, T. A., M. G. Mehaffey, et al. (1993). "Adenovirus mediated expression of therapeutic plasma levels of human factor IX in mice." Nat Genet **5**(4): 397-402.

Sorrell, D. A. and A. F. Kolb (2005). "Targeted modification of mammalian genomes." Biotechnol Adv **23**(7-8): 431-469.

Stehle, I. M., M. F. Scinteie, et al. (2003). "Exploiting a minimal system to study the epigenetic control of DNA replication: the interplay between transcription and replication." Chromosome Res **11**(5): 413-421.

Stewart, P. L., R. M. Burnett, et al. (1991). "Image reconstruction reveals the complex molecular organization of adenovirus." Cell **67**(1): 145-154.

Stewart, P. L., S. D. Fuller, et al. (1993). "Difference imaging of adenovirus: bridging the resolution gap between X-ray crystallography and electron microscopy." Embo J **12**(7): 2589-2599.

Strunze, S., M. F. Engelke, et al. (2011). "Kinesin-1-mediated capsid disassembly and disruption of the nuclear pore complex promote virus infection." Cell Host Microbe **10**(3): 210-223.

Sumida, S. M., D. M. Truitt, et al. (2005). "Neutralizing antibodies to adenovirus serotype 5 vaccine vectors are directed primarily against the adenovirus hexon protein." J Immunol **174**(11): 7179-7185.

Suomalainen, M., M. Y. Nakano, et al. (1999). "Microtubule-dependent plus- and minus end-directed motilities are competing processes for nuclear targeting of adenovirus." J Cell Biol **144**(4): 657-672.

Svensson, U., R. Persson, et al. (1981). "Virus-receptor interaction in the adenovirus system I. Identification of virion attachment proteins of the HeLa cell plasma membrane." J Virol **38**(1): 70-81.

Takeuchi, J. K. and B. G. Bruneau (2009). "Directed transdifferentiation of mouse mesoderm to heart tissue by defined factors." Nature **459**(7247): 708-711.

Terashima, T., K. Oka, et al. (2009). "DRG-targeted helper-dependent adenoviruses mediate selective gene delivery for therapeutic rescue of sensory neuronopathies in mice." J Clin Invest **119**(7): 2100-2112.

Thomas, C. E., A. Ehrhardt, et al. (2003). "Progress and problems with the use of viral vectors for gene therapy." Nat Rev Genet **4**(5): 346-358.

Tichy, E. D., R. Pillai, et al. (2010). "Mouse embryonic stem cells, but not somatic cells, predominantly use homologous recombination to repair double-strand DNA breaks." Stem Cells Dev **19**(11): 1699-1711.

Tollefson, A. E., A. Scaria, et al. (1992). "The 11,600-MW protein encoded by region E3 of adenovirus is expressed early but is greatly amplified at late stages of infection." J Virol **66**(6): 3633-3642.

Trotman, L. C., N. Mosberger, et al. (2001). "Import of adenovirus DNA involves the nuclear pore complex receptor CAN/Nup214 and histone H1." Nat Cell Biol **3**(12): 1092-1100.

Tuve, S., H. Wang, et al. (2006). "A new group B adenovirus receptor is expressed at high levels on human stem and tumor cells." J Virol **80**(24): 12109-12120.

Van Spall, H. G., A. Toren, et al. (2007). "Eligibility criteria of randomized controlled trials published in high-impact general medical journals: a systematic sampling review." JAMA **297**(11): 1233-1240.

Vassiliou, G. S., J. L. Cooper, et al. (2011). "Mutant nucleophosmin and cooperating pathways drive leukemia initiation and progression in mice." Nat Genet **43**(5): 470-475.

Vierbuchen, T., A. Ostermeier, et al. (2010). "Direct conversion of fibroblasts to functional neurons by defined factors." Nature **463**(7284): 1035-1041.

Waddington, S. N., J. H. McVey, et al. (2008). "Adenovirus serotype 5 hexon mediates liver gene transfer." Cell **132**(3): 397-409.

Wang, H., Z. Y. Li, et al. (2010). "Desmoglein 2 is a receptor for adenovirus serotypes 3, 7, 11 and 14." Nat Med.

Wang, H., D. M. Shayakhmetov, et al. (2005). "A capsid-modified helper-dependent adenovirus vector containing the beta-globin locus control region displays a nonrandom integration pattern and allows stable, erythroid-specific gene expression." J Virol **79**(17): 10999-11013.

Wang, S., Y. Zhao, et al. (2009). "A new positive/negative selection scheme for precise BAC recombineering." Mol Biotechnol **42**(1): 110-116.

Warlich, E., J. Kuehle, et al. (2011). "Lentiviral vector design and imaging approaches to visualize the early stages of cellular reprogramming." Mol Ther **19**(4): 782-789.

Warming, S., N. Costantino, et al. (2005). "Simple and highly efficient BAC recombineering using galK selection." Nucleic Acids Res **33**(4): e36.

Warrington, K. H., Jr. and R. W. Herzog (2006). "Treatment of human disease by adeno-associated viral gene transfer." Hum Genet **119**(6): 571-603.

Weatherall, D. J. (2001). "Phenotype-genotype relationships in monogenic disease: lessons from the thalassaemias." Nat Rev Genet **2**(4): 245-255.

Weber, J. M. (1995). "Adenovirus endopeptidase and its role in virus infection." Curr Top Microbiol Immunol **199 (Pt 1)**: 227-235.

Webster, A., S. Russell, et al. (1989). "Characterization of the adenovirus proteinase: substrate specificity." J Gen Virol **70 (Pt 12)**: 3225-3234.

Wickham, T. J., M. E. Carrion, et al. (1995). "Targeting of adenovirus penton base to new receptors through replacement of its RGD motif with other receptor-specific peptide motifs." Gene Ther **2**(10): 750-756.

Wickham, T. J., P. Mathias, et al. (1993). "Integrins alpha v beta 3 and alpha v beta 5 promote adenovirus internalization but not virus attachment." Cell **73**(2): 309-319.

Wiethoff, C. M., H. Wodrich, et al. (2005). "Adenovirus protein VI mediates membrane disruption following capsid disassembly." J Virol **79**(4): 1992-2000.

Wilson, J. M. (2005). "Gendicine: the first commercial gene therapy product." Hum Gene Ther **16**(9): 1014-1015.

Wilson, M. H., J. M. Kaminski, et al. (2005). "Functional zinc finger/sleeping beauty transposase chimeras exhibit attenuated overproduction inhibition." FEBS Lett **579**(27): 6205-6209.

Wodrich, H., D. Henaff, et al. (2010). "A capsid-encoded PPxY-motif facilitates adenovirus entry." PLoS Pathog **6**(3): e1000808.

Wold, W. S., K. Doronin, et al. (1999). "Immune responses to adenoviruses: viral evasion mechanisms and their implications for the clinic." Curr Opin Immunol **11**(4): 380-386.

Wold, W. S., A. E. Tollefson, et al. (1995). "E3 transcription unit of adenovirus." Curr Top Microbiol Immunol **199 (Pt 1)**: 237-274.

Wolff, L. J., J. A. Wolff, et al. (2009). "Effect of tissue-specific promoters and microRNA recognition elements on stability of transgene expression after hydrodynamic naked plasmid DNA delivery." Hum Gene Ther **20**(4): 374-388.

Wood, A. J., T. W. Lo, et al. (2011). "Targeted genome editing across species using ZFNs and TALENs." Science **333**(6040): 307.

Wortmann, A., S. Vohringer, et al. (2008). "Fully detargeted polyethylene glycol-coated adenovirus vectors are potent genetic vaccines and escape from pre-existing anti-adenovirus antibodies." Mol Ther **16**(1): 154-162.

Wu, S. C., Y. J. Meir, et al. (2006). "piggyBac is a flexible and highly active transposon as compared to sleeping beauty, Tol2, and Mos1 in mammalian cells." Proc Natl Acad Sci U S A **103**(41): 15008-15013.

Yang, Y., F. A. Nunes, et al. (1994). "Cellular immunity to viral antigens limits E1-deleted adenoviruses for gene therapy." Proc Natl Acad Sci U S A **91**(10): 4407-4411.

Yang, Y., E. F. Vanin, et al. (1995). "Inducible, high-level production of infectious murine leukemia retroviral vector particles pseudotyped with vesicular stomatitis virus G envelope protein." Hum Gene Ther **6**(9): 1203-1213.

Yant, S. R., A. Ehrhardt, et al. (2002). "Transposition from a gutless adeno-transposon vector stabilizes transgene expression in vivo." Nat Biotechnol **20**(10): 999-1005.

Yant, S. R., Y. Huang, et al. (2007). "Site-directed transposon integration in human cells." Nucleic Acids Res **35**(7): e50.

Yant, S. R., J. Park, et al. (2004). "Mutational analysis of the N-terminal DNA-binding domain of sleeping beauty transposase: critical residues for DNA binding and hyperactivity in mammalian cells." Mol Cell Biol **24**(20): 9239-9247.

Yant, S. R., X. Wu, et al. (2005). "High-resolution genome-wide mapping of transposon integration in mammals." Mol Cell Biol **25**(6): 2085-2094.

Yates, J. L., N. Warren, et al. (1985). "Stable replication of plasmids derived from Epstein-Barr virus in various mammalian cells." Nature **313**(6005): 812-815.

Yei, S., N. Mittereder, et al. (1994). "Adenovirus-mediated gene transfer for cystic fibrosis: quantitative evaluation of repeated in vivo vector administration to the lung." Gene Ther **1**(3): 192-200.

Yi, Y., S. H. Hahm, et al. (2005). "Retroviral gene therapy: safety issues and possible solutions." Curr Gene Ther **5**(1): 25-35.

Yotnda, P., H. Onishi, et al. (2001). "Efficient infection of primitive hematopoietic stem cells by modified adenovirus." Gene Ther **8**(12): 930-937.

Youil, R., T. J. Toner, et al. (2002). "Hexon gene switch strategy for the generation of chimeric recombinant adenovirus." Hum Gene Ther **13**(2): 311-320.

Yusa, K., R. Rad, et al. (2009). "Generation of transgene-free induced pluripotent mouse stem cells by the piggyBac transposon." Nat Methods **6**(5): 363-369.

Yusa, K., L. Zhou, et al. (2011). "A hyperactive piggyBac transposase for mammalian applications." Proc Natl Acad Sci U S A **108**(4): 1531-1536.

Zabner, J., L. A. Couture, et al. (1993). "Adenovirus-mediated gene transfer transiently corrects the chloride transport defect in nasal epithelia of patients with cystic fibrosis." Cell **75**(2): 207-216.

Zayed, H., Z. Izsvak, et al. (2004). "Development of hyperactive sleeping beauty transposon vectors by mutational analysis." Mol Ther **9**(2): 292-304.

Zhang, W. W. (1999). "Development and application of adenoviral vectors for gene therapy of cancer." Cancer Gene Ther **6**(2): 113-138.

Zhang, Y., F. Buchholz, et al. (1998). "A new logic for DNA engineering using recombination in Escherichia coli." Nat Genet **20**(2): 123-128.

Zhou, D., X. Zhou, et al. (2010). "An efficient method of directly cloning chimpanzee adenovirus as a vaccine vector." Nat Protoc **5**(11): 1775-1785.

7.3. Curriculum vitae

Persönliche Daten:

Name:	Martin Andreas Mück-Häusl
Geburtstag:	02.03.1981
Geburtsort:	Bad Reichenhall
Nationalität:	Deutsch

Schulausbildung:

1987 – 1991	Grundschule Karlstein, Bad Reichenhall
1991 – 2000	Karlsgymnasium Bad Reichenhall

Hochschulausbildung:

2000 – 2004	Studiengang *Biochemie (B. Sc.)*, TU München
2004 – 2007	Studiengang *Biochemie (M. Sc.)*, TU München
2007 – 2011	Promotion in der Abteilung für Virologie des Max von Pettenkofer-Instituts, medizinische Fakultät der Ludwig-Maximilians-Universität München; Betreuerin: Prof. Dr. Anja Ehrhardt (Universität Witten/Herdecke); Thema der Promotion: „Genetic engineering of adenoviral vectors for improved therapeutic applications“

7.4. Acknowledgement

First of all, I want to thank Prof. Dr. Roland Beckmann for taking care of the supervision of this thesis, for the time and efforts he spent and for representing this thesis at the Department of Biochemistry at the LMU Munich. Furthermore, I want to thank the members of my committee Prof. Dr. Klaus Förstemann, PD Dr. Manfred Ogris, Prof. Dr. Christian Wahl-Schott and Prof. Dr. Karl-Peter Hopfner for their instant readiness to spend their time and efforts to support this work.

It is a major concern to me to thank my supervisor and mentor Prof. Dr. Anja Ehrhardt. Anja, I think there are no better words than Tina used in her thesis: I thank you for the excellent support, the confidence and especially for the great atmosphere you provided throughout the four years I worked in your lab. With the words of Brian: You deserve the "Best Boss in the World" button on your car!

Furthermore, I want to thank all my collaborators Philip Ng, PhD (Baylor College), Mark Kay, PhD (Stanford University), Timothy Nichols, PhD (University of North Carolina, Chapel Hill), Elizabeth Merricks (University of North Carolina, Chapel Hill), Helen Franck (University of North Carolina, Chapel Hill), Dr. Zsolt Ruzsics (LMU), Stefan Jordan (LMU), Andrew Baker, PhD (University of Glasgow) and Raul Alba, PhD (University of Glasgow).

Special thanks goes to my current lab mates Nadja, Nadine, Tina, Ricki, Wenli and Manish. It was a great pleasure to work with you during the last years. I cannot imagine getting such nice colleagues again. Thanks a lot for the nice evenings at the Wiesn, at the "beach" and all the time we spent together. You got real friends to me. At this part I also want to mention my former lab members I started with 4 years ago or worked with during the last years, Nina, Leo, Ines, Lorenz, Raphi and Nicci. I also want to thank you for the nice atmosphere in the lab.

Moreover, I wish to thank all the people at the Pettenkofer-Institute. In particular, the clinical virology for their support and of course the AG Spaß and all the coffee and lunch mates, it was a fruitful get together and you made the time here so enjoyable.

However, it is impossible to overstate the support of my family, loved ones and friends who have been my foundation in all I achieved. Especially, I would like to thank my parents for their love and patience. You always trust in me and were instrumental during this thesis. Last but not least, I want to say a special thank to my most favourite person Tanja for her ambitious support and patience during the last months.